APPLICATIONS OF EFFECTIVE THEORIES OF QCD IN COLLIDER PHYSICS

by

Wai Kin Lai

B.S., Chinese University of Hong Kong, 2005

M.S., University of Pittsburgh, 2009

Submitted to the Graduate Faculty of

the Kenneth P. Dietrich School of Arts and Sciences in partial fulfillment

of the requirements for the degree of

Doctor of Philosophy

University of Pittsburgh

2016

UNIVERSITY OF PITTSBURGH

KENNETH P. DIETRICH SCHOOL OF ARTS AND SCIENCES

This dissertation was presented

by

Wai Kin Lai

It was defended on

September 21, 2016

and approved by

Adam Leibovich, Professor, Chair of Department, University of Pittsburgh

Ayres Freitas, Associate Professor, University of Pittsburgh

Vittorio Paolone, Professor, University of Pittsburgh

Ira Rothstein, Professor, Carnegie Mellon University

Xiao-lun Wu, Professor, University of Pittsburgh

Dissertation Director: Adam Leibovich, Professor, Chair of Department, University of Pittsburgh

APPLICATIONS OF EFFECTIVE THEORIES OF QCD IN COLLIDER PHYSICS

Wai Kin Lai, PhD

University of Pittsburgh, 2016

In this thesis, we apply effective theories of Quantum Chromodynamics (QCD) in collider physics.

First, we apply heavy quark effective theory (HQET) on the production asymmetries of heavy hadrons in collider experiments. Asymmetries of the partial widths of a heavy hadron and its antiparticle contain information about CP violation. In collider experiments, partial widths are inevitably entangled with production rates. Therefore, understanding production asymmetries is essential in extracting information about CP violation from collider experiments. At leading twist in perturbative QCD, such production asymmetries are absent. Using heavy quark effective theory (HQET), we examine the subleading-twist processes which can produce the productions asymmetries. By fitting several non-perturbative parameters to data, the production asymmetries of D^+/D^- measured at LHCb can be explained reasonably well. We also make predictions on production asymmetries of $\Lambda_Q/\overline{\Lambda}_Q$ at the LHC. The asymmetries are found to be significant in the forward region and should be measurable by LHCb. In addition, for further investigation in the future, we compute the partonic cross sections for P waves.

Second, we apply soft-collinear effective theory (SCET) to resum large logarithms $\ln^n(1-m_{VH}^2/\hat{s})$ in the threshold region $m_{VH}^2 \to \hat{s}$ for the associated production of the Higgs boson with a vector boson at the LHC. The effect of NNNLL resummation on the total cross section at NNLO is found to be negligible. For the distribution in $\tau = M_{VH}^2/s$, the NNLL resummation increases the fixed-order NLO result by $\sim 10\%$ at $\tau \sim 0.1$, suggesting the

importance of threshold resummation at τ of moderate size.

TABLE OF CONTENTS

LIST OF TABLES

LIST OF FIGURES

PREFACE

I would like to thank Prof. Adam Leibovich for his guidance on my research during my years in Pittsburgh. I am also debted to Prof. Tao Han, Dr. Sally Dawson and Dr. Ian Lewis, from whom I learned a lot during our collaboration.

1.0 INTRODUCTION

The Standard Model of particle physics and general relativity, the foundations of modern physics, have passed countless experimental tests to great precision. However, only about 5% of the energy content of the universe is explained by particles in the Standard Model. Dark matter constitutes about 25% of the total energy content, while dark energy makes up the remaining 70% [1]. Explanations of dark matter and dark energy by particle physics are actively being looked for. Even within the Standard Model, there are long-standing problems to be solved. For instance, the origin of the tiny neutrino masses is unknown. The ultra-violet stability of the Higgs mass is yet to be explained. To try to answer all these questions, one needs to probe physics at very short distances. For this purpose, the Large Hadron Collider was built.

Since the discovery of the Higgs boson at the LHC in 2012 [2][3], particle physics has entered a new era of excitement. The Higgs boson was the latest discovered elementary particle in the Standard Model. It is responsible for the electroweak symmetry breaking and giving masses to the $W^{\pm}, Z$ bosons as well as the quarks and leptons. Precision measurements of properties of the Higgs boson will provide valuable information on new physics. To date the couplings of the Higgs to various Standard Model particles are roughly consistent with those predicted by the Standard Model (see Fig. (1)). It should be noted that the smallness of the theoretical errors are largely due to advances in perturbative QCD. As part of this thesis, We will apply soft-collinear effective theory to improve QCD predictions for the associated Higgs production with a vector boson at the LHC.

On the other hand, the LHCb experiment is looking for new physics in the heavy flavor sector. CP violation has been one of the central topics in particle physics since its discovery in 1964 [5]. The non-zero baryon asymmetry in the universe can be explained with a symmetric

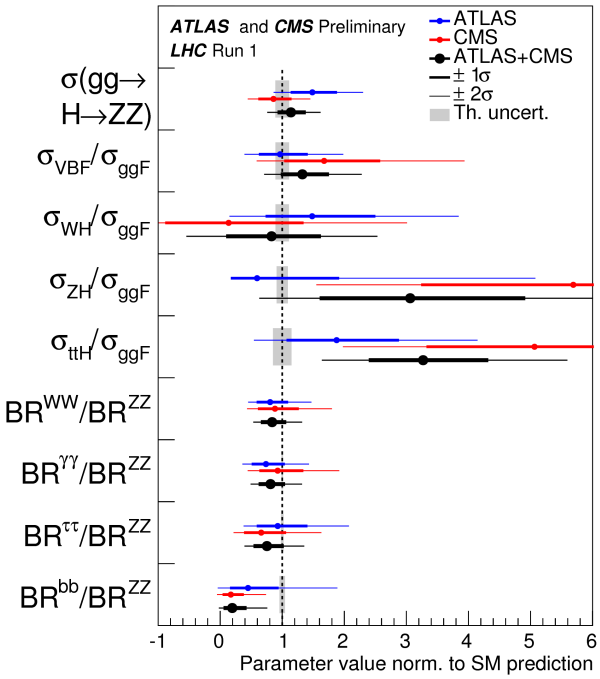

Figure 1: Couplings of Higgs to Standard Model particles from LHC Run I [4].

initial condition at the Big Bang only if CP is violated in the fundamental physical theory [6]. CP violation in the quark sector in the Standard Model is too small to explain the observed abundance of baryons [7][8]. New forms of CP violations are actively being searched at the LHCb experiment. CP violations have been observed in decays of neutral kaons [5] and B mesons [9][10]. CP violations in D meson systems, although not yet observed, are highly expected. A key observable which signals CP violation in D meson decays is the D decay asymmetry a^f_{CP}:

$$a^f_{CP} = \frac{\Gamma(D \to f) - \Gamma(\overline{D} \to \overline{f})}{\Gamma(D \to f) + \Gamma(\overline{D} \to \overline{f})}, \tag{1.1}$$

where f denotes some final state. However, even without CP violation, QCD implies that D and $\overline{D}$ are produced at different amounts at the LHC. Therefore, To extract the a^f_{CP} it is important to understand the production asymmetry A_p:

$$A_p = \frac{\sigma(D) - \sigma(\overline{D})}{\sigma(D) + \sigma(\overline{D})}. \tag{1.2}$$

Production asymmetries for $D^{\pm}$ have been oberved at LHCb [11]. We will apply heavy quark effective theory to explain them.

In the rest of this chapter, we will first review the Standard Model briefly. Then we will review the basic elements of perturbative QCD and the general framework of effective field theory. Chapter 2 and 3 are respectively devoted to introductions of heavy quark effective theory (HQET) and soft-collinear effective theory (SCET), the two effective theories of QCD which we will use throughout the thesis. The following two chapters are the core of the thesis. Chapter 4 is on the application of HQET to predictions of production asymmetries of $D^{\pm}$ and $\Lambda_Q/\overline{\Lambda}_Q$. Chapter 5 is on threshold resummation of the associated Higgs production with a vector boson, based on the SCET framework. Finally, Chapter 6 is the conclusion.

1.1 THE STANDARD MODEL

The Standard Model is a gauge theory with local gauge group $SU(3)_c \times SU(2)_W \times U(1)_Y$. It describes the strong and electroweak interactions. The field content consists of gauge fields (A^a_μ, W^I_μ, B_μ), quark fields (Q^i_L, u^i_R, d^i_R), lepton fields (L^i_L, e^i_R), and the Higgs field H, as listed in Table (1). The full Lagrangian has the form

$$\mathcal{L}_{SM} = \mathcal{L}_{gauge\,field} + \mathcal{L}_{fermion} + \mathcal{L}_{Higgs} + \mathcal{L}_{Yukawa}\,. \tag{1.3}$$

$\mathcal{L}_{gauge\,field}$ contains the kinetic terms of the gauge fields:

$$\mathcal{L}_{gauge\,field} = -\frac{1}{4}G^{a\mu\nu}G^a_{\mu\nu} - \frac{1}{4}W^{I\mu\nu}W^I_{\mu\nu} - \frac{1}{4}B^{\mu\nu}B_{\mu\nu}\,, \tag{1.4}$$

where $G^a_{\mu\nu}$, $W^I_{\mu\nu}$ and $B_{\mu\nu}$ are the field strengths:

$$G^a_{\mu\nu} = \partial_\mu A^a_\nu - \partial_\nu A^a_\mu + g f^{abc} A^b_\mu A^c_\nu\,, \tag{1.5a}$$

$$W^I_{\mu\nu} = \partial_\mu W^I_\nu - \partial_\nu W^I_\mu + g_2 \epsilon^{IJK} W^J_\mu W^K_\nu\,, \tag{1.5b}$$

$$B_{\mu\nu} = \partial_\mu B_\nu - \partial_\nu B_\mu\,. \tag{1.5c}$$

f^{abc} and ϵ^{IJK} are the structure constants defined by $[t^a, t^b] = i f^{abc} t^c$ and $[T^I, T^J] = i\epsilon^{IJK} T^K$, where t^a, $a = 1, \ldots, 8$, are the eight generators of $SU(3)_c$, and T^I, $I = 1, 2, 3$, are the three

Table 1: Field content in the Standard Model

Field	$SU(3)_c$	$SU(2)_W$	$U(1)_Y$	Lorentz
A^a_μ	**8**	**1**	0	$(1/2, 1/2)$
W^I_μ	**1**	**3**	0	$(1/2, 1/2)$
B_μ	**1**	**1**	0	$(1/2, 1/2)$
$Q^i_L = \begin{pmatrix} u^i_L \\ d^i_L \end{pmatrix}$	**3**	**2**	$1/6$	$(1/2, 0)$
u^i_R	**3**	**1**	$2/3$	$(0, 1/2)$
d^i_R	**3**	**1**	$-1/3$	$(0, 1/2)$
$L^i_L = \begin{pmatrix} \nu^i_L \\ e^i_L \end{pmatrix}$	**1**	**2**	$-1/2$	$(1/2, 0)$
e^i_R	**1**	**1**	-1	$(0, 1/2)$
$H = \begin{pmatrix} H^+ \\ H^0 \end{pmatrix}$	**1**	**2**	$1/2$	$(0, 0)$

The index $i = 1, 2, 3$ labels fermion family. The second and third column list the dimensions of the $SU(3)_c$ and $SU(2)_Y$ irreducible representations respecively. The $U(1)_Y$ charges Y are listed in the fourth column. The last column lists the type of irreducible representations of the Lorentz group $SO(3, 1)$ in the (J_L, J_R) notation.

generators of $SU(2)_W$. $\mathcal{L}_{fermion}$ contains the kinetic terms and gauge interactions of the fermions:

$$\mathcal{L}_{fermion} = \bar{Q}_L^i i\not{D} Q_L^i + \bar{u}_R^i i\not{D} u_R^i + \bar{d}_R^i i\not{D} d_R^i + \bar{L}_L^i i\not{D} L_L^i + \bar{e}_R^i i\not{D} e_R^i \,, \tag{1.6}$$

where D_μ is the covariant derivative

$$D_\mu = \partial_\mu - igt^a A_\mu^a - ig_2 T^I W_\mu^I - ig_1 Y B_\mu \,. \tag{1.7}$$

$\mathcal{L}_{Higgs}$ contains the kinetic term, gauge interactions, and self interactions of the Higgs field:

$$\mathcal{L}_{Higgs} = (D_\mu H)^\dagger (D^\mu H) - V(H) \,, \tag{1.8}$$

where the Higgs potential is given by

$$V(H) = \frac{\lambda}{4}\left(H^\dagger H - \frac{v^2}{2}\right)^2 \,. \tag{1.9}$$

$\mathcal{L}_{Yukawa}$ contains the Yukawa couplings between the fermions and the Higgs field:

$$\mathcal{L}_{Yukawa} = g_u^{ij} \bar{u}_R^i H^T \epsilon Q_L^j - g_d^{ij} \bar{d}_R^i H^\dagger Q_L^j - g_e^{ij} \bar{e}_R^i H^\dagger L_L^j + h.c. \,, \tag{1.10}$$

where $\epsilon = \begin{pmatrix} 0 & 1 \\ -1 & 0 \end{pmatrix}$. Neutrinos are treated as massless. Upon spontaneously symmetry breaking, H acquires a non-zero vacuum expectation value, which at tree level can be taken as

$$\langle H \rangle = \begin{pmatrix} 0 \\ \frac{v}{\sqrt{2}} \end{pmatrix} \tag{1.11}$$

with $v > 0$. After spontaneous symmetry breaking, $SU(2)_W \times U(1)_Y$ is broken down to $U(1)_{EM}$, which has generator $Q = T^3 + Y$ and is identify with the local gauge group for electromagnetism. Expanded around the vacuum expectation value, the Higgs field is

$$H(x) = \begin{pmatrix} h^+(x) \\ \frac{v}{\sqrt{2}} + h^0(x) \end{pmatrix} \,. \tag{1.12}$$

h^+ and Im h^0, corresponding to the Goldstone bosons, can be eliminated by a local $SU(2)_W \times U(1)_Y$ gauge transformation. This defines the unitary gauge. Therefore, in unitary gauge, we have

$$H(x) = \begin{pmatrix} 0 \\ \frac{v}{\sqrt{2}} + \text{Re } h^0(x) \end{pmatrix} . \tag{1.13}$$

$h \equiv \sqrt{2}\text{Re } h^0$ is the Higgs Boson, which at tree level has mass $m_h = \sqrt{\frac{\lambda}{2}}v$. Three among the four gauge bosons for $SU(2)_W \times U(1)_Y$ acquire a mass. They are the $W^\pm$ and Z bosons, with masses at tree level given by

$$M_W = \frac{g_2 v}{2} , \qquad M_Z = \frac{M_W}{\cos\theta_W} , \tag{1.14}$$

where θ_W is the Weinberg angle defined by $\sin\theta_W = \frac{g_1}{\sqrt{g_1^2+g_2^2}}$. The electromagnetic potential $\mathcal{A}_\mu$ is massless. In terms of the $SU(2)_W \times U(1)_Y$ gauge fields, the mass eigenstates $W_\mu^\pm$, Z_μ, and $\mathcal{A}_\mu$ are

$$W_\mu^\pm = \frac{W_\mu^1 \mp i W_\mu^2}{\sqrt{2}} , \tag{1.15a}$$

$$Z_\mu = \cos\theta_W W_\mu^3 - \sin\theta_W B_\mu , \tag{1.15b}$$

$$\mathcal{A}_\mu = \sin\theta_W W_\mu^3 + \cos\theta_W B_\mu . \tag{1.15c}$$

The quarks and leptons acquire masses from the Higgs vacuum expectation value according to Eq. (1.10), with mass terms given by

$$\mathcal{L}_{fermion\,mass} = -M_u^{ij}\bar{u}^i u^j - M_d^{ij}\bar{d}^i d^j - M_e^{ij}\bar{e}^i e^j , \tag{1.16}$$

where the mass matrices are $M_u = \frac{v g_u}{\sqrt{2}}$, $M_d = \frac{v g_d}{\sqrt{2}}$, and $M_e = \frac{v g_e}{\sqrt{2}}$. It is always possible to diagonalize the mass matrices by unitary transformations on the family index i for the various fermion fields. In terms of the fermion mass eigenstates, for which we will use the same symbols u^i, d^i, e^i, and ν^i as the gauge eigenstates from now on, we have

$$\mathcal{L}_{Yukawa} = \sum_i \left[-m_u^i \left(1 + \frac{h}{v}\right) \bar{u}^i u^i - m_d^i \left(1 + \frac{h}{v}\right) \bar{d}^i d^i - m_e^i \left(1 + \frac{h}{v}\right) \bar{e}^i e^i \right] . \tag{1.17}$$

Other terms in the full Lagrangian are not changed by the mass diagonalization, except for the quark charged current interactions with $W^{\pm}$, for which the change is

$$\frac{g_2}{\sqrt{2}} W^+_\mu \bar{u}^i_L \gamma^\mu d^i_L \to \frac{g_2}{\sqrt{2}} W^+_\mu \bar{u}^i_L \gamma^\mu V^{ij} d^j_L \,. \tag{1.18}$$

V is called the Cabibbo-Kobayashi-Maskawa (CKM) matrix. It contains three angles and one CP-violating phase. Therefore, the total number of free parameters in the Standard Model is 3 (three gauge couplings) + 6 (quark masses) + 3 (charged lepton masses) + 1 (Higgs vev v) + 1 (Higgs mass) + 4 (CKM matrix) = 18. Table 2 lists the masses of all particles in the Standard Model. The magnitudes of the CKM matrix elements are [12]

$$\begin{pmatrix} |V_{ud}| & |V_{us}| & |V_{ub}| \\ |V_{cd}| & |V_{cs}| & |V_{cb}| \\ |V_{td}| & |V_{ts}| & |V_{tb}| \end{pmatrix} = \begin{pmatrix} 0.97427 \pm 0.00014 & 0.22536 \pm 0.00061 & 0.00355 \pm 0.00015 \\ 0.22522 \pm 0.00061 & 0.97343 \pm 0.00015 & 0.0414 \pm 0.0012 \\ 0.00886^{+0.00033}_{-0.00032} & 0.0405^{+0.0011}_{-0.0012} & 0.99914 \pm 0.00005 \end{pmatrix} . \tag{1.19}$$

1.2 PERTURBATIVE QCD

Quantum Chromdynamics (QCD) is the theory of strong interactions. It is the $SU(3)_c$ gauge theory in the Standard Model. The Lagrangian of QCD is given by

$$\mathcal{L} = -\frac{1}{4} G^{a\mu\nu} G^a_{\mu\nu} + \bar{\psi}_i (i \not{D}_{ij} - m\delta_{ij}) \psi_j \,, \tag{1.20}$$

where only one flavor of quark ψ is included for simplicity. Generalization to multiple quark flavors is trivial. i is the quark color index. $D^\mu_{ij} = \delta_{ij}\partial^\mu - igt^a_{ij}A^{a\mu}$ is the $SU(3)_c$ covariant derivative. t^a is the $SU(3)_c$ generators in the fundamental representation, renormalized to

$$\mathrm{tr}[t^a t^b] = T_F \delta^{ab} \,, \; T_F = \frac{1}{2} \,. \tag{1.21}$$

Table 2: Particle masses in the Standard Model [12]

Quark	Mass
u	$2.3^{+0.7}_{-0.5}$ MeV (current)
d	$4.8^{+0.5}_{-0.3}$ MeV (current)
c	$1.275^{+0.025}_{-0.025}$ GeV ($\overline{MS}$)
s	95^{+5}_{-5} MeV (current)
t	$176.7^{+4.0}_{-3.4}$ GeV (pole)
b	$4.18^{+0.03}_{-0.03}$ GeV ($\overline{MS}$)
e	$0.510998928 \pm 0.000000011$ MeV
μ	$105.6583715 \pm 0.0000035$ MeV
τ	1776.82 ± 0.16 MeV
ν	$\sum_{i=1}^{3} m_{\nu_i} < 0.176$ eV
$W^{\pm}$	80.385 ± 0.015 GeV
Z	91.1876 ± 0.0021 GeV
h	125.7 ± 0.4 GeV

The quadratic Casimir operators for the fundamental and adjoint representations are given respectively by

$$t^a t^a = C_F \mathbf{I}\,,\ C_F = \frac{N_c^2 - 1}{2N_c} = \frac{4}{3}\,; \tag{1.22}$$

$$f^{abc} f^{abd} = C_A \delta^{cd}\,,\ C_A = N_c = 3\,. \tag{1.23}$$

The Lagrangian Eq. (1.20) is invariant under the $SU(3)_c$ gauge transformation:

$$\begin{aligned} \psi_i &\to U_{ij}\psi_j\,, \\ A_\mu^a t^a &\to U A_\mu^a t^a U^\dagger + \frac{i}{g} U \partial_\mu U^\dagger\,, \end{aligned} \tag{1.24}$$

where $U(x) \in SU(3)_c$. To get a well-behaved tree level gluon propagator for perturbative calculations, one adopts the Faddeev-Popov procedure to fix the gauge. The resultant Lagrangian for covariant gauge is

$$\mathcal{L} = -\frac{1}{4} F^{a\mu\nu} F^a_{\mu\nu} - \frac{1}{2\xi}(\partial^\mu A^a_\mu)^2 + \partial^\mu \bar{c}^a D^{ac}_\mu c^c + \bar{\psi}_i (i \not{D}_{ij} - m\delta_{ij})\psi_j\,. \tag{1.25}$$

c^a is the ghost field, which tranforms as a $SU(3)_c$ adjoint representation. $D^{ac}_\mu = \delta^{ac}\partial_\mu + g f^{abc} A^b_\mu$ is the covariant derivative in the adjoint representation. The various Feynman rules resulting from Eq. (1.25) is given by Fig. 2.

High-order perturbative calculations necessarily require renormalization to remove UV-divergences. This leads to running of the fields, the mass and the coupling constant. Most striking is the running of the coupling constant g. Define $\alpha_s \equiv g^2/4\pi$. Renormalization to one loop yields [13]

$$Q^2 \frac{d\alpha_s(Q)}{dQ^2} \equiv \beta(\alpha_s) = -\frac{1}{4\pi}\left(11 - \frac{2}{3} n_f\right) \alpha_s^2(Q)\,, \tag{1.26}$$

where n_f is the number of quark flavors. Equation (1.26) has the solution

$$\alpha_s(Q) = \frac{12\pi}{(33 - 2n_f)\ln(Q^2/\Lambda^2_{QCD})}\,. \tag{1.27}$$

Equation (1.27) shows that α_s decreases as the energy scale Q increases for $n_f < 17$. This phenomenon is called asymptotic freedom. Λ_{QCD} is the scale at which α_s blows up to infinity in perturbation theory. It represents the energy scale below which perturbation theory fails.

Fitting to data yields $\Lambda_{QCD} \sim 200$ MeV. To date, running of α_s has been calculated to four loops. Figure (3) shows the fitting of the theoretical running of α_s to data.

It is believed that all physical particles are color singlets. This phenomenon is called color confinement. [1] Most hadrons are either a meson (bound colorless $q\bar{q}$ pair) or a baryon (colorless qqq bound state). When two hadrons collide in a high energy experiment, the partons (quarks and gluons) inside an initial-state hadron collide with those inside the other as if they were free particles. This is because the hard partonic collision happens on a time scale $\sim 1/\sqrt{s}$, $\sqrt{s}$ being the hadronic center-of-mass energy; while the quarks and gluons inside an initial-state hadron interact on a time scale $\sim 1/\Lambda_{QCD} \gg 1/\sqrt{s}$. The partons coming out from the partonic collision will fragment into hadrons on a time scale $\sim 1/\Lambda_{QCD}$. Since the hard scale $\sqrt{s}$ and the hadronic scale Λ_{QCD} are widely separated, one expects the cross section to factorize. For instance, the cross section to produce a Higgs boson h at the LHC is schematically given by

$$\begin{aligned} d\sigma(p+p \to h+X) &= \sum_{i,j} \int dx_1 \int dx_2 \, f_{i/p}(x_1,\mu) f_{j/p}(x_2,\mu) d\hat{\sigma}(ij \to h+X,\mu) \\ &= \sum_{i,j} f_{i/p} \otimes f_{j/p} \otimes d\hat{\sigma}(ij \to h+X) \,. \end{aligned} \tag{1.28}$$

The parton distribution function (PDF) $f_{i/p}(x,\mu)$ describes the probability distribution for parton i in a proton to have momentum fraction x at scale μ. $d\hat{\sigma}$ is the hard partonic cross section. Similarly, to produce a specific hadron H, we have

$$\begin{aligned} d\sigma(p+p \to H+X) &= \sum_{i,j,k} \int dx_1 \int dx_2 \int dz \, f_{i/p}(x_1,\mu) f_{j/p}(x_2,\mu) d\hat{\sigma}(ij \to k+X,\mu) D_{H/k}(z,\mu) \\ &= \sum_{i,j,k} f_{i/p} \otimes f_{j/p} \otimes d\hat{\sigma}(ij \to k+X) \otimes D_{H/k} \,. \end{aligned} \tag{1.29}$$

where the fragmentation function $D_{H/k}(z,\mu)$ describes the probability distribution for parton k to fragment into hadron H with momentum fraction z at scale μ. Since the parton distribution functions and the fragmentation functions encode the long-distance physics, they are intrinsically non-perturbative. They are determined by fitting to various experimental

[1] To date, there is no rigorous theoretical proof for color confinement. However, there are several clues hinting at it. For example, one can derive an attractive linear potential between a quark-antiquark pair in the large coupling limit using lattice QCD.

data. Some other non-perturbative elements, typically those involving heavy quarks, can be calculated by lattice QCD, a method in which path integrals are numerically calculated in a discretized spacetime. Factorization of QCD cross sections are the basic assumption and tool for every cross section calculation for hadronic collisions. Factorization primarily works for the so called "leading twist" contribution, which is the contribution at leading power of $\Lambda_{QCD}/\sqrt{s}$ [14]. Although rigorous proof of factorization at leading twist exists only for a handful of processes, for most processes one can show by direct perturbative calculations that factorization does work for the first few orders in α_s at leading twist.

Nowadays, perturbative QCD has entered the precision era. Theoretical errors of next-to-next-to-leading-order (NNLO) QCD predictions are typically only a few percent [15]. A handful of processes have been calculated even to N^3LO [16]. In addition, effective field theories of QCD are applied to resum large logarithms in processes with widely separated scales.

1.3 EFFECTIVE FIELD THEORY

Effective field theory is a powerful tool to handle problems with widely separated scales. The best way to understand the idea of effective field theory is through the Wilsonian approach. Consider a scalar field theory with action

$$S(\Lambda) = \int d^4x \left[\frac{1}{2}(\partial\phi)^2 + \sum_j g_j \phi^j \right] , \tag{1.30}$$

which is used with a cutoff Λ when evaluating a path integral. Let $\Lambda' < \Lambda$. One can write ϕ as a sum of low-energy modes ϕ_l and high-energy modes ϕ_h:

$$\phi = \phi_l + \phi_h \, . \tag{1.31}$$

ϕ_l contains modes with Euclidean momentum $|k| \leq \Lambda'$ while ϕ_h contains modes with $\Lambda' < |k| \leq \Lambda$. The n-point function of the low energy modes ϕ_l is given by

$$\begin{aligned}
&= \langle T\left[\phi_l(x_1)\cdots\phi_l(x_n)\right]\rangle_{S(\Lambda)} \\
&= \int\limits_{|k|\leq\Lambda} \mathcal{D}\phi\, \phi_l(x_1)\cdots\phi_l(x_n) e^{iS(\Lambda)} \\
&= \int\limits_{|k|\leq\Lambda'} \mathcal{D}\phi \int\limits_{\Lambda'<|k|\leq\Lambda} \mathcal{D}\phi\, \phi_l(x_1)\cdots\phi_l(x_n) e^{iS(\Lambda)} \\
&= \int\limits_{|k|\leq\Lambda'} \mathcal{D}\phi\, \phi_l(x_1)\cdots\phi_l(x_n) \int\limits_{\Lambda'<|k|\leq\Lambda} \mathcal{D}\phi\, e^{iS(\Lambda)} \\
&= \int\limits_{|k|\leq\Lambda'} \mathcal{D}\phi\, \phi_l(x_1)\cdots\phi_l(x_n) e^{iS(\Lambda')} \\
&= \langle T\left[\phi_l(x_1)\cdots\phi_l(x_n)\right]\rangle_{S(\Lambda')} \, ,
\end{aligned} \tag{1.32}$$

where

$$S(\Lambda') = -i \ln \int\limits_{\Lambda'<|k|\leq\Lambda} \mathcal{D}\phi\, e^{iS(\Lambda)} \, . \tag{1.33}$$

Equation (1.33) defines $S(\Lambda)$ for any Λ. Now consider the n-point function for ϕ,

$$G(x_i, g_j(\Lambda), \Lambda) \equiv \langle T\left[\phi(x_1)\cdots\phi(x_n)\right]\rangle_{S(\Lambda)} \, . \tag{1.34}$$

We want to relate the low energy physics to the high energy physics. To do so, we first define a simple scaling by

$$x = bx' \,, \;\; \phi(x) = b^{-1}\phi'(x') \,, \tag{1.35}$$

When $b > 1$. Then one immediately sees that

$$\begin{aligned} S[\phi] &= \int d^4x \left[(\partial'\phi'(x'))^2 + \sum_j b^{4-j} g_j \phi'^j(x') \right] \\ &\equiv S'[\phi'] \,. \end{aligned} \tag{1.36}$$

Therefore, we have

$$G(bx_i, g_j(\Lambda), \Lambda) = b^{-n} G(x_i, b^{4-j} g_j\,(\Lambda), b\Lambda) \;. \tag{1.37}$$

Next, we look at the running of $G(x_i, g_j(\Lambda), \Lambda)$ with respect to Λ. The renormalized n-point function G is related to the bare n-point function $G^{(0)}$ by $G^{(0)} = Z_G G$, with $G^{(0)} = G^{(0)}(x_i, g_j^{(0)})$ being independent of Λ. Differentiating this relation with respect to Λ one gets

$$\Lambda \frac{d}{d\Lambda} G = -\gamma_G G \tag{1.38}$$

with $\gamma_G = \frac{\Lambda}{Z_G}\frac{dZ_G}{d\Lambda}$. Equation (1.38) is the renormalization group equation (RGE). Its solution is

$$G(x_i, g_j(\Lambda), \Lambda) = e^{-\int_{\Lambda'}^{\Lambda} \gamma_G \, d\ln\Lambda} G(x_i, g_j(\Lambda'), \Lambda') \,. \tag{1.39}$$

It should also be noted that, $\frac{d}{d\Lambda} = \Lambda\frac{\partial}{\partial\Lambda} + \sum_j \beta_j \frac{\partial}{\partial g_j}$, with $\beta_j = \Lambda \frac{dg_j(\Lambda)}{d\Lambda}$ being the beta function for the coupling g_j. Applying first Eq. (1.38) and then (1.37), we have

$$\begin{aligned} G(bx_i, g_j(\Lambda), \Lambda) &= e^{-\int_{\Lambda/b}^{\Lambda} \gamma_G \, d\ln\Lambda} G(bx_i, g_j(\Lambda/b), \Lambda/b) \\ &= b^{-n} e^{\int_{\Lambda}^{\Lambda/b} \gamma_G \, d\ln\Lambda} G(x_i, b^{4-j} g_j(\Lambda/b), \Lambda) \\ &= b^{-n} e^{\int_{\Lambda}^{\Lambda/b} \gamma_G \, d\ln\Lambda} G(x_i, b^{4-j} e^{\int_{\Lambda}^{\Lambda/b} \beta_j \, d\ln\Lambda} g_j(\Lambda), \Lambda) \end{aligned} \tag{1.40}$$

Equation (1.40) relate the low energy n-point function $G(bx_i, g_j(\Lambda), \Lambda)$ to the high energy one $G(x_i, b^{4-j} g_j(\Lambda/b), \Lambda)$, with both having the same cutoff Λ. On the right hand side, there is an overall scaling factor $b^{-n} e^{\int_{\Lambda}^{\Lambda/b} \gamma_G \, d\ln\Lambda}$. The factor b^{-n} is the canonical classical scaling factor solely due to the simple scaling Eq. (1.35). The factor $e^{\int_{\Lambda}^{\Lambda/b} \gamma_G \, d\ln\Lambda}$, due to the momentum

shell integration, is of quantum origin. For this reason γ_G is called the anomalous dimension of G. Similarly, b^{j-4} is the canonical scaling of g_j and β_j is the corresponding anomalous dimension. As far as only canonical scaling is concerned, in the low-energy limit $b \to \infty$, the coupling $b^{4-j} g_j$ in the action grows for $j < 4$, stays still for $j = 4$ and diminishes for $j > 4$. Accordingly, for any operator O in the Lagrangian, O is called relevant if its mass dimension $[O] < 4$, marginal if $[O] = 4$ and irrelvant if $[O] > 4$. The relevance of an operator at low energies can deviate from this conclusion from the naive canonical scaling if the anomalous dimension is taken into account.

Now consider a theory with action S_{full} with two particles of widely separated masses m and M, with $m \ll M$. This theory can be regarded as having a cutoff $\Lambda \sim M$. A typical low-energy observable would be of the form $\langle f|O_{full}|i\rangle$, where $|i\rangle$ and $|f\rangle$ are respectively certain initial and final states involving only the light particle. A perturbative calculation of the observable would typically contain large logarithms of the form $\ln^n(m/M)$, which can potentially spoil the convergence of the perturbative expanison. Let us go to an effective low-energy theory for which the cutoff is $\Lambda' \sim m$. In this theory the massive particle does not exist. It is "integrated out" in the language of Wilsonian momentum shell integration. This low-energy theory necessarily has a different action S_{eff} from S_{full}. Borrowing from the idea of operator product expansion, it is reasonable to assume that the operator O_{full} can be expanded in terms of a set of operators $\{O_i\}$ in the effective theory:

$$O_{full} = \sum_i C_i(\mu) O_i(\mu)\,, \tag{1.41}$$

where μ is some arbitrary factorization scale. Equation (1.41) represents a factorization of short-distance physics (encoded in C_i) and long-distance physics (encoded in O_i). In principle, one should include all possible O_i with the same quantum number as O_{full}. However, since $[C_i] = [O_{full}] - [O_i]$, C_i is suppressed by powers of $1/M$ if $[O_i] > [O_{full}]$. One can therefore keep only operators up to some mass dimension on the right hand side of Eq. (1.41), with neglected terms suppressed by powers of m/M. The Wilson coefficients C_i can be calculated by matching, that is, sandwiching Eq. (1.41) between any two states $|a\rangle$ and $|b\rangle$ involving the light particle only:

$$\langle a|O_{full}|b\rangle = \sum_i C_i(\mu) \langle a|O_i(\mu)|b\rangle\,, \tag{1.42}$$

where the left hand side is expanded as a power series in $1/M$ up to the highest power chosen for the right hand side. Note that in performing the matching Eq. (1.42), IR divergences may arise in both $\langle a|O_{full}|b\rangle$ and $\langle a|O_i(\mu)|b\rangle$. However, since the full theory and the effective theory agree in the IR, these divergences should cancel each other in the matching condition. The resultant $C_i(\mu)$ are free of IR divergence. Since O_i contains only the low-energy degrees of freedom, it has only one physical scale, namely m. $\langle f|O_i(\mu)|i\rangle$ would therefore contain $\ln^n(m/\mu)$. Since high-energy physics is contained in the Wilson coefficients $C_i(\mu)$, they would contain $\ln^n(M/\mu)$. Here comes the trick. One can use the renormalization group equations to run C_i and O_i to the common scale μ from a high scale $\sim M$ and a low scale $\sim m$ respectively, thus resumming the large logarithms. To be specific, differentiating $O_i^{(0)} = Z_{ij}(\mu)O_j(\mu)$ with respect to μ, we have the RGE

$$\mu\frac{d}{d\mu}O_j = -\gamma_{ji}O_i\,,\ \ \gamma_{ji} = Z^{-1}_{jk}\mu\frac{d}{d\mu}Z_{ki}\,. \tag{1.43}$$

Equation (1.43) has the solution

$$O_j(\mu) = P\exp\left(\int_{\mu'}^{\mu} -\gamma_{ji}\,d\ln\mu\right)O_i(\mu')\,, \tag{1.44}$$

where P denotes μ-ordering. On the other hand, differentiating Eq. (1.41) with respect to μ gives

$$\mu\frac{d}{d\mu}C_i = C_j\gamma_{ji}\,, \tag{1.45}$$

which has the solution

$$C_i(\mu) = C_j(\mu')P\exp\left(\int_{\mu}^{\mu'} -\gamma_{ji}\,d\ln\mu\right)\,. \tag{1.46}$$

Applying Eqs. (1.44) and (1.46) to Eq. (1.41) and running O_i and C_i from m and M respectively, we get

$$\langle f|O_{full}|i\rangle = C_i(M)P\exp\left(\int_{m}^{M} -\gamma_{ij}\,d\ln\mu\right)\langle f|O_j(m)|i\rangle\,. \tag{1.47}$$

In Eq. (1.47), neither $C_i(M)$ nor $\langle f|O_j(m)|i\rangle$ contains large logarithms. The running kernel $P\exp\left(\int_m^M -\gamma_{ij}\,d\ln\mu\right)$ resums the large logarithms $\ln^n(m/M)$.

The Wilsonian effective theory has the draw back that it requires a hard cutoff, which spoils gauge invariance in the case of gauge theories. Therefore, in practice, we use the approach of continuum effective theory, in which the cutoff is always taken as infinite. In a continuum effective theory, dimensional regularization is used. The effective theory differs from the full theory because a different field content is introduced explicitly in the effective theory. This approach has the advantage of preserving gauge invariance in all calculations. However, the drawback is that the decoupling of the heavy states has to be introduced by hand, instead of follows naturally from the RGE, as guaranteed by the decoupling theorem. In this thesis, we will only use continuum effective theory.

The low-energy effective theory should inherit all the symmetries of the full theory. In principle, all operators consistent with the symmetries of the full theory have to be introduced in the effective Lagrangian. Therefore, the effective Lagrangian typically contains infinitely many operators:

$$\mathcal{L}_{eff} = \sum_i g_i \mathcal{L}_i \,. \tag{1.48}$$

The coefficients g_i are obtained by matching physical amplitudes such as S-matrix elements calculated from the full theory and the effective theory respectively. Like the Wilson coefficients, g_i contains information of the high energy modes. Note that the mass dimension of g_i is $[g_i] = 4 - [\mathcal{L}_i]$. Therefore, operators with dimension greater than four have their corresponding coupling suppressed by powers of $1/M$. This is consistent with our previous discussion of canonical scaling. One can truncate the infinite series (1.48) and only keep operators up to some mass dimesion. The terms neglected will be suppressed by powers of m/M. In this way, one have an effective Lagrangian with finitely many terms. Apparently, operators kept with dimension greater than four would render the theory non-renormalizable, since loop diagrams involving those vertices require counterterms not in the Lagrangian. However, those counterterms are of a even higher mass dimension, which can be neglected up to errors suppressed by powers of m/M. In this sense, the effective theory is renormalizable and thus have full predictive power, up to power corrections.

As usual, one can use integration by parts to express certain terms in $\mathcal{L}_{eff}$ in terms of the others. Another way to remove redundant operators in the Lagrangian is through redefinitions of the fields which have the same 1-particle states and preserve the symmetries

of the theory. This second way leads to a handy theorem: one can apply the equations of motion derived from operators with dimension less than n to operators with dimension n without changing observables of the theory to all loop orders.

In principle, any quantum field theory can be regarded as an low-energy effective field theory of some full theory. For example, regarding the Standard Model as a low-energy effective theory, one can introduce operators with dimension higher than four to the Lagrangian. Phenomenological constraints on these higher dimensional operators can tell the validity of candidate full theories via the matching and running. For certain effective field theories, the matching conditions cannot be implemented perturbatively. An example is chiral perturbation theory, which is an effective theory for low energy $E \lesssim \Lambda_{QCD}$ scatterings of pions. In that case, one leaves the couplings in the effective Lagrangian as free parameters to be determined from experimental data. In this thesis, we will apply two effective theories of QCD for which matching can be performed perturbatively. The first is heavy quark effective theory (HQET), which describes hadrons with one heavy valence quark. The second is soft-collinear effective theory (SCET), which describes the interactions of soft and collinear quarks and gluons. SCET is particularly useful in describing energetic jets and observables in high energy experiments near phase space boundaries.

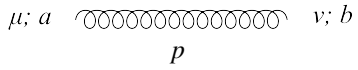

$$= \frac{i\left(-g^{\mu\nu} + (1-\xi)\frac{p^\mu p^\nu}{p^2}\right)}{(p^2 + i0^+)}\delta^{ab}\,,$$

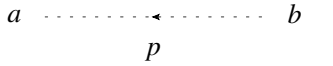

$$= \frac{i\delta^{ab}}{p^2 + i0^+}\,,$$

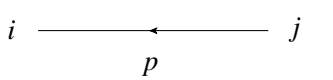

$$= \frac{i\delta^{ij}}{\not{p} - m + i0^+}\,,$$

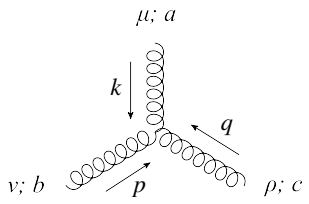

$$= g f^{abc}[g^{\mu\nu}(k-p)^\rho + g^{\nu\rho}(p-q)^\mu + g^{\rho\mu}(q-k)^\nu]\,,$$

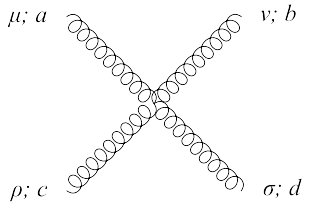

$$\begin{aligned} =& ig^2[f^{abe}f^{cde}(g^{\mu\rho}g^{\nu\sigma} - g^{\mu\sigma}g^{\nu\rho}) \\ &+ f^{ace}f^{bde}(g^{\mu\nu}g^{\rho\sigma} - g^{\mu\sigma}g^{\nu\rho}) \\ &+ f^{ade}f^{bce}(g^{\mu\nu}g^{\rho\sigma} - g^{\mu\rho}g^{\nu\sigma})]\,, \end{aligned}$$

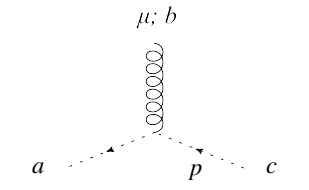

$$= -g f^{abc} p^\mu\,,$$

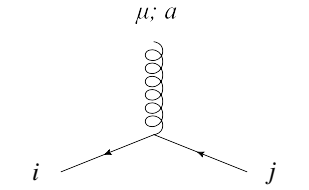

$$= ig\gamma^\mu t^a_{ij}\,.$$

Figure 2: Feynman rules of perturbative QCD in covariant gauge.

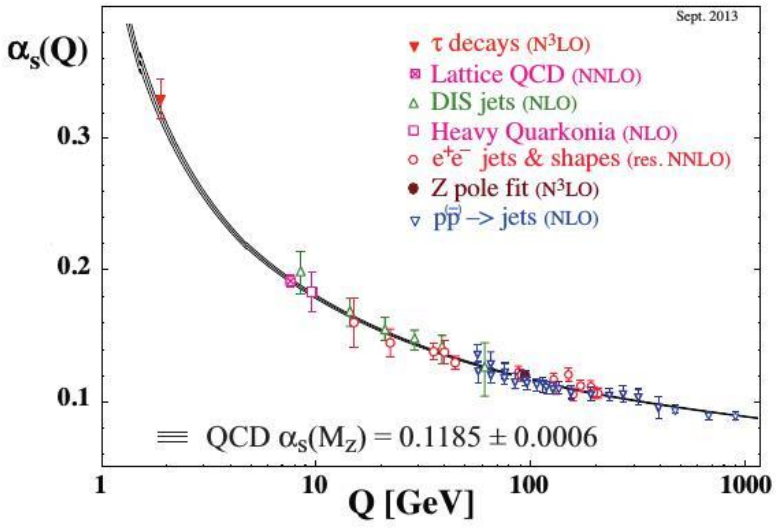

Figure 3: Running of $\alpha_s(Q)$ [12].

2.0 HEAVY QUARK EFFECTIVE THEORY (HQET)

Heavy quarks are quarks with masses $m_Q \gg \Lambda_{QCD} \sim 200$ MeV. In the Standard Model, these are the charm, the bottom and the top quarks. Inside a hadron with a single valence heavy quark, the light degrees of freedom (light quarks and gluons) interact with the heavy quark with momenta $\sim \Lambda_{QCD}$. As a result, the heavy quark is almost undisturbed. To study phenomena involving such heavy hadrons, one is led to consider the effective field theory in which the degrees of freedom are the light degrees of freedom together with a heavy quark with low virtuality [17]. This effective theory will help resum $\ln^n(\Lambda_{QCD}/M_Q)$ in observables. The effective theory also exhibits an extra symmetry, the heavy quark symmetry, at leading power in Λ_{QCD}/m_Q. This symmetry can be used to relate various non-perturbative parameters and simplifies phenomenological analyses.

2.1 HEAVY QUARK SYMMETRY

Consider the infinite mass limit $m_Q \to \infty$ of the heavy quarks. In this limit, as far as only strong interactions are concerned, all heavy quarks behave in the same way. This is the heavy quark flavor symmetry, $U(N_h)_f$, where N_h is the number of heavy quark flavors. In addition, since the spin-dependent interactions of a heavy quark with a gluon are proportional to the chromomagnetic moment $\sim \mathbf{S}_Q/m_Q$, the interactions is spin-independent in the infinite mass limit. This heavy quark spin symmetry combines with heavy quark flavor symmetry to form a larger group, the heavy quark symmetry $U(2N_h)$. Since the heavy quark spin $\mathbf{S}_Q$ is a good quantum number, the total angular momentum of the light degrees of freedom defined by $\mathbf{S}_l \equiv \mathbf{J} - \mathbf{S}_Q$ is also a good quantum number. To a fixed light valence quark content and

s_l, there corresponds a heavy quark symmetry $U(2N_h)$ multiplet, and a heavy quark spin symmetry multiplet for a fixed flavor of heavy quark. To appreciate how well the heavy quark symmetry approximates the real world, Table 3 shows the masses of the lowest-lying charm and bottom hadrons. From Table 3, one sees heavy quark spin symmetry works well. The approximate heavy quark flavor symmetry is manifest in the similarity of patterns of mass differences within a given light quark flavor $SU(3)$ multiplet for the charm and bottom quarks. The heavy quark symmetry provides a way to relates non-perturbative matrix elements involving heavy quarks, namely

$$\langle a|O|b\rangle = \langle a|U^\dagger O U|b\rangle \quad \text{for any } U \in U(2N_h)\,. \tag{2.1}$$

Deviations from heavy quark symmetry are of order Λ_{QCD}/m_Q. For the charm quark, $m_c = 1.275$ GeV and so $\Lambda_{QCD}/m_c \sim 0.2$. For the bottom quark, $m_b = 4.18$ GeV and so $\Lambda_{QCD}/m_b \sim 0.05$.

2.2 HQET LAGRANGIAN

The tree-level Lagrangian for HQET at leading power in Λ/m_Q can be obtained by matching to QCD at tree level. A heavy quark Q interacting with the light degrees of freedom inside a hadron has momentum given by

$$p = m_Q v + k\,. \tag{2.2}$$

The four-velocity v, with $v^2 = 1$, is chosen such that $p = m_Q v$ for an on shell heavy quark. So v has the power counting $v \sim 1$. k, representing the deviation from being on-shell, has the power counting $k \sim \Lambda_{QCD}$. At tree level, the heavy quark field $Q_v(x)$ in HQET is defined in terms of the heavy quark field $Q(x)$ in QCD by

$$Q(x) = e^{-im_Q v\cdot x}\left[Q_v(x) + \mathfrak{Q}_v(x)\right]\,, \tag{2.3}$$

where

$$Q_v(x) = e^{im_Q v\cdot x}\frac{1+\not{v}}{2}Q(x)\,,\ \ \mathfrak{Q}_v(x) = e^{im_Q v\cdot x}\frac{1-\not{v}}{2}Q(x)\,. \tag{2.4}$$

Table 3: The lowest-lying hadrons containing a c or b quark

Charm Hadron	Mass (MeV)	Quark Content	Bottom Hadron	Mass (MeV)	Quark Content	J^p	s_l
D^+	1869.61 ± 0.10	$c\bar{d}$	B^0	5279.58 ± 0.17	$b\bar{d}$	0^-	$1/2$
D^{*+}	2010.26 ± 0.07		B^{*0}	5325.2 ± 0.4		1^-	
D^0	1864.84 ± 0.07	$c\bar{u}$	B^-	5279.26 ± 0.17	$b\bar{u}$	0^-	$1/2$
D^{*0}	2006.96 ± 0.10		B^{*-}	5325.2 ± 0.4		1^-	
D_s^+	1968.30 ± 0.11	$c\bar{s}$	B_s^0	5366.7 ± 0.24	$b\bar{u}$	0^-	$1/2$
D_s^{*+}	2112.1 ± 0.4		B_s^{*0}	$5415.4^{+2.4}_{-2.1}$		1^-	
Λ_c^+	2286.46 ± 0.14	$c[ud]$	Λ_b^0	5619.5 ± 0.4	$b[ud]$	$1/2^+$	0
Ξ_c^+	$2467.8^{+0.4}_{-0.6}$	$c[us]$	Ξ_b^0	5793.1 ± 2.5	$b[us]$	$1/2^+$	0
Ξ_c^0	$2470.88^{+0.34}_{-0.80}$	$c[ds]$	Ξ_b^-	5794.9 ± 0.9	$b[ds]$	$1/2^+$	0
Σ_c^{++}	2453.98 ± 0.16	$c(uu)$	Σ_b^+	5811.3 ± 1.9	$b(uu)$	$1/2^+$	1
Σ_c^{*++}	2517.9 ± 0.6		Σ_b^{*+}	5832.1 ± 1.9		$3/2^+$	
Σ_c^+	2452.9 ± 0.4	$c(ud)$	Σ_b^0		$b(ud)$	$1/2^+$	1
Σ_c^{*+}	2517.5 ± 2.3		Σ_b^{*0}			$3/2^+$	
Σ_c^0	2453.74 ± 0.16	$c(dd)$	Σ_b^-	5815.5 ± 1.8	$b(dd)$	$1/2^+$	1
Σ_c^{*0}	2518.8 ± 0.6		Σ_b^{*-}	5835.1 ± 1.9		$3/2^+$	
$\Xi_c^{\prime+}$	2575.6 ± 3.1	$c(us)$	$\Xi_b^{\prime 0}$		$b(us)$	$1/2^+$	1
Ξ_c^{*+}	$2645.9^{+0.5}_{0.6}$		Ξ_b^{*0}	5949.3 ± 1.2		$3/2^+$	
$\Xi_c^{\prime 0}$	2577.9 ± 2.9	$c(ds)$	$\Xi_b^{\prime -}$		$b(ds)$	$1/2^+$	1
Ξ_c^{*0}	2645.9 ± 0.5		Ξ_b^{*-}			$3/2^+$	
Ω_c^0	2695.2 ± 1.7	$c(ss)$	Ω_b^-	6048.8 ± 3.2	$b(ss)$	$1/2^+$	1
Ω_c^{*0}	2765.9 ± 2.0		Ω_b^{*-}			$3/2^+$	

Heavy quark spin symmetry multiplets are separated by single horizontal lines. Light quark flavor $SU(3)$ multiplets are separated by double horizontal lines. ( ) and [ ] stand for symmetrization and anti-symmetrization respectively.

The projector operators $\frac{1+\not{v}}{2}$ and $\frac{1-\not{v}}{2}$ project out the particle and anti-particle components respectively. This can be easily seen by going to the rest frame of v, in which case $\frac{1+\not{v}}{2} = \frac{1+\gamma^0}{2} = \begin{pmatrix} 1 & 0 \\ 0 & 0 \end{pmatrix}$ and $\frac{1-\not{v}}{2} = \frac{1-\gamma^0}{2} = \begin{pmatrix} 0 & 0 \\ 0 & 1 \end{pmatrix}$ in the Pauli-Dirac basis. The two projectors satisfy $\left(\frac{1+\not{v}}{2}\right)^2 = \left(\frac{1-\not{v}}{2}\right)^2 = 1$ and $\left(\frac{1+\not{v}}{2}\right)\left(\frac{1-\not{v}}{2}\right) = 0$. Therefore,

$$\left(\frac{1+\not{v}}{2}\right) Q_v = Q_v = \not{v} Q_v \,. \tag{2.5}$$

Q_v is a leading degree of freedom in the effective theory, while $\mathfrak{Q}_v$ is suppressed by Λ_{QCD}/m_Q. Therefore, at leading power in Λ_{QCD}/m_Q, $\mathfrak{Q}_v$ can be simply neglected. Dropping $\mathfrak{Q}_v$ and substituting Eq. (2.3) into the QCD heavy quark Lagrangian $\bar{Q}\left(i\not{D} - m_Q\right) Q$ gives $\bar{Q}_v i\not{D} Q_v$, which upon insertion of $\frac{1+\not{v}}{2}$ on both sides of $\not{D}$ yields

$$\mathcal{L} = \bar{Q}_v iv \cdot D Q_v \,. \tag{2.6}$$

To check that the matching to QCD works for all tree-level amplitudes, one simply needs to check whether the propagator and vertex in QCD reduces to those derived from Eq. (2.6) in the heavy quark limit $m_Q \to \infty$. [1] In the heavy quark limit, the quark propagator in QCD becomes

$$\frac{i(\not{p} + m_Q)}{p^2 - m_Q^2 + i0^+} = \frac{i(m_Q \not{v} + m_Q + \not{k})}{2m_Q v \cdot k + k^2 + i0^+} \to \left(\frac{1+\not{v}}{2}\right) \frac{i}{v \cdot k + i0^+} \,, \tag{2.7}$$

which coincides with the propagator derived from Eq. (2.6). The heavy-quark-gluon vertex in QCD is $igt^a\gamma^\mu$. This vertex is always sandwiched between two heavy-quark propagator, which as we have just showed is proportional to $\left(\frac{1+\not{v}}{2}\right)$ in the heavy quark limit. Therefore, in the vertex one can replace γ^μ by

$$\gamma^\mu \to \left(\frac{1+\not{v}}{2}\right) \gamma^\mu \left(\frac{1+\not{v}}{2}\right) = v^\mu \left(\frac{1+\not{v}}{2}\right) \to v^\mu \,. \tag{2.8}$$

The heavy-quark-gluon vertex in QCD in the heavy quark limit is thus $igt^a v^\mu$, which is the same as the vertex derived from Eq. (2.6). Generalization of Eq. (2.6) to multiple heavy quark flavors is trivial:

$$\mathcal{L} = \sum_{i=1}^{N_h} \bar{Q}_v^{(i)} iv \cdot D Q_v^{(i)} \,. \tag{2.9}$$

[1] At loop level, in general, $\langle p|Q|0\rangle \neq \langle p|Q_v|0\rangle$ and so one has to take into account the LSZ external-leg factors in QCD and HQET respectively in the matching conditions.

The effective Lagrangian (2.9) is independent of the masses and spins of the heavy quarks, and so is manifestly invariant under the heavy quark symmetry $U(2N_h)$. That Eq. (2.9) is unchanged by loop-level matching can be seen from a simple symmetry argument: Equation (2.9) is the most general dimension-4 operator bilinear in Q_v which is consistent with Poincare symmetry, gauge symmetry and heavy quark symmetry. There is no simple relation between Q and Q_v beyond tree level. The relation $\not{v} Q_v = Q_v$ is treated as always valid by definition though.

Power corrections to Eq. (2.6) can be derived in a way similar to above. Keeping $\mathfrak{Q}_v$ and substituting Eq. (2.3) into the QCD Lagrangian one gets, by noting that $\not{v} Q_v = Q_v$ and $\not{v} \mathfrak{Q}_v = -\mathfrak{Q}_v$,

$$\mathcal{L} = \bar{Q}_v (iv \cdot D) Q_v - \bar{\mathfrak{Q}}_v (iv \cdot D + 2m_Q) \mathfrak{Q}_v + \bar{Q}_v i \not{D} \mathfrak{Q}_v + \bar{\mathfrak{Q}}_v i \not{D} Q_v \,. \tag{2.10}$$

Define the perpendicular component of any four vector w^μ by $w_\perp \equiv w^\mu - w \cdot v v^\mu$. Then $\not{D}$ in the last two terms of Eq. (2.10) can be replaced by $\not{D}_\perp$. One can perform a Gaussian integration in the path integral with respect to $\mathfrak{Q}_v$ to eliminate $\mathfrak{Q}_v$ in the Lagrangian. The resulting determinant factor corresponds to heavy-quark loops, which can be neglected at tree level. The overall tree-level effect of this Gaussian integration is thus replacing $\mathfrak{Q}_v$ in the Lagrangian (2.10) by the solution of its equation of motion

$$(iv \cdot D + 2m_q) \mathfrak{Q}_v = i \not{D}_\perp Q_v \,. \tag{2.11}$$

The result is

$$\begin{aligned} \mathcal{L} &= \bar{Q}_v \left(iv \cdot D + i \not{D}_\perp \frac{1}{2m_Q + iv \cdot D} i \not{D}_\perp \right) Q_v \\ &= \bar{Q}_v \left(iv \cdot D - \frac{1}{2m_Q} \not{D}_\perp \not{D}_\perp \right) Q_v + \mathcal{O}(1/m_Q^2) \,. \end{aligned} \tag{2.12}$$

Recalling that $[D_\mu, D_\nu] = -igG_{\mu\nu} = -igG^a_{\mu\nu} t^a$ and $\sigma_{\mu\nu} = \frac{i}{2}[\gamma_\mu, \gamma_\nu]$, we can write Eq. (2.12) as

$$\mathcal{L} = \mathcal{L}_0 + \mathcal{L}_1 + \mathcal{O}(1/m_Q^2) \,, \tag{2.13}$$

where $\mathcal{L}_0$ is the leading power Lagrangian $\mathcal{L}_0 = \bar{Q}_v iv \cdot DQ_v$ and $\mathcal{L}_1$ is the leading power correction $\sim 1/m_Q$ given by

$$\mathcal{L}_1 = -\bar{Q}_v \frac{D_\perp^2}{2m_Q} Q_v + g\bar{Q}_v \frac{\sigma_{\mu\nu} G^{\mu\nu}}{4m_Q} Q_v \,. \tag{2.14}$$

The first term in Eq. (2.14) gives the non-relativistic kinetic energy $\mathbf{p}_Q^2/2m_Q$. Although it breaks heavy quark flavor symmetry owing to the appearance of m_Q, heavy quark spin symmetry is preserved. The second term describes interactions of gluons with the chromo-magnetic moment of the heavy quark. It breaks both heavy quark flavor and spin symmetries.

It is useful to assign a power of the small parameter $\lambda = \Lambda_{QCD}/m_Q$ to the fields in order to estimate the size of various operators. Momenta in HQET scale as $p^\mu \sim \lambda m_Q$, so $x \sim 1/\lambda m_Q$. The leading power action $S^{(0)} = \int d^4x\, \bar{Q}_v iv \cdot DQ_v$ by definition scales as λ^0. This implies $Q_v \sim \lambda^{3/2}$. Since the gluon field A_μ always goes with the momentum in the covariant derivative $D_\mu = \partial_\mu - igA_\mu$ by gauge invariance, we have $A_\mu \sim \lambda$. Therefore, $\mathcal{L}_0$ and $\mathcal{L}_1$ scale as λ^4 and λ^5 respectively.

2.3 REPARAMETRIZATION INVARIANCE (RPI)

In HQET, the necessity to choose a specfic four-velocity v means that Lorentz invariance is violated. However, one should note that decomposition of the heavy quark momentum p into $m_Q v$ and k, $p = m_Q + k$, is not unique. Any deposition which preserves the power counting ($v \sim 1$, $k \sim \Lambda_{QCD}$) should be regarded as valid. Therefore, one can resume Lorentz symmetry partially by requiring the effective theory to be invariant under a change of v for which the power counting is preserved. Consider the transformation

$$\begin{aligned} v &\to v + \frac{\epsilon}{m_Q} \,, \\ k &\to k - \epsilon \,, \end{aligned} \tag{2.15}$$

where $\epsilon \sim \Lambda_{QCD}$ in order to preserve the power counting. ϵ is treated as infinitesimal and so is kept to linear order only in all equations. The requirement $v^2 = 1$ to $\mathcal{O}(\epsilon)$ gives

$$v \cdot \epsilon = 0 \,. \tag{2.16}$$

To preserve the relation $\not{v} Q_v = Q_v$, Q_v has to transform $Q_v \to Q_v + \delta Q_v$ in such a way that

$$\left(\not{v} + \frac{\not{\ell}}{m_Q}\right)(Q_v + \delta Q_v) = Q_v + \delta Q_v \,, \tag{2.17}$$

which to order $\mathcal{O}(\epsilon)$ implies

$$(1 - \not{v})\delta Q_v = \frac{\not{\ell}}{m_Q} Q_v \,. \tag{2.18}$$

A simple choice of δQ_v satisfying Eq. (2.18) is

$$\delta Q_v = \frac{\not{\ell}}{2m_Q} Q_v \,. \tag{2.19}$$

For this choice of δQ_v, the full reparametrization transformation is given by

$$\begin{aligned} v &\to v + \frac{\epsilon}{m_Q} \,, \\ Q_v &\to e^{i\epsilon\cdot x}\left(1 + \frac{\not{\ell}}{2m_Q}\right) Q_v \,, \end{aligned} \tag{2.20}$$

where the factor $e^{i\epsilon\cdot x}$ implements $k \to k - \epsilon$. The effective Lagrangian is required to be invariant under the transformation Eq. (2.20) to any order in $1/m_Q$. This is the reparametrization invariance (RPI). The reparametrization transformation (2.20) connects operators of different powers in $1/m_Q$. For instance, under the reparametrization transformation, the tree-level $\mathcal{L}_0$ and $\mathcal{L}_1$ transform as

$$\begin{aligned} \mathcal{L}_0 &\to \mathcal{L}_0 + \frac{1}{m_Q}\bar{Q}_v(i\epsilon\cdot D)Q_v + \mathcal{O}(1/m_Q^2) \,, \\ \mathcal{L}_1 &\to \mathcal{L}_1 - \frac{1}{m_Q}\bar{Q}_v(i\epsilon\cdot D)Q_v + \mathcal{O}(1/m_Q^2) \,. \end{aligned} \tag{2.21}$$

The term $-\frac{1}{m_Q}\bar{Q}_v(i\epsilon\cdot D)Q_v$ in the transformed $\mathcal{L}_1$ is solely from the transformation of the kinetic energy term $-\bar{Q}_v\frac{D_\perp^2}{2m_Q}Q_v$. Therefore, the coefficient of the kinetic energy term has to be unaltered by radiative corrections in order to preserve reparametrization invariance. The most general effective Lagrangian bilinear in Q_v and consistent with heavy quark symmetry at leading power, Poincare symmetry, gauge symmetry and reparametrization invariance for a single quark flavor is thus

$$\mathcal{L} = \bar{Q}_v iv\cdot D Q_v - \bar{Q}_v\frac{D_\perp^2}{2m_Q}Q_v + a(\mu)g\bar{Q}_v\frac{\sigma_{\mu\nu}G^{\mu\nu}}{4m_Q}Q_v + \mathcal{O}(1/m_Q^2) \,, \tag{2.22}$$

where $a(\mu)$ is obtained by matching to QCD. Since $a(\mu)$ encodes the short-distance physics, it has the property $a(m_Q) = 1 + \mathcal{O}(\alpha_s(m_Q))$, without any large logarithms at $\mu = m_Q$. Tree-level matching and 1-loop running gives [17]

$$a(\mu) = \left(\frac{\alpha_s(m_Q)}{\alpha_s(\mu)}\right)^{9/(33-2N_q)} , \tag{2.23}$$

where N_q is the number of light quark flavors.

Reparametrization invariance is often used to relate various Wilson coefficients in the expansions of QCD operators in terms of HQET operators. Specifically, for the expansion $O_{QCD} = \sum_i C_i O_i^{HQET}$, the right hand side has to be RPI-invariant since O_{QCD} is manifestly RPI-invariant. This imposes a constraint on the relative sizes of the Wilson coefficients C_i and would help in simplifying the matching precedure.

3.0 SOFT-COLLINEAR EFFECTIVE THEORY (SCET)

3.1 IR STRUCTURE OF PERTURBATIVE QCD

There are two reasons why QCD predictions are challenging in high energy experiments. The first is color confinement. It entails that asymptotic states are hadrons, which are different from the degrees of freedom that enter the hard scatterings, namely the quarks and gluons. The second is the sizable coupling constant at high energy. At $\mu \sim M_Z \sim 100$ GeV, $\alpha_s(M_Z) \sim 0.1$, which is still large compared to the fine structure constant $\alpha(M_z) \sim \alpha(0) \sim 0.01$. The first difficulty forces one to find proofs for factorization of cross sections into a perturbative and a non-perturbative part. The second difficulty concerns observables with widely-separated scales. For QCD with massless fermions, there are naturally two widely separated scales in any high energy collision. They are the initial-state center-of-mass energy $\sqrt{s}$ and the hadronic scale Λ_{QCD}. In the case of jets, the mass m_J of a jet is typically in the range $\Lambda_{QCD} \ll m_J \ll \sqrt{s}$, so that there are three widely separated scales. Observables with widely separated scales Λ and Λ' ($\Lambda' \ll \Lambda$) contain terms of the form $\alpha_s^m \ln^n(\Lambda/\Lambda')$ in their perturbative expansion. These logarithms could potentially spoil the convergence of the perturbative series. For example, for $\sqrt{s} = 1$ TeV amd $m_J = 10$ GeV, the Sudokov log term $\alpha_s \ln\left(\frac{\sqrt{s}}{m_J}\right) \ln\left(\frac{m_J}{\Lambda_{QCD}}\right) \sim 2$, which is not a small parameter to expand in.

Logarithms in perturbative quantum field theory are tied to infrared divergences. For instance, in a theory with a particle of mass m, the logarithm $\ln(Q/m)$ signals an IR divergence in the limit $m \to 0$. As discussed in Section 1.3, one can construct an effective field theory in the IR to resum logarithms. Therefore, in order to construct an effective field theory to resum logarithms in QCD, one has to determine the IR degrees of freedom in QCD which produce the IR divergences.

Singularities of Feynman diagrams can be located by the Landau equations and IR power counting [18][19]. The idea is as follows. In a general theory with massive particles, after Feynman parametrization, any 1PI diagram has the form

$$G(\{p_s\}) = \prod_{lines\, i} \int_0^1 d\alpha_i \, \delta\left(\sum_i \alpha_i - 1\right) \prod_{loops\, r} \int d^4 k_r \frac{F(k_r, p_s)}{[D(\alpha_i, k_r, p_s)]^N} \,, \tag{3.1}$$

where

$$D(\alpha_i, k_r, p_s) = \sum_j \alpha_j \left(l_j^2(p,k) - m_j^2\right) + i0^+ \,. \tag{3.2}$$

Here p_s are the external momenta, k_r the loop momenta, α_j the Feynman parameters and l_j the momentum of line j. Note that l_j is linear in k_r and p_s:

$$l_j = \sum_r \eta_{jr} k_r + \sum_s \hat{\eta}_{js} p_s \,. \tag{3.3}$$

Let ζ be one of the variables $\{k_i^\mu, \alpha_j\}$. Then $G(\{p_s\})$ is a multi-integral over all ζ's along some contours in the complex (k, α)-space. $G(\{p_s\})$ is singular at $\bar{p}_s$ only if, for every ζ on which D has depends, the ζ contours pass through some points $(\bar{k}, \bar{\alpha})$ such that $D(\bar{\alpha}_i, \bar{k}_r, p_s) = 0$ and the contours are unable to deform away from $(\bar{k}, \bar{\alpha})$ locally. These points $(\bar{k}, \bar{\alpha})$ form the so-called pinch surfaces in the (k, α)-space.

There are two ways for a ζ-contour to be trapped at $(\bar{k}, \bar{\alpha})$. If ζ is a momentum variable $\zeta = k_j^\nu$, i.e., the ν-th component of the loop momentum for loop j, then the ζ-contour is trapped at $(\bar{k}, \bar{\alpha})$ iff the contour is pinched between two infinitely close zeros of D. Dependence of D on ζ means $\alpha_m \neq 0$ for some line m in loop j, in which case $D(\bar{\alpha}_i, \bar{k}_r, p_s) = 0$ gives two poles. The condition of the two poles being degenerate is $\frac{\partial}{\partial k_j^\nu} D(\alpha_i, k_r, p_s)\big|_{(\bar{k}, \bar{\alpha})} = 0$, which gives

$$\sum_i \eta_{ij} \alpha_i l_i = 0 \,. \tag{3.4}$$

If $\zeta = \alpha_j$, a Feynman parameter, then D depends on ζ iff $l_j^2 \neq m_j^2$. The criteria $D(\bar{\alpha}_i, \bar{k}_r, p_s) = 0$ and that the ζ-contour is trapped are equivalent to $\bar{\alpha}_j = 0$. In summary, a set of points in (k, α)-space is a pinch surface if and only if the Landau equations are satisfied:

Landau equations:

I) For lines with $l_i^2 = m_i^2$, $\sum_i \eta_{ij} \alpha_i l_i = 0$ for every loop j including line i.

II) For lines with $l_i^2 \neq m_i^2$, $\alpha_i = 0$.

The Landau equations can be summarized by a simple physical picture as follows. Given a 1PI-diagram, shrink each off-shell line into a point, thus forming a reduced diagram. Treat the reduced diagram is a diagram in spacetime literally. Assign a straight spacetime displacement vector $\Delta x_i = \alpha_i l_i$ for each on-shell line. Then the Landau equations are equivalent to requiring all loops in the spacetime diagram to close. A reduced diagram satisfying this criterion is called a physical spacetime diagram. It corresponds to the classical picture in which on-shell lines propagate for a proper time $\tau_i = m_i \alpha_i$ with definite momentum l_i while off-shell lines do not propagate at all. Figure (4) shows an example of the construction of a physical spacetime diagram. The totality of pinch surfaces for a 1PI diagram with a fixed set of external momenta $\{p_s\}$ can be determined by listing all possible physical spacetime diagrams. Note that the existence of pinch surfaces is only a necessary condition for singularity of $G(\{p_s\})$ at $\{p_s\}$. For a massless theory, like QCD with massless fermions, the integration measure and the numerator $F(k_r, p_s)$ in Eq. (3.1) may tame the singularities and render the integral finite at pinch surfaces. The rigorous analysis of singularities in massless theory involves counting powers of coordinates normal to the pinch surfaces in a neighborhood of the pinch surfaces in the integral Eq. (3.1). The details of this IR power counting will not concern us here. The lesson from the Landau equations is that singularities of 1PI diagrams come from degrees of freedom close to the mass shell. In massless theories, these are the soft ($k \sim 0$) and collinear ($k^2 \sim 0$, $k^0 \neq 0$) degrees of freedom. We will collectively call the singularities caused by the soft and collinear degrees of freedom IR singularities. Singularities in 1PI diagrams are branch points. They are the origin of the large logarithms. For non-1PI diagrams, there are additional mass pole singularities coming from lines connecting the 1PI components. These pole singularities do not give rise to large logarithms. They can be located by drawing physical spacetime diagrams though.

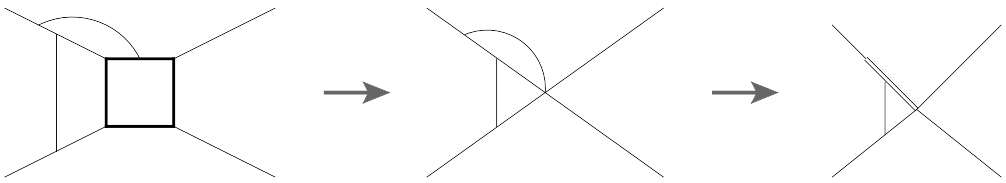

Figure 4: Contruction of a physical spacetime diagram. The bold lines are off-shell. They are shrunk to a point to form the reduced diagram. The remaining on-shell lines are drawn as straight lines to form the physical spacetime diagram.

3.2 SCET$_{\mathbf{I}}$ AND SCET$_{\mathbf{II}}$

In Section (3.1), we saw that the IR degrees of freedom for QCD wth massless fermions are the soft and collinear degrees of freedom. One is thus led to construct an effective field theory of QCD which contains exclusively these degrees of freedom. Soft-collinear effective theory is such an effective theory [20][21]. Collinear degrees of freedom are best described in terms of a pair of light-like vectors n and $\bar{n}$ which satisfy

$$n^2 = \bar{n}^2 = 0\,, \tag{3.5}$$

$$n \cdot \bar{n} = 2\,. \tag{3.6}$$

Any 4-momentum p^μ can be expanded in terms of n and $\bar{n}$ as

$$p^\mu = \frac{n^\mu}{2}\bar{n}\cdot p + \frac{\bar{n}^\mu}{2} n\cdot p + p_\perp^\mu \tag{3.7}$$

with

$$n \cdot p_\perp = \bar{n}\cdot p_\perp = 0\,, \tag{3.8}$$

so that we can write $p^\mu = (\bar{n}\cdot p, n\cdot p, p_\perp) \equiv (p^-, p^+, p_\perp)$. The invariant mass is given by

$$p^2 = (\bar{n}\cdot p)(n\cdot p) + p_\perp^2 = p^- p^+ + p_\perp^2\,. \tag{3.9}$$

SCET$_{\mathbf{I}}$

Consider the momenta $p^\mu = (p^-, p^+, p_\perp)$ of the collinear degrees of freedom within an energetic jet in the direction of n. The jet is produced from a hard collision at a scale Q. A jet

typically contains dozens of hadron, so the jet mass has a scale $\Delta \gg \Lambda_{QCD}$. On the other hand, a jet is well defined only when it is collimated, which means $\Delta \ll Q$. Since the energy of the jet is of order Q, we have $p^- \sim Q$. $p^2 = p^- p^+ + p_\perp^2 \sim \Delta^2$ implies $p^+ \sim \Delta^2/Q$ and $p_\perp \sim \Delta$. Therefore, the collinear momenta p_n scale as

$$p_n^\mu = (p_n^-, p_n^+, p_{n\perp}) \sim Q(1, \lambda^2, \lambda)\,, \tag{3.10}$$

where $\lambda = \Delta/Q \ll 1$ is a small parameter. To preserve the scaling Eq. (3.10) under interactions between the collinear and the soft modes, the momenta p_{us} of the soft modes should scale as

$$p_{us}^\mu = (p_{us}^-, p_{us}^+, p_{us\perp}) \sim Q(\lambda^2, \lambda^2, \lambda^2)\,. \tag{3.11}$$

We shall call modes with momentum scaling as Eq. (3.11) ultrasoft modes. The effective theory with power counting Eqs. (3.10) and (3.11) is called SCET_I. The locations of the collinear modes, the ultrasoft modes and the hard modes in momentum space are shown in Figure (5).

SCET_II

Consider a highly boosted hadron in the direction of n produced from a hard collision at a scale Q. The collinear degrees of freedom within the hadron have energy $\sim Q$. So their momenta have $p^- \sim Q$. They invariant masses should be of the order of the hadronic scale Λ_{QCD}, i.e., $p^2 = p^- p^+ + p_\perp^2 \sim \Lambda_{QCD}^2$. This gives the scaling

$$p_n^\mu = (p_n^-, p_n^+, p_{n\perp}) \sim Q(1, \lambda^2, \lambda)\,, \tag{3.12}$$

where $\lambda = \Lambda_{QCD}/Q \ll 1$ is a small parameter. The soft modes are naturally at the scale Λ_{QCD} and so have momenta scaling as

$$p_s^\mu = (p_s^-, p_s^+, p_{s\perp}) \sim Q(\lambda, \lambda, \lambda)\,. \tag{3.13}$$

We shall call modes with momentum scaling as Eq. (3.13) soft modes. The effective theory with power counting Eqs. (3.12) and (3.13) is called SCET_II. The locations of the collinear modes, the soft modes and the hard modes in momentum space are shown in Figure (6). SCET_II can be regarded as a low energy effective theory of SCET_I with modes of invariant

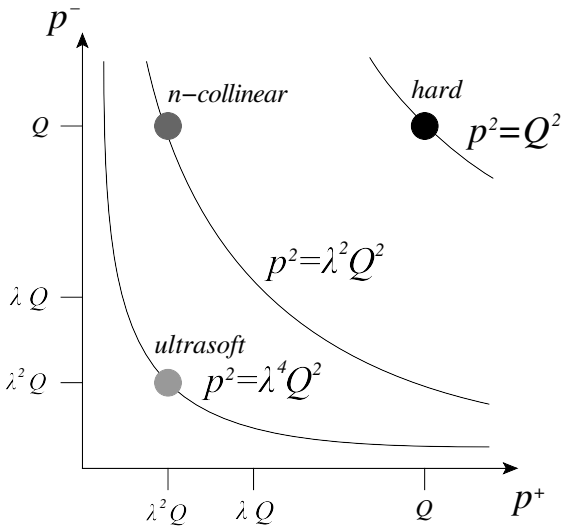

Figure 5: Modes in $\mathrm{SCET_I}$.

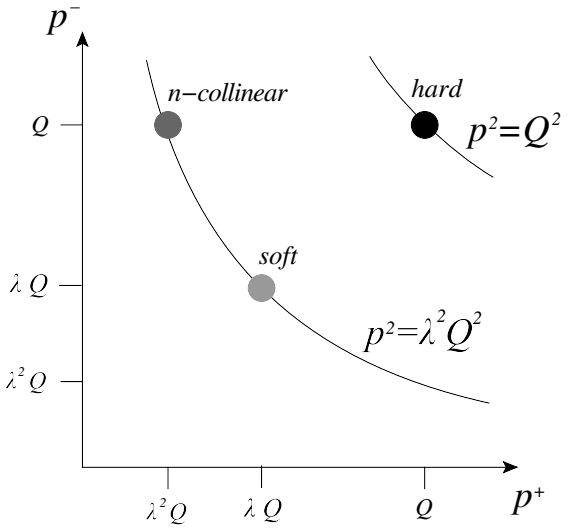

Figure 6: Modes in $\mathrm{SCET_{II}}$.

mass $p^2 \gtrsim \lambda Q^2$ integrated out.

3.3 POWER COUNTING

Before constructing the Lagrangian for SCET, it is necessary to assign a power of the small parameter λ to the various fields in the effective theory [22]. The power counting is non-trivial because the collinear modes are not only defined by the sizes of their invariant masses but also their locations on the invariant-mass hyperbolas (see Figs. 5 and 6). In addition, there are two widely separated invariant-mass shells in SCET_I.

As shown in Section 3.2, collinear momenta scale as $p_n^\mu = (p_n^-, p_n^+, p_{n\perp}) \sim (1, \lambda^2, \lambda)$. The collinear quark field ξ_n and its corresponding Lagrangian in SCET are by definition constructed to recover QCD in the collinear limit. The tree-level fermion propagator in QCD in the collinear limit is

$$\frac{i\not{p}}{p^2 + i0^+} \to \frac{i\not{n}\bar{n}\cdot p}{2(p^2 + i0^+)} = \frac{i\not{n}}{2} \frac{1}{\left(n\cdot p + \frac{p_\perp^2}{\bar{n}\cdot p} + i0^+ \text{sign}(\bar{n}\cdot p)\right)} \,. \tag{3.14}$$

Therefore, at leading power the tree-level collinear quark action in SCET has the form

$$S_{n\xi}^{(0)} = \int d^4x \bar{\xi}_n \frac{\bar{\not{n}}}{2} (in\cdot\partial + \cdots)\xi_n \,. \tag{3.15}$$

Note that $x = (x^-, x^+, x_\perp) \sim (\lambda^2, 1, \lambda)$ and $in\cdot D \sim \lambda^2$. The leading power action by definition scales as $\mathcal{L}^{(0)} \sim \lambda^0$. Therefore, Eq. (3.15) implies $\xi_n \sim \lambda$. A similar argument applied to the soft quark field q_s and the ultra soft quark field q_{us} gives $q_s \sim \lambda^{3/2}$ and $q_{us} \sim \lambda^3$ respectively. Note that the gluon field A^μ always goes with the momentum in the covariant derivative $D_\mu = \partial_\mu - igA_\mu$, as required by gauge invariance. Therefore, A^μ should scale like p^μ. As a result, we have $A_n^\mu \sim (1, \lambda^2, \lambda)$, $A_s^\mu \sim (\lambda, \lambda, \lambda)$ and $A_{us}^\mu \sim (\lambda^2, \lambda^2, \lambda^2)$. The power counting of various fields in SCET is listed in Table 4,

Table 4: Power counting in SCET

Type	$p^\mu = (p^-, p^+, p_\perp)$	Fields	Power Counting
Collinear	$p^\mu \sim (1, \lambda^2, \lambda)$	ξ_n	λ
		A_n^μ	$(1, \lambda^2, \lambda)$
Soft	$p^\mu \sim (\lambda, \lambda, \lambda)$	q_s	$\lambda^{3/2}$
		A_s^μ	$(\lambda, \lambda, \lambda)$
Ultrasoft	$p^\mu \sim (\lambda^2, \lambda^2, \lambda^2)$	q_{us}	λ^3
		A_{us}^μ	$(\lambda^2, \lambda^2, \lambda^2)$

3.4 SCET LAGRANGIAN

Like HQET, the tree-level SCET Lagrangian can be obtained by substituting in the QCD Lagrangian the tree-level relation between the fields in QCD and the EFT and eliminating power-suppressed modes by the equations of motion. We will focus on SCET_I. For collinear quarks in the n direction, we decompose the quark field ψ as

$$\psi(x) = \hat{\xi}_n(x) + \hat{\varphi}_{\bar{n}}(x)\,, \tag{3.16}$$

where

$$\hat{\xi}_n = \frac{\not{n}\bar{\not{n}}}{4}\psi\,,\ \ \hat{\varphi}_{\bar{n}}\frac{\bar{\not{n}}\not{n}}{4}\psi\,. \tag{3.17}$$

$\hat{\xi}$ is the large component in the collinear limit $p \propto n$. $\hat{\varphi}$ is power suppressed. Substituting Eq. (3.16) into the QCD Lagrangian for a massless fermion $\mathcal{L}_\psi = \bar{\psi} i \not{D} \psi$ gives

$$\mathcal{L}_{n\xi} = \bar{\hat{\xi}}_n \frac{\bar{\not{n}}}{2} in\cdot D \hat{\xi}_n + \bar{\hat{\varphi}}_{\bar{n}}\frac{\not{n}}{2} i\bar{n}\cdot D\hat{\varphi}_{\bar{n}} + \bar{\hat{\varphi}}_{\bar{n}} i\not{D}_\perp \hat{\xi}_n + \bar{\hat{\xi}}_n i\not{D}_\perp \hat{\varphi}_{\bar{n}}\,. \tag{3.18}$$

The equation of motion of $\hat{\varphi}_{\bar{n}}$ gives

$$\hat{\varphi}_{\bar{n}} = \frac{1}{i\bar{n}\cdot D} i\not{D}_\perp \frac{\bar{\not{n}}}{2}\hat{\xi}_n\,. \tag{3.19}$$

Substituted Eq. (3.19) back into Eq. (3.18) gives

$$\mathcal{L}_{n\xi} = \bar{\hat{\xi}}_n \frac{\bar{n}\!\!\!/}{2} \left(in\cdot D + i\not{D}_\perp \frac{1}{i\bar{n}\cdot D} i\not{D}_\perp \right) \hat{\xi}_n \,. \tag{3.20}$$

It is convenient to define fields in the effective theory in such a way that the large momentum components are factor out, so that x-dependence always refers to ultrasoft fluctuations. This procedure is called the multipole expanison. To do this, any momentum is decomposed as

$$p^\mu = p_l^\mu + p_r^\mu \,, \tag{3.21}$$

where $p_l^\mu = (p_l^-, p_l^+, p_l^\perp) \sim (1, 0, \lambda)$ are large, called the label momenta, and $p_r^\mu = (p_r^-, p_r^+, p_r^\perp) \sim (\lambda^2, \lambda^2, \lambda^2)$ are small, called the residual momenta. One can think of the momentum space as being divided into cells of linear size $\lambda^2 Q$. Any momentum p is described by the label momentum p_l which labels the cell to which p belongs and the residual momentum p_r which describes where p is within the cell. From this picture we have

$$\int d^4p = \sum_{p_l \neq 0} \int d^4p_r \;\; \text{for collinear modes} \,, \tag{3.22}$$

$$\int d^4p = \int d^4p_r \;\; \text{for ultrasoft modes} \,, \tag{3.23}$$

$$\int d^4x e^{i(p-q)\cdot x} = (2\pi)^4 \delta_{p_l,q_l} \delta^4(p_r - q_r) \,. \tag{3.24}$$

Consider the Fourier transform of $\hat{\xi}(x)$, $\hat{\xi}(p) = \int d^4x\, e^{ip\cdot x} \hat{\xi}(x)$. We can write $\hat{\xi}(p) = \xi_{n,p_l}(p_r)$. In position space, $\xi_{n,p_l}(x) = \int \frac{d^4p_r}{(2\pi)^4} e^{-ip_r\cdot x} \xi_{n,p_l}(p_r)$. Define $\xi_n(x)$ by

$$\xi_n(x) = \sum_{p_l \neq 0} \xi_{n,p_l}(x) \,. \tag{3.25}$$

Then $\hat{\xi}_n$ is related to ξ_n by

$$\begin{aligned}
\hat{\xi}_n(x) &= \int \frac{d^4p}{(2\pi)^4} e^{-ip\cdot x} \hat{\xi}_n(p) \\
&= \sum_{p_l \neq 0} \int \frac{d^4p_r}{(2\pi)^4} e^{-ip_l\cdot x} e^{-ip_r\cdot x} \xi_{n,p_l}(p_r) \\
&= \sum_{p_l \neq 0} e^{-ip_l\cdot x} \xi_{n,p_l}(x) \\
&= e^{-i\mathcal{P}\cdot x} \sum_{p_l \neq 0} \xi_{n,p_l}(x) \\
&= e^{-i\mathcal{P}\cdot x} \xi_n(x) \,,
\end{aligned} \tag{3.26}$$

where $\mathcal{P}$ is the label momentum operator. In terms of ξ_n, keeping only terms of order λ^0, the collinear Lagrangian Eq. (3.20) becomes

$$\mathcal{L}^{(0)}_{n\xi} = e^{-i\mathcal{P}\cdot x}\bar{\xi}_n \frac{\bar{n}\!\!\!/}{2}\left(in\cdot D + iD\!\!\!/_{n\perp}\frac{1}{i\bar{n}\cdot D_n}iD\!\!\!/_{n\perp}\right)\xi_n\,, \tag{3.27}$$

where

$$\begin{aligned} iD^\mu_{n\perp} &\equiv \mathcal{P}^\mu_\perp + gA^\mu_{n\perp}\,,\\ i\bar{n}\cdot D_n &\equiv \overline{\mathcal{P}} + g\bar{n}\cdot A_n\,. \end{aligned} \tag{3.28}$$

The Feynman rules to $\mathcal{O}(g)$ derived from $\mathcal{L}^{(0)}_{n\xi}$ are listed in Figure **??**. For the gluon modes, at tree level we have $A^\mu(x) = \hat{A}^\mu_n(x) + A^\mu_{us} + \mathcal{O}(\lambda^3)$. The multipole-expanded collinear gluon field A^μ_n is by defined by $\hat{A}^\mu_n(x) = e^{-i\mathcal{P}\cdot x}A^\mu_n(x)$. Recall that the gluon Lagrangian in QCD is

$$\mathcal{L}_g = -\frac{1}{2}\mathrm{tr}\left\{G^{\mu\nu}G_{\mu\nu}\right\} + \frac{1}{\tau}\mathrm{tr}\left\{\left[i\partial_\mu, A^\mu\right]^2\right\} + 2\mathrm{tr}\left\{\bar{c}[i\partial^\mu,[iD_\mu,c]]\right\}\,, \tag{3.29}$$

where $G_{\mu\nu} = \frac{i}{g}\left[D_\mu, D_\nu\right] = G^a_{\mu\nu}t^a$, $A_\mu = A^a_\mu t^a$, $c = c^a t^a$ and $D_\mu = \partial_\mu - igA_\mu$. The ultrasoft gluon field A^μ_{us} is a slowly varying field. It behaves like a classical background field from the perspective of the collinear fields. Therefore, in the collinear gluon Lagrangian, the gauge fixing term should be invariant under gauge transformation $U(x)$ with ultrasoft fluctuations $\partial_\mu U \sim Q(\lambda^2,\lambda^2,\lambda^2)$. This means replacing ∂_μ by

$$i\mathcal{D}^\mu_{us} \equiv \frac{n^\mu}{2}\overline{\mathcal{P}} + \mathcal{P}^\mu_\perp + \frac{\bar{n}^\mu}{2}\left(in\cdot\partial + gn\cdot A_{us}\right)\,. \tag{3.30}$$

In addition, one should replace D_μ by the covariant derivative to leading power in λ^0

$$i\mathcal{D}^\mu \equiv \frac{n^\mu}{2}\left(\overline{\mathcal{P}} + g\bar{n}\cdot A_n\right) + \mathcal{P}^\mu_\perp + gA^\mu_{n\perp} + \frac{\bar{n}^\mu}{2}\left(in\cdot\partial + gn\cdot A_n + gn\cdot A_{us}\right)\,. \tag{3.31}$$

The resulting leading-power Lagrangian for the collinear gluon field is

$$\mathcal{L}^{(0)}_{ng} = e^{-i\mathcal{P}\cdot x}\left\{\frac{1}{2g^2}\mathrm{tr}\left\{\left[i\mathcal{D}^\mu, i\mathcal{D}^\nu\right]^2\right\} + \frac{1}{\tau_n}\mathrm{tr}\left\{\left[i\mathcal{D}^\mu_{us}, A_{n\mu}\right]^2\right\} + 2\mathrm{tr}\left\{\bar{c}_n\left[i\mathcal{D}^\mu_{us},[i\mathcal{D}_\mu,c_n]\right]\right\}\right\}\,. \tag{3.32}$$

The Lagrangian for the ultrasoft modes is obtained by simply replacing ψ and A^μ by q_{us} and A^μ_{us} respectively in the QCD Lagrangian. So

$$\mathcal{L}^{(0)}_{us} = \bar{q}_{us} i \not{D}_{us} q_{us} - \frac{1}{2}\mathrm{tr}\left\{[iD^\mu_{us}, iD^\nu_{us}]^2\right\} + \frac{1}{\tau_{us}}\mathrm{tr}\left\{[i\partial_\mu, A^\mu_{us}]^2\right\} + 2\mathrm{tr}\left\{\bar{c}_{us}[i\partial_\mu, [iD^\mu_{us}, c_{us}]]\right\}\,, \tag{3.33}$$

where $iD^\mu_{us} \equiv i\partial^\mu + gA^\mu_{us}$. The gauge-fixing paramters τ_n and τ_{us} can be chosen to be different from each other, since there are two types of gauge symmetry, as will be shown in Section 3.5. The full leading-power Lagrangian in $\mathrm{SCET_I}$ with a single collinear sector at tree-level is given by

$$\mathcal{L}^{(0)} = \mathcal{L}^{(0)}_{n\xi} + \mathcal{L}^{(0)}_{ng} + \mathcal{L}^{(0)}_{us}\,. \tag{3.34}$$

Generalization to multiple collinear sectors is trivial:

$$\mathcal{L}^{(0)} = \sum_i \left[\mathcal{L}^{(0)}_{n_i\xi} + \mathcal{L}^{(0)}_{n_i g}\right] + \mathcal{L}^{(0)}_{us}\,, \tag{3.35}$$

where n_i is the light-like direction of the i-th collinear sector. For $i \neq j$, n_i and n_j have to satisfy $n_i \cdot n_j \gg \lambda^2$ in order to be well separated from each other.

3.5 GAUGE SYMMETRY

Gauge transformations in QCD might connect modes with momenta of different sizes. For instance, a slowly varying field $\psi(x)$ would turn into a fast varying field after a gauge transformation $\psi(x) \to U(x)\psi(x)$ if $U(x)$ is fast varying. Since the hard degrees of freedom are integrated out in SCET, the gauge transformations in SCET has to preserve the momentum scaling of various modes. Again we will focus on $\mathrm{SCET_I}$. There are two types of gauge transformations in $\mathrm{SCET_I}$ [21]. The first is the collinear gauge transformations $U_n(x)$, which satisfy

$$i\partial^\mu U_n \sim Q(\underset{-}{1}, \underset{+}{\lambda^2}, \underset{\perp}{\lambda})\,, \tag{3.36}$$

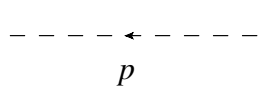

$$= i\frac{\not{\bar{n}}}{2}\frac{\bar{n}\cdot p_l}{\bar{n}\cdot p_l n\cdot p_r + p_{l\perp}^2 + i0}\,,$$

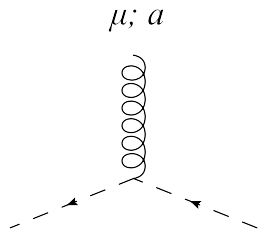

$$= igt^a n^\mu \frac{\not{\bar{n}}}{2}\,,$$

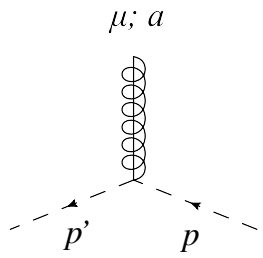

$$= igt^a\left[n^\mu + \frac{\gamma_\perp^\mu \not{p}_{l\perp}}{\bar{n}\cdot p_l} + \frac{\not{p}'_{l\perp}\gamma_\perp^\mu}{\bar{n}\cdot p'_l} - \frac{\not{p}'_{l\perp}\not{p}_{l\perp}}{\bar{n}\cdot p_l \bar{n}\cdot p'_l}\bar{n}^\mu\right]\frac{\not{\bar{n}}}{2}\,.$$

Figure 7: Feynman rules to $\mathcal{O}(g)$ derived from $\mathcal{L}_{n\xi}^{(0)}$ in $\mathrm{SCET_I}$. Collinear quarks are represented by dashed lines, ultrasoft gluons by curly lines and collinear gluons by curly lines with a central line.

i.e., $U_n(x)$ is a collinear field. In the spirit of multipole expansion, we can write $U_n(x) = \sum_{p_l\neq 0} U_{n,p_l}(x)$. Under a collinear gauge transformation, the various fields transform as

$$\begin{aligned}
&\xi_n \to U_n \xi_n\,,\\
&A_n^\mu \to U_n\left(A_n^\mu + \frac{i}{g}\mathcal{D}_{us}^\mu\right)U_n^\dagger\,,\\
&q_{us} \to q_{us}\,,\\
&A_{us}^\mu \to A_{us}^\mu\,.
\end{aligned} \tag{3.37}$$

The second type of gauge transformations is the ulrasoft gauge transformations $U_{us}(x)$, which satisfy

$$i\partial^\mu U_{us} \sim Q(\lambda_-^2, \lambda_+^2, \lambda_\perp^2)\,, \tag{3.38}$$

Under an ultrasoft gauge transformation, the various fields transform as

$$\begin{aligned}
\xi_n &\to U_{us}\xi_n\,, \\
A_n^\mu &\to U_{us}A_n^\mu U_{us}^\dagger\,, \\
q_{us} &\to U_{us}q_{us}\,, \\
A_{us}^\mu &\to U_{us}\left(A_{us}^\mu + \frac{i}{g}\partial^\mu\right)U_{us}^\dagger\,.
\end{aligned} \tag{3.39}$$

The gauge transformations (3.37) and (3.39) are consistent with the picture that ultrasoft fields are classical background fields from the perspective of the collinear fields. To avoid double counting, collinear gauge transformations at spacetime infinity is taken to be $U_n(\infty) = 1$, since $x \to \infty$ corresponds to the ultrasoft modes. The Lagrangian and operators in $\mathrm{SCET_I}$ are required to be invariant under the collinear and ultrasoft gauge transformations. For instance, the leading power Lagrangian (3.34) is invariant under these gauge transformations.

A useful tool which helps in constructing gauge-invariant operators in SCET is the collinear Wilson line

$$W_n(x,-\infty) = \mathrm{P}\exp\left(ig\int_{-\infty}^{0} ds\,\bar{n}\cdot A_n(x+\bar{n}s)\right)\,. \tag{3.40}$$

In momentum space, we have

$$W_n(\{q_i\}) = \sum_{k=0}^{\infty}\sum_{perms}\frac{(-g)^k}{k!}\left[\frac{\bar{n}\cdot A_n(q_1)\cdots\bar{n}\cdot A_n(q_k)}{(\bar{n}\cdot q_1)\cdots\left(\bar{n}\cdot\sum_{i=1}^{k}q_i\right)}\right] = \sum_{perms}\exp\left(\frac{-g}{\bar{n}\cdot\mathcal{P}}\bar{n}\cdot A_n\right)\,, \tag{3.41}$$

where the momenta q_i come to x from infinity. W_n is the solution to the differential equation

$$i\bar{n}\cdot D_n W_n = 0 \tag{3.42}$$

with $W_n(x=\infty) = 1$, where $\bar{n}\cdot D_n = \overline{\mathcal{P}} + g\bar{n}\cdot A_n$. Also, W_n satisfies $W_nW_n^\dagger = 1$. Therefore, for any operator $O(x)$, we have

$$i\bar{n}\cdot D_n\left(W_nO\right) = W_n\overline{\mathcal{P}}O\,, \tag{3.43}$$

which implies

$$\overline{\mathcal{P}} = W_n^\dagger i\bar{n}\cdot D_n W_n \tag{3.44}$$

and so $\frac{1}{in\cdot D_n} = W_n \frac{1}{in\cdot\partial} W_n^\dagger$. Substituting this into $\mathcal{L}_{n\xi}^{(0)}$ yields

$$\mathcal{L}_{n\xi}^{(0)} = e^{-i\mathcal{P}\cdot x}\bar{\xi}_n \frac{\bar{n}\!\!\!/}{2}\left(in\cdot D + i\not{D}_{n\perp} W_n \frac{1}{in\cdot\partial} W_n^\dagger i\not{D}_{n\perp}\right)\xi_n\,, \tag{3.45}$$

which is manifestly collinear gauge invariant, for under a collinear gauge transformation

$$\begin{aligned} W_n(x,-\infty) &\to U_n(x) W_n(x,-\infty) U_n^\dagger(-\infty) \\ &= U_n(x) W_n(x,-\infty) \end{aligned} \tag{3.46}$$

with $U_n(-\infty) = 1$ by definition.

3.6 REPARAMETRIZATION INVARIANCE

The choice of the pair of light-like vectors n and $\bar{n}$ satisfying $n\cdot\bar{n} = 2$ is not unique. Any choice which preserves the power counting $p_n \sim (1, \lambda^2, \lambda)$ is equally valid. Like HQET, the Lorentz symmetry in SCET is partially restored by imposing the reparametrization invariance [23]. There are three types of reparametrization transformations:

Type I	**Type II**	**Type III**
$n^\mu \to n^\mu + \Delta_\perp^\mu$	$n^\mu \to n^\mu$	$n^\mu \to (1+\alpha) n^\mu$
$\bar{n}^\mu \to \bar{n}^\mu$	$\bar{n}^\mu \to \bar{n}^\mu + \epsilon_\perp^\mu$	$\bar{n}^\mu \to (1-\alpha)\bar{n}^\mu$

(3.47)

where $\Delta_\perp^\mu$, $\epsilon_\perp^\mu$ and α are infinitesimal. $\Delta_\perp^\mu$ and $\epsilon_\perp^\mu$ satisfy $n\cdot\Delta_\perp = \bar{n}\cdot\Delta_\perp = n\cdot\epsilon_\perp = \bar{n}\cdot\epsilon_\perp = 0$. Preservation of the power counting $p_n \sim (1, \lambda^2, \lambda)$ implies $\Delta_\perp^\mu \sim \lambda$ and $\epsilon_\perp^\mu \sim \lambda^0$. $p_\perp^\mu$ has to transform $p_\perp^\mu \to p_\perp^\mu + \delta p_\perp^\mu$ in such a way to make p^μ invariant under the reparametrization. For instance, for Type-I transformations, we have

$$\begin{aligned} p^\mu &= \frac{n^\mu}{2}\bar{n}\cdot p + \frac{\bar{n}^\mu}{2} n\cdot p + p_\perp^\mu \\ &= \frac{n^\mu}{2}\bar{n}\cdot p + \frac{\bar{n}^\mu}{2} n\cdot p + p_\perp^\mu + \frac{\Delta_\perp^\mu}{2}\bar{n}\cdot p + \frac{\bar{n}}{2}\Delta_\perp\cdot p + \delta_I p_\perp^\mu\,, \end{aligned} \tag{3.48}$$

which means

$$p_\perp^\mu \to p_\perp^\mu - \frac{\Delta_\perp^\mu}{2}\bar{n}\cdot p - \frac{\bar{n}}{2}\Delta_\perp\cdot p\,. \tag{3.49}$$

Table 5: Reparametrization transformations in SCET

Type I	**Type II**	**Type III**
$n \to n + \Delta_\perp$	$n \to n$	$n \to n + \alpha n$
$\bar{n} \to \bar{n}$	$\bar{n} + \epsilon_\perp$	$\bar{n} \to \bar{n} - \alpha \bar{n}$
$n \cdot D \to n \cdot D + \Delta_\perp \cdot D_\perp$	$n \cdot D \to n \cdot D$	$n \cdot \to n \cdot D + \alpha n \cdot D$
$D_\perp^\mu \to D_\perp^\mu - \frac{\Delta_\perp^\mu}{2} \bar{n} \cdot D - \frac{\bar{n}^\mu}{2} \Delta_\perp \cdot D$	$D_\perp^\mu \to D_\perp^\mu - \frac{\epsilon_\perp^\mu}{2} n \cdot D - \frac{n^\mu}{2} \epsilon_\perp \cdot D$	$D_\perp^\mu \to D_\perp^\mu$
$\bar{n} \cdot D \to \bar{n} \cdot D$	$\bar{n} \cdot D \to \bar{n} \cdot D + \epsilon_\perp \cdot D_\perp$	$\bar{n} \cdot D \to \bar{n} \cdot D - \alpha \bar{n} \cdot D$
$\xi_n \to \left(1 + \frac{1}{4} \not{\Delta}_\perp \not{\bar{n}}\right) \xi_n$	$\xi_n \to \left(1 + \frac{1}{2} \not{\epsilon}_\perp \frac{1}{\bar{n} \cdot D} \not{D}_\perp\right) \xi_n$	$\xi \to \xi$
$W_n \to W_n$	$W_n \to \left[\left(1 - \frac{1}{\bar{n} \cdot D} \epsilon_\perp \cdot D_\perp\right) W_n\right]$	$W_n \to W_n$

The invariance of $\psi = Ce^{-i\mathcal{P}\cdot x}\left(1 + \frac{1}{\bar{n}\cdot D}\not{D}_\perp \frac{\not{\bar{n}}}{2}\right)\xi_n$ under the reparametrizations also forces ξ_n to transform accordingly. The transformations of various objects in SCET for Type-I, Type-II and Type III transformations are summarized in Table 5. It can be shown that the collinear quark Lagrangian $\mathcal{L}_{n\xi}^{(0)}$ Eq. (3.27) is the only possible dimension-4 operator bilinear in ξ_n which scales as λ^4 and is consistent with Poincare symmetry, gauge symmetry and reparametrization invariance [23]. Therefore, $\mathcal{L}_{n\xi}^{(0)}$ is unaltered by radiative corrections and thus is the true leading power collinear quark Lagrangian for SCET_I to all orders in α_s. Just as in HQET, reparametrization transformations relate operators of different powers. This would provide constraints on the Wilson coefficients in operator expansions.

3.7 ULTRASOFT-COLLINEAR FACTORIZATION

Apparently there are non-trivial couplings between the collinear and soft modes in the leading power Lagrangian $\mathcal{L}^{(0)}$ of SCET_I Eq. (3.34). A remarkable feature of SCET_I is that the collinear and soft modes decouple from each other after a redefinition of the collinear fields.

The details are as follows. First, define the soft Wilson line by

$$Y_n(x) = \mathrm{P}\exp\left(ig\int_{-\infty}^{0} ds n\cdot A_{us}(x+ns)\right). \tag{3.50}$$

In momentum space, we have

$$Y_n(\{q_i\}) = \sum_{k=0}^{\infty}\sum_{perms}\frac{(-g)^k}{k!}\left[\frac{n\cdot A_{us}(q_1)\cdots n\cdot A_{us}(q_k)}{(n\cdot q_1)\cdots\left(n\cdot\sum_{i=1}^{k} q_i\right)}\right], \tag{3.51}$$

where the momenta q_i come to x from infinity. Y_n satisfies

$$in\cdot D_{us} Y_n = 0 \tag{3.52}$$

and $Y_n Y_n^\dagger = 1$. Define new collinear fields by $\xi'_n(x)$ and $A'^{\mu}_n(x)$ by

$$\begin{aligned}
\xi_n &= Y_n(x)\xi'_n(x)\,,\\
A^\mu_n(x) &= Y_n(x)A'^{\mu}_n(x)Y_n^\dagger(x)\,,\\
c_n(x) &= Y_n(x)c'_n(x)Y_n^\dagger(x)\,.
\end{aligned} \tag{3.53}$$

Equation (3.53) is called the BPS field refinition [21]. The collinear Wilson line transforms accordingly as

$$W_n(x) = Y_n(x)W'_n(x)Y_n^\dagger(x)\,. \tag{3.54}$$

Note that for any operator $O(x)$, we have

$$in\cdot D_{us}\left(Y_n O\right) = Y_n in\cdot\partial O\,, \tag{3.55}$$

where $iD^\mu_{us} = i\partial^\mu + gA^\mu_{us}$. In terms of the newly defined fields, the collinear quark Lagrangian $\mathcal{L}^{(0)}_{n\xi}$ Eq. (3.45) becomes

$$\begin{aligned}
\mathcal{L}^{(0)}_{n\xi} &= e^{-i\mathcal{P}\cdot x}\bar\xi_n\frac{\bar n\!\!\!/}{2}\left(in\cdot D + i\not{D}_{n\perp}W_n\frac{1}{\overline{\mathcal{P}}}W_n^\dagger i\not{D}_{n\perp}\right)\xi_n\\
&= e^{-i\mathcal{P}\cdot x}\bar\xi'_n Y_n^\dagger\frac{\bar n\!\!\!/}{2}\left(in\cdot D_{us} + gn\cdot Y_n A'_n Y_n^\dagger + iY_n\not{D}'_{n\perp}Y_n^\dagger Y_n W'_n Y_n^\dagger\frac{1}{\overline{\mathcal{P}}}Y_n W'^{\dagger}_n Y_n^\dagger Y_n i\not{D}'_{n\perp}Y_n^\dagger\right)Y_n\xi'_n\\
&= e^{-i\mathcal{P}\cdot x}\bar\xi'_n\frac{\bar n\!\!\!/}{2}\left(in\cdot\partial + gn\cdot A'_n + i\not{D}'_{n\perp}W'_n\frac{1}{\overline{\mathcal{P}}}W'^{\dagger}_n i\not{D}'_{n\perp}\right)\xi'_n\\
&= e^{-i\mathcal{P}\cdot x}\bar\xi'_n\frac{\bar n\!\!\!/}{2}\left(in\cdot D'_n + i\not{D}'_{n\perp}W'_n\frac{1}{\overline{\mathcal{P}}}W'^{\dagger}_n i\not{D}'_{n\perp}\right)\xi'_n\,,
\end{aligned} \tag{3.56}$$

where

$$
\begin{aligned}
i\bar{n}\cdot D'_n &\equiv \overline{\mathcal{P}} + g\bar{n}\cdot A'_n = Y_n^\dagger i\bar{n}\cdot D_n Y_n\,,\\
iD'^{\mu}_{n\perp} &\equiv \mathcal{P}^\mu_\perp + gA'^{\mu}_{n\perp} = Y_n^\dagger iD^\mu_{n\perp} Y_n\,,\\
in\cdot D'_n &\equiv in\cdot\partial + gn\cdot A'_n = Y_n^\dagger in\cdot DY_n\,.
\end{aligned}
\tag{3.57}
$$

Therefore, we have

$$
\mathcal{L}^{(0)}_{n\xi}(\xi_n, A_n, n\cdot A_{us}) = \mathcal{L}^{(0)}_{n\xi}(\xi'_n, A'_n, 0)\,,
\tag{3.58}
$$

which does not contain A_{us}. By a similar manipulation, it can be shown that for the collinear gluon Lagrangian we also have

$$
\mathcal{L}^{(0)}_{ng}(\xi_n, A_n, n\cdot A_{us}) = \mathcal{L}^{(0)}_{ng}(\xi'_n, A'_n, 0)\,,
\tag{3.59}
$$

that is

$$
\mathcal{L}^{(0)}_{ng} = e^{-i\mathcal{P}\cdot x}\left\{\frac{1}{2g^2}\mathrm{tr}\left\{\left[i\mathcal{D}'^{\mu}, i\mathcal{D}'^{\nu}\right]^2\right\} + \frac{1}{\tau_n}\mathrm{tr}\left\{\left[i\mathcal{D}'^{\mu}_{us}, A'_{n\mu}\right]^2\right\} + 2\mathrm{tr}\left\{\bar{c}'_n\left[i\mathcal{D}'^{\mu}_{us}, \left[i\mathcal{D}'_\mu, c'_n\right]\right]\right\}\right\}\,,
\tag{3.60}
$$

where

$$
\begin{aligned}
i\mathcal{D}'^{\mu} &\equiv \frac{n^\mu}{2}\left(\overline{\mathcal{P}} + g\bar{n}\cdot A'_n\right) + \mathcal{P}^\mu_\perp + gA'^{\mu}_{n\perp} + \frac{\bar{n}^\mu}{2}\left(in\cdot\partial + gn\cdot A'_n\right) = Y_n^\dagger i\mathcal{D}'^{\mu} Y_n\,,\\
i\mathcal{D}'^{\mu}_{us} &\equiv \frac{n^\mu}{2}\overline{\mathcal{P}} + \mathcal{P}^\mu_\perp + \frac{\bar{n}^\mu}{2} in\cdot\partial\,.
\end{aligned}
\tag{3.61}
$$

That the ultrasoft and collinear modes decouple at the Lagrangian level implies that the decoupling is valid to all orders in α_s.

4.0 HEAVY HADRON PRODUCTION ASYMMETRIES

4.1 INTRODUCTION

Observation and proper interpretation of CP violation in heavy hadron system could provide an outstanding opportunity for indirect searches for physics beyond the standard model. Even already available bounds on CP-violating interactions provide rather stringent constraints on the models of new physics because of availability of large statistical samples of charm and bottom data from the LHCb, Belle, and BaBar experiments. Larger samples will be available soon from both pp and e^+e^- machines [24].

One of the simplest signals for CP violation in heavy hadron systems is obtained by comparing partial decay widths of heavy hadrons H to those of anti-heavy hadron $\overline{H}$. While CPT symmetry requires the total widths of H and $\overline{H}$ to be the same, the partial decay widths $\Gamma(H \to f)$ and $\Gamma(\overline{H} \to \overline{f})$ are different in the presence of CP violation, which is signaled by a nonzero value of the asymmetry

$$a_{CP}^{f} = \frac{\Gamma(H \to f) - \Gamma(\overline{H} \to \overline{f})}{\Gamma(H \to f) + \Gamma(\overline{H} \to \overline{f})} \,. \tag{4.1}$$

This signal is reasonably robust for D^+/D^- mesons, provided that the number of decaying particles and antiparticles is the same. However, at the Large Hadron Collider (LHC), the number of produced D^+ and D^- mesons might not be the same due to the fact that the initial state contains two protons. With CP-violating asymmetries expected to be at the per mille levels [25], it is important to examine the production asymmetry of D mesons both experimentally and theoretically. Indeed, fixed-target experiments have already observed large asymmetries of charmed mesons and baryons in the forward region. In hadroproduction, the charmed hadrons are preferentially produced with a light valence quark of the same type

as what appears in the hadronic beam, for example [26]. This has been termed the "leading particle effect". More recently, a similar asymmetry in $D^{\pm}$ production, defined as

$$A_p = \frac{d\sigma(D^+) - d\sigma(D^-)}{d\sigma(D^+) + d\sigma(D^-)}\,, \tag{4.2}$$

has been measured in the forward region to be $\sim -1\%$ by the LHCb Collaboration [11]. What are the theoretical expectations for this asymmetry?

Factorization theorems of perturbative QCD [27] state that heavy hadron production cross section can be written in a factorized form. At the LHC, the cross section for producing a D $(c\bar{q})$ meson in a pp collision, at leading order in a $1/p_T$ expansion, is given by

$$d\sigma[pp \to D + X] = \sum_{i,j} f_{i/p} \otimes f_{j/p} \otimes d\hat{\sigma}[ij \to c + X] \otimes D_{c\to D}\,, \tag{4.3}$$

where $f_{i/p}$ is the parton distribution function for parton i in the proton, $d\hat{\sigma}(ij \to c + X)$ is the partonic cross section and $D_{c\to D}$ is the fragmentation function describing hadronization of a c quark into a D meson. The corresponding equation for $\overline{D}$ is obtained by replacing c by $\bar{c}$ and D by $\overline{D}$. Owing to charge conjugation symmetry and that $f_{c/p} = f_{\bar{c}/p}$, perturbative QCD Eq. (4.3) predicts that $A_p = 0$, which is at least true at leading order in the $1/p_T$ expansion.

This conclusion led theorists to examine other mechanisms for generating the production asymmetry of Eq. (4.61), including attempts to describe the effect phenomenologically. The main idea of those approaches is to identify phenomenological mechanisms that can lead to enhanced production asymmetries, such as "meson cloud" effects. The results of these model-dependent calculations can be found in Refs. [28, 29]. We note that it might be challenging to interpret some of those mechanisms in QCD.

To reconcile the experimental observations with QCD, we note that there are corrections to Eq. (4.3) that scale as powers of $\Lambda_{\rm QCD}/m_c$ and $\Lambda_{\rm QCD}/p_T$. In principle, one can expect nonvanishing power-suppressed contributions to A_p at low p_T. A QCD-based model for these power corrections is the heavy quark recombination mechanism [30, 31, 32, 33]. In this scenario, a light quark involved in the hard scattering process combines with the heavy quark produced in that interaction to form the final state meson, leading to corrections of order $\Lambda_{\rm QCD} m_c/p_T^2$.

We apply the heavy quark recombination mechanism to explain the D^+/D^- production asymmetry data from LHCb. The heavy quark recombination mechanism is reviewed and developed in Section 4.2. Section 4.3 presents predictions of the heavy quark recombination mechanism in comparison with the D^+/D^- production asymmetry data from LHCb. Section 4.4 presents a rough prediction on the Λ_c^+/Λ_c^- and $\Lambda_b^0/\overline{\Lambda}_b^0$ production asymmetry at LHCb. Section 4.5 discusses possible improvements on predictions from the the heavy quark recombination mechanism, as well as other possible explanations of production asymmetries of heavy hadrons. Section 4.6 summarizes our results. Part of the work in this chapter was published in Refs. [34] and [35].

4.2 HEAVY QUARK RECOMBINATION MECHANISM

4.2.1 Hadronic Production of Heavy Mesons

Imagine production of a lowest lying charm meson with the light valence quark of the same flavor as that appears as a valence quark in the beam. For instance, for a proton beam we could have D^- or $\overline{D}^0$ states, which we shall generically call $\overline{D}$. The recombination process, shown in Fig. 8, comes in as a power-suppressed correction to Eq. (4.3). As mentioned, the light quark in the production of $\overline{D}$ comes from the incident proton. The contribution to the cross section at the parton level is given by

$$d\hat{\sigma}[\overline{D}] = \sum_n d\hat{\sigma}[qg \to (\bar{c}q)^n + c + X]\rho[(\bar{c}q)^n \to \overline{D}]\,, \tag{4.4}$$

where $(\bar{c}q)^n$ indicates that the light quark of flavor q with momentum of order $\Lambda_{\rm QCD}$ in the $\bar{c}$ rest frame is produced in the state n, where $n = {}^{2S+1}L_J^{(c)}$ labels the color and angular momentum quantum numbers of the quark pair. The cross section is factored into a perturbatively calculable piece $d\hat{\sigma}[qg \to (\bar{c}q)^n + c + X]$ and a nonperturbative factor $\rho[(\bar{c}q)^n \to \overline{D}]$ encoding the probability for the quark pair with quantum number n to hadronize into a final state including a $\overline{D}$. Equation (4.4) must then be convoluted with the proton parton distribution functions to get the final hadronic cross section.

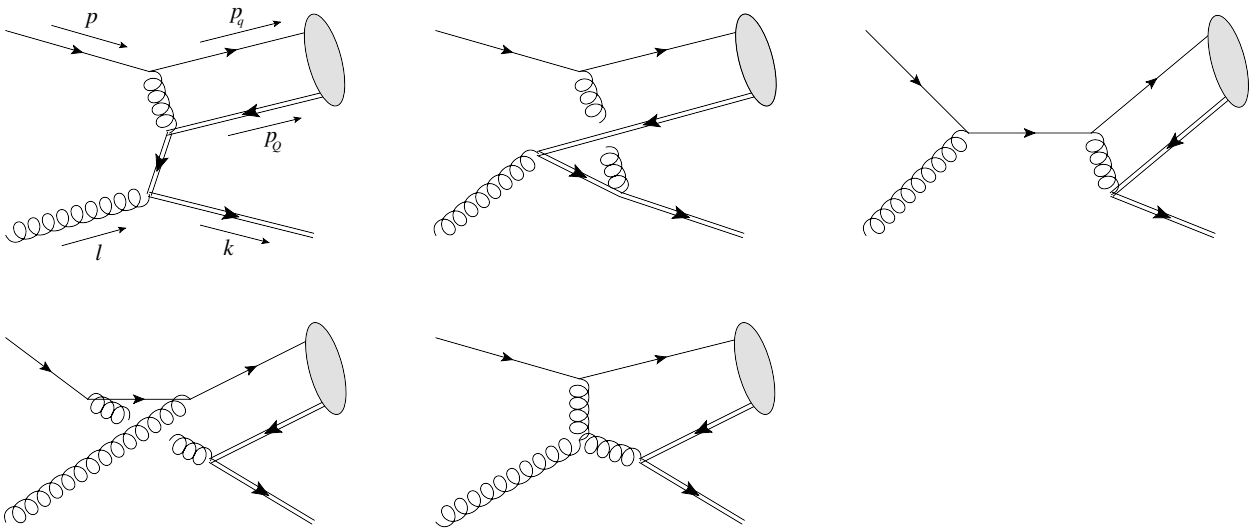

Figure 8: Diagrams for production of a $\overline{D}$ meson by the heavy quark recombination mechanism described by Eq. (4.4) at lowest order of α_s. They describes the partonic process $qg \to (\bar{Q}q)^n + Q$.

Since the ρ's are only sensitive to the soft physics between q and $\bar{c}$ in the $\bar{c}$ rest frame, they are governed by HQET. Let us list out all possible n at leading power in Λ_{QCD}/m_Q. Since $\mathbf{3} \times \bar{\mathbf{3}} = \mathbf{1} + \mathbf{8}$, there are two possible color states, namely the color singlet and the color octet. Since the D meson is in the state ${}^1S_0^{(1)}$, the one obvious leading parameter is $\rho_1^{sm} = \rho[\bar{c}q({}^1S_0^{(1)}) \to \overline{D}]$. Recall that in HQET, $\partial_\mu \sim A_\mu \sim \Lambda_{QCD}$ and $q \sim Q_v \sim \Lambda_{QCD}^{3/2}$ Although a spin flip on the heavy quark is through an insertion of the power-suppressed Lagrangian $\int d^4x g\bar{Q}_v \frac{\sigma_{\mu\nu}G^{\mu\nu}}{4m_Q} Q_v$, a spin flip on the light quark is through $\int d^4x \bar{q}\not{A}q$, which is not power-suppressed. So $\rho_1^{sf} = \rho[\bar{c}q({}^3S_1^{(1)}) \to \overline{D}]$ is also leading. Moreover, a soft gluon emission is through the leading Lagrangians $\int d^4x \bar{Q}_v v \cdot A Q_v$ and $\int d^4x \bar{q}\not{A}q$. Therefore, the color octet contributions $\rho_8^{sm} = \rho[\bar{c}q({}^1S_0^{(8)}) \to \overline{D}]$ and $\rho_8^{sf} = \rho[\bar{c}q({}^3S_1^{(8)}) \to \overline{D}]$ are also leading. Contributions from $L > 0$ are suppressed since they involve factors of $\partial/m_Q \sim \Lambda_{QCD}/m_Q$ in the definition of ρ. Charge conjugation symmetry implies that $\rho[(\bar{c}q)^n \to \overline{D}] = \rho[(c\bar{q})^n \to D]$. Therefore, for production of D or $\overline{D}$, we have four different ρ's at leading power:

$$\begin{aligned} \rho_1^{sm} &= \rho[c\bar{d}({}^1S_0^{(1)}) \to D]\,, & \rho_1^{sf} &= \rho[c\bar{d}({}^3S_1^{(1)}) \to D]\,, \\ \rho_8^{sm} &= \rho[c\bar{d}({}^1S_0^{(8)}) \to D]\,, & \rho_8^{sf} &= \rho[c\bar{d}({}^3S_1^{(8)}) \to D]\,. \end{aligned} \tag{4.5}$$

The factorization Eq. (4.4) is an operator expansion in the EFT language:

$$d\hat{\sigma}[\overline{D}] = \sum_n d\hat{\sigma}[qg \to (\bar{c}q)^n + c + X]\langle 0|O(\overline{D})_n|0\rangle\,, \tag{4.6}$$

where $O(\overline{D})_n$ is some HQET operator and we identify $\rho[(\bar{c}q)^n \to \overline{D}]$ with $\langle 0|O_n(\overline{D})|0\rangle$. The definition of O_n is arbitrary except that it should (1) project out the correct quantum number n, (2) create the meson $\overline{D}$ in the final state, (3) be gauge invariant, and (4) absorb all residual infrared divergences that appear in the matching. Inspired by the result of matching at tree level, a simple set of definitions are given by

$$\begin{aligned}
&\rho[Q\bar{q}(^1S_0^{(1)}) \to H] \\
&= -\frac{1}{8m_Q}\int \frac{d\eta_1}{\eta_1}\frac{d\eta_2}{\eta_2}\frac{dw_1}{2\pi}\frac{dw_2}{2\pi}e^{-i\eta_1 w_1 + i\eta_2 w_2} \\
&\quad\times \langle 0|\bar{\mathbf{T}}\left[\bar{q}(w_2 v)\gamma_5 S(w_2 v, 0)Q_v(0)\right] a_H^\dagger a_H \mathbf{T}\left[\bar{Q}_v(0)\gamma_5 S(0, w_1 v)q(w_1 v)\right]|0\rangle\,, \qquad (4.7a)\\
&\rho[Q\bar{q}(^3S_1^{(1)}) \to H] \\
&= -\frac{1}{24m_Q}\int \frac{d\eta_1}{\eta_1}\frac{d\eta_2}{\eta_2}\frac{dw_1}{2\pi}\frac{dw_2}{2\pi}e^{-i\eta_1 w_1 + i\eta_2 w_2} \\
&\quad\times \langle 0|\bar{\mathbf{T}}\left[\bar{q}(w_2 v)\gamma_T^\mu S(w_2 v, 0)Q_v(0)\right] a_H^\dagger a_H \mathbf{T}\left[\bar{Q}_v(0)\gamma_{T\mu} S(0, w_1 v)q(w_1 v)\right]|0\rangle\,, \qquad (4.7b)\\
&\rho[Q\bar{q}(^1S_0^{(8)}) \to H] \\
&= -\frac{3}{32m_Q}\int \frac{d\eta_1}{\eta_1}\frac{d\eta_2}{\eta_2}\frac{dw_1}{2\pi}\frac{dw_2}{2\pi}e^{-i\eta_1 w_1 + i\eta_2 w_2} \\
&\quad\times \langle 0|\bar{\mathbf{T}}\left[\bar{q}(w_2 v)\gamma_5 t^a S(w_2 v, 0)Q_v(0)\right] a_H^\dagger a_H \mathbf{T}\left[\bar{Q}_v(0)\gamma_5 S(0, w_1 v)t^a q(w_1 v)\right]|0\rangle\,, \qquad (4.7c)\\
&\rho[Q\bar{q}(^3S_1^{(8)}) \to H] \\
&= -\frac{1}{16m_Q}\int \frac{d\eta_1}{\eta_1}\frac{d\eta_2}{\eta_2}\frac{dw_1}{2\pi}\frac{dw_2}{2\pi}e^{-i\eta_1 w_1 + i\eta_2 w_2} \\
&\quad\times \langle 0|\bar{\mathbf{T}}\left[\bar{q}(w_2 v)\gamma_T^\mu t^a S(w_2 v, 0)Q_v(0)\right] a_H^\dagger a_H \mathbf{T}\left[\bar{Q}_v(0)\gamma_{T\mu} S(0, w_1 v)t^a q(w_1 v)\right]|0\rangle\,, \qquad (4.7d)
\end{aligned}$$

where v is the four velocity of the hadron H and $\gamma_T^\mu = \gamma^\mu - v\cdot\gamma v^\mu$. $S(wv, 0)$ is the soft Wilson line defined by

$$S(wv, 0) = \mathrm{P}\exp\left(ig\int_0^w ds\; v\cdot A(sv)\right)\,. \tag{4.8}$$

The factor $1/\eta_1\eta_2$ is constructed to absorb the residual IR divergences in the matching. From the power counting $q \sim Q_v \sim \Lambda_{QCD}^{3/2}$, $a_H \sim \Lambda_{QCD}^{-3/2}$, $w \sim 1/\Lambda_{QCD}$ and $\eta \sim \Lambda_{QCD}$, we see that the ρ's in Eqs. (4.23) scale as Λ_{QCD}/m_Q.

The perturbative piece $d\hat{\sigma}[qg \to (\bar{c}q)^n + c + X]$ is calculated by matching. It was calculated to lowest order in α_s in Ref. [30]. Here we give a brief review of the method. Going to the rest frame of the outgoing heavy anti-quark, taking $p_q \to 0$ and keeping only terms which blow up as $p_q \to 0$, the amplitude for the five diagrams in Fig. 8 with partonic final state is found to be

$$\mathcal{M} = g^3 \mathrm{Tr}\left[v_i(p_Q)\bar{u}_j(p_q)\left(\frac{A_1}{2p\cdot p_q} + \frac{A_2}{2l\cdot p_q}\right)\right], \tag{4.9}$$

where the trace is over Dirac indices and i, j are color indices. A_1 ans A_2 are given by

$$\begin{aligned} A_1 = \epsilon_\nu t^b \gamma_\mu u(p)\bar{v}(k)\Bigg\{ & t^b\gamma^\mu \frac{1}{\not{l} - \not{p}_Q - m_Q} t^a \gamma^\nu + t^a \gamma^\nu \frac{1}{\not{k} - \not{l} - m_Q} t^b \gamma^\mu \\ & + \frac{i f^{abc} t^c}{(k+p_Q)^2}\left[(\not{l} - \not{p})g^{\mu\nu} + 2p^\nu\gamma^\mu - 2l^\mu\gamma^\nu\right]\Bigg\}, \end{aligned} \tag{4.10}$$

$$A_2 = -\frac{1}{(k+p_Q)^2}\epsilon_\nu t^a \gamma^\nu \not{l} t^b \gamma^\mu u(p)\bar{v}(k) t^b \gamma_\mu, \tag{4.11}$$

where ϵ^μ and a are the polarization vector and color state of the incoming gluon respectively. Let v be the four velocity of the $\bar{Q}q$ pair forming the $\overline{D}$ meson. In a general frame, we can write $p_q = (v\cdot p_q)v + p_{qT}$, where parametrically $p_{qT} \ll (v\cdot p_q)v$. So we can replace p_q by $(v\cdot p_q)v$. Therefore, we have

$$\mathcal{M} = g^3 \mathrm{Tr}\left[v_i(p_Q)\bar{u}_j(p_q)\left(\frac{A_1}{2(p\cdot v)(p_q\cdot v)} + \frac{A_2}{2(l\cdot v)(p_q\cdot v)}\right)\right], \tag{4.12}$$

To leading order in Λ_{QCD}/m_Q, p_Q can also be approximated by $m_Q v$. The ρ's in Eqs. (4.23) are normalized in such a way that the matching at tree level corresponds to the replacement

$$\frac{1}{(p\cdot v)(p_q\cdot v)} \to \frac{1}{p\cdot p_Q} \tag{4.13a}$$

$$\frac{1}{(l\cdot v)(p_q\cdot v)} \to \frac{1}{l\cdot p_Q} \tag{4.13b}$$

and

$$v_i(p_Q)\bar{u}_j(p_q) \to \frac{m_Q}{N_c}\delta_{ij}(\not{p}_Q - m_Q)\gamma_5\sqrt{\rho[Q\bar{q}(^1S_0^{(1)}) \to H]}\,, \quad \text{for } q\bar{Q} \to q\bar{Q}(^1S_0^{(1)}) + g\,, \tag{4.14a}$$

$$v_i(p_Q)\bar{u}_j(p_q) \to \frac{m_Q}{N_c}\delta_{ij}(\not{p}_Q - m_Q)\not{\epsilon}^*_H\sqrt{\rho[Q\bar{q}(^3S_1^{(1)}) \to H]}\,, \quad \text{for } q\bar{Q} \to q\bar{Q}(^3S_1^{(1)}) + g\,, \tag{4.14b}$$

$$v_i(p_Q)\bar{u}_j(p_q) \to \sqrt{\frac{2}{N_c}}m_Q t^a_{ij}(\not{p}_Q - m_Q)\gamma_5\sqrt{\rho[Q\bar{q}(^1S_0^{(8)}) \to H]}\,, \quad \text{for } q\bar{Q} \to q\bar{Q}(^1S_0^{(8)}) + g\,, \tag{4.14c}$$

$$v_i(p_Q)\bar{u}_j(p_q) \to \sqrt{\frac{2}{N_c}}m_Q t^a_{ij}(\not{p}_Q - m_Q)\not{\epsilon}^*_H\sqrt{\rho[Q\bar{q}(^3S_1^{(8)}) \to H]}\,, \quad \text{for } q\bar{Q} \to q\bar{Q}(^3S_1^{(8)}) + g\,, \tag{4.14d}$$

in the amplitude Eq. (4.12). Here ϵ_H is the polarization vector of the producd meson in the intermediate $J = 1$ states. The partonic cross section is given by

$$\frac{d\hat{\sigma}}{d\hat{t}} = \frac{1}{16\pi\hat{s}^2}\overline{\sum}|\mathcal{M}|^2 \tag{4.15}$$

Here we quote the result from [30]:

$$\begin{aligned}
&\frac{d\hat{\sigma}}{dt}\left[qg \to \bar{Q}q(^1S_0^{(1)}) + Q\right] \\
=&\frac{2\pi^2\alpha_s^3}{243}\frac{m_Q^2}{S^3}\left[-\frac{64U}{S} + \frac{m_Q^2}{T}\left(79 - \frac{112U}{T} - \frac{64U^2}{T^2}\right) - \frac{16m_Q^4 S}{UT^2}\left(1 - \frac{8U}{T}\right)\right]\,, \qquad (4.16a)\\
&\frac{d\hat{\sigma}}{dt}\left[qg \to \bar{Q}q(^3S_1^{(1)}) + Q\right] \\
=&\frac{2\pi^2\alpha_s^3}{243}\frac{m_Q^2}{S^3}\left[-\frac{64U}{S}\left(1 + \frac{2U^2}{T^2}\right) - \frac{m_Q^2}{T}\left(19 - \frac{28T}{U} + \frac{368U}{T} + \frac{4T^2}{U^2} - \frac{64U^2}{T^2}\right)\right. \\
&\left.\qquad -\frac{48m_Q^4 S}{UT^2}\left(1 - \frac{8U}{T}\right)\right]\,, \qquad (4.16b)\\
&\frac{d\hat{\sigma}}{dt}\left[qg \to \bar{Q}q(^1S_0^{(8)}) + Q\right] \\
=&\frac{4\pi^2\alpha_s^3}{243}\frac{m_Q^2}{S^3}\left[-\frac{U}{S}\left(4 + \frac{9T}{U} + \frac{9T^2}{U^2}\right) - \frac{m_Q^2}{2T}\left(79 + \frac{14U}{T} + \frac{8U^2}{T^2} - \frac{18T^2}{U^2}\right)\right. \\
&\left.\qquad +\frac{m_Q^4 S}{UT^2}\left(8 + \frac{9T}{U} + \frac{8U}{T}\right)\right]\,, \qquad (4.16c)
\end{aligned}$$

$$
\begin{aligned}
&\frac{d\hat{\sigma}}{dt}\left[qg\to\bar{Q}q(^3S_1^{(8)})+Q\right]\\
=&\frac{4\pi^2\alpha_s^3}{243}\frac{m_Q^2}{S^3}\left[-\frac{U}{S}\left(22+\frac{9T}{U}+\frac{18U}{T}+\frac{9T^2}{U^2}+\frac{8U^2}{T^2}\right)\right.\\
&\left.-\frac{m_Q^2}{2T}\left(233+\frac{10U}{T}+\frac{316T}{U}+\frac{266T^2}{U^2}-\frac{8U^2}{T^2}\right)+\frac{8m_Q^4S}{UT^2}\left(8+\frac{9T}{U}+\frac{8U}{T}\right)\right],
\end{aligned}
\tag{4.16d}
$$

where $S=\hat{s}=(p+l)^2$, $T=\hat{t}-m_Q^2=(p_Q-p)^2-m_Q^2$ and $U=\hat{u}-m_Q^2=(k-p)^2-m_Q^2$ (see Fig. 8). Note that these partonic cross sections when multiplied by the ρ's are suppressed by $\alpha_s\Lambda_{QCD}m_Q/S$ compared to the leading twist partonic cross sections in Eq. (4.3).

Besides the $qg\to(\bar{c}q)^n+c+X$ process, there are also contributions from $q\bar{c}\to(\bar{c}q)^n+g+X$, as shown in Fig. 9. Using a similar method, we calculate $d\hat{\sigma}[q\bar{c}\to(\bar{c}q)^n+g+X]$ to lowest order in α. The resulting partonic cross sections are calculated to be

$$
\begin{aligned}
&\frac{d\hat{\sigma}}{d\hat{t}}[q\bar{Q}\to\bar{Q}q(^1S_0^{(1)})+g]\\
=&\frac{16\pi^2\alpha_s^3}{729}\frac{m_Q^2}{S^3}\left[\frac{64S^2}{T^2}-\frac{m_Q^2S}{UT}\left(79-\frac{112S}{U}-\frac{64S^2}{U^2}\right)+\frac{16m_Q^4}{U^2}\left(1-\frac{8S}{U}\right)\right]
\end{aligned}
\tag{4.17a}
$$

$$
\begin{aligned}
&\frac{d\hat{\sigma}}{d\hat{t}}[q\bar{Q}\to\bar{Q}q(^3S_1^{(1)})+g]\\
=&\frac{16\pi^2\alpha_s^3}{729}\frac{m_Q^2}{S^3}\left[\frac{64S^2}{T^2}\left(1+\frac{2S^2}{U^2}\right)-\frac{m_Q^2}{T}\left(28-\frac{4U}{S}-\frac{19S}{U}-\frac{368S^2}{U^2}+\frac{64S^3}{U^3}\right)\right.\\
&\left.+\frac{48m_Q^4}{U^2}\left(1-\frac{8S}{U}\right)\right],
\end{aligned}
\tag{4.17b}
$$

$$
\begin{aligned}
&\frac{d\hat{\sigma}}{d\hat{t}}[q\bar{Q}\to\bar{Q}q(^1S_0^{(8)})+g]\\
=&\frac{32\pi^2\alpha_s^3}{729}\frac{m_Q^2}{S^3}\left[\left(9+\frac{9S}{T}+\frac{4S^2}{T^2}\right)-\frac{m_Q^2}{T}\left(\frac{9U}{S}-\frac{79S}{2U}-\frac{7S^2}{U^2}-\frac{4S^3}{U^3}\right)\right.\\
&\left.-\frac{m_Q^4}{U^2}\left(8+\frac{8S}{U}+\frac{9U}{S}\right)\right],
\end{aligned}
\tag{4.17c}
$$

$$
\begin{aligned}
&\frac{d\hat{\sigma}}{d\hat{t}}[q\bar{Q}\to\bar{Q}q(^3S_1^{(8)})+g]\\
=&\frac{32\pi^2\alpha_s^3}{729}\frac{m_Q^2}{S^3}\left[\left(16+\frac{13U}{T}+\frac{14T}{U}+\frac{12U^2}{T^2}+\frac{8T^2}{U^2}\right)\right.\\
&\left.+\frac{m_Q^2}{T}\left(158+\frac{133U}{S}+\frac{233S}{2U}+\frac{5S^2}{U^2}-\frac{4S^3}{U^3}\right)-\frac{3m_Q^4}{U^2}\left(8+\frac{8S}{U}+\frac{9U}{S}\right)\right],
\end{aligned}
\tag{4.17d}
$$

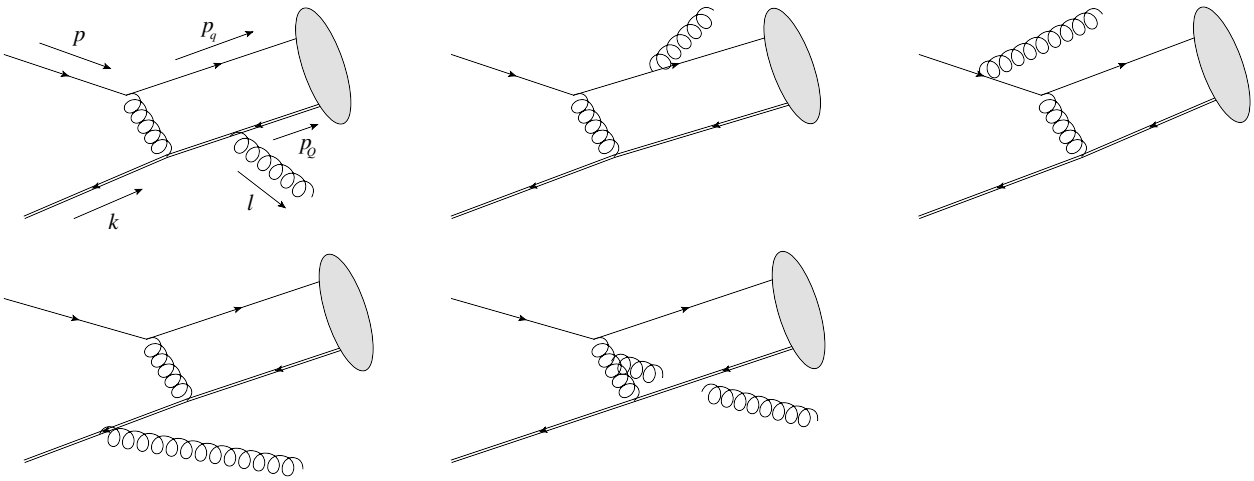

Figure 9: Diagrams for production of a $\overline{D}$ meson by the heavy quark recombination mechanism for the partonic process $q\bar{Q} \to (\bar{Q}q)^n + g$ at lowest order in α_s.

where we have defined $S = \hat{s} - m_Q^2 = (k+p)^2 - m_Q^2, T = \hat{t} = (k - p_Q)^2$, and $U = \hat{u} - m_Q^2 = (k-l)^2 - m_Q^2$. Note that the results for $Qq \to (\bar{Q}q)^n + g$ (Eqs. (4.17)) can be obtained from those for $qg \to (\bar{Q}q)^n + Q$ (Eqs. (4.16)) by carefully applying crossing symmetry. We chose to compute the cross sections from scratch. As a cross check, we are able to reproduce the results in Eqs. (4.16). To obtain Eqs. (4.17) by crossing symmetry, one starts from Eqs. (4.16). First, formally the flux factor is not changed, i.e.

$$\frac{1}{S^2} \to \frac{1}{S^2} \quad \text{for the prefactor}\,. \tag{4.18}$$

Then beside this flux factor, for all the appearances of S, T and U, the following replacements are implemented:

$$\begin{aligned} S &\to T\,, \\ T &\to U\,, \\ U &\to S\,. \end{aligned} \tag{4.19}$$

After all these, one has to multiply the resulting expression by $-8/3$. The final result is equal to Eqs. (4.17).

The c quark in Eq. (4.4) could fragment into a D meson, this time of opposite flavor, i.e., a D^+ or D^0, generically labeled D. Thus, to get the full rate due to recombination for producing $\overline{D}$ mesons, we also need to account for the contribution where a light antiquark comes from the proton, while the $\bar{c}$ fragments into a $\overline{D}$. We thus have three contributions:

$$(a) \qquad d\hat{\sigma}[\overline{D}] = \sum_n d\hat{\sigma}[qg \to (\bar{c}q)^n + c + X]\rho[(\bar{c}q)^n \to \overline{D}]\,, \tag{4.20a}$$

$$(b) \qquad d\hat{\sigma}[\overline{D}] = \sum_n d\hat{\sigma}[q\bar{c} \to (\bar{c}q)^n + g + X]\rho[(\bar{c}q)^n \to \overline{D}]\,, \tag{4.20b}$$

$$(c) \qquad d\hat{\sigma}[\overline{D}] = \sum_n d\hat{\sigma}[\bar{q}g \to (c\bar{q})^n + \bar{c} + X] \sum_H \rho[(c\bar{q})^n \to H] \otimes D_{\bar{c}\to\overline{D}}\,, \tag{4.20c}$$

where H can be any hadron. Eq. (4.20c) will be called the opposite-side recombination. The recombination cross section for producing a D is obtained by taking the charge conjugate of the above equations.

4.2.2 Hadronic Production of Heavy Baryons

The heavy quark recombination mechanism can be easily generalized to baryon productions. For instance, for the production of the Λ_Q (Qud) mesons, the contributions from the heavy quark recombination mechanism are given by

$$(a) \qquad d\hat{\sigma}[\Lambda_Q] = \sum_n d\hat{\sigma}[qg \to (Qq)^n + \overline{Q} + X]\rho[(Qq)^n \to \Lambda_Q]\,, \tag{4.21a}$$

$$(b) \qquad d\hat{\sigma}[\Lambda_Q] = \sum_n d\hat{\sigma}[Qq \to (Qq)^n + g + X]\rho[(Qq)^n \to \Lambda_Q]\,, \tag{4.21b}$$

$$(c) \qquad d\hat{\sigma}[\Lambda_Q] = \sum_n d\hat{\sigma}[qg \to (\overline{Q}q)^n + Q] \sum_{\overline{H}} \rho[(\overline{Q}q)^n \to \overline{H}] \otimes D_{Q\to\Lambda_Q}\,. \tag{4.21c}$$

The processes (a) and (b) are shown in Fig. 10. Since $\mathbf{3} \times \mathbf{3} = \bar{\mathbf{3}} + \mathbf{6}$, the two possible color states are the antisymmetric $\bar{\mathbf{3}}$ and the symmetric $\mathbf{6}$. Again, by similar reasons as in the case of meson production, to leading order in Λ_{QCD}/m_Q there are four non-perturbative parameters:

$$\eta_{\bar{3}} = \rho[Qq(^1S_0^{(\bar{3})}) \to \Lambda_Q]\,, \qquad \tilde{\eta}_{\bar{3}} = \rho[Qq(^3S_1^{(\bar{3})}) \to \Lambda_Q]\,,$$
$$\eta_6 = \rho[Qq(^1S_0^{(6)}) \to \Lambda_Q]\,, \qquad \tilde{\eta}_6 = \rho[Qq(^3S_1^{(6)}) \to \Lambda_Q]\,. \tag{4.22}$$

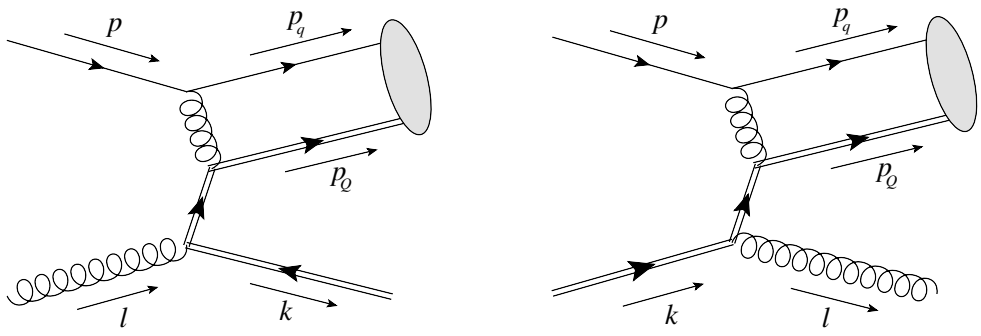

Figure 10: Examples of diagrams for production of a Λ_Q baryon by the heavy-quark recombination mechanism for (a) $qg \to (Qq)^n + \overline{Q}$ and (b) $Qq \to (Qq)^n + g$. Each process has five diagrams. Single lines represent light quarks, double lines heavy quarks, and the shaded blob the Λ_Q baryon.

The field-theoretical definitions of these non-perturbative parameters are given by

$$\begin{aligned}
&\rho[Qq(^1S_0^{(\bar{3})}) \to H] \\
&= -\frac{1}{m_Q}\int \frac{d\eta_1}{\eta_1}\frac{d\eta_2}{\eta_2}\frac{dw_1}{2\pi}\frac{dw_2}{2\pi}e^{-i\eta_1 w_1 + i\eta_2 w_2} \\
&\quad \times \langle 0|\bar{\mathbf{T}}\left[\bar{q}(w_2 v)\mathcal{C}^\dagger\gamma_5 K^a S(w_2 v, 0)Q_v(0)\right] a_H^\dagger a_H \mathbf{T}\left[\bar{Q}_v(0)\gamma_5 S(0, w_1 v)K^a\mathcal{C}q(w_1 v)\right]|0\rangle\,,
\end{aligned} \tag{4.23a}$$

$$\begin{aligned}
&\rho[Qq(^3S_1^{(\bar{3})}) \to H] \\
&= -\frac{1}{m_Q}\int \frac{d\eta_1}{\eta_1}\frac{d\eta_2}{\eta_2}\frac{dw_1}{2\pi}\frac{dw_2}{2\pi}e^{-i\eta_1 w_1 + i\eta_2 w_2} \\
&\quad \times \langle 0|\bar{\mathbf{T}}\left[\bar{q}(w_2 v)\mathcal{C}^\dagger\gamma_T^\mu K^a S(w_2 v, 0)Q_v(0)\right] a_H^\dagger a_H \mathbf{T}\left[\bar{Q}_v(0)\gamma_{T\mu} S(0, w_1 v)K^a\mathcal{C}(w_1 v)\right]|0\rangle\,,
\end{aligned} \tag{4.23b}$$

$$\begin{aligned}
&\rho[Qq(^1S_0^{(6)}) \to H] \\
&= -\frac{1}{m_Q}\int \frac{d\eta_1}{\eta_1}\frac{d\eta_2}{\eta_2}\frac{dw_1}{2\pi}\frac{dw_2}{2\pi}e^{-i\eta_1 w_1 + i\eta_2 w_2} \\
&\quad \times \langle 0|\bar{\mathbf{T}}\left[\bar{q}(w_2 v)\mathcal{C}^\dagger\gamma_5 L^a S(w_2 v, 0)Q_v(0)\right] a_H^\dagger a_H \mathbf{T}\left[\bar{Q}_v(0)\gamma_5 S(0, w_1 v)L^a\mathcal{C}q(w_1 v)\right]|0\rangle\,,
\end{aligned} \tag{4.23c}$$

$$
\begin{aligned}
&\rho[Qq(^3S_1^{(6)}) \to H] \\
&= -\frac{1}{m_Q}\int \frac{d\eta_1}{\eta_1}\frac{d\eta_2}{\eta_2}\frac{dw_1}{2\pi}\frac{dw_2}{2\pi}e^{-i\eta_1 w_1 + i\eta_2 w_2} \\
&\quad \times \langle 0|\bar{\mathbf{T}}\left[\bar{q}(w_2 v)\mathcal{C}^\dagger \gamma_T^\mu L^a S(w_2 v, 0) Q_v(0)\right] a_H^\dagger a_H \mathbf{T}\left[\bar{Q}_v(0)\gamma_{T\mu} S(0, w_1 v) L^a \mathcal{C} q(w_1 v)\right]|0\rangle\,,
\end{aligned}
\tag{4.23d}
$$

where K^a and L^a are the color matrices for $\bar{\mathbf{3}}$ and $\mathbf{6}$ respectively:

$$
K^1 = \frac{1}{\sqrt{2}}\begin{pmatrix} 0 & 0 & 0 \\ 0 & 0 & 1 \\ 0 & -1 & 0 \end{pmatrix}, \quad K^2 = \frac{1}{\sqrt{2}}\begin{pmatrix} 0 & 0 & -1 \\ 0 & 0 & 0 \\ 1 & 0 & 0 \end{pmatrix}, \quad K^3 = \frac{1}{\sqrt{2}}\begin{pmatrix} 0 & 1 & 0 \\ -1 & 0 & 0 \\ 0 & 0 & 0 \end{pmatrix},
\tag{4.24}
$$

$$
\begin{aligned}
L^1 &= \begin{pmatrix} 1 & 0 & 0 \\ 0 & 0 & 0 \\ 0 & 0 & 0 \end{pmatrix}, \quad L^2 = \frac{1}{\sqrt{2}}\begin{pmatrix} 0 & 1 & 0 \\ 1 & 0 & 0 \\ 0 & 0 & 0 \end{pmatrix}, \quad L^3 = \begin{pmatrix} 0 & 0 & 0 \\ 0 & 1 & 0 \\ 0 & 0 & 0 \end{pmatrix}, \\
L^4 &= \frac{1}{\sqrt{2}}\begin{pmatrix} 0 & 0 & 0 \\ 0 & 0 & 1 \\ 0 & 1 & 0 \end{pmatrix}, \quad L^5 = \begin{pmatrix} 0 & 0 & 0 \\ 0 & 0 & 0 \\ 0 & 0 & 1 \end{pmatrix}, \quad L^6 = \frac{1}{\sqrt{2}}\begin{pmatrix} 0 & 0 & 1 \\ 0 & 0 & 0 \\ 1 & 0 & 0 \end{pmatrix}.
\end{aligned}
\tag{4.25}
$$

The perturbative pieces $d\hat{\sigma}[qg \to (Qq)^n + \overline{Q}]$ and $d\hat{\sigma}[Qq \to (Qq)^n + \bar{g}]$ can be calculated in a similar way as in the case of meson production. One can first charge-conjugate the heavy quark line in Fig. 10 and then apply replacement

$$
v_i(p_Q)\bar{u}_j(p_q) \to \frac{m_Q}{N_c}K^a_{ij}(\not{p}_Q - m_Q)\gamma_5\sqrt{\rho[Q\bar{q}(^1S_0^{(\bar{3})}) \to H]}\,, \quad \text{for } q\bar{Q} \to q\bar{Q}(^1S_0^{(\bar{3})}) + g\,,
\tag{4.26a}
$$

$$
v_i(p_Q)\bar{u}_j(p_q) \to \frac{m_Q}{N_c}K^a_{ij}(\not{p}_Q - m_Q)\not{\epsilon}\sqrt{\rho[Q\bar{q}(^3S_1^{(\bar{3})}) \to H]}\,, \quad \text{for } q\bar{Q} \to q\bar{Q}(^3S_1^{(\bar{3})}) + g\,,
\tag{4.26b}
$$

$$
v_i(p_Q)\bar{u}_j(p_q) \to \sqrt{\frac{2}{N_c}}m_Q L^a_{ij}(\not{p}_Q - m_Q)\gamma_5\sqrt{\rho[Q\bar{q}(^1S_0^{(6)}) \to H]}\,, \quad \text{for } q\bar{Q} \to q\bar{Q}(^1S_0^{(6)}) + g\,,
\tag{4.26c}
$$

$$
v_i(p_Q)\bar{u}_j(p_q) \to \sqrt{\frac{2}{N_c}}m_Q L^a_{ij}(\not{p}_Q - m_Q)\not{\epsilon}\sqrt{\rho[Q\bar{q}(^3S_1^{(6)}) \to H]}\,, \quad \text{for } q\bar{Q} \to q\bar{Q}(^3S_1^{(6)}) + g\,.
\tag{4.26d}
$$

The perturbative pieces $d\hat{\sigma}[qg \to (Qq)^n + \overline{Q} + X]$ (Fig. 10(a)) were calculated to lowest order in α_s in Ref. [33]. Here we quote the result:

$$\frac{d\hat{\sigma}}{d\hat{t}}[Qq \to (Qq)^n + g] = -\frac{2\pi^2\alpha_s^3 m_Q^2}{27S^3} F(n|S,T), \tag{4.27}$$

$$\begin{aligned} &F(^1S_0^{(\bar{3})}|S,T) \\ =&-\frac{16U}{S}\left(1-\frac{ST}{U^2}\right) - \frac{m_Q^2}{T}\left(3+\frac{28U}{T}+\frac{16U^2}{T^2}-\frac{16T^2}{U^2}\right) + \frac{4m_Q^4 S}{UT^2}\left(3+\frac{4T}{U}+\frac{8U}{T}\right), \end{aligned} \tag{4.28a}$$

$$\begin{aligned} &F(^3S_1^{(\bar{3})}|S,T) \\ =&3F(^1S_0^{(\bar{3})}|S,T) - 32\left(\frac{T}{U}-\frac{U^2}{T^2}\right) - \frac{4m_Q^2}{T}\left(8-\frac{6U}{T}-\frac{16U^2}{T^2}+\frac{13T}{U}+\frac{15T^2}{U^2}\right), \end{aligned} \tag{4.28b}$$

$$\begin{aligned} &F(^1S_0^{(6)}|S,T) \\ =&-\frac{4U}{S}\left(2-\frac{5ST}{U^2}\right) - \frac{m_Q^2}{T}\left(27+\frac{14U}{T}+\frac{8U^2}{T^2}-\frac{20T^2}{U^2}\right) + \frac{2m_Q^4 S}{UT^2}\left(9+\frac{10T}{U}+\frac{8U}{T}\right), \end{aligned} \tag{4.28c}$$

$$\begin{aligned} &F(^3S_1^{(6)}|S,T) \\ =&3F(^1S_0^{(6)}|S,T) - \frac{8U}{S}\left(3+\frac{5ST}{U^2}+\frac{5U}{T}+\frac{2U^2}{T^2}\right) + \frac{4m_Q^2 S}{U^2}\left(27-\frac{U}{T}-\frac{U^2}{T^2}-\frac{8U^3}{T^3}\right), \end{aligned} \tag{4.28d}$$

where $S = \hat{s} = (p+l)^2$, $T = \hat{t} - m_Q^2 = (p_Q - p)^2 - m_Q^2$ and $U = \hat{u} - m_Q^2 = (k-p)^2 - m_Q^2$. Using a similar method, we calculate $d\hat{\sigma}[Qq \to (Qq)^n + g + X]$ (Fig. 10(b)) to lowest order in α_s. The result is

$$\frac{d\hat{\sigma}}{d\hat{t}}[Qq \to (Qq)^n + g] = -\frac{16\pi^2\alpha_s^3 m_Q^2}{81S^2T} G(n|S,T), \tag{4.29}$$

$$\begin{aligned} &G(^1S_0^{(\bar{3})}|S,T) \\ =&-\frac{16S}{T}\left(1-\frac{TU}{S^2}\right) - \frac{m_Q^2}{U}\left(3+\frac{28S}{U}+\frac{16S^2}{U^2}-\frac{16U^2}{S^2}\right) + \frac{4m_Q^4 T}{SU^2}\left(3+\frac{4U}{S}+\frac{8S}{U}\right), \end{aligned} \tag{4.30a}$$

$$
\begin{aligned}
&G(^3S_1^{(\bar{3})}|S,T)\\
=&3G(^1S_0^{(\bar{3})}|S,T) - 32\left(\frac{U}{S}-\frac{S^2}{U^2}\right) - \frac{4m_Q^2}{U}\left(8-\frac{6S}{U}-\frac{16S^2}{U^2}+\frac{13U}{S}+\frac{15U^2}{S^2}\right), \qquad (4.30b)\\
&G(^1S_0^{(6)}|S,T)\\
=&-\frac{4S}{T}\left(2-\frac{5TU}{S^2}\right) - \frac{m_Q^2}{U}\left(27+\frac{14S}{U}+\frac{8S^2}{U^2}-\frac{20U^2}{S^2}\right) + \frac{2m_Q^4T}{SU^2}\left(9+\frac{10U}{S}+\frac{8S}{U}\right), \qquad (4.30c)\\
&G(^3S_1^{(6)}|S,T)\\
=&3G(^1S_0^{(6)}|S,T) - \frac{8S}{T}\left(3+\frac{5TU}{S^2}+\frac{5S}{U}+\frac{2S^2}{U^2}\right) + \frac{4m_Q^2T}{S^2}\left(27-\frac{S}{U}-\frac{S^2}{U^2}-\frac{8S^3}{U^3}\right), \qquad (4.30d)
\end{aligned}
$$

where $S=\hat{s}-m_Q^2=(k+p)^2-m_Q^2, T=\hat{t}=(k-p_Q)^2$, and $U=\hat{u}-m_Q^2=(k-l)^2-m_Q^2$. Alternatively, one can obtain these results by implementing crossing symmetry as described in Eqs. (A.14) and (4.19) and multiplying by $-8/3$.

4.2.3 Photoproduction of Heavy Mesons

The heavy quark recombination mechanism can be likewise applied to photoproduction of heavy mesons. Consider photoproduction of the $\overline{D}$ meson, $\gamma N \to \overline{D}+X$, where N is a nucleon. The leading twist contribution in perturbative QCD is given by

$$
d\sigma[\gamma N\to\overline{D}+X] = \sum_i f_{i/N}\otimes d\hat{\sigma}[i\gamma\to\bar{c}+X]\otimes D_{\bar{c}\to\overline{D}}\,. \qquad (4.31)
$$

The subleading-twist contributions from the heavy quark recombination mechanism which give a non-vanishing production asymmetry are given by

$$
(a)\qquad d\hat{\sigma}[\overline{D}] = \sum_n d\hat{\sigma}[q\gamma\to(\bar{c}q)^n+c+X]\rho[(\bar{c}q)^n\to\overline{D}]\,, \qquad (4.32a)
$$

$$
(b)\qquad d\hat{\sigma}[\overline{D}] = \sum_n d\hat{\sigma}[\bar{q}\gamma\to(c\bar{q})^n+\bar{c}+X]\sum_H \rho[(c\bar{q})^n\to H]\otimes D_{\bar{c}\to\overline{D}}\,. \qquad (4.32b)
$$

The leading non-perturbative parameters are the same as in the case of hadronic production, i.e. ρ_1^{sm}, ρ_1^{sf}, ρ_8^{sm} and ρ_8^{sf} (Eqs. (4.5)). To lowest order in α and α_s, the diagrams for the partonic process $q\gamma\to(\bar{Q}q)^n+Q+X$ are as shown in Fig. 11. Keeping only terms singular

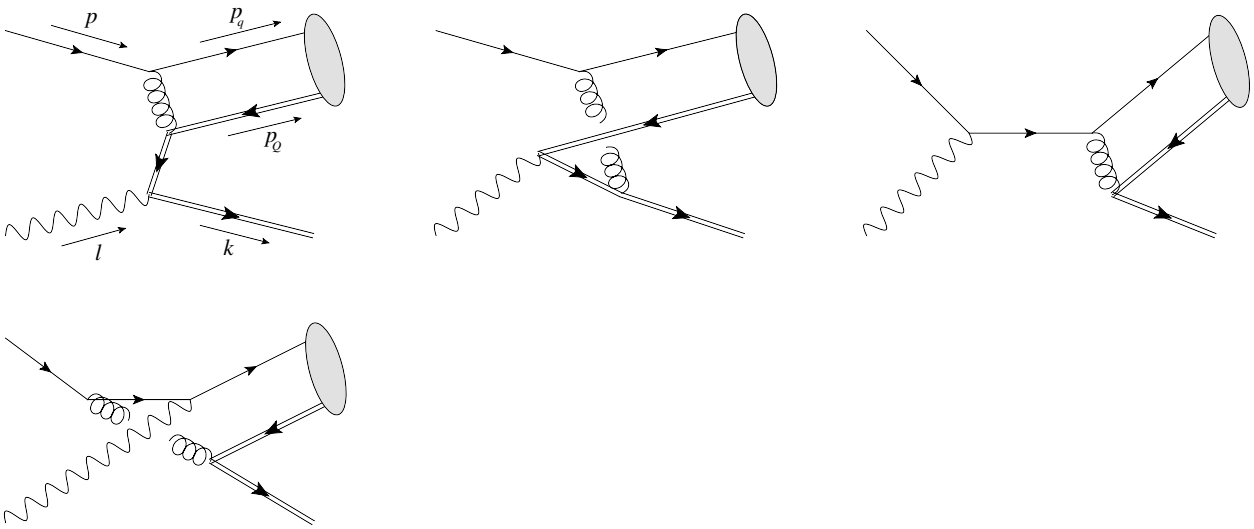

Figure 11: Diagrams for photoproduction of a $\overline{D}$ meson by the heavy quark recombination mechanism described by Eq. (4.32a) at lowest order in α and α_s.

as $p_q \to 0$, the partonic amplitude of the four diagrams in Fig. 11 is given by

$$\mathcal{M} = eg^2 \mathrm{Tr}\left[v_i(p_Q)\bar{u}_j(p_q)\left(\frac{A_1}{2p\cdot p_q} + \frac{A_2}{2l\cdot p_q}\right)\right], \tag{4.33}$$

where the trace is over Dirac indices and i, j are color indices. A_1 ans A_2 are given by

$$A_1 = e_Q \epsilon_\nu t^b \gamma_\mu u(p)\bar{v}(k)\left(t^b\gamma^\mu \frac{1}{\not{l} - \not{p}_Q - m_Q}\gamma^\nu + \gamma^\nu \frac{1}{\not{k} - \not{l} - m_Q} t^b \gamma^\mu\right), \tag{4.34}$$

$$\tag{4.35}$$

$$A_2 = -\frac{e_q}{(k+p_Q)^2}\epsilon_\nu \gamma^\nu \not{l} t^b \gamma^\mu u(p)\bar{v}(k) t^b \gamma_\mu, \tag{4.36}$$

where ϵ^μ is the polarization vector of the incoming photo. $e_q e$ and $e_Q e$ are the electric charges of the incoming light quark and outgoing heavy quark respectively. The absorption of IR

divergences and projection onto various state n are as in Eqs. (4.13) and (4.14) respectively. The resulting partonic cross sections were calculated in Ref. [31]. Here we quote the result:

$$\begin{aligned}
&\frac{d\hat{\sigma}}{dt}\left[q\gamma \to \bar{Q}q({}^1S_0^{(1)}) + Q\right] \\
=&\frac{256\pi^2 e_Q^2 \alpha \alpha_s^2 m_Q^2}{81 S^3}\left[-\frac{S}{U}\left(1+\frac{\kappa T}{S}\right)^2 + \frac{m_Q^2 S}{U^2}\left(-\frac{S^3}{T^3} + \frac{2(1+\kappa)S}{T} + 4\kappa + \frac{\kappa^2 T}{S}\right)\right. \\
&\left. + \frac{2m_Q^4 S^3}{T^3 U^2}\left(1+\frac{\kappa T}{S}\right)\right], \qquad (4.37a)\\
&\frac{d\hat{\sigma}}{dt}\left[q\gamma \to \bar{Q}q({}^3S_1^{(1)}) + Q\right] \\
=&\frac{256\pi^2 e_Q^2 \alpha \alpha_s^2 m_Q^2}{81 S^3}\left[-\frac{S}{U}\left(1+\frac{2U^2}{T^2}\right)\left(1+\frac{\kappa T}{S}\right)^2 + \frac{m_Q^2 S}{U^2}\left(\frac{S^3}{T^3} + \frac{4(2+\kappa)S^2}{T^2} + \frac{2(3+7\kappa)S}{T}\right.\right. \\
&\left.\left. + 4\kappa(3+\kappa) + \frac{3\kappa^2 T}{S}\right) + \frac{6m_Q^4 S^3}{T^3 U^2}\left(1+\frac{\kappa T}{S}\right)\right], \qquad (4.37b)
\end{aligned}$$

where $\kappa \equiv e_q/e_Q$, $S = \hat{s} = (p+l)^2$, $T = \hat{t} - m_Q^2 = (p_Q - p)^2 - m_Q^2$ and $U = \hat{u} - m_Q^2 = (k-p)^2 - m_Q^2$. The color-octet cross sections are given by

$$\begin{aligned}
\frac{d\hat{\sigma}}{dt}\left[q\gamma \to \bar{Q}q({}^1S_0^{(8)}) + Q\right] &= \frac{1}{8}\frac{d\hat{\sigma}}{dt}\left[q\gamma \to \bar{Q}q({}^1S_0^{(1)}) + Q\right], \qquad (4.38a)\\
\frac{d\hat{\sigma}}{dt}\left[q\gamma \to \bar{Q}q({}^3S_1^{(8)}) + Q\right] &= \frac{1}{8}\frac{d\hat{\sigma}}{dt}\left[q\gamma \to \bar{Q}q({}^3S_1^{(1)}) + Q\right]. \qquad (4.38b)
\end{aligned}$$

4.2.4 Perturbative Cross Sections for P waves

As discussed in Section 4.2.1, in productions of D mesons, the contributions from P waves ($L = 1$) are suppressed by Λ_{QCD}/m_Q relative to the contributions from S waves ($L = 0$). For the purpose of of more detailed phenomenological analyses in the future, we calculate the perturbative cross sections for these leading power-suppressed contributions.

For P waves in meson productions, there are 8 non-perturbative parameters, corresponding to $n = {}^1P_1^{(1)}$, ${}^3P_0^{(1)}$, ${}^3P_1^{(1)}$, ${}^3P_2^{(1)}$, ${}^1P_1^{(8)}$, ${}^3P_0^{(8)}$, ${}^3P_1^{(8)}$, ${}^3P_2^{(8)}$. The definitions of the corresponding non-perturbative parameters $\rho[Q\bar{q}({}^{2S+1}P_J^{(c)}) \to H]$ involve one derivative on each

side of the cut. For example, for $n = {}^1P_1^{(1)}$,

$$\begin{aligned}\rho[Q\bar{q}({}^1P_1^{(1)}) \to H] =& \frac{1}{m_Q^3}\int \frac{d\eta_1}{\eta_1}\frac{d\eta_2}{\eta_2}\frac{dw_1}{2\pi}\frac{dw_2}{2\pi}e^{-i\eta_1 w_1 + i\eta_2 w_2} \\ & \times \langle 0|\bar{\mathbf{T}}\left[\bar{q}(w_2 v)\left(-\frac{i}{2}\overleftrightarrow{D}_T^{\mu}\right)S(w_2 v, 0)Q_v(0)\right]a_H^\dagger \\ & \times a_H \mathbf{T}\left[\bar{Q}_v(0)\left(-\frac{i}{2}\overleftrightarrow{D}_{T\mu}\right)S(0, w_1 v)q(w_1 v)\right]|0\rangle\,, \end{aligned} \tag{4.39}$$

where $D_T^\mu \equiv D^\mu - (v\cdot D)v^\mu$. The definitions for other n are listed in Appendix A. We will calculate $d\hat{\sigma}[qg \to (\bar{Q}q)^n + Q + X]$ to lowest order in α_s for P waves. The corresponding results for $d\hat{\sigma}[\bar{Q}q \to (\bar{Q}q)^n + g + X]$ can be obtained by applying crossing symmetry (see Appendix A).

Consider again Fig. 8. We have to keep p_q to first order in the numerator of the amplitude. We should write the outgoing heavy quark momentum as $p_Q = p_H - p_q$, where p_H is the momentum of the outgoing meson. To first order in p_q in the numerator, keeping only the terms which blow up at $p_q \to 0$, the amplitude for the five diagrams has the form

$$\mathcal{M} = g^3 \mathrm{Tr}\left[v(p_Q)\bar{u}(p_q)\left(\frac{A_1^{(0)} + A_1^{(1)}}{2p\cdot p_q} + \frac{A_2^{(0)} + A_2^{(1)}}{2l\cdot p_q}\right)\right], \tag{4.40}$$

where (0) and (1) denote zeroth order and linear order in p_q respectively. $A_1^{(0)}$ and $A_2^{(0)}$ are given by

$$\begin{aligned} A_1^{(0)} =& \epsilon_\nu t^b \gamma_\mu u(p)\bar{u}(k)\left\{t^b\gamma^\mu \frac{1}{\not{l} - \not{p}_H - m_Q}t^a\gamma^\nu + t^a\gamma^\nu\frac{1}{\not{k} - \not{l} - m_Q}t^b\gamma^\mu \right. \\ & \left. + \frac{if^{abc}t^c}{(k+p_H)^2}\left[(\not{l} - \not{p})g^{\mu\nu} + 2p^\nu\gamma^\mu - 2l^\mu\gamma^\nu\right]\right\}, \end{aligned} \tag{4.41}$$

$$A_2^{(0)} = -\frac{1}{(k+p_H)^2}\epsilon_\nu t^a\gamma^\nu \not{l} t^b\gamma^\mu u(p)\bar{u}(k)t^b\gamma_\mu\,. \tag{4.42}$$

$A_1^{(1)}$ and $A_2^{(1)}$ are given by

$$\begin{aligned} A_1^{(1)} =& \epsilon_\nu t^b\gamma_\mu u(p)\bar{u}(k)\left\{\frac{t^b\gamma^\mu}{(l-p_H)^2 - m_Q^2}\left[\frac{-2(\not{l} - \not{p}_H + m_Q)(l-p_H)\cdot p_q}{(l-p_H)^2 - m_Q^2} + \not{p}_q\right]t^a\gamma^\nu \right. \\ & + \frac{if^{abc}t^c}{(k+p_H)^2}\left[\frac{2(k+p_H)\cdot p_q}{(k+p_H)^2}\left((\not{l} - \not{p})g^{\mu\nu} + (p+k+p_H)\gamma^\mu + (-k-p_H-p)^\mu\gamma^\nu\right)\right. \\ & \left.\left. + \not{p}_q g^{\mu\nu} - 2p_q^\nu\gamma^\mu + p_q^\mu\gamma^v\right]\right\}, \end{aligned} \tag{4.43}$$

$$A_2^{(2)} = \frac{1}{(k+p_H)^2}\epsilon_\nu t^a\gamma^\nu\left[\not{p}_q - \frac{2(k+p_H)\cdot p_q \not{l}}{(k+p_H)^2}\right]t^b\gamma^\mu u(p)\bar{u}(k)t^b\gamma_\mu\,. \tag{4.44}$$

To project on a specific spin state, we apply the replacement

$$v(p_Q)\bar{u}(p_q) \to \mathbb{P}\,, \tag{4.45}$$

where $\mathbb{P}$ is the spin state projection operator. We can write

$$\mathbb{P} = \mathbb{P}^{(0)} + \mathbb{P}^{(1)}\,, \tag{4.46}$$

where again (0) and (1) denote zeroth order and linear order in p_q respectively. For $s = 0$, we have

$$\mathbb{P}^{(0)}_{s=0} = \frac{1}{2\sqrt{2}}(\not{p}_H - m_H)\gamma_5\,, \tag{4.47a}$$

$$\mathbb{P}^{(1)}_{s=0} = -\frac{1}{\sqrt{2}m_H}\gamma_5 \not{p}_q \not{p}_H\,. \tag{4.47b}$$

For $s = 1$, we have

$$\mathbb{P}^{(0)}_{s=1} = \frac{1}{2\sqrt{2}}\not{\epsilon}^*(s_z)(\not{p}_H + m_H)\gamma_5\,, \tag{4.48a}$$

$$\mathbb{P}^{(1)}_{s=1} = -\frac{1}{\sqrt{2}m_H}\left[\not{p}_q \not{p}_H \not{\epsilon}^*_H(s_z) + \epsilon^*_H(s_z)\cdot p_q(\not{p}_H - m_H)\right]\,. \tag{4.48b}$$

The amplitude in a specific spin state and of linear order in p_q in the numerator is thus

$$\mathcal{M}^{(1)}(s, s_z) = g^3 \mathrm{Tr}\left[\mathbb{P}^{(1)}\left(\frac{A_1^{(0)}}{2p\cdot p_q} + \frac{A_2^{(0)}}{2l\cdot p_q}\right) + \mathbb{P}^{(0)}\left(\frac{A_1^{(1)}}{2p\cdot p_q} + \frac{A_2^{(1)}}{2l\cdot p_q}\right)\right]\,. \tag{4.49}$$

Note that $\mathcal{M}^{(1)}(s, s_z)$ has the form $p_q^\mu \tilde{\mathcal{M}}_\mu(s, s_z)$. The projection on a specific orbital angular momentum state with $L = 1$ is given by

$$\begin{aligned}\mathcal{M}(L = 1, L_z; s, s) &= \int \frac{d\Omega}{|\vec{p}_q|} Y^*_{1L_z}(\hat{\vec{p}}_q) p_q^\mu \tilde{\mathcal{M}}_\mu(s, s_z) \\ &= 2\sqrt{\frac{\pi}{3}}\epsilon^{*\mu}_H(L_z)\tilde{\mathcal{M}}_\mu(s, s_z)\,.\end{aligned} \tag{4.50}$$

Finally, the projection on a specific total angular momentum state is given by

$$\mathcal{M}(J, J_z) = \sum_{L_z, s_z} \langle L, L_z; s, s_z | J, J_z\rangle \mathcal{M}(L, L_z; s, s_z)\,. \tag{4.51}$$

For this step, the following identities are useful:

$$\sum_{L_z,s_z} \langle 1, L_z; 1, s_z | 0, 0\rangle \epsilon_H^{*\alpha}(L_z)\epsilon_H^{*\beta}(s_z) = \sqrt{\frac{1}{3}}\left(g^{\alpha\beta} - \frac{p_H^\alpha p_H^\beta}{m_H^2}\right), \tag{4.52}$$

$$\sum_{L_z,s_z} \langle 1, L_z; 1, s_z | 1, J_z\rangle \epsilon_H^{*\alpha}(L_z)\epsilon_H^{*\beta}(s_z) = \frac{-i}{\sqrt{2}m_H}\epsilon^{\alpha\beta\gamma\delta} p_{H\gamma}\epsilon^*_{H\delta}(J_z)\,, \tag{4.53}$$

$$\sum_{L_z,s_z} \langle 1, L_z; 1, s_z | 2, J_z\rangle \epsilon_H^{*\alpha}(L_z)\epsilon_H^{*\beta}(s_z) = \epsilon_H^{*\alpha\beta}(J_z)\,, \tag{4.54}$$

where $\epsilon_H^{*\alpha\beta}(J_z)$ is the traceless symmetric polarization tensor for $J = 2$. To square the amplitude, we will use the following polarization sums:

$$\sum_{J_z=-1}^{1} \epsilon_H^\mu \epsilon_H^{*\nu} = -g^{\mu\nu} + \frac{p_H^\mu p_H^\nu}{m_H^2} \equiv P_H^{\mu\nu}\,, \tag{4.55}$$

$$\sum_{J_z=-2}^{2} \epsilon_H^{\mu\nu} \epsilon_H^{*\alpha\beta} = \frac{1}{2}\left(P_H^{\mu\alpha}P_H^{\nu\beta} + P_H^{\nu\alpha}P_H^{\mu\beta}\right) - \frac{1}{3}P_H^{\mu\nu}P_H^{\alpha\beta}\,. \tag{4.56}$$

The resulting perturbative cross sections are listed in Appendix A.

Similarly, we calculate the perturbative cross sections for P waves for hadronic production of heavy baryons and photoproduction of heavy mesons. The results are listed in Appendix A.

4.3 $D^\pm$ PRODUCTION ASYMMETRIES

In this section, we will apply the heavy quark recombination mechanism to explain the D^+/D^- production asymmetry,

$$A_p = \frac{d\sigma(D^+) - d\sigma(D^-)}{d\sigma(D^+) + d\sigma(D^-)}\,, \tag{4.57}$$

observed at LHCb. We will only include contributions leading in Λ_{QCD}/m_Q, i.e. the S-wave contributions:

$$\rho_1^{sm} = \rho[c\bar{d}(^1S_0^{(1)}) \to D]\,, \qquad \rho_1^{sf} = \rho[c\bar{d}(^3S_1^{(1)}) \to D]\,,$$
$$\rho_8^{sm} = \rho[c\bar{d}(^1S_0^{(8)}) \to D]\,, \qquad \rho_8^{sf} = \rho[c\bar{d}(^3S_1^{(8)}) \to D]\,. \tag{4.58}$$

For simplicity, in the opposite-side recombination Eq. (4.20c) we will restrict H to be D or D^* only and sum over $\bar{q} = \bar{u}, \bar{d}$ and $\bar{s}$ with $SU(3)$ flavor symmetry assumed. Neglecting ρ_1^{sf} and ρ_8^{sf}, the combination $\rho_1^{sm} + \rho_8^{sm}/8$ was determined to be 0.15 by fitting to the E687 and E691 fixed-target photoproduction data [31]. Neglecting ρ_8^{sm}, ρ_1^{sf} and ρ_8^{sf}, the parameter ρ_1^{sm} was determined to be 0.06 by fitting to data from the E791 experiment [32]. We will take $\rho_1^{sm} \sim 0.06$ and $\rho_8^{sm} \sim 0.72$. It turns out that these two contributions only account for $\sim 30\%$ of the measured asymmetry $A_p = (-0.96 \pm 0.26 \pm 0.18)\%$ at LHCb in Ref. [11]. Therefore, we include ρ_1^{sf} and ρ_8^{sf} and, given the arguments above, choose values of similar size as the spin-matched parameters. We also include feed down from $D^{*\pm}$. From heavy quark spin symmetry, we have

$$\begin{aligned} \rho[c\bar{d}(^1S_0^{(c)}) \to D^+] &= \rho[c\bar{d}(^3S_1^{(c)}) \to D^{*+}]\,, \\ \rho[c\bar{d}(^3S_1^{(c)}) \to D^+] &= \rho[c\bar{d}(^1S_0^{(c)}) \to D^{*+}]\,. \end{aligned} \tag{4.59}$$

We use MSTW 2008 LO central PDFs with $m_c = 1.275$ GeV and the Peterson parametrization for the fragmentation function [36] is used for $D_{c\to H}$:

$$D_{c\to H}(z) = \frac{N_H}{z\left(1 - \frac{1}{z} - \frac{\epsilon_c}{1-z}\right)^2}\,. \tag{4.60}$$

$\epsilon_c \sim (m_q/m_c)^2$ was measured to be 0.062 ± 0.007 for the D^{*+} meson [37]. Charge conjugation symmetry and approximate heavy quark symmetry implies that ϵ_c is approximately the same for $D^\pm$ and $D^{*\pm}$. We will take $\epsilon_c = 0.06$ for both $D^\pm$ and $D^{*\pm}$. N_H are determined by the averages of the measured fragmentation probabilities listed in [38]. For the perturbative QCD rate, Eq. (4.3), which has no asymmetry if we ignore C violation but enters into the denominator of Eq. (4.61), we use the LO cross section. The factorization scale is set to be $\mu_f = \sqrt{p_T^2 + m_c^2}$.

When integrated over 2 GeV $< p_T <$ 18 GeV and $2.2 < \eta < 4.75$, excluding the region with 2 GeV $< p_T <$ 3.2 GeV, $2.2 < \eta < 2.8$, the asymmetry A_p for $D^\pm$ is found to be $-0.85\% < A_p < -1.06\%$ with $0.055 < \rho_1^{sm} < 0.065$, $0.65 < \rho_8^{sm} < 0.8$, $0.14 < \rho_1^{sf} < 0.18$ and $0.14 < \rho_8^{sf} < 0.18$. Figure 12 shows A_p as a function of pseudorapidity η and transverse momentum p_T of the $D^\pm$ mesons as predicted by the heavy quark recombination mechanism. Data from Ref. [11] are shown as well. The grey band is from varying the ρ parameters

within the ranges above. The dashed line is obtained using the central value of the ρ parameters and varying ϵ_c within its error bars. The calculated distributions are reasonably consistent with the data. Figure 13 shows the independence of A_p on the factorization scale μ_f when μ_f is varied the the range $\frac{1}{2}\sqrt{p_T^2+m_c^2} < \mu_f < 2\sqrt{p_T^2+m_c^2}$. The scale dependence is significant ($\sim 100\%$) at the high η and low p_T ends. An NLO calculation for the heavy quark recombination mechanism in the future will presumably reduce this theoretical uncertainty.

4.4 $\Lambda_Q/\overline{\Lambda}_Q$ PRODUCTION ASYMMETRIES

In this section, we make predictions for the rapidity and transverse momentum distributions of the asymmetries of heavy baryon productions using the heavy quark recombination mechanism in the forward region. The LHCb experiment should see an asymmetry in both Λ_c^+/Λ_c^- and $\Lambda_b^0/\overline{\Lambda}_b^0$ productions.

The production asymmetry A_p of a Λ_Q (udQ) baryon is defined by

$$A_p = \frac{d\sigma(\Lambda_Q) - d\sigma(\overline{\Lambda}_Q)}{d\sigma(\Lambda_Q) + d\sigma(\overline{\Lambda}_Q)}\,, \tag{4.61}$$

where Q is either c or b. The opposite-side recombination Eq. (4.21c) has two contributions:

$$(1) \qquad d\hat{\sigma}[\Lambda_Q] = \sum_n d\hat{\sigma}[qg \to (\overline{Q}q)^n + Q] \sum_{\overline{H}_{meson}} \rho[(\overline{Q}q)^n \to \overline{H}_{meson}] \otimes D_{Q\to\Lambda_Q}\,, \tag{4.62a}$$

$$(2) \qquad d\hat{\sigma}[\Lambda_Q] = \sum_n d\hat{\sigma}[\bar{q}g \to (\overline{Q}\bar{q})^n + Q] \sum_{\overline{H}_{baryon}} \eta[(\overline{Q}\bar{q})^n \to \overline{H}_{baryon}] \otimes D_{Q\to\Lambda_Q}\,, \tag{4.62b}$$

where H_{meson} and H_{baryon} are any heavy meson and heavy baryon respectively. For simplicity, we will take H to be a low-lying heavy hadron. Thus, for Λ_c production we will take H_{meson} to be either D or D^*, and H_{baryon} be any baryon from the lowest mass $J^p = \frac{1}{2}^+$ and $\frac{3}{2}^+$ heavy baryon $SU(3)$ flavor multiplets, and similarly for Λ_b production. We will also assume $SU(3)$ flavor symmetry.

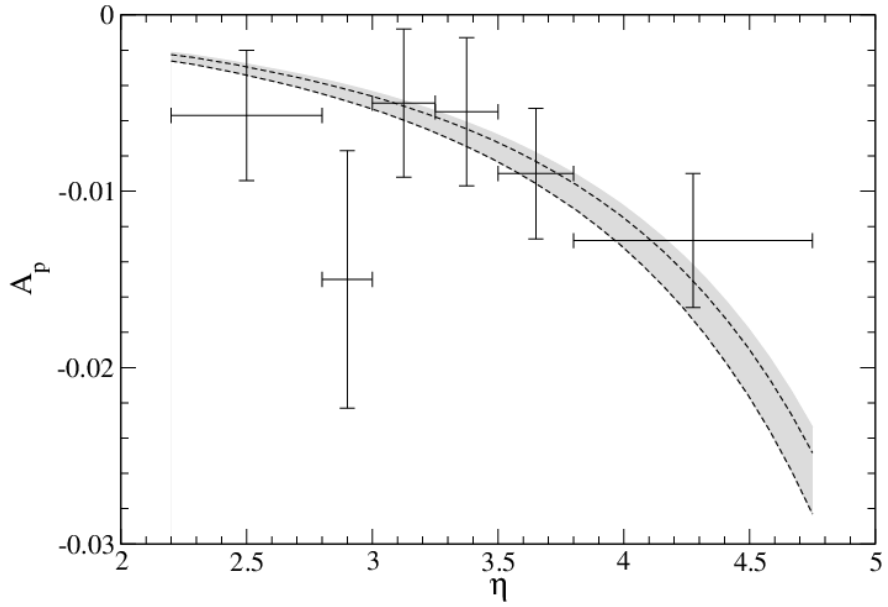

(a)

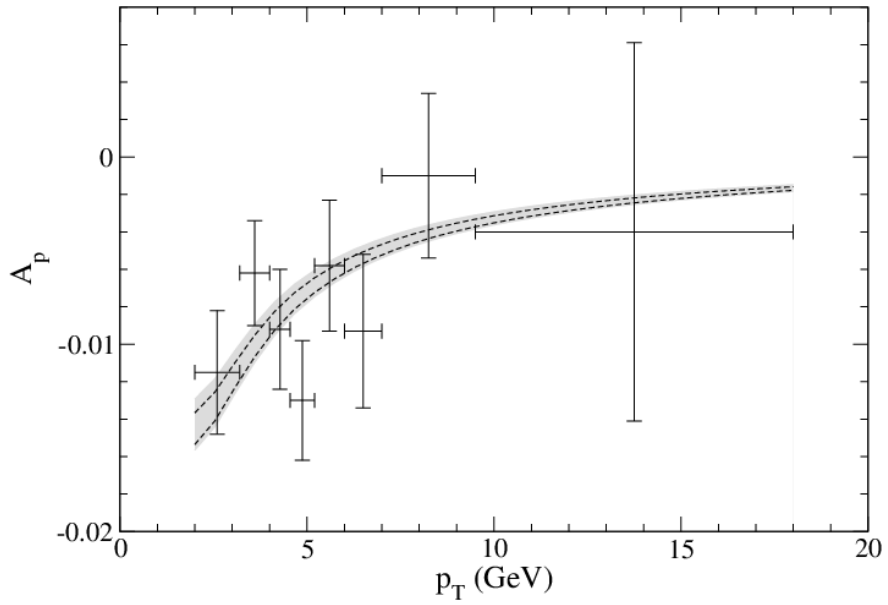

(b)

Figure 12: Asymmetry in $D^{\pm}$ production A_p as a function of (a) pseudorapidity η and (b) transverse momentum p_T in 7 TeV pp collisions. The data points are from LHCb [11]. The grey band is obtained by varying the ρs in the intervals $0.055 < \rho_1^{sm} < 0.065$, $0.65 < \rho_8^{sm} < 0.8$, $0.14 < \rho_1^{sf} < 0.18$ and $0.14 < \rho_8^{sf} < 0.18$ respectively. The dashed lines are from varying $0.055 < \epsilon_c < 0.69$.

We will only consider contributions leading in Λ_{QCD}/m_Q. The leading nonperturbative parameters $\rho[(c\bar{q})^n \to D]$ for D mesons are

$$\begin{aligned} \rho_1^{sm} &= \rho[c\bar{d}(^1S_0^{(1)}) \to D]\,, & \rho_1^{sf} &= \rho[c\bar{d}(^3S_1^{(1)}) \to D]\,, \\ \rho_8^{sm} &= \rho[c\bar{d}(^1S_0^{(8)}) \to D]\,, & \rho_8^{sf} &= \rho[c\bar{d}(^3S_1^{(8)}) \to D]\,. \end{aligned} \tag{4.63}$$

For D^* mesons, we can exploit heavy quark spin symmetry and get

$$\begin{aligned} \rho[c\bar{q}(^1S_0^{(c)}) \to D] &= \rho[c\bar{q}(^3S_1^{(c)}) \to D^*]\,, \\ \rho[c\bar{q}(^3S_1^{(c)}) \to D] &= \rho[c\bar{q}(^1S_0^{(c)}) \to D^*]\,. \end{aligned} \tag{4.64}$$

Similar relations are also true for B and B^*. The leading nonperturbative parameters $\eta[(Qq)^n \to \Lambda_Q]$ for Λ_Q baryons are

$$\begin{aligned} \eta_3 &= \eta[Qq(^1S_0^{(\bar{3})}) \to \Lambda_Q]\,, & \tilde{\eta}_3 &= \eta[Qq(^3S_1^{(\bar{3})}) \to \Lambda_Q]\,, \\ \eta_6 &= \eta[Qq(^1S_0^{(6)}) \to \Lambda_Q]\,, & \tilde{\eta}_6 &= \eta[Qq(^3S_1^{(6)}) \to \Lambda_Q]\,. \end{aligned} \tag{4.65}$$

All the ρ's and η's scale as Λ_{QCD}/m_Q. Contributions of feeddown from heavier baryons in processes Eqs. (4.21a) and (4.21b) can be taken into account by using the inclusive parameter η_{inc}:

$$\eta_{inc}[(Qq)^n \to \Lambda_Q] = \eta[(Qq)^n \to \Lambda_Q] + \sum_{H_{baryon} \neq \Lambda_Q} \eta[(Qq)^n \to H_{baryon}] Br[H_{baryon} \to \Lambda_Q + X]\,. \tag{4.66}$$

Here again we assume H_{baryon} is a member of the lowest mass $J^p = \frac{1}{2}^+$ and $\frac{3}{2}^+$ heavy baryon $SU(3)$ flavor multiplets. With our choice of possible $\overline{H}_{baryon}$ in the opposite-side recombination, by a simple quark counting and the fact that $Br[H_{baryon} \to \Lambda_Q + X] \approx 1$ for $H_{baryon} = \Sigma_Q$ or Σ_Q^*, we have

$$\sum_{\overline{H}_{baryon}} \eta[(\overline{Q}\bar{q}')^n \to \overline{H}_{baryon}] \approx \frac{3}{2} \eta_{inc}[(Qq)^n \to \Lambda_Q]\,, \tag{4.67}$$

where $q' = u, d, s$ and $q = u, d$. From Section 4.3, a reasonable fit to $D^\pm$ asymmetry at LHCb gives $0.055 < \rho_1^{sm} < 0.065$, $0.65 < \rho_8^{sm} < 0.8$, $0.14 < \rho_1^{sf} < 0.18$ and $0.14 < \rho_8^{sf} < 0.18$ for $\rho[(c\bar{d})^n \to D^+]$. Best single-parameter fit to $\Lambda_c^\pm$ asymmetry in fixed target experiments gives

$\tilde{\eta}_{3,inc} = 0.058$ for Λ_c [33]. We will take $\eta_{3,inc} = \eta_{6,inc} = \tilde{\eta}_{6,inc} = 0$ and $0.052 < \tilde{\eta}_{3,inc} < 0.064$ for Λ_c. For the η's for Λ_b and ρ's for B, we simply multiply the Λ_c and D counterparts by the theoretical scaling factor m_c/m_b. We use MSTW 2008 LO central PDFs with $m_c = 1.275$ GeV and $m_b = 4.18$ GeV. The fragmentation function $D_{Q\to\Lambda_Q}$ is taken as

$$D_{Q\to\Lambda_Q}(z) = f_{\Lambda_Q}\delta(1-z)\,, \tag{4.68}$$

where f_{Λ_Q} is the inclusive fragmentation probability. This form of fragmentation function was found to be better than the Peterson form when fitting to fixed target Λ_c^+/Λ_c^- asymmetry data [33]. We take $f_{\Lambda_c^+} = 0.101$, which is the average of the values listed in [38]. $f_{\Lambda_b^0}$ is taken to be 0.09 from [39]. We use the LO cross section for the perturbative QCD rate Eq. (4.3). The factorization scale is set to be $\mu_f = \sqrt{p_T^2 + m_Q^2}$.

For Λ_c^+/Λ_c^- production, the kinematic region is taken to be $2 < y < 5$ and 2 GeV $< p_T <$ 20 GeV. The integrated A_p is found to be $2.0\% < A_p(\Lambda_c^+/\Lambda_c^-) < 2.4\%$ for $\sqrt{s} = 7$ TeV and $1.2\% < A_p(\Lambda_c^+/\Lambda_c^-) < 1.5\%$ for $\sqrt{s} = 14$ TeV. For $\Lambda_b^0/\overline{\Lambda}_b^0$ production, the kinematic region is taken to be $2 < y < 5$ and 5 GeV $< p_T <$ 20 GeV. The integrated A_p is found to be $2.2\% < A_p(\Lambda_b^0/\overline{\Lambda}_b^0) < 2.6\%$ for $\sqrt{s} = 7$ TeV and $1.1\% < A_p(\Lambda_b^0/\overline{\Lambda}_b^0) < 1.4\%$ for $\sqrt{s} = 14$ TeV. Figures 14 and 15 show the rapidity and transverse momentum distributions of A_p for Λ_c^+/Λ_c^- and $\Lambda_b^0/\overline{\Lambda}_b^0$ respectively. The asymmetry is significant at the high-rapidity and low-p_T ends ($\sim 2 - 15\%$). Because of this, the integrated A_p is sensitive to the upper rapidity cut and lower p_T cut. Figures 16 and 17 show the dependence of the integrated A_p on the upper rapidity cut and lower p_T cut for Λ_c^+/Λ_c^- and $\Lambda_b^0/\overline{\Lambda}_b^0$ respectively. The kinematic regions are the same as in Figs. 14 and 15 except for the variations in the upper rapidity cut and lower p_T cut. In order to give an idea of the size of the recombination cross section relative to the standard perturbative QCD cross section, the ratio of the two cross sections is plotted in Fig. 18 as a function of rapidity and transverse momentum respectively for Λ_c^+ and Λ_c^- productions in 7 TeV pp collisions.

It should also be noted that Eqs. (4.21a), (4.21b), (4.62a) and (4.62b) have corrections suppressed by powers of Λ_{QCD}/p_T and m_Q/p_T, which we have neglected in our calculations. As a result, in principle our calculations should have large theoretical uncertainties for $p_T \sim m_Q$. However, as shown in Section 4.3, the heavy quark recombination works reasonably

well at regions of p_T as low as $p_T \sim 2$ GeV in explaining the $D^{\pm}$ asymmetries at LHCb. Therefore, it seems reasonable to include the $p_T \sim m_Q$ region in our calculations.

Shown in Fig. 19 are the CMS data [40], which are the rapidity and transverse momentum distributions of $\sigma(\overline{\Lambda}_b^0)/\sigma(\Lambda_b^0)$ for 7 TeV pp collisions in the kinematic region $0 < y < 2$ and 10 GeV $< p_T <$ 50 GeV. The CMS data, in spite of the large error bars, do have a slight trend of surplus of Λ_b^0 over $\overline{\Lambda}_b^0$ in the regions of high rapidity and low transverse momentum respectively. However, with the values of η's we used above, the asymmetry predicted from the heavy quark recombination mechanism is negligible in this kinematic region. To see the limit of the heavy quark recombination mechanism in explaining the data, in Fig. 19 we also plot the prediction with larger values of η's. Here all η_{inc}'s are set equal to each other, with the range being $\Lambda_{QCD}/m_b \sim 0.2 < \eta_{inc} < 1$. The ranges of the ρs are as those used in Fig. 15. Although the prediction shows a significant asymmetry $\sim 10\%$ at the high-rapidity and low-p_T ends, it still fails to hit the bin with the largest rapidity. Fig. 20 shows the prediction in the forward region $2 < y < 5$ and 5 GeV $< p_T <$ 20 GeV for 7 TeV pp collisions with the ranges of η's and ρ's as in Fig. 19. The asymmetry is huge ($\sim 50\%$). We believe that our previous predictions with smaller η_{inc}'s (Figs. 14-17) are more reasonable since those values of η's were obtained from better fit to fixed-target experiments. Moreover, the surplus of $\overline{\Lambda}_b^0$ over Λ_b^0 at $y \sim 1$ and $p_T > 20$ GeV in the CMS data cannot be explained by any existing model. We hope that data from LHCb in the future will settle the issue.

4.5 DISCUSSION

In the heavy quark recombination mechanism, it is assumed that the quark pair $Q\bar{q}$ coming out from the hard partonic collision hadronizes into the heavy hadron H with no momentum loss. In principle, only a fraction z of the momentum of the quark pair hadronizes into H. However, this would inevitably introduce a z dependence in the non-perturbative parameters ρ's which has to be determined by a large mount of data. Therefore, in this sense, the heavy quark recombination mechanism is a model.

An appealing feature of the heavy quark recombination mechanism is that it has its

basis in perturbative QCD and HQET and so the theoretical errors can be systematically reduced. One obvious direction of improvement is to include the power-suppressed contributions from P waves. Another direction of improvement is to calculate to higher orders in α_s. Note that there are three separately scales: $p_T \gg m_Q \gg \Lambda_{QCD}$. One should be able to resum $\ln^n(m_Q/p_T)$ by SCET. However, since we are looking at low-p_T (non-leading twist) phenomena, we expect that $\ln^n(m_Q/p_T)$ is not large. $\ln^n(\Lambda_{QCD}/m_Q)$ can be resummed by HQET. At a low scale $\mu \sim \Lambda_{QCD}$, the heavy quark symmetry holds well and so we have $\rho[(Q\bar{q})^n \to H_b, \mu] \approx (m_c/m_b)\rho[(Q\bar{q})^n \to H_c, \mu]$. If the running of the ρ's is known, one can derive a relation between $\rho[(Q\bar{q})^n \to H_b, m_b]$ and $\rho[(Q\bar{q})^n \to H_c, m_c]$. This would lead to non-trivial relations between the predictions on charm hadron productions and bottom hadron productions.

It should be emphasized that the heavy quark recombination mechanism is not the only possible way to give rise to production asymmtries of heavy hadrons at the LHC. Other models for soft processes in QCD also give qualitatively similar asymmetries. While a quantitative analysis of the differences of these models is beyond the scope of this thesis, we discuss the qualitative properties of a few of the models below.

The first example of another model is the valon model [41]. In this model, initial-state hadrons involved in soft scatterings are composed of valons, which are valence quarks dressed by gluons and quark-antiquark pairs. A heavy quark induced by fluctuations in a valon would combine with light quarks in the valons from the same initial-state hadron to form a heavy hadron. The valon distributions are non-perturbative and were obtained by fitting to data of soft hadronic scattering, so are the distributions of light valence and sea quarks inside a valon. Since a heavy quark-antiquark pair is a tightly bound system in a valon, it has a wide momentum spread. The probability to find a heavy quark in a valon is therefore assumed to be uniform in momentum fraction. The probability for a heavy quark and quarks to combine and form a heavy hadron has its dependence on momentum fractions determined by a counting rule. The model predicts a surplus of the produced H over $\overline{H}$ in pp collisions since the light valence quarks of the H or $\overline{H}$ come from the valons of the initial-state protons. This model has the nice feature of the absence of free parameters in the prediction of A_p. However, it makes no prediction on the p_T distribution of the produced heavy hadron since

the effect of a transverse kick is neglected [41].

The second model is the intrinsic heavy quark model [42]. In this model, an initial-state proton is in a superposition of Fock states $|uud\ldots\rangle$, where "$\ldots$" denotes an arbitrary number of quark-antiquark pairs and gluons. The heavy quark Q in $|uudQ\overline{Q}\rangle$ can combine with the valence light quarks to form a heavy hadron H. The probability for Fock state $|uudQ\overline{Q}\rangle$ with a given momentum fraction distribution among the quarks is assumed a simple form proportional to $\alpha_s^4(m_{Q\overline{Q}})$. The produced H has momentum fraction given simply by the sum of those of the light quarks and Q forming it. The idea is therefore very similar to that of the valon model. Formally, this model gives an asymmetry suppressed by an extra power of α_s relative to that predicted by the heavy quark recombination mechanism.

The third model is the string-drag model [43], in which a heavy quark produced by parton fusion is dragged toward the spectator quarks by color strings connecting them. The surplus of the produced H over $\overline{H}$ is due to the surplus of spectator valence quarks over the sea quarks. The dragging effect is non-perturbative and can only be taken into account by Monte Carlo simulations.

Comparison of predictions on the asymmetry from the heavy quark recombination mechanism and these three models will be an interesting work to follow up. Qualitatively all the models are similar since in order to have any asymmetry, some type of interaction that distinguishes the initial state is necessary. The interaction is with a spectator quark or the proton remnant, giving rise to the possibility of a hadron-antihadron asymmetry. Given the fact that we are dealing with hadronic initial and final states, there will always be some nonperturbative input into any calculation. Of note, however, is that the heavy quark recombination model only has standard PDFs in the initial state. The other models mentioned above must include additional nonperturbative inputs for the initial state.

4.6 SUMMARY

In this chapter, motivated by the relevance in the search for CP violation at the LHC, we investigated the production asymmetries of heavy hadrons using the heavy quark recombi-

nation mechanism. After a brief review of the heavy quark recombination mechanism, we calculated the partonic cross sections for P-waves in heavy quark recombination mechanism. After that, we applied the heavy quark recombination mechanism to explain the production asymmetries of D^+/D^- observed at LHCb. We found that with suitably chosen sizes of several non-perturbative parameters, the p_T and η distributions of the production asymmetry can be explained well. We also made preliminary predictions on production asymmetries for heavy baryons Λ_c^+/Λ_c^- and $\Lambda_b/\overline{\Lambda}_b$. We found that the asymmetries are significant in the forward region and should be measurable at LHCb.

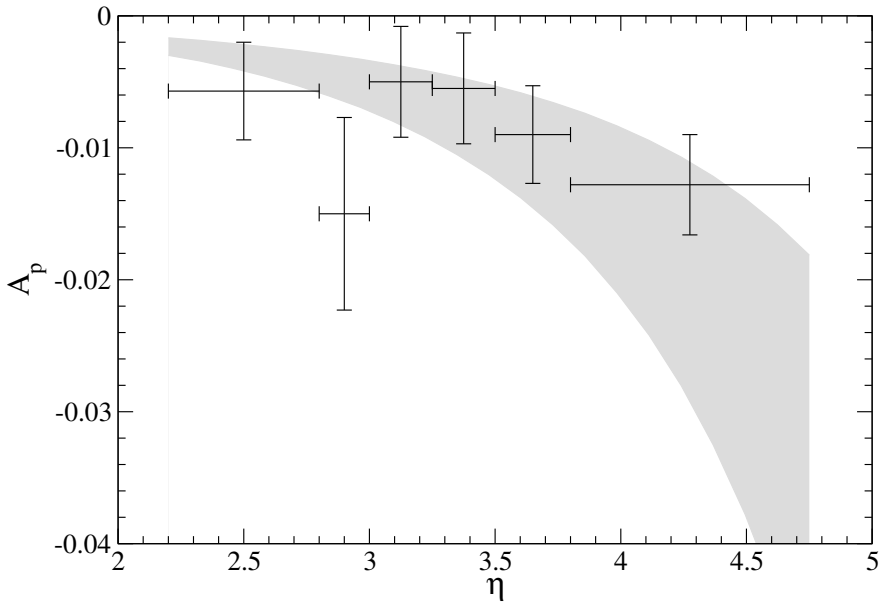

(a)

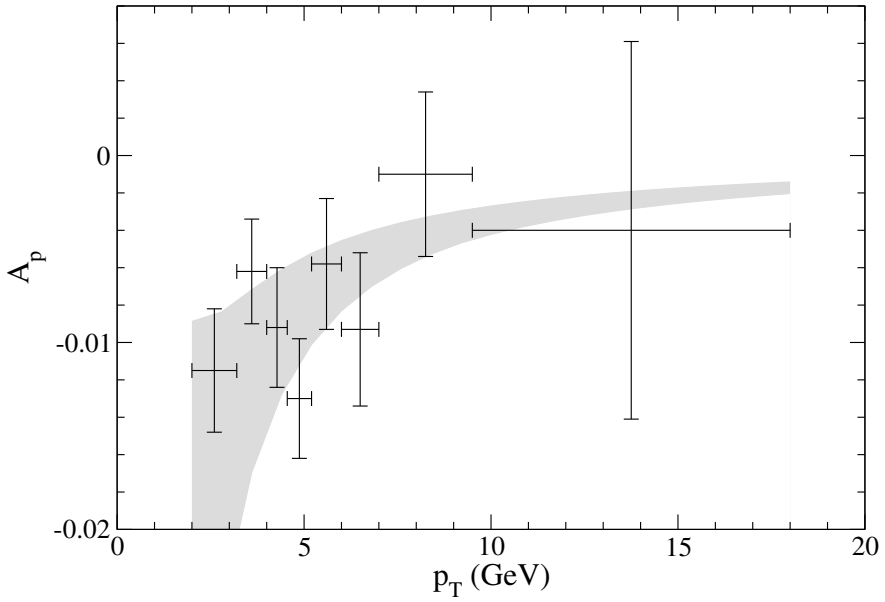

(b)

Figure 13: Asymmetry in $D^{\pm}$ production A_p as a function of (a) pseudorapidity η and (b) transverse momentum p_T in 7 TeV pp collisions. The data points are from LHCb [11]. The grey band is obtained by varying μ_f in the interval $\frac{1}{2}\sqrt{p_T^2 + m_c^2} < \mu_f < 2\sqrt{p_T^2 + m_c^2}$. The ρ's are taken to be central values of the ranges in Fig. 12. ϵ_c is taken to be 0.06.

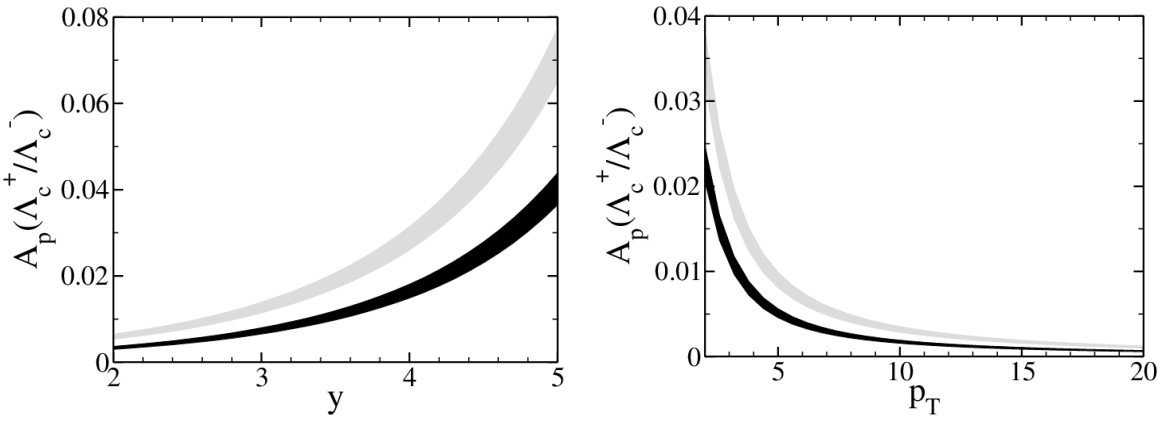

(a) (b)

Figure 14: Asymmetry in Λ_c^+/Λ_c^- production as a function of (a) rapidity y and (b) transverse momentum p_T in the kinematic region $2 < y < 5$ and 2 GeV $< p_T <$ 20 GeV in 7 TeV (grey band) and 14 TeV (black band) pp collisions.

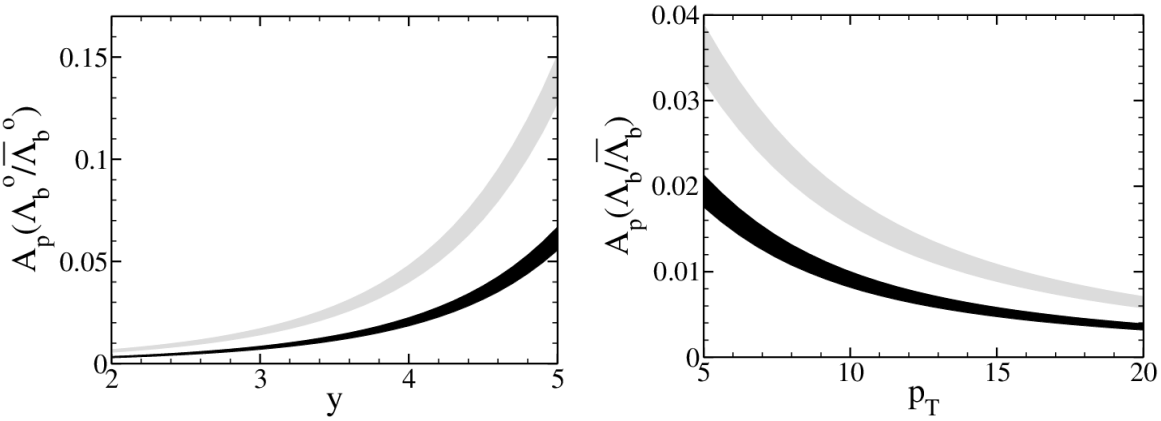

(a) (b)

Figure 15: Asymmetry in $\Lambda_b^0/\overline{\Lambda}_b^0$ production as a function of (a) rapidity y and (b) transverse momentum p_T in the kinematic region $2 < y < 5$ and 5 GeV $< p_T <$ 20 GeV in 7 TeV (grey band) and 14 TeV (black band) pp collisions.

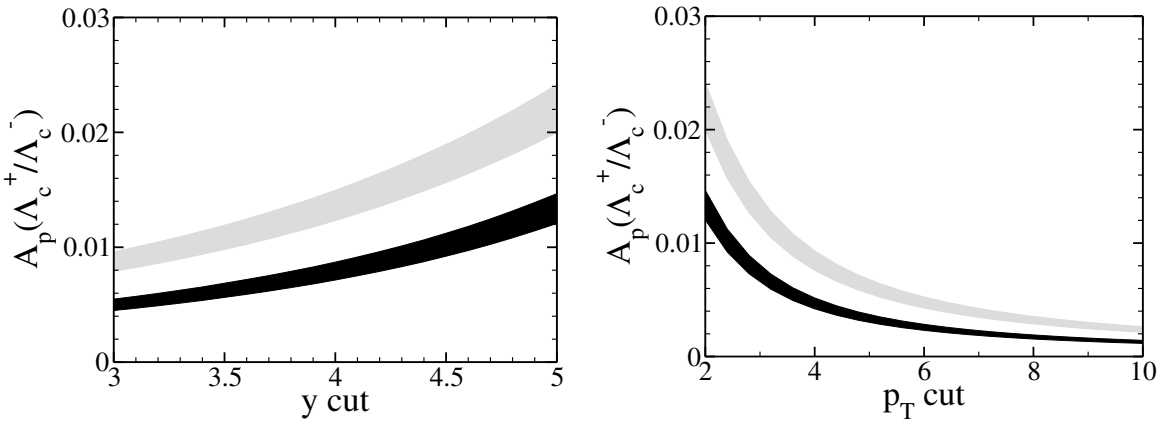

(a) (b)

Figure 16: Integrated asymmetry in Λ_c^+/Λ_c^- production as a function of (a) upper y cut and (b) lower p_T cut in the kinematic region $2 < y < 5$ and 2 GeV $< p_T <$ 20 GeV in 7 TeV (grey band) and 14 TeV (black band) pp collisions.

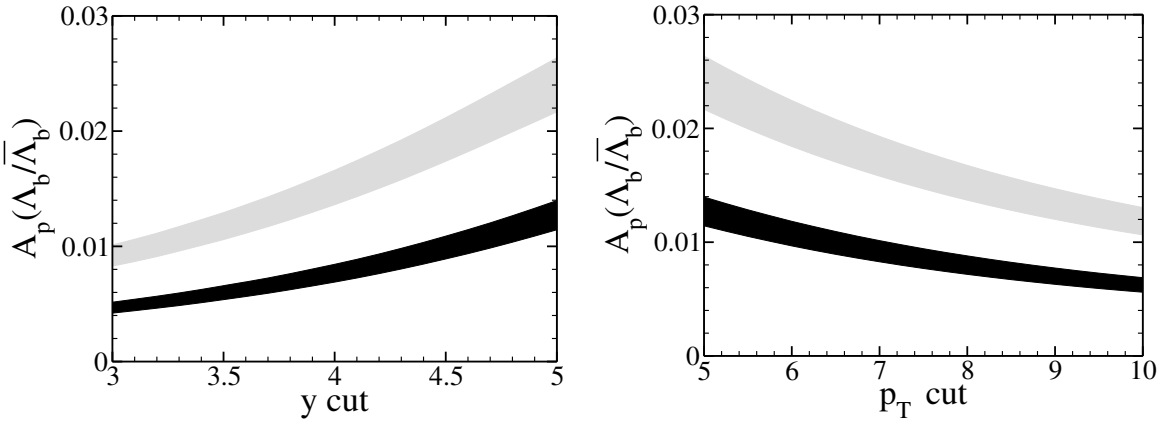

(a) (b)

Figure 17: Integrated asymmetry in $\Lambda_b^0/\overline{\Lambda}_b^0$ production as a function of (a) upper y cut and (b) lower p_T cut in the kinematic region $2 < y < 5$ and 5 GeV $< p_T <$ 20 GeV in 7 TeV (grey band) and 14 TeV (black band) pp collisions.

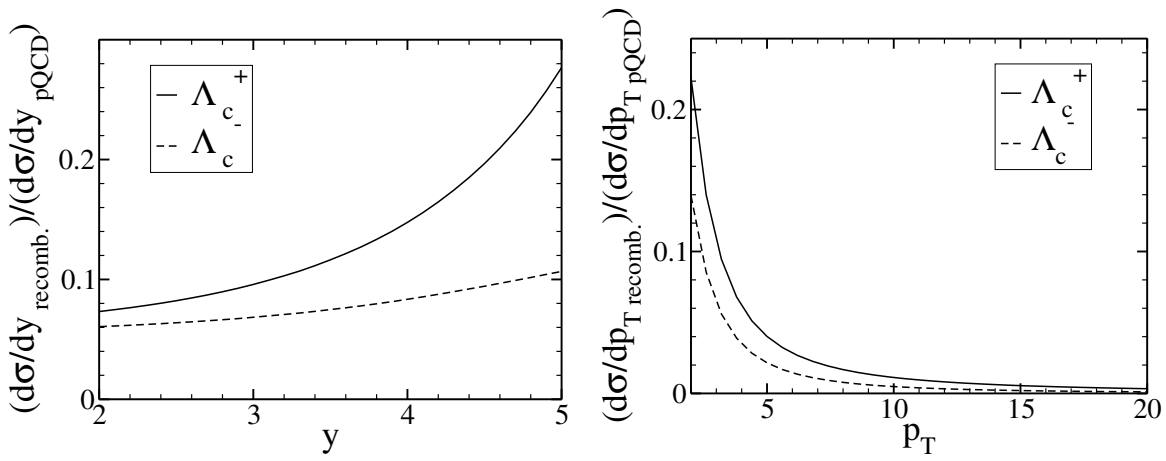

(a) (b)

Figure 18: Distributions in (a) rapidity and (b) transverse momentum of ratio of recombination cross section to standard perturbative QCD cross section for Λ_c^+ and Λ_c^- productions in 7 TeV pp collisions. ρ's and η's are taken to be central values of those used in Fig. 14.

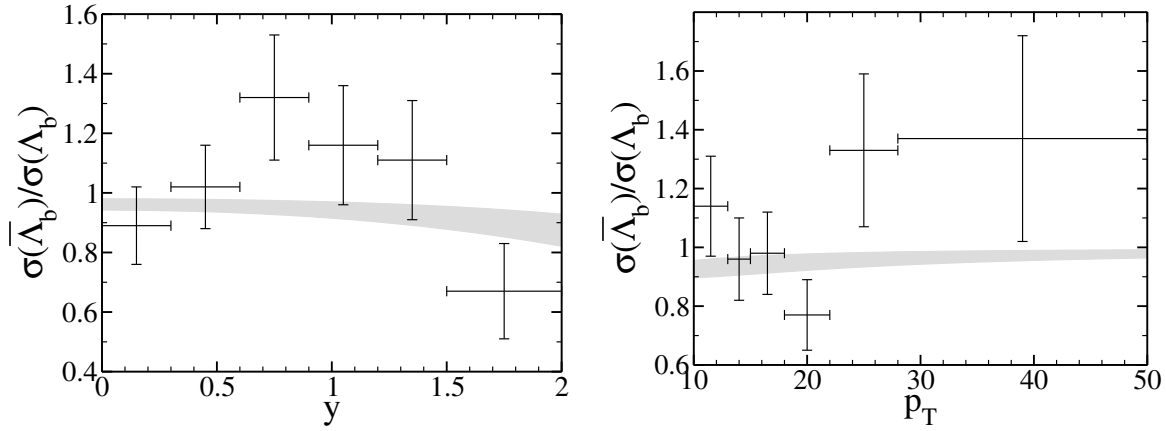

(a) (b)

Figure 19: $\sigma(\overline{\Lambda}_b^0)/\sigma(\Lambda_b^0)$ as a function of (a) rapidity y and (b) transverse momentum p_T in the kinematic region $0 < y < 2$ and 10 GeV $< p_T <$ 50 GeV for 7 TeV pp collisions. The data are from CMS [40]. The grey band is our prediction from the heavy quark recombination mechanism with all η_{inc}'s set equal to each other, the range being $0.2 < \eta_{inc} < 1$. The ranges of ρ's are as those used in Fig. 15.

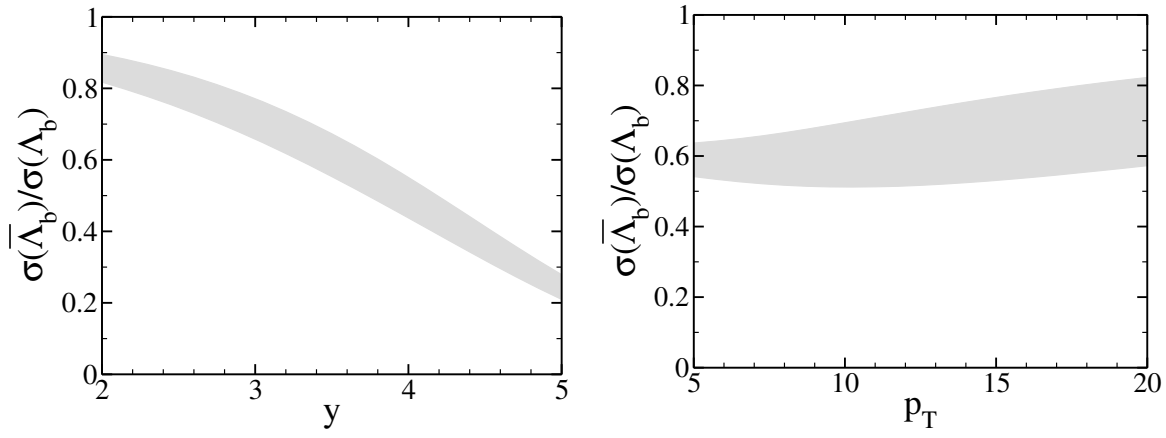

(a) (b)

Figure 20: $\sigma(\overline{\Lambda}_b^0)/\sigma(\Lambda_b^0)$ as a function of (a) rapidity y and (b) transverse momentum p_T in the kinematic region $2 < y < 5$ and 5 GeV $< p_T <$ 20 GeV for 7 TeV pp collisions. The grey band is our prediction from the heavy quark recombination mechanism with all η_{inc}s set equal to each other, the range being $0.2 < \eta_{inc} < 1$. The ranges of ρ's are as those used in Fig. 15.

5.0 THRESHOLD RESUMMATION IN ASSOCIATED HIGGS PRODUCTION WITH A VECTOR BOSON

5.1 INTRODUCTION

The recent discovery of a Higgs-like particle [2, 3] has brought our understanding of electroweak symmetry breaking to a deeper level. Now it is imperative to study the detailed properties of this particle in the hope of finding any hints for new physics beyond the Standard Model (SM). An important Higgs production mechanism at hadron colliders is the associated production of a Higgs boson and a vector boson, VH ($V = W^{\pm}, Z$) [44]. At the Tevatron, the process $q\overline{q}' \to VH$ with the decay of the vector boson to leptons and of the Higgs to the $b\bar{b}$ and W^+W^- channels has provided important sensitivity to a light Higgs boson [45, 46]. At the LHC, the production rate for associated VH production is small, but with ~ 30 fb^{-1} a light Higgs in association with a W or Z can potentially be observed in the boosted regime via $H \to b\bar{b}$ [47]. Reliable predictions are essential for the observation and study of the VVH couplings in this channel [48, 49].

The rate for associated VH production is perturbatively known to next-to-next-to-leading order (NNLO), i.e. $\mathcal{O}(\alpha_s^2)$ [50, 51]. At next-to-leading order (NLO), the QCD corrections are identical to those of the Drell-Yan process for an off-shell gauge boson, $q\overline{q}' \to V^*$ [52, 53, 54]. At NNLO, however, the ZH process receives a small additional contribution from the gg initial state, $gg \to ZH$ [50]. The NLO rates are available in the general purpose MCFM [55] program, while the total rate can be found to NNLO using the VH@NNLO code [50].

Infrared finite results in higher-order QCD processes occur due to a cancellation of virtual and real soft divergences. The fixed-order calculation is reliable providing all of the scales

are of the same order of magnitude. When the invariant mass M_{VH} of the final state particles WH or ZH approaches the center-of-mass energy of the colliding partons, there is less phase space available for real emission. While the infrared divergences will still cancel, large Sudakov logarithms will remain. These logarithms can spoil the convergence of the perturbative series and need to be resummed to all orders for reliable results in this threshold region. Threshold corrections involve terms of the form $\alpha_s^n \frac{\log^{2n-1}(1-z)}{(1-z)}$, which are large when $z = M_{VH}^2/\hat{s} \sim 1$, where $\hat{s}$ is the partonic center-of-mass (c.m.) energy-squared [56, 57, 58].

We present for the threshold resummation of the process $pp \to VH + X$ at the LHC in the SCET framework. Since the final state particles are color-singlets, the resummation can be straight-forwardly adopted from results in the literature for the Drell-Yan process [58]. Section 5.2 contains a brief review of the resummation formalism we apply. Section 5.3 presents results for the total cross section and the M_{VH} distribution including the resummation of threshold logarithms and a discussion of the theoretical uncertainties. Finally, Section 5.4 summarizes our results and discusses the relevance of them to searches at the LHC. The work of this chapter was published in Ref. [59].

5.2 THRESHOLD RESUMMATION IN SCET

In the original approach to threshold resummation [56, 60], the resummation is performed after taking the Mellin transformation of the hadronic cross section [61, 62]. The Mellin-transformed hadronic cross section can then be factored into the product of the partonic cross section and the parton luminosity. The threshold logarithms for VH production are of the form $\ln^n(1-z)$, where $z = M_{VH}^2/\hat{s}$, and are contained in the partonic cross section. After resummation, an inverse-Mellin transformation is performed to obtain the physical cross section. This leads to a new divergence due to the presence of the Landau pole in α_s. Prescriptions for how to perform the inverse-Mellin transformation have been developed to remove this problem. The resummation of threshold logarithms for Drell-Yan production has been extensively studied [63, 64, 65, 66].

More recently, techniques using soft-collinear effective theory (SCET) [20, 21, 67] have

been developed in which the resummation is performed in momentum space, obviating the need to go to Mellin space. This in turn removes the problem of the Landau pole. In this section, we will generalize the SCET resummation formulation of [58] to the case of VH production.

To lowest electroweak order, the differential cross section of the process $pp \to VH + X$ (Fig. 21) in the invariant mass M_{VH} of the VH pair is given by

$$\frac{d\sigma}{dM_{VH}^2} = -\frac{N_c \hat{\sigma}_0}{2\pi(c_v^2 + c_a^2)} \int \frac{d^3q}{(2\pi)^3 2q^0} \int d^4x\, e^{-iq\cdot x} \langle p_1 p_2 | J_V^{\mu\dagger}(x) J_{V\mu}(0) | p_1 p_2 \rangle \,, \tag{5.1}$$

where q is the momentum of the virtual vector boson V^* and $\hat{\sigma}$ is the leading order partonic cross section

$$\hat{\sigma}_0(M^2) = (c_v^2 + c_a^2) \frac{G_F^2 M_V^4 \lambda^{1/2}(M_V^2, M_H^2, M^2)}{96\pi N_c \left(1 - M_V^2/M^2\right)^2} \left(\lambda(M_V^2, M_H^2, M^2) + \frac{12 M_V^2}{M^2} \right) , \tag{5.2}$$

with

$$\begin{aligned} c_v &= 2T_3 - 4Q \sin^2\theta_W \,, \quad \text{for } V = Z \,, \\ c_v &= -c_a = \sqrt{2} \,, \qquad\qquad \text{for } V = W \,, \end{aligned}$$

and

$$\lambda(x, y, z) = \left(1 - \frac{x}{z} - \frac{y}{z}\right)^2 - \frac{4xy}{z^2} \,. \tag{5.3}$$

J_V^μ is the quark current coupled to the vector boson V:

$$\begin{aligned} J_W^\mu &= \sum_{i=1}^{3} V^{ij} W^+ \bar{u}^i \gamma^\mu (1 - \gamma_5) d^j + h.c. \,, \\ J_Z^\mu &= \sum_{i=1}^{3} \left\{ \bar{u}^i \gamma^\mu \left[\left(1 - \frac{8}{3}\sin^2\theta_W\right) - \gamma_5 \right] u^i + \bar{d}^i \gamma^\mu \left[\left(-1 + \frac{4}{3}\sin^2\theta_W\right) + \gamma_5 \right] d^i \right\} . \end{aligned} \tag{5.4}$$

In the threshold region $z = M_{VH}^2/\hat{s}^2 \sim 1$, we have the SCET_I scenario with small parameter $\lambda = \sqrt{1-z}$. Let n and $\bar{n}$ be the light-like vectors parallel to the two beams respectively (n along p_1 and $\bar{n}$ along p_2). We have three types of modes

$$\begin{aligned} \text{hard}: &\quad p_h \sim \sqrt{\hat{s}}(1, 1, 1) \,, \\ \text{collinear}: &\quad p_n \sim \sqrt{\hat{s}}(1, \lambda^2, \lambda) \,, \\ \text{anti-collinear}: &\quad p_{\bar{n}} \sim \sqrt{\hat{s}}(\lambda^2, \lambda) \,, \\ \text{ultrasoft}: &\quad p_{us} \sim \sqrt{\hat{s}}(\lambda^2, \lambda^2, \lambda^2) \,. \end{aligned} \tag{5.5}$$

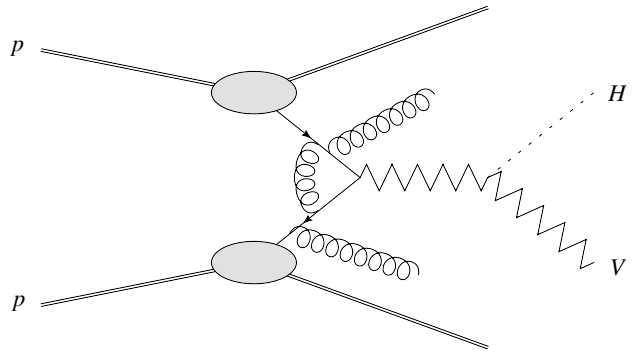

Figure 21: $pp \to VH + X$ to lowest electroweak order.

Note that the currents have the form $J_V^\mu = \bar{\psi}\,(c_v + c_a\gamma_5)\,\psi$ with J_V^μ is thus matched to a SCET current at leading power in λ as

$$J^\mu(0) = \int_{-\infty}^{\infty} ds\,dt\,\tilde{C}_V(s,t,\mu_f)\bar{\chi}_{\bar{n}}(0)e^{in\cdot\mathcal{P}_{\bar{n}}^\dagger s}\gamma_\perp^\mu\,(c_v' + c_a'\gamma_5)\,e^{-i\bar{n}\cdot\mathcal{P}_n t}\chi_n(0) + h.c.\,, \tag{5.6}$$

where $\chi_n \equiv W_n^\dagger\xi_n$ and $\chi_{\bar{n}} \equiv W_{\bar{n}}^\dagger\xi_{\bar{n}}$ are the collinear-gauge invariant collinear quark fields. Applying the BPS field redefinition, we have

$$\bar{\chi}_{\bar{n}}(0)e^{in\cdot\mathcal{P}_{\bar{n}}^\dagger s}\gamma_\perp^\mu\,(c_v' + c_a'\gamma_5)\,e^{-i\bar{n}\cdot\mathcal{P}_n t}\chi_n(0) \to \bar{\chi}_{\bar{n}}(0)e^{in\cdot\mathcal{P}_{\bar{n}}^\dagger s}\gamma_\perp^\mu\,(c_v' + c_a'\gamma_5)\,Y_{\bar{n}}^\dagger(0)Y_n(0)e^{-i\bar{n}\cdot\mathcal{P}_n t}\chi_n(0)\,. \tag{5.7}$$

Here comes the question of whether $c_v'/c_a' = c_v/c_a$ when the matching is done to high orders in α_s. We now show that this is true at NNLO. We adopt the 't Hooft-Veltman covention of γ_5 in dimensional regularization, that is

$$\begin{aligned} \{\gamma_5, \gamma^\mu\} &= 0\,, \ \text{for}\,\mu = 0,1,2,3, \\ [\gamma_5, \gamma^\mu] &= 0\,, \ \text{for}\,\mu > 3. \end{aligned} \tag{5.8}$$

The matching at NLO is shown in Fig. 22. On the QCD side, the γ_5 in the axial part can pass through a quark-gluon vertex using Eqn. (5.8) and so we get the same radiative correction for both the vector and axial parts. On the SCET side, it is trivial that γ_5 is not involved in the loops, since the n-collinear sector is decoupled from the $\bar{n}$-collinear sector after the BPS field redefinition. For the matching at NNLO, the γ_5 on the SCET side is not

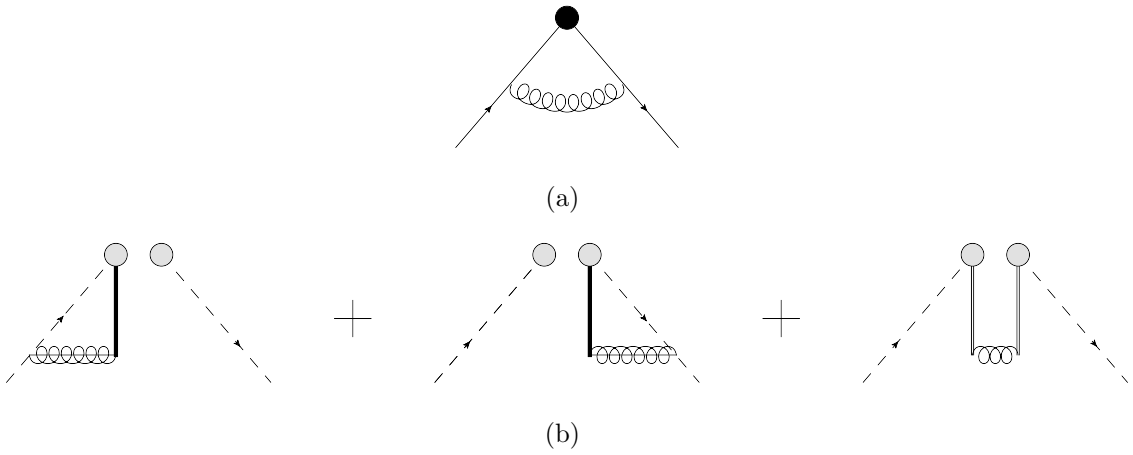

Figure 22: Matching of the QCD current J_V^μ (a) to the SCET current (b) at NLO. The Collinear Wilson lines and ultrasoft Wilson lines are denoted by bold lines and double lines respectively.

involved in the loops by the same reason. However, on the QCD side, γ_5 can pass through quark-gluon vertices and get out of all loops except for one graph, which is shown in Fig. 23. This graph involves a anomalous triangle, which is proportional to $k_1^\mu k_2^\nu$, with k_1^μ and k_2^μ being the momenta of the two virtual gluons. The contraction of these gluon momenta on the external-leg fermion line gives zero by the $U(1)$ Ward identity. For the vector part in the same graph, the triangle gives zero owing to Furry's theorem. Therefore, the QCD diagram in Fig. 23 vanishes. As a result, at NNLO, we have $c_v'/c_a' = c_v/c_a$ and so are free to set $c_v' = c_v$ and $c_a' = c_a$.

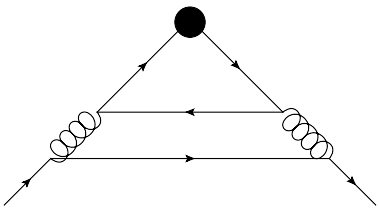

Figure 23: The graph on the QCD side in the matching of currents at NNLO which involves an anomalous triangle.

Define the Wilson coefficient in momentum space by

$$C_V(-\omega_1\omega_2 - i\epsilon, \mu_f) \equiv \int_{-\infty}^{\infty} d\omega_1 d\omega_2\, e^{-i\omega_2 s + i\omega_1 t} \tilde{C}_V(s,t,\mu_f)\,, \tag{5.9}$$

where the prescription $-i\epsilon$ denotes the relevant side along the branch cut. Note that C only depends on the product $\omega_1\omega_2$ of the hard components of the momenta of the quark and anti-quark going into the hard vertex. Substituting Eqn. (5.9) into (5.6) yields

$$J^\mu(0) = \int_{-\infty}^{\infty} d\omega_1 d\omega_2\, C_V(-\omega_1\omega_2 - i\epsilon, \mu_f) \bar{\chi}_{\bar{n},\omega_2}(0) \gamma_\perp^\mu \left(c_v + c_a\gamma_5\right) Y_{\bar{n}}^\dagger(0) Y_n(0) \chi_{n,\omega_1}(0) + h.c.\,, \tag{5.10}$$

where $\chi_{n,\omega}(x) \equiv \delta(\bar{\mathcal{P}} - \omega)\chi_n(x)$. Using Eqn. (5.10), after a Fierz transformation and averaging over initial state colors in Eqn. (5.1), we have

$$\begin{aligned}\frac{d\sigma}{dM_{VH}^2} = \hat{\sigma}_0 |C_V(-M_{VH}^2 - i\epsilon, \mu_f)|^2 \sum_{q,q'} \int_0^1 dx_1 dx_2 \left[f_{q/N}(x_1,\mu_f) f_{\bar{q}'}(x_2,\mu_f) + (q \leftrightarrow \bar{q}')\right] \\ \times \int \frac{d^3q}{(2\pi)^3 2q^0} \frac{1}{2\pi} \int d^4x\; e^{i\left(x_1 \bar{n}\cdot p_1 \frac{n}{2} + x_2 n\cdot p_2 \frac{\bar{n}}{2} - q\right)\cdot x} \hat{W}_{DY}(x,\mu_f)\,,\end{aligned} \tag{5.11}$$

where

$$f_{q/p}(x,\mu) = \langle p | \bar{\chi}_n(0) \frac{\bar{n}\!\!\!/}{2} \chi_{n, x\bar{n}\cdot p}(0) |p\rangle\,, \tag{5.12}$$

$$f_{\bar{q}/p}(x,\mu) = -f_{q/p}(-x,\mu)\,, \tag{5.13}$$

are the quark and anti-quark PDFs respectively and

$$\hat{W}_{\rm DY}(x,\mu) = \frac{1}{N_c} \langle 0 | {\rm Tr} \bar{\mathbf{T}} \left[Y_{\bar{n}}^\dagger(x) Y_n(x)\right] \mathbf{T} \left[Y_{\bar{n}}^\dagger(0) Y_n(0)\right] |0\rangle \tag{5.14}$$

is the Drell-Yan soft function. In Eqn. (5.1), the quark flavors q and q' to be summed depends on V being Z or $W^\pm$. The squared CKM matrix elements are absorbed into the definition of $\hat{\sigma}_0$. In the partonic c.m. frame, $q^0 \gg |\vec{q}|$ in the $z \to 1$ limit. So q^0 is independent of $|\vec{q}|$. Integrating over d^3q yields a $\delta^3(\vec{x})$. Also note that in the partonic c.m. frame,

$$x_1 \bar{n}\cdot p_1 \frac{n^0}{2} + x_2 n\cdot p_2 \frac{\bar{n}^0}{2} - q^0 = \sqrt{\hat{s}}(1-z)\,. \tag{5.15}$$

Define the momentum-space soft function

$$W_{\rm DY}(\omega,\mu) = \int \frac{dx^0}{4\pi}\; e^{i\omega x^0} \hat{W}_{\rm DY}(x^0, \vec{x}=0, \mu)\,. \tag{5.16}$$

We have

$$\frac{d\sigma}{dM_{VH}^2} = \frac{\hat{\sigma}_0}{s}|C_V(-M_{VH}^2 - i\epsilon, \mu_f)|^2 \sum_{q,q'} \int_0^1 \frac{dx_1}{x_1}\frac{dx_2}{x_2}\left[f_{q/N}(x_1,\mu_f) f_{\bar{q}'}(x_2,\mu_f) + (q \leftrightarrow \bar{q}')\right]$$
$$\times \sqrt{\hat{s}} W_{DY}(\sqrt{\hat{s}}(1-z), \mu_f)\,. \tag{5.17}$$

Changing the integration variable from x_2 to z, we arrive at the final form of hadronic the cross section

$$\frac{d\sigma}{dM_{VH}^2} = \frac{\hat{\sigma}}{s}\int_\tau^1 \frac{dz}{z} C(z, M_{VH}, \mu_f)\mathcal{L}\left(\frac{\tau}{z}, \mu_f\right), \tag{5.18}$$

where $\tau = M_{VH}^2/s$ and $\mathcal{L}$ is the parton luminosity,

$$\mathcal{L}(y,\mu_f) = \sum_{q,q'}\int_y^1 \frac{dx}{x} f_q(x,\mu_f) f_{\bar{q}'}\left(\frac{y}{x},\mu_f\right) + (q \leftrightarrow \overline{q}')\,, \tag{5.19}$$

where C is factorized into a hard function H and a soft function S:

$$C(z, M_{VH}, \mu_f) = \mathcal{H}(M_{VH},\mu_f)\mathcal{S}(M_{VH}(1-z),\mu_f),, \tag{5.20}$$

with

$$\mathcal{H}(M_V H, \mu_f) = |C_V(-M_{VH}^2 - i\epsilon, \mu_f)|^2 \tag{5.21}$$

and

$$\mathcal{S}(M_{VH}(1-z),\mu_f) = \sqrt{\hat{s}} W_{DY}(M_{VH}(1-z),\mu_f), \tag{5.22}$$

where we used $\sqrt{\hat{s}}(1-z) = M_{VH}(1-z) + \mathcal{O}(\lambda^4)$.

Eqn. (5.18) was first derived in fixed-order perturbative QCD [68] without a factorization of $C(z, M_{VH}, \mu_f)$ into a hard and a soft part. Perturbative QCD gives $C(z, M_{VH}, \mu_f) = \delta(1-z) + \mathcal{O}(\alpha_s)$. What we have shown is that $C(z, M_{VH}, \mu_f)$ factorizes in the threshold region $z \to 1$. The hard function $H(M_{VH}, \mu_f)$ and soft function $S(M_{VH}(1-z), \mu_f)$, evaluated at μ_f, are obtained by renormalization group running from the hard scale $\mu_h \sim M_{VH}$ and soft scale $\mu_s \sim M_{VH}(1-\tau)$, respectively, to sum the threshold logarithms to all orders in α_s. The final result is obtained from that for the Drell-Yan process using the technique of momentum space renormalization group [58]

$$C(z, M_{VH}, \mu_f) = \left|C_V(-M_{VH}^2 - i\epsilon, \mu_h)\right|^2 U(M_{VH}, \mu_h, \mu_s, \mu_f)\frac{z^{-\eta}}{(1-z)^{1-2\eta}}$$
$$\times \tilde{s}_{DY}\left(\ln\frac{M_{VH}^2(1-z)^2}{\mu_s^2 z} + \partial_\eta, \mu_s\right)\frac{e^{-2\gamma_E\eta}}{\Gamma(2\eta)}. \tag{5.23}$$

Here $U(M_{VH}, \mu_h, \mu_s, \mu_f)$ is the evolution kernel. $\tilde{s}_{DY}$ is the the Laplace transform of $\hat{W}_{DY}$:

$$\tilde{s}_{\rm DY}(L, \mu_s) = \int_0^\infty d\omega \; e^{-s\omega} W_{\rm DY}(\omega, \mu_s) \,, \;\; s = \frac{1}{e^{\gamma_E} \mu_s e^{L/2}} \,. \tag{5.24}$$

η is defined by $\eta \equiv 2a_\Gamma(\mu_s, \mu_f)$, where $a_\Gamma(\nu, \mu)$ is the anomalous exponent of the cusp anomalous dimension:

$$a_\Gamma(\nu, \mu) = -\int_{\alpha_s(\nu)}^{\alpha_s(\mu)} d\alpha \frac{\Gamma_{\rm cusp}}{\beta(\alpha_s)} \,. \tag{5.25}$$

The analytic expressions for C_V, $\tilde{s}_{\rm DY}$, U and the various anomalous dimensions which are necessary for our numerical calculations are listed in Appendix B. Eq. (5.18) with C given by Eq. (5.23) is defined only for $\eta > 0$. For $\eta < 0$, an analytic continuation is required. For example, for $-\frac{1}{2} < \eta < 0$, we have to use the identity

$$\int_0^\Omega dx \frac{f(x)}{x^{1-2\eta}} = \int_0^\Omega dx \frac{f(x) - f(0)}{x^{1-2\eta}} + \frac{f(0)}{2\eta} \Omega^{2\eta} \,. \tag{5.26}$$

For $\eta < -\frac{1}{2}$ additional substraction terms are required.

Eq. (5.18) is only valid in the threshold region $z \sim 1$. To obtain a formula valid for all values of z, we match the threshold-resummed result with the fixed-order result,

$$\left[\frac{d\sigma}{dM_{VH}^2}\right]_{matched} = \left[\frac{d\sigma}{dM_{VH}^2}\right]_{threshold\ resum} - \left[\frac{d\sigma}{dM_{VH}^2}\right]_{threshold\ f.o.} + \left[\frac{d\sigma}{dM_{VH}^2}\right]_{f.o.} \,. \tag{5.27}$$

Here $\left[\frac{d\sigma}{dM_{VH}^2}\right]_{threshold\ resum}$ is the result obtained using the threshold resummation formula of Eq. (5.23), $\left[\frac{d\sigma}{dM_{VH}^2}\right]_{f.o.}$ is the fixed-order perturbative result and $\left[\frac{d\sigma}{dM_{VH}^2}\right]_{threshold\ f.o.}$ is obtained from the fixed-order result by keeping only the leading threshold singularity in C. The order of the logarithmic approximation in the resummed result and the corresponding fixed-order results used in the matching of Eq. (5.27) are summarized in Table 6.

Table 6: Approximation schemes for threshold resummation given a fixed order matched to a logarithmic approximation as in Eq. (5.27).

Fixed order	Log.	Accuracy$\sim \alpha_s^n L^k$	$\Gamma_{\rm cusp}$	γ^V, γ^ϕ	$C_V, \tilde{s}_{DY}$
LO	NLL	$2n-1 \le k \le 2n$	2-loop	1-loop	tree-level
NLO	NNLL	$2n-3 \le k \le 2n$	3-loop	2-loop	1-loop
NNLO	NNNLL	$2n-5 \le k \le 2n$	4-loop	3-loop	2-loop

5.3 NUMERICAL RESULTS

In this section, we study the scale dependence of the total cross section for VH production at the LHC, beginning with the sensitivity of the resummed threshold distributions to the hard, soft, and factorization scales. Near the threshold, $\tau \equiv M_{VH}^2/s \to 1$, the threshold logarithms are enhanced, leading to potentially large scale variations. The naive choice for the soft scale is $\mu_s \sim M_{VH}(1-\tau)$. We follow the prescription of Ref. [58] to determine a sensible range for the soft scale. We consider the correction to $\left[\frac{d\sigma}{dM_{VH}^2}\right]_{threshold\ resum}$ due to the one-loop correction to $\tilde{s}_{DY}$ in Eq. (5.23). We use C_V at NNLO and the running at NNNLL. We take $\mu_h = \mu_f = M_{VH}$ and use the NNLO MSTW2008 68% confidence PDF set [69]. A low value of μ_s is found empirically from the scale where the correction to $\left[\frac{d\sigma}{dM_{VH}^2}\right]_{threshold\ resum}$ due to the one-loop correction to $\tilde{s}_{DY}$ is minimal,

$$\mu_s^{(I)} = \frac{M_{VH}(1-\tau)}{2\sqrt{1+100\tau}}\,. \tag{5.28}$$

In obtaining this result, a functional form $\mu_s^{(I)} = \frac{M_{VH}(1-\tau)}{\sqrt{a+b\tau}}$ is assumed, as in Ref. [58]. Alternatively, an upper scale for the soft variation can be chosen as the value where the correction to $\left[\frac{d\sigma}{dM_{VH}^2}\right]_{threshold\ resum}$ due to the one-loop correction to $\tilde{s}_{DY}$ drops below 10%,

$$\mu_s^{(II)} = \frac{M_{VH}(1-\tau)}{0.9+12\tau}\,. \tag{5.29}$$

Again, a functional form $\mu_s^{(II)} = \frac{M_{VH}(1-\tau)}{a+b\tau}$ is assumed. Empirically, the forms of $\frac{\mu_s^{(I,II)}}{M_{VH}}$ are insensitive to M_{VH}. Here and henceforth, we adopt the Higgs mass value

$$M_H = 125 \text{ GeV}. \tag{5.30}$$

We investigate the numerical effects of the scale variation by plotting the differential cross section of the threshold resummation of Eq. (5.23) and varying the soft, hard, and factorization scales. It is customary to measure the size of QCD corrections by a K-factor (K) typically defined as the ratio of a higher order cross section to the lowest order cross section:

$$\frac{d\sigma}{dM_{VH}^2} \equiv K \frac{d\sigma}{dM_{VH}^2}\bigg|_{\text{LO}}, \tag{5.31}$$

where $\frac{d\sigma}{dM_{VH}^2}$ is a distribution defined at higher order in QCD.

To study the scale variation arising from threshold resummation, we investigate the K-factor of Eq. (5.31) defined with

$$\frac{d\sigma}{dM_{VH}^2} \equiv \left[\frac{d\sigma}{dM_{VH}^2}\right]_{threshold-resum}. \tag{5.32}$$

To isolate the effects of the scale variation due to threshold resummation from effects of the scale variation due to parton distribution functions (PDFs) and running α_s, the K-factor is evaluated by using the NNLO MSTW2008 68% confidence PDF set and the 3-loop value of α_s for all orders of the threshold resummed cross section and the LO cross section. Figure 24 shows the scale variation of this choice of K-factor as a function of τ at NLL between the dotted curves, NNLL between the dashed curves, and NNNLL between the solid curves for ZH production at $M_{ZH} = 1$ TeV. The soft scale variation in $pp \to ZH$, with μ_h and μ_f held constant, is shown in Fig. 24(a). The variation in the NLL result is significant, but the NNLL and NNNLL curves have little dependence on the soft scale, justifying the *ad hoc* choices of $\mu_s^{(I,II)}$. The K-factor grows rapidly as τ increases, as expected. The sensitivity to the hard scale is shown in Fig. 24(b), with fixed μ_s and μ_f. The hard scale is set by the invariant mass of the VH pair, and again we find that at NNLL and NNNLL, there is little dependence on μ_h, showing excellent convergence of the perturbation series. Finally, we show the factorization scale dependence in Fig. 24(c). The factorization scale dependence is small even at NLL.

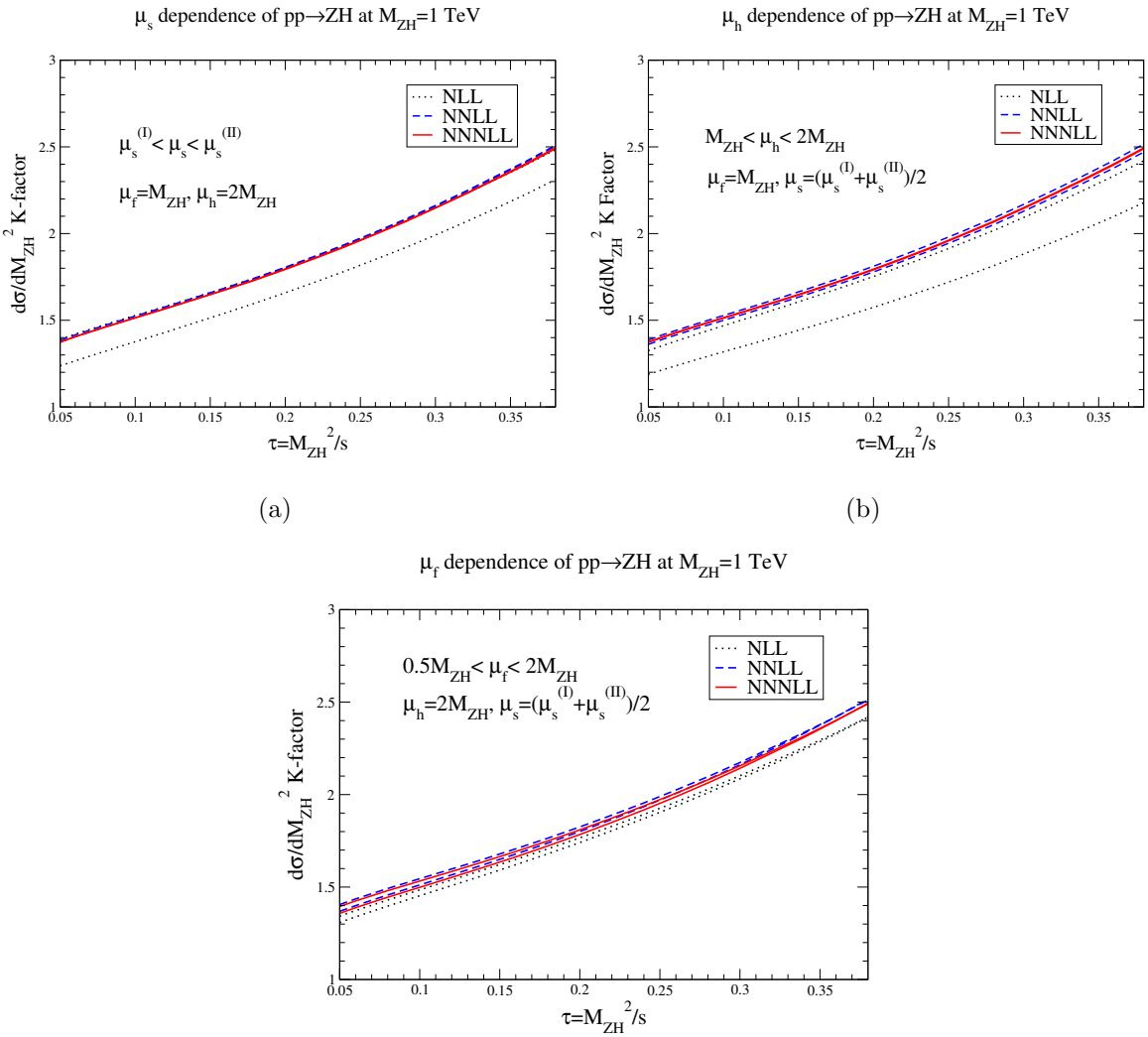

Figure 24: The (a) soft scale, (b) hard scale, and (c) factorization scale dependence of the threshold resummed cross section for $pp \to ZH$ at NLL between the dotted lines dotted, NNLL between the dashed lines, and NNNLL between the solid lines normalized to the LO result (the K-factor is defined in Eqs. (5.31) and (5.32)). The invariant mass M_{ZH} is fixed at 1 TeV.

We have also considered the scale dependence of the matched result for the total cross section. Analytic expressions for the LO and NLO fixed order results are found in Refs. [53, 54, 52, 50], and we use the computer code VH@NNLO for the fixed order NNLO results. The matched curves are found using the threshold resummation results of Eq. (5.27). In Fig. 2, we use the MSTW2008 68% confidence level PDFs, and use LO PDFs for the LO and the NLL-LO matched curves, NLO PDFs for the NLO and NNLL-NLO matched curves, and NNLO PDFs for the NNLO and NNNLL-NNLO matched curves, and use $1, 2$ and 3-loop evolution of α_s respectively. We include the small contribution from the gg initial state in the ZH NNLO and NNNLL-NNLO matched curves.

The results for ZH production at $\sqrt{s} = 8$ TeV and $\sqrt{s} = 14$ TeV are shown in Figs. 25(a) and 25(b), respectively. We have chosen the central scale to be $\mu_0 = M_{ZH}$. The gg initial state contributes $\sigma_{gg} = 0.06$ pb at $\sqrt{s} = 14$ TeV with $\mu_f = \mu_0$. This is the reason for the larger splitting between the NLO and NNLO curves than is seen in the WH results below. The fixed-order and matched curves have the renormalization/factorization scales set equal, $\mu_r = \mu_f$. The matched and resummed curves have the hard scale, $\mu_h = 2M_{VH}$, and the soft scale, $\mu_s = \frac{1}{2}(\mu_s^{(I)} + \mu_s^{(II)})$. The NNNLL-NNLO matched curve is almost identical to the NNLO fixed order curve, and the resummation has little effect at this order. On the other hand, the NNLL-NLO matched curve increases the fixed order NLO result (at $\mu_f = \mu_0$) by about 7%.

The matched cross sections for WH production at $\sqrt{s} = 8$ TeV and 14 TeV are shown in Figs. 25(c) and 25(d). These figures show the sum of W^+H and W^-H production. As in the ZH case, the NNLO and NNNLL-NNLO matched results for WH production are quite close and show little scale variation. The NNLL resummation increases the NLO fixed order result by $\sim 3\%$.

The uncertainties in the ZH and WH cross sections from PDFs, renormalization and factorization scale dependence, and the determination of α_s have been investigated by the LHC Higgs Cross Section Working Group for the NNLO total cross section [48]. They find a total uncertainty at $\sqrt{s} = 8$ TeV of $\mathcal{O}(4\%)$ for WH and $\mathcal{O}(5\%)$ for ZH production for a 125 GeV Higgs boson. Our results show that including the resummation of threshold logarithms to NNNLL accuracy does not induce any further uncertainties. We note that

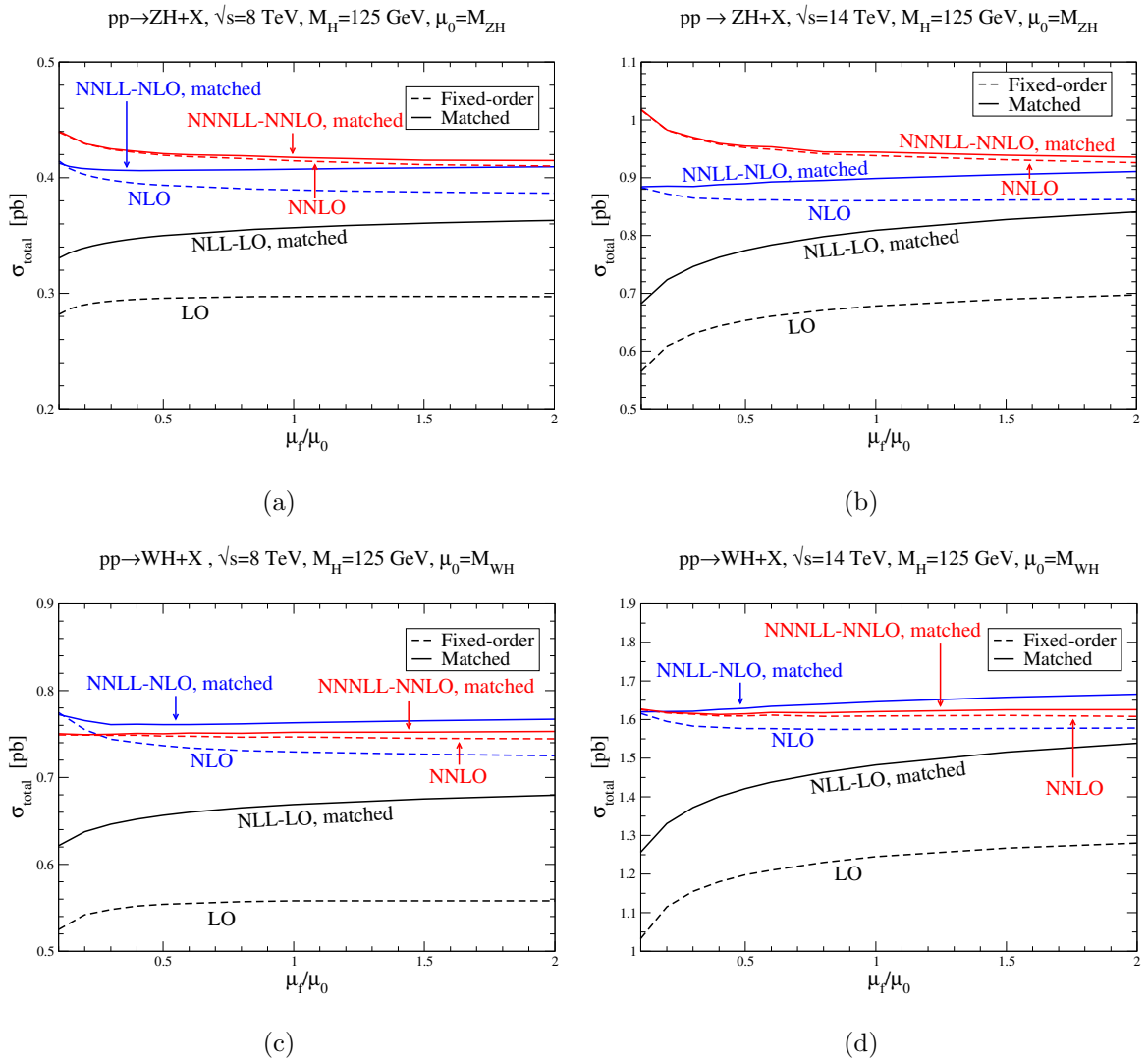

Figure 25: Scale dependence of the fixed order (dashed) and threshold resummed matched (solid) cross sections for (a,b) ZH and (c,d) WH production at (a,c)$\sqrt{s} = 8$ TeV and (b,d) $\sqrt{s} = 14$ TeV. The NNLO and NNNLL-NNLO matched ZH results include the contribution from the gg initial state.

Ref. [48] also includes the NLO electroweak effects [70], assuming complete factorization of the QCD and electroweak corrections. In the G_μ renormalization scheme, these corrections reduce the total Higgs and vector boson associated rates by about $\mathcal{O}(5\%)$.

Next, we examine the invariant-mass distributions including threshold resummation and matching. Since the distributions vary over many orders of magnitude, it is easier to see the effects in the K-factor, as defined in Eq. (5.31). Figures 26(a) and 26(b) show the K-factor versus τ at NNLL-NLO with $\sqrt{s} = 14$ TeV for $pp \to ZH+X$ and $pp \to WH+X$, respectively. The K-factor for the matched result of Eq. (5.27) is shown with solid lines, the threshold-resummed contribution with dot-dashed lines, the fixed-order perturbative contribution with dashed lines, and the contribution from the leading threshold singularity of the fixed-order perturbative piece with dotted lines. Here again we use the MSTW2008 68% confidence level PDFs. The scales are chosen to be $\mu_f = M_{ZH}$, $\mu_h = 2M_{ZH}$ and $\mu_s = \frac{1}{2}(\mu_s^I + \mu_s^{II})$. For the NLO fixed-order result, the leading threshold singularity of the NLO fixed-order result and the threshold-resummed result at NNLL, the NLO PDFs and 2-loop α_s are used, whereas for the LO fixed-order denominator of the K-factor, we use the LO PDFs and 1-loop α_s. As expected, the leading singularity and fixed-order results (the two lower curves) are close to each other, since the leading singularity dominates in the fixed-order result. On the other hand, the resummation effect is significant at high τ, as seen by the large enhancement of the NNLL (the two upper curves) from the NLO result of $\sim 20\%$ for both ZH and WH at $\tau = 0.3$.

The decrease of the K-factor at higher τ values is due to the PDF effect. To see this, we artificially adopt the NLO MSTW2008 68% confidence level PDFs and 2-loop α_s for the NLO fixed-order result, the leading threshold singularity of the NLO-fixed-order result and the threshold-resummed result at NNLL, as well as the LO denominator, and show the K-factors of these results with $\sqrt{s} = 14$ TeV for $pp \to ZH + X$ and $pp \to WH + X$ in Fig. 27(a) and 27(b) respectively. This is to isolate the effects of PDFs from a dynamical origin. The choice of scales is the same as in Fig. 26. We note that the monotonic increase of the K-factor distributions in Fig. 27 is drastically different from that in Fig. 26. This is a PDF induced effect, showing the importance of a consistent choice of PDFs as in Fig. 26.

To examine the convergence of the perturbative series, we plot the K-factors for the

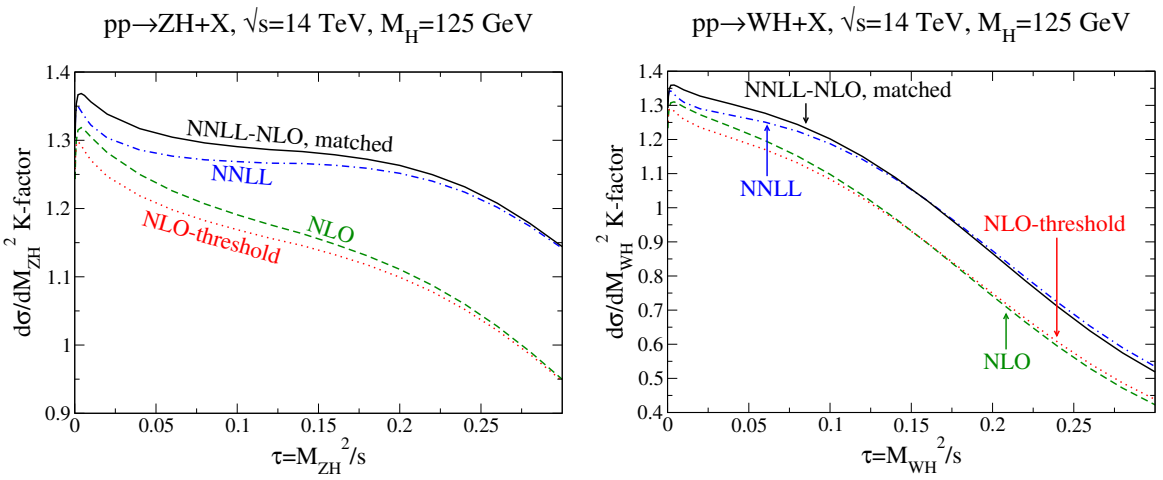

Figure 26: K-factor distributions at $\sqrt{s} = 14$ TeV for (a) ZH and (b) WH production. The NNLL-NLO matched result is shown with solid lines, the NNLL threshold resummed result with dot-dashed lines, the leading threshold singularity of the NLO fixed-order result with dashed lines, and the NLO fixed-order result with dotted lines.

resummed results at NLL, NNLL and NNNLL with $\sqrt{s} = 14$ TeV for $pp \to ZH + X$ in Fig. 28, using NNLO MSTW2008 68% confidence level PDFs and 3-loop α_s for all the resummed results as well as the LO denomintor. We see from Fig. 28 that the difference between NNLL and NNNLL is tiny ($< 1\%$), confirming the excellent convergence of the perturbative series at this order especially after leaving out the PDF effect.

5.4 SUMMARY

Given the exciting discovery of a Higgs-like particle at the LHC [2, 3], it becomes imperative to determine its properties. Thus its production rate at the LHC must be calculated as accurately as possible. Since the gauge boson-Higgs associated production is one of the channels that unambiguously probes the VVH coupling with $V = W^{\pm}$ or Z, it is of particular interest. We combined the long-known fixed-order perturbative QCD calculations for VH

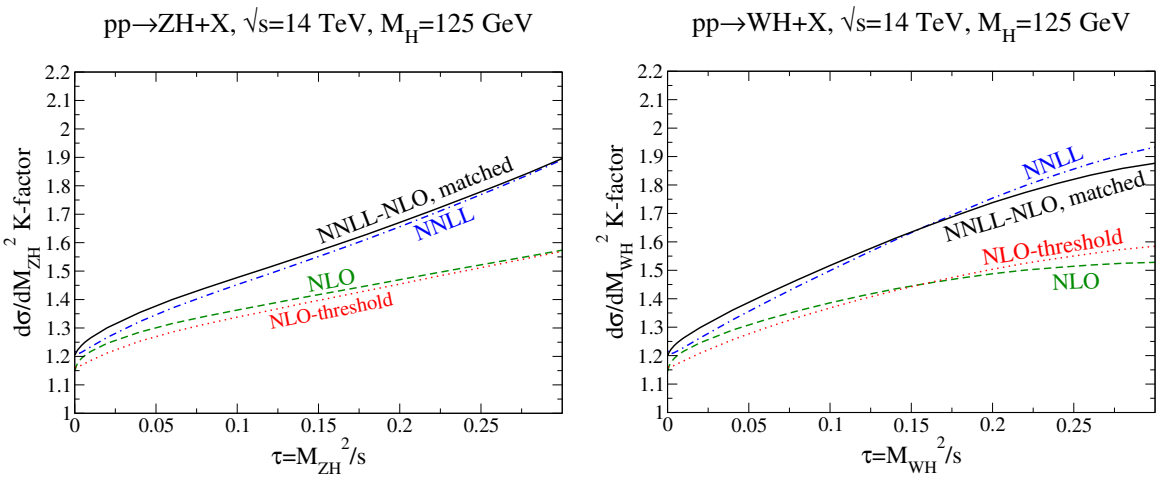

(a) (b)

Figure 27: K-factor distributions at $\sqrt{s} = 14$ TeV for (a) ZH and (b) WH production. The NNLL-NLO matched result is shown with solid lines, the NNLL threshold resummed result with dot-dashed lines, the leading threshold singularity of the NLO fixed-order result with dashed lines, and the NLO fixed-order result with dotted lines. The NLO PDFs and 2-loop α_s are adopted for all the results as well as the LO denominator.

production [50] with soft-gluon resummation of threshold logarithms.

After a brief overview of the resummation formalism, we carried out detailed numerical analyses at the LHC for $\sqrt{s} = 8$ TeV and 14 TeV. The overall corrections from NNLO fixed order calculations are sizable, increaing the LO rate by a factor as large as about 30% [48]. After implementing threshold resummation, the dependence of the total cross section and the τ distributions on the soft and hard scales, as well as on the factorization scale is very weak at the NNLO-NNNLL order, indicating the reliability of the calculations. The NNLL threshold resummed total cross section increases the fixed-order NLO result by about 7%, while the NNNLL resummed result has little impact on the NNLO fixed order rate, demonstrating the excellent convergence of the perturbation series. For the τ distributions, the NNLL threshold resummed result increases the fixed-order NLO result by about 10% at $\tau \sim 0.1$, suggesting importance of threshold resummation at τ of moderate size. A calculation of the τ distributions at NNLO and NNNLL in the future will possibly settle the issue.

As a final remark, our calculations can be easily extended to other electroweak pair

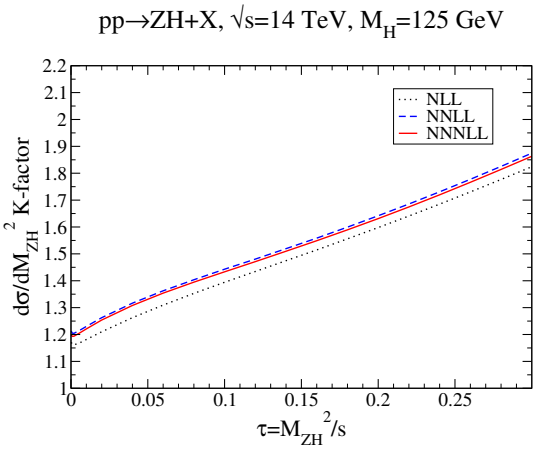

Figure 28: $pp \to ZH + X$ K factor distribution at $\sqrt{s} = 14$ TeV for the threshold resummed piece at various orders of the logarithmic approximation, using the same PDFs for all curves.

production processes with the same color structures which arise via $q\bar{q}'$ annihilation at leading order, such as the EW gauge boson pairs and the Higgs pair production H^0A^0, $H^0H^\pm$, $A^0H^\pm$ and H^+H^- [71].

6.0 CONCLUSION

In this thesis, we applied effective theories of QCD to two problems in Collider Physics.

First, motivated by the relevance in the search for CP violation at the LHC, we investigated the production asymmetries of heavy hadrons using the heavy quark recombination mechanism based on HQET. We applied the heavy quark recombination mechanism to explain the production asymmetries of D^+/D^- observed at LHCb. We found that with suitably chosen sizes of several non-perturbative parameters, the p_T and η distributions of the production asymmetry can be explained well. We also made preliminary predictions on production asymmetries for heavy baryons Λ_c^+/Λ_c^- and $\Lambda_b/\overline{\Lambda}_b$. We found that the asymmetries are significant in the forward region and should be measurable at LHCb. For further investigation in the future, we also calculate the partonic cross sections for P waves to leading order in α_s for hadronic production of heavy mesons and heavy baryons, as well as photoproduction of heavy mesons.

Second, we applied SCET to resum threshold logs in the associated production of a Higgs boson and a vector boson at the LHC. The total cross section is resummed to NNNLL. We found that resummation has negligible effect on the total cross section at NNLO. The distribution in $\tau = M_{VH}^2/s$ is resummed to NNLL. We found that resummation increases the fixed-order NLO result by $\sim 10\%$ at $\tau \sim 0.1$, suggesting the importance of threshold resummation at τ of moderate size.

APPENDIX A

LIST OF PARTONIC CROSS SECTIONS FOR P WAVES IN HEAVY QUARK RECOMBINATION MECHANISM

In this appendix, we list our result for the P-wave partonic cross sections in the heavy quark recombination mechanism. In obtaining these results, we used Feyn Calc [72] to deal with the Dirac algebra, and Ref. [73] and *Mathematica* to deal with the color algebra.

A.1 HADRONIC PRODUCTION OF HEAVY MESONS

For P waves in meson productions, there are 8 non-perturbative parameters, corresponding to $n = {}^1P_1^{(1)},\ {}^3P_0^{(1)},\ {}^3P_1^{(1)},\ {}^3P_2^{(1)},\ {}^1P_1^{(8)},\ {}^3P_0^{(8)},\ {}^3P_1^{(8)},\ {}^3P_2^{(8)}$. They are defined by

$$\begin{aligned}
\rho[Q\bar{q}({}^1P_1^{(1)}) \to H] =& \frac{1}{m_Q^3}\int \frac{d\eta_1}{\eta_1}\frac{d\eta_2}{\eta_2}\frac{dw_1}{2\pi}\frac{dw_2}{2\pi}e^{-i\eta_1 w_1 + i\eta_2 w_2} \\
& \times \langle 0|\bar{\mathbf{T}}\left[\bar{q}(w_2 v)\left(-\frac{i}{2}\overleftrightarrow{D}_T^{\mu}\right)S(w_2 v,0)Q_v(0)\right]a_H^\dagger \\
& \times a_H \mathbf{T}\left[\bar{Q}_v(0)\left(-\frac{i}{2}\overleftrightarrow{D}_{T\mu}\right)S(0,w_1 v)q(w_1 v)\right]|0\rangle\,, \qquad \text{(A.1a)} \\
\rho[Q\bar{q}({}^3P_0^{(1)}) \to H] =& \frac{1}{m_Q^3}\int \frac{d\eta_1}{\eta_1}\frac{d\eta_2}{\eta_2}\frac{dw_1}{2\pi}\frac{dw_2}{2\pi}e^{-i\eta_1 w_1 + i\eta_2 w_2} \\
& \times \langle 0|\bar{\mathbf{T}}\left[\bar{q}(w_2 v)\left(-\frac{i}{2}\overleftrightarrow{D}_T^{\mu}\Sigma_\mu\right)S(w_2 v,0)Q_v(0)\right]a_H^\dagger \\
& \times a_H \mathbf{T}\left[\bar{Q}_v(0)\left(-\frac{i}{2}\overleftrightarrow{D}_T^{\nu}\Sigma_\nu\right)S(0,w_1 v)q(w_1 v)\right]|0\rangle\,, \qquad \text{(A.1b)} \\
\rho[Q\bar{q}({}^3P_1^{(1)}) \to H] =& \frac{1}{m_Q^3}\int \frac{d\eta_1}{\eta_1}\frac{d\eta_2}{\eta_2}\frac{dw_1}{2\pi}\frac{dw_2}{2\pi}e^{-i\eta_1 w_1 + i\eta_2 w_2} \\
& \times \langle 0|\bar{\mathbf{T}}\left[\bar{q}(w_2 v)\left(-\frac{i}{2}\epsilon_{\mu\nu\alpha\beta}v^\nu\overleftrightarrow{D}_T^{\alpha}\Sigma^\beta\right)S(w_2 v,0)Q_v(0)\right]a_H^\dagger \\
& \times a_H \mathbf{T}\left[\bar{Q}_v(0)\left(-\frac{i}{2}\epsilon^{\mu}{}_{\rho\sigma\delta}v^\rho\overleftrightarrow{D}_T^{\sigma}\Sigma^\delta\right)S(0,w_1 v)q(w_1 v)\right]|0\rangle\,, \qquad \text{(A.1c)} \\
\rho[Q\bar{q}({}^3P_2^{(1)}) \to H] =& \frac{1}{m_Q^3}\int \frac{d\eta_1}{\eta_1}\frac{d\eta_2}{\eta_2}\frac{dw_1}{2\pi}\frac{dw_2}{2\pi}e^{-i\eta_1 w_1 + i\eta_2 w_2} \\
& \times \langle 0|\bar{\mathbf{T}}\left[\bar{q}(w_2 v)\left(-\frac{i}{2}\overleftrightarrow{D}_T^{(\mu}\overleftrightarrow{D}_T^{\nu)}\right)S(w_2 v,0)Q_v(0)\right]a_H^\dagger \\
& \times a_H \mathbf{T}\left[\bar{Q}_v(0)\left(-\frac{i}{2}\overleftrightarrow{D}_{T(\mu}\overleftrightarrow{D}_{T\nu)}\right)S(0,w_1 v)q(w_1 v)\right]|0\rangle\,, \qquad \text{(A.1d)}
\end{aligned}$$

$$\rho[Q\bar{q}(^1P_1^{(8)}) \to H] = \frac{1}{m_Q^3}\int \frac{d\eta_1}{\eta_1}\frac{d\eta_2}{\eta_2}\frac{dw_1}{2\pi}\frac{dw_2}{2\pi}e^{-i\eta_1 w_1 + i\eta_2 w_2} \times \langle 0|\bar{\mathbf{T}}\left[\bar{q}(w_2 v)\left(-\frac{i}{2}\overleftrightarrow{D}^{\mu}_{T}\right)t^a S(w_2 v, 0)Q_v(0)\right]a_H^\dagger \times a_H \mathbf{T}\left[\bar{Q}_v(0)\left(-\frac{i}{2}\overleftrightarrow{D}_{T\mu}\right)S(0, w_1 v)t^a q(w_1 v)\right]|0\rangle\,, \tag{A.1e}$$

$$\rho[Q\bar{q}(^3P_0^{(8)}) \to H] = \frac{1}{m_Q^3}\int \frac{d\eta_1}{\eta_1}\frac{d\eta_2}{\eta_2}\frac{dw_1}{2\pi}\frac{dw_2}{2\pi}e^{-i\eta_1 w_1 + i\eta_2 w_2} \times \langle 0|\bar{\mathbf{T}}\left[\bar{q}(w_2 v)\left(-\frac{i}{2}\overleftrightarrow{D}^{\mu}_{T}\Sigma_\mu\right)t^a S(w_2 v, 0)Q_v(0)\right]a_H^\dagger \times a_H \mathbf{T}\left[\bar{Q}_v(0)\left(-\frac{i}{2}\overleftrightarrow{D}^{\nu}_{T}\Sigma_\nu\right)S(0, w_1 v)t^a q(w_1 v)\right]|0\rangle\,, \tag{A.1f}$$

$$\rho[Q\bar{q}(^3P_1^{(8)}) \to H] = \frac{1}{m_Q^3}\int \frac{d\eta_1}{\eta_1}\frac{d\eta_2}{\eta_2}\frac{dw_1}{2\pi}\frac{dw_2}{2\pi}e^{-i\eta_1 w_1 + i\eta_2 w_2} \times \langle 0|\bar{\mathbf{T}}\left[\bar{q}(w_2 v)\left(-\frac{i}{2}\epsilon_{\mu\nu\alpha\beta}v^\nu\overleftrightarrow{D}^{\alpha}_{T}\Sigma^\beta\right)t^a S(w_2 v, 0)Q_v(0)\right]a_H^\dagger \times a_H \mathbf{T}\left[\bar{Q}_v(0)\left(-\frac{i}{2}\epsilon^{\mu}{}_{\rho\sigma\delta}v^\rho\overleftrightarrow{D}^{\sigma}_{T}\Sigma^\delta\right)S(0, w_1 v)t^a q(w_1 v)\right]|0\rangle\,, \tag{A.1g}$$

$$\rho[Q\bar{q}(^3P_2^{(8)}) \to H] = \frac{1}{m_Q^3}\int \frac{d\eta_1}{\eta_1}\frac{d\eta_2}{\eta_2}\frac{dw_1}{2\pi}\frac{dw_2}{2\pi}e^{-i\eta_1 w_1 + i\eta_2 w_2} \times \langle 0|\bar{\mathbf{T}}\left[\bar{q}(w_2 v)\left(-\frac{i}{2}\overleftrightarrow{D}^{(\mu}_{T}\overleftrightarrow{D}^{\nu)}_{T}\right)t^a S(w_2 v, 0)Q_v(0)\right]a_H^\dagger \times a_H \mathbf{T}\left[\bar{Q}_v(0)\left(-\frac{i}{2}\overleftrightarrow{D}_{T(\mu}\overleftrightarrow{D}_{T\nu)}\right)S(0, w_1 v)t^a q(w_1 v)\right]|0\rangle\,, \tag{A.1h}$$

Here $\bar{\psi}\overleftrightarrow{D}_\mu\chi \equiv \bar{\psi}D^\mu\chi - (\overline{D^\mu\psi})\chi$, $D_T^\mu \equiv D^\mu - (v\cdot D)v^\mu$ and $\gamma_T^\mu \equiv \gamma^\mu - (v\cdot\gamma)v^\mu$. Σ_μ is the spin 4-vector defined by

$$\Sigma_\mu \equiv \epsilon_{\mu\nu\alpha\beta}v^\nu\sigma^{\alpha\beta}\,, \tag{A.2}$$

where $\sigma^{\alpha\beta} = \frac{i}{2}[\gamma^\alpha, \gamma^\beta]$. For any transverse tensor $T_T^{\mu\nu}$, i.e. $T_T^{\mu\nu}v_\mu = T_T^{\mu\nu}v_\nu = 0$, we define

$$T_T^{(\mu\nu)} \equiv \frac{1}{2}\left(T_T^{\mu\nu} + T_T^{\nu\mu}\right) - \frac{T_{T\alpha}^{\alpha}}{3}\left(g^{\mu\nu} - v^\mu v^\nu\right)\,. \tag{A.3}$$

The resulting perturbative cross sections for $qg \to \bar{Q}q(^{2S+1}P_J^{(c)}) + Q$ have the form

$$\frac{d\hat{\sigma}}{d\hat{t}}[qg \to \bar{Q}q(^{2S+1}P_J^{(c)}) + Q] = -\frac{\pi^2\alpha_s^3 m_H^2}{6S^2}\frac{N(^{2S+1}P_J^{(c)}|S,T)}{D(^{2S+1}P_J^{(c)}|S,T)}\,, \tag{A.4}$$

where $S = \hat{s} = (p+l)^2$ and $T = \hat{t} - m_H^2 = (p_H - p)^2 - m_H^2$. We will distinguish m_H from m_Q and write $m_Q = r m_H$. The numerator $N(^{2S+1}P_J^{(c)}|S,T)$ is a power expansion in m_H:

$$N(^{2S+1}P_J^{(c)}|S,T) = \sum_{n=0}^{6} a_{2n}(^{2S+1}P_J^{(c)}|S,T) m_H^{2n} \,. \tag{A.5}$$

For $\bar{Q}q(^1P_1^{(1)})$, we have

$$\begin{aligned}
&D(^1P_1^{(1)}|S,T) \\
=&72S^4T^2(S+T)^4[(1-r^2)+S+T]^2 \,, &\text{(A.6a)}\\
&a_0(^1P_1^{(1)}|S,T) \\
=&-64S^2(S+T)^5(12S^4+32S^3T+48S^2T^2+41ST^3+12T^4) \,, &\text{(A.6b)}\\
&a_2(^1P_1^{(1)}|S,T) \\
=&S(S+T)^4\,[\,\left(3584r^2-576r-3488\right)S^5+\left(9459r^2-1532r-10300\right)S^4T \\
&+\left(11902r^2-4052r-13612\right)S^3T^2+\left(9707r^2-5836r-8560\right)S^2T^3 \\
&+\left(4064r^2-2756r-1120\right)ST^4+\left(512r^2+512\right)T^5\big] \,, &\text{(A.6c)}\\
&a_4(^1P_1^{(1)}|S,T) \\
=&(S+T)^3\left[\left(-256r^4+512r^2-256\right)T^6+\left(-6912r^4+3328r^3+11151r^2+210r-4765\right)S^6\right. \\
&+\left(-19067r^4+10310r^3+32023r^2+1744r-15756\right)S^5T \\
&+\left(-21203r^4+17974r^3+36261r^2-4300r-19102\right)S^4T^2 \\
&+\left(-15317r^4+19974r^3+19577r^2-14572r-6324\right)S^3T^3 \\
&+\left(-8653r^4+10546r^3+4084r^2-10286r+4259\right)S^2T^4 \\
&\left.+\left(-2688r^4+1540r^3+536r^2-1540r+2152\right)ST^5\right] \,, &\text{(A.6d)}\\
&a_6(^1P_1^{(1)}|S,T) \\
=&(S+T)^2\left[\left(800r^6-2400r^4+2400r^2-800\right)T^6\right. \\
&+\left(7168r^6-7552r^5-13500r^4+3318r^3+11086r^2+5098r-5442\right)S^6 \\
&+\left(22416r^6-27406r^5-39839r^4+9564r^3+38902r^2+19570r-22887\right)S^5T \\
&+\left(26296r^6-41948r^5-42308r^4+21840r^3+48340r^2+20972r-33048\right)S^4T^2 \\
&+\left(17787r^6-34920r^5-23124r^4+34168r^3+21543r^2+752r-16206\right)S^3T^3
\end{aligned}$$

$$
\begin{aligned}
&+\left(10886r^6-15804r^5-13496r^4+24498r^3+1292r^2-8694r+1318\right)S^2T^4\\
&+\left(4915r^6-2962r^5-8701r^4+5924r^3+2657r^2-2962r+1129\right)ST^5\big]\ , \qquad \text{(A.6e)}\\
&a_8({}^1P_1^{(1)}|S,T)\\
=&(S+T)\big[\left(-913r^8+3652r^6-5478r^4+3652r^2-913\right)T^6\\
&+\left(-4352r^8+8448r^7+8299r^6-12678r^5-8223r^4\right.\\
&\left.-1716r^3+10333r^2+5946r-6057\right)S^6\\
&+\left(-16716r^8+35678r^7+29647r^6-53624r^5-32117r^4\right.\\
&\left.-3242r^3+44973r^2+21188r-25787\right)S^5T\\
&+\left(-24660r^8+58386r^7+41775r^6-93564r^5-48149r^4\right.\\
&\left.+10242r^3+71053r^2+24936r-40019\right)S^4T^2\\
&+\left(-19309r^8+46066r^7+35857r^6-84512r^5-40781r^4\right.\\
&\left.+30826r^3+51227r^2+7620r-26994\right)S^3T^3\\
&+\left(-10659r^8+17510r^7+27358r^6-39678r^5-30450r^4\right.\\
&\left.+26826r^3+21462r^2-4658r-7711\right)S^2T^4\\
&+\left(-4539r^8+2592r^7+15532r^6-7776r^5-19362r^4\right.\\
&\left.+7776r^3+10284r^2-2592r-1915\right)ST^5\big]\ , \qquad \text{(A.6f)}\\
&a_{10}({}^1P_1^{(1)}|S,T)\\
&=\left(450r^{10}-2250r^8+4500r^6-4500r^4+2250r^2-450\right)T^6\\
&+\left(1536r^{10}-4672r^9-3262r^8+14562r^7+1898r^6-14790r^5\right.\\
&\left.-2170r^4+4582r^3+4014r^2+318r-2016\right)S^6\\
&+\left(7445r^{10}-22718r^9-16341r^8+71580r^7+10198r^6-76704r^5\right.\\
&\left.-8406r^4+29540r^3+14357r^2-1698r-7253\right)S^5T\\
&+\left(14166r^{10}-42564r^9-33722r^8+138008r^7+24908r^6-157776r^5\right.\\
&\left.-14772r^4+71784r^3+18878r^2-9452r-9458\right)S^4T^2\\
&+\left(13734r^{10}-38064r^9-38150r^8+129180r^7+37536r^6-159156r^5\right.\\
&\left.-21048r^4+83028r^3+13418r^2-14988r-5490\right)S^3T^3\\
&+\left(7560r^{10}-16012r^9-26550r^8+58054r^7+36270r^6-78090r^5\right.
\end{aligned}
$$

$$
\begin{aligned}
&-25110r^4+46066r^3+9810r^2-10018r-1980\big)\,S^2T^4\\
&+\big(2529r^{10}-2466r^9-11277r^8+9864r^7+19818r^6-14796r^5\\
&-17082r^4+9864r^3+7173r^2-2466r-1161\big)\,ST^5\,,
\end{aligned}
\tag{A.6g}
$$

$$
\begin{aligned}
&a_{12}({}^1P_1^{(1)}|S,T)\\
=&\big(-81r^{12}+486r^{10}-1215r^8+1620r^6-1215r^4+486r^2-81\big)\,T^5\\
&+\big(-648r^{12}+1296r^{11}+2916r^{10}-6480r^9-4860r^8+12960r^7+3240r^6\\
&-12960r^5+6480r^3-972r^2-1296r+324\big)\,ST^4\\
&+\big(-256r^{12}+1024r^{11}+800r^{10}-5412r^9+4r^8+11408r^7-2896r^6\\
&-11992r^5+4504r^4+6288r^3-2800r^2-1316r+644\big)\,S^5\\
&+\big(-1233r^{12}+4644r^{11}+4010r^{10}-23852r^9-1203r^8+48968r^7-10628r^6\\
&-50232r^5+17497r^4+25748r^3-10950r^2-5276r+2507\big)\,S^4T\\
&+\big(-2196r^{12}+7560r^{11}+7596r^{10}-38124r^9-4860r^8+76896r^7-12600r^6\\
&-77544r^5+23940r^4+39096r^3-15444r^2-7884r+3564\big)\,S^3T^2\\
&+\big(-1782r^{12}+5220r^{11}+6804r^{10}-26100r^9-7290r^8+52200r^7-3240r^6\\
&-52200r^5+12150r^4+26100r^3-8748r^2-5220r+2106\big)\,S^2T^3\,.
\end{aligned}
\tag{A.6h}
$$

For $\bar{Q}q({}^3P_0^{(1)})$, we have

$$
\begin{aligned}
&D({}^3P_0^{(1)}|S,T)\\
=&72S^4T^2(S+T)^4\left[T+\left(1-r^2\right)m_H^2\right]^2\left[\left(1-r^2\right)m_H^2+S+T\right]^2\,,
\end{aligned}
\tag{A.7a}
$$

$$
\begin{aligned}
&a_0({}^3P_0^{(1)}|S,T)\\
=&-64S^2T^2(S+T)^5\left(4S^4+9ST^3+4T^4\right)\,,
\end{aligned}
\tag{A.7b}
$$

$$
\begin{aligned}
&a_2({}^3P_0^{(1)}|S,T)\\
=&ST(S+T)^4\left[\left(512r^2-3072r+8704\right)S^6+\left(2048r^2-8320r+34080\right)S^5T\right.\\
&+\left(1489r^2-10812r+49196\right)S^4T^2+\left(1602r^2-11412r+27340\right)S^3T^3\\
&\left.+\left(4233r^2-8572r+1304\right)S^2T^4+\left(2976r^2-2740r-1576\right)ST^5+\left(512r^2+512\right)T^6\right]\,,
\end{aligned}
\tag{A.7c}
$$

$$
\begin{aligned}
&a_4({}^3P_0^{(1)}|S,T)\\
=&(S+T)^3\left[\left(-256r^4+512r^2-256\right)T^8+\left(-256r^4+3072r^3-8704r^2-3072r+8960\right)S^8\right.\\
&+\left(-3584r^4+27200r^3-54336r^2-33152r+60800\right)S^7T\\
&+\left(-10146r^4+71992r^3-128905r^2-99374r+150465\right)S^6T^2\\
&+\left(-11899r^4+101146r^3-140893r^2-144604r+169400\right)S^5T^3\\
&+\left(-12675r^4+94658r^3-59291r^2-120576r+80314\right)S^4T^4\\
&+\left(-17205r^4+57802r^3+6533r^2-58840r+8712\right)S^3T^5\\
&+\left(-13035r^4+17286r^3+7724r^2-14434r+3045\right)S^2T^6\\
&\left.+\left(-3712r^4+820r^3+160r^2-820r+3552\right)ST^7\right]\,, \qquad \text{(A.7d)}\\
&a_6({}^3P_0^{(1)}|S,T)\\
=&(S+T)^2\left[\left(1312r^6-3936r^4+3936r^2-1312\right)T^8\right.\\
&+\left(1536r^6-15808r^5+29984r^4+37568r^3-49024r^2-21760r+17504\right)S^8\\
&+\left(12241r^6-101628r^5+125872r^4+260900r^3-241599r^2-160040r+102718\right)S^7T\\
&+\left(32654r^6-262208r^5+200670r^4+700162r^3-467944r^2-440330r+233908\right)S^6T^2\\
&+\left(45196r^6-372010r^5+133521r^4+976252r^3-434894r^2-606530r+257041\right)S^5T^3\\
&+\left(47028r^6-323652r^5+4212r^4+777016r^3-193400r^2-454044r+143000\right)S^4T^4\\
&+\left(46242r^6-170948r^5-46108r^4+354940r^3-53074r^2-183992r+52940\right)S^3T^5\\
&+\left(32504r^6-46508r^5-32042r^4+84510r^3-28278r^2-38002r+27816\right)S^2T^6\\
&\left.+\left(11315r^6-3558r^5-14413r^4+7116r^3-5119r^2-3558r+8217\right)ST^7\right]\,, \qquad \text{(A.7e)}\\
&a_8({}^3P_0^{(1)}|S,T)\\
=&(S+T)\left[\left(-2769r^8+11076r^6-16614r^4+11076r^2-2769\right)T^8\right.\\
&+\left(-3840r^8+32960r^7-31827r^6-123190r^5+94223r^4+148268r^3\right.\\
&\left.-76837r^2-58038r+18281\right)S^8\\
&+\left(-25365r^8+198586r^7-106383r^6-759616r^5+407971r^4\right.\\
&\left.+928994r^3-393141r^2-367964r+116918\right)S^7T\\
&+\left(-67819r^8+509178r^7-93761r^6-1940848r^5+684929r^4\right.\\
&\left.+2365938r^3-818483r^2-934268r+295134\right)S^6T^2
\end{aligned}
$$

$$
\begin{aligned}
&+\left(-101456r^8+719382r^7+60513r^6-2652108r^5+562813r^4\right.\\
&\left.+3155782r^3-907197r^2-1223056r+385327\right)S^5T^3\\
&+\left(-104318r^8+600874r^7+171900r^6-2078586r^5+261186r^4\right.\\
&\left.+2357238r^3-624112r^2-879526r+295344\right)S^4T^4\\
&+\left(-85494r^8+291712r^7+156782r^6-925308r^5+95858r^4\right.\\
&\left.+975480r^3-320086r^2-341884r+152940\right)S^3T^5\\
&+\left(-52758r^8+73204r^7+103944r^6-214000r^5+6632r^4\right.\\
&\left.+208388r^3-114064r^2-67592r+56246\right)S^2T^6\\
&+\left(-19169r^8+6528r^7+50452r^6-19584r^5-36342r^4\right.\\
&\left.+19584r^3-1996r^2-6528r+7055\right)ST^7\Big]\ , \qquad \text{(A.7f)}\\
&a_{10}({}^3P_0^{(1)}|S,T)\\
=&\left(3076r^{10}-15380r^8+30760r^6-30760r^4+15380r^2-3076\right)T^8\\
&+\left(5120r^{10}-35200r^9+2304r^8+175442r^7-62294r^6-317502r^5\right.\\
&\left.+121146r^4+249478r^3-90226r^2-72218r+23950\right)S^8\\
&+\left(32810r^{10}-215378r^9-31049r^8+1062016r^7-250616r^6-1905716r^5\right.\\
&\left.+611242r^4+1486896r^3-510490r^2-427818r+148103\right)S^7T\\
&+\left(90312r^{10}-561076r^9-181656r^8+2705408r^7-363184r^6-4770688r^5\right.\\
&\left.+1285704r^4+3669456r^3-1206792r^2-1043100r+375616\right)S^6T^2\\
&+\left(142172r^{10}-798596r^9-385082r^8+3725940r^7-196028r^6-6401588r^5\right.\\
&\left.+1489144r^4+4819740r^3-1560736r^2-1345496r+510530\right)S^5T^3\\
&+\left(146620r^{10}-661940r^9-444036r^8+2961734r^7+49230r^6-4917546r^5\right.\\
&\left.+1055222r^4+3597650r^3-1215090r^2-979898r+408054\right)S^4T^4\\
&+\left(108442r^{10}-313678r^9-340269r^8+1338012r^7+174716r^6-2131968r^5\right.\\
&\left.+433046r^4+1504612r^3-571374r^2-396978r+195439\right)S^3T^5\\
&+\left(58248r^{10}-76520r^9-198272r^8+311720r^7+196664r^6-476040r^5\right.\\
&\left.+17160r^4+323000r^3-122464r^2-82160r+48664\right)S^2T^6
\end{aligned}
$$

$$
\begin{aligned}
&+\left(19948r^{10}-7084r^{9}-80656r^{8}+28336r^{7}+123144r^{6}-42504r^{5}\right.\\
&\left.-84976r^{4}+28336r^{3}+23404r^{2}-7084r-864\right)ST^{7}\,, \qquad \text{(A.7g)}\\
&a_{12}({}^{3}P_{0}^{(1)}|S,T)\\
=&\left(-1894r^{12}+11364r^{10}-28410r^{8}+37880r^{6}-28410r^{4}+11364r^{2}-1894\right)T^{7}\\
&+\left(-3840r^{12}+19840r^{11}+16345r^{10}-119510r^{9}-9663r^{8}+282088r^{7}-48878r^{6}\right.\\
&\left.-327604r^{5}+98762r^{4}+187784r^{3}-70923r^{2}-42598r+18197\right)S^{7}\\
&+\left(-21802r^{12}+107570r^{11}+95782r^{10}-629226r^{9}-82510r^{8}+1449108r^{7}-196716r^{6}\right.\\
&\left.-1647668r^{5}+454418r^{4}+927066r^{3}-336746r^{2}-206850r+87574\right)S^{6}T\\
&+\left(-52410r^{12}+237156r^{11}+235414r^{10}-1346276r^{9}-253884r^{8}+3021624r^{7}-297652r^{6}\right.\\
&\left.-3358776r^{5}+848270r^{4}+1852004r^{3}-650658r^{2}-405732r+170920\right)S^{5}T^{2}\\
&+\left(-70114r^{12}+269056r^{11}+318620r^{10}-1481192r^{9}-404958r^{8}+3236832r^{7}-167304r^{6}\right.\\
&\left.-3513904r^{5}+797170r^{4}+1896800r^{3}-645012r^{2}-407592r+171598\right)S^{4}T^{3}\\
&+\left(-58336r^{12}+162888r^{11}+268849r^{10}-869258r^{9}-401911r^{8}+1848152r^{7}+85874r^{6}\right.\\
&\left.-1957788r^{5}+340394r^{4}+1033712r^{3}-324995r^{2}-217706r+90125\right)S^{3}T^{4}\\
&+\left(-31938r^{12}+48606r^{11}+153982r^{10}-251382r^{9}-277970r^{8}+519468r^{7}+210820r^{6}\right.\\
&\left.-536172r^{5}-25390r^{4}+276438r^{3}-48082r^{2}-56958r+18578\right)S^{2}T^{5}\\
&+\left(-11158r^{12}+5364r^{11}+59176r^{10}-26820r^{9}-128510r^{8}+53640r^{7}+145440r^{6}\right.\\
&\left.-53640r^{5}-89650r^{4}+26820r^{3}+28088r^{2}-5364r-3386\right)ST^{6}\,. \qquad \text{(A.7h)}
\end{aligned}
$$

For $\bar{Q}q({}^{3}P_{1}^{(1)})$, we have

$$
\begin{aligned}
&D({}^{3}P_{1}^{(1)}|S,T)\\
=&36S^{4}T^{2}(S+T)^{4}\left[T+\left(1-r^{2}\right)m_{H}^{2}\right]^{2}\left[\left(1-r^{2}\right)m_{H}^{2}+S+T\right]^{2}\,, \qquad \text{(A.8a)}\\
&a_{0}({}^{3}P_{1}^{(1)}|S,T)\\
=&-256S^{2}T^{2}(S+T)^{7}\left(S^{2}+2ST+3T^{2}\right)\,, \qquad \text{(A.8b)}\\
&a_{2}({}^{3}P_{1}^{(1)}|S,T)\\
=&ST(S+T)^{4}\left[\left(1024r^{2}-1024r+512\right)S^{6}+\left(6720r^{2}-6752r-288\right)S^{5}T\right.\\
&\left.+\left(17715r^{2}-16298r-5271\right)S^{4}T^{2}+\left(24802r^{2}-17984r-10254\right)S^{3}T^{3}\right.
\end{aligned}
$$

$$+\left(18819r^2-9054r-8211\right)S^2T^4+\left(6560r^2-1672r-1968\right)ST^5+\left(512r^2+512\right)T^6\big]\,, \tag{A.8c}$$

$$\begin{aligned}
&a_4({}^3P_1^{(1)}|S,T)\\
=&(S+T)^3\left[\left(-768r^4+1024r^3-1024r+768\right)S^8+\left(-256r^4+512r^2-256\right)T^8\right.\\
&+\left(-8768r^4+14080r^3+3968r^2-14784r+2432\right)S^7T\\
&+\left(-38182r^4+62068r^3+28854r^2-65172r+2256\right)S^6T^2\\
&+\left(-84837r^4+127448r^3+76140r^2-132124r+2881\right)S^5T^3\\
&+\left(-106077r^4+134428r^3+98472r^2-137468r+8065\right)S^4T^4\\
&+\left(-75027r^4+71848r^3+65196r^2-72700r+11727\right)S^3T^5\\
&+\left(-27581r^4+17080r^3+18890r^2-17120r+8999\right)S^2T^6\\
&\left.+\left(-4224r^4+1152r^3+1400r^2-1152r+2824\right)ST^7\right]\,,
\end{aligned} \tag{A.8d}$$

$$\begin{aligned}
&a_6({}^3P_1^{(1)}|S,T)\\
=&(S+T)^2\left[\left(1312r^6-3936r^4+3936r^2-1312\right)T^8\right.\\
&+\left(3584r^6-6304r^5-1056r^4+13312r^3-3200r^2-7008r+672\right)S^8\\
&+\left(29619r^6-61034r^5-27585r^4+131284r^3-10775r^2-70506r+8485\right)S^7T\\
&+\left(107070r^6-226364r^5-137566r^4+483216r^3-15490r^2-257456r+45630\right)S^6T^2\\
&+\left(213990r^6-425592r^5-306728r^4+892152r^3-23178r^2-466840r+115916\right)S^5T^3\\
&+\left(253040r^6-438228r^5-368544r^4+899444r^3-39552r^2-461148r+155140\right)S^4T^4\\
&+\left(177802r^6-244372r^5-251770r^4+491976r^3-40450r^2-247604r+114418\right)S^3T^5\\
&+\left(70972r^6-66692r^5-98840r^4+132556r^3-16112r^2-65864r+43980\right)S^2T^6\\
&\left.+\left(14583r^6-6542r^5-23867r^4+13084r^3+3985r^2-6542r+5299\right)ST^7\right]\,,
\end{aligned} \tag{A.8e}$$

$$\begin{aligned}
&a_8({}^3P_1^{(1)}|S,T)\\
=&(S+T)\left[\left(-2769r^8+11076r^6-16614r^4+11076r^2-2769\right)T^8\right.\\
&+\left(-6912r^8+15712r^7+8802r^6-52544r^5+7738r^4\right.\\
&\left.+58208r^3-13978r^2-21376r+4350\right)S^8\\
&+\left(-52539r^8+130180r^7+90434r^6-427632r^5+24012r^4\right.\\
&\left.+466188r^3-108202r^2-168736r+46295\right)S^7T
\end{aligned}$$

$$
\begin{aligned}
&+\left(-176297r^8+440024r^7+348526r^6-1412044r^5+12148r^4\right.\\
&\left.+1506224r^3-364030r^2-534204r+179653\right)S^6T^2\\
&+\left(-334442r^8+786660r^7+700902r^6-2461940r^5-47354r^4\right.\\
&\left.+2564660r^3-670678r^2-889380r+351572\right)S^5T^3\\
&+\left(-386084r^8+799936r^7+828048r^6-2445156r^5-112840r^4\right.\\
&\left.+2490264r^3-714488r^2-845044r+385364\right)S^4T^4\\
&+\left(-274318r^8+458892r^7+604068r^6-1376648r^5-147308r^4\right.\\
&\left.+1376620r^3-420316r^2-458864r+237874\right)S^3T^5\\
&+\left(-116346r^8+135716r^7+277208r^6-403428r^5-133116r^4\right.\\
&\left.+399708r^3-100008r^2-131996r+72262\right)S^2T^6\\
&+\left(-27125r^8+15648r^7+78256r^6-46944r^5-72018r^4\right.\\
&\left.+46944r^3+17768r^2-15648r+3119\right)ST^7\Big]\ ,
\end{aligned}
\tag{A.8f}
$$

$$
\begin{aligned}
&a_{10}({}^3P_1^{(1)}|S,T)\\
&=\left(3076r^{10}-15380r^8+30760r^6-30760r^4+15380r^2-3076\right)T^8\\
&+\left(7168r^{10}-20288r^9-19336r^8+90128r^7+3628r^6-149260r^5\right.\\
&\left.+33096r^4+109288r^3-35572r^2-29868r+11016\right)S^8\\
&+\left(54224r^{10}-155368r^9-154478r^8+671224r^7+54696r^6-1083832r^5\right.\\
&\left.+219940r^4+775464r^3-257176r^2-207488r+82794\right)S^7T\\
&+\left(179296r^{10}-498960r^9-526796r^8+2099076r^7+248376r^6-3306208r^5\right.\\
&\left.+623244r^4+2311028r^3-780912r^2-604936r+256792\right)S^6T^2\\
&+\left(335496r^{10}-867252r^9-1006324r^8+3563128r^7+578640r^6-5486536r^5\right.\\
&\left.+948456r^4+3752696r^3-1285016r^2-962036r+428748\right)S^5T^3\\
&+\left(385444r^{10}-876960r^9-1185592r^8+3534540r^7+829436r^6-5341548r^5\right.\\
&\left.+771380r^4+3587316r^3-1215920r^2-903348r+415252\right)S^4T^4\\
&+\left(276604r^{10}-512980r^9-891646r^8+2041192r^7+787728r^6-3045696r^5\right.\\
&\left.+220652r^4+2019736r^3-620924r^2-502252r+227586\right)S^3T^5
\end{aligned}
$$

$$
\begin{aligned}
&+\left(120664r^{10}-159576r^{9}-424776r^{8}+632536r^{7}+493320r^{6}-940152r^{5}\right.\\
&\left.-137944r^{4}+621000r^{3}-108288r^{2}-153808r+57024\right)S^{2}T^{6}\\
&+\left(29328r^{10}-20184r^{9}-119432r^{8}+80736r^{7}+184448r^{6}-121104r^{5}\right.\\
&\left.-130032r^{4}+80736r^{3}+37808r^{2}-20184r-2120\right)ST^{7}\,, \qquad \text{(A.8g)}\\
&a_{12}({}^{3}P_{1}^{(1)}|S,T)\\
=&\left(-1894r^{12}+11364r^{10}-28410r^{8}+37880r^{6}-28410r^{4}+11364r^{2}-1894\right)T^{7}\\
&+\left(-4352r^{12}+14272r^{11}+18090r^{10}-76124r^{9}-20782r^{8}+162216r^{7}-10788r^{6}\right.\\
&\left.-172624r^{5}+41436r^{4}+91736r^{3}-31718r^{2}-19476r+8114\right)S^{7}\\
&+\left(-29260r^{12}+91396r^{11}+119640r^{10}-475304r^{9}-140964r^{8}+988216r^{7}-47992r^{6}\right.\\
&\left.-1026784r^{5}+232260r^{4}+533156r^{3}-179328r^{2}-110680r+45644\right)S^{6}T\\
&+\left(-83002r^{12}+240020r^{11}+338228r^{10}-1222116r^{9}-417534r^{8}+2488608r^{7}-53136r^{6}\right.\\
&\left.-2533328r^{5}+527362r^{4}+1289196r^{3}-418308r^{2}-262380r+106390\right)S^{5}T^{2}\\
&+\left(-127894r^{12}+328920r^{11}+528040r^{10}-1648444r^{9}-703322r^{8}+3304400r^{7}+90360r^{6}\right.\\
&\left.-3311736r^{5}+586862r^{4}+1659448r^{3}-504352r^{2}-332588r+130306\right)S^{4}T^{3}\\
&+\left(-114808r^{12}+246640r^{11}+491330r^{10}-1224684r^{9}-731806r^{8}+2432336r^{7}+310084r^{6}\right.\\
&\left.-2415304r^{5}+269404r^{4}+1199136r^{3}-309638r^{2}-238124r+85434\right)S^{3}T^{4}\\
&+\left(-59664r^{12}+95404r^{11}+273192r^{10}-473132r^{9}-472044r^{8}+938488r^{7}+349536r^{6}\right.\\
&\left.-930712r^{5}-53304r^{4}+461468r^{3}-61800r^{2}-91516r+24084\right)S^{2}T^{5}\\
&+\left(-16562r^{12}+14804r^{11}+84608r^{10}-74020r^{9}-174610r^{8}+148040r^{7}+183600r^{6}\right.\\
&\left.-148040r^{5}-100790r^{4}+74020r^{3}+25552r^{2}-14804r-1798\right)ST^{6}\,. \qquad \text{(A.8h)}
\end{aligned}
$$

For $\bar{Q}q({}^{3}P_{2}^{(1)})$, we have

$$
\begin{aligned}
&D({}^{3}P_{2}^{(1)}|S,T)\\
=&216S^{4}T^{2}(S+T)^{4}\left[m_{H}^{2}\left(1-r^{2}\right)+S+T\right]^{2}\,, \qquad \text{(A.9a)}\\
&a_{0}({}^{3}P_{2}^{(1)}|S,T)\\
=&-128S^{2}(S+T)^{5}(10S^{4}+24S^{3}T+36S^{2}T^{2}+33ST^{3}+10T^{4})\,, \qquad \text{(A.9b)}
\end{aligned}
$$

$$
\begin{aligned}
&a_2({}^3P_2^{(1)}|S,T)\\
=&S(S+T)^4\left[\left(7680r^2-3104r+2656\right)S^5+\left(22805r^2-11250r+12745\right)S^4T\right.\\
&+\left(34014r^2-14352r+17258\right)S^3T^2+\left(31781r^2-7646r+11837\right)S^2T^3\\
&\left.+\left(15200r^2-1472r+7520\right)ST^4+\left(2560r^2+2560\right)T^5\right]\,, \qquad \text{(A.9c)}\\
&a_4({}^3P_2^{(1)}|S,T)\\
=&(S+T)^3\left[\left(-1280r^4+2560r^2-1280\right)T^6\right.\\
&+\left(-19200r^4+15520r^3-4608r^2-3840r+4408\right)S^6\\
&+\left(-67945r^4+62504r^3-21414r^2-10556r+12331\right)S^5T\\
&+\left(-107121r^4+91980r^3-13318r^2-10220r+9599\right)S^4T^2\\
&+\left(-100191r^4+60432r^3+27326r^2-5508r+4397\right)S^3T^3\\
&+\left(-55399r^4+17012r^3+35670r^2-3532r+4409\right)S^2T^4\\
&\left.+\left(-14976r^4+1472r^3+14720r^2-1472r+256\right)ST^5\right]\,,\\
&a_6({}^3P_2^{(1)}|S,T)\\
=&(S+T)^2\left[\left(4000r^6-12000r^4+12000r^2-4000\right)T^6\right.\\
&+\left(25600r^6-31040r^5-8128r^4+27996r^3-10048r^2+4448r-8092\right)S^6\\
&+\left(105170r^6-137516r^5-47114r^4+121720r^3-15106r^2+18540r-44294\right)S^5T\\
&+\left(180504r^6-228168r^5-141636r^4+210796r^3+48480r^2+18712r-88008\right)S^4T^2\\
&+\left(172017r^6-175854r^5-229429r^4+183380r^3+140151r^2-7526r-82739\right)S^3T^3\\
&+\left(98398r^6-62340r^5-192810r^4+82536r^3+136890r^2-20196r-42478\right)S^2T^4\\
&\left.+\left(31307r^6-8066r^5-78135r^4+16132r^3+62349r^2-8066r-15521\right)ST^5\right]\,, \qquad \text{(A.9d)}\\
&a_8({}^3P_2^{(1)}|S,T)\\
=&(S+T)\left[\left(-4565r^8+18260r^6-27390r^4+18260r^2-4565\right)T^6\right.\\
&+\left(-19200r^8+31040r^7+25472r^6-60948r^5-3692r^4\right.\\
&\left.+25968r^3+9104r^2+3940r-11684\right)S^6\\
&+\left(-89810r^8+150024r^7+142376r^6-302400r^5-68060r^4\right.\\
&\left.+149176r^3+70944r^2+3200r-55450\right)S^5T\\
&+\left(-169806r^8+276144r^7+334904r^6-586196r^5-264056r^4\right.
\end{aligned}
$$

$$
\begin{aligned}
&+341216r^3+203968r^2-31164r-105010\big)\,S^4T^2\\
&+\big(-169355r^8+241712r^7+425320r^6-554920r^5-446646r^4\\
&+384704r^3+294752r^2-71496r-104071\big)\,S^3T^3\\
&+\big(-97149r^8+100564r^7+306448r^6-258132r^5-382530r^4\\
&+214572r^3+234312r^2-57004r-61081\big)\,S^2T^4\\
&+\big(-31563r^8+15972r^7+117500r^6-47916r^5-163122r^4\\
&+47916r^3+99996r^2-15972r-22811\big)\,ST^5\big]\,, \qquad \text{(A.9e)}\\
&a_{10}({}^3P_2^{(1)}|S,T)\\
=&\big(2250r^{10}-11250r^8+22500r^6-22500r^4+11250r^2-2250\big)\,T^6\\
&+\big(7680r^{10}-15520r^9-21408r^8+53268r^7+19896r^6-65280r^5\\
&-8708r^4+32836r^3+4960r^2-5304r-2420\big)\,S^6\\
&+\big(40297r^{10}-81266r^9-121479r^8+281864r^7+132522r^6-355188r^5\\
&-73030r^4+189848r^3+32925r^2-35258r-11235\big)\,S^5T\\
&+\big(84162r^{10}-163944r^9-277918r^8+580588r^7+351156r^6-756696r^5\\
&-228264r^4+427404r^3+93922r^2-87352r-23058\big)\,S^4T^2\\
&+\big(89862r^{10}-159360r^9-330238r^8+581736r^7+479796r^6-789048r^5\\
&-356580r^4+470328r^3+145414r^2-103656r-28254\big)\,S^3T^3\\
&+\big(52380r^{10}-74752r^9-217024r^8+284104r^7+359200r^6-403800r^5\\
&-299256r^4+254296r^3+127108r^2-59848r-22408\big)\,S^2T^4\\
&+\big(16317r^{10}-13590r^9-75915r^8+54360r^7+140490r^6-81540r^5\\
&-129150r^4+54360r^3+58905r^2-13590r-10647\big)\,ST^5\,, \qquad \text{(A.9f)}\\
&a_{12}({}^3P_2^{(1)}|S,T)\\
=&\big(-405r^{12}+2430r^{10}-6075r^8+8100r^6-6075r^4+2430r^2-405\big)\,T^5\\
&+\big(-1280r^{12}+3104r^{11}+6016r^{10}-16476r^9-10564r^8+34864r^7+7696r^6\\
&-36776r^5-664r^4+19344r^3-1904r^2-4060r+700\big)\,S^5\\
&+\big(-6165r^{12}+14400r^{11}+28870r^{10}-74152r^9-51123r^8+152608r^7+39092r^6\\
&-156912r^5-6763r^4+80608r^3-6618r^2-16552r+2707\big)\,S^4T
\end{aligned}
$$

$$
\begin{aligned}
&+\left(-10980r^{12}+23940r^{11}+51840r^{10}-120816r^{9}-94104r^{8}+243864r^{7}+77616r^{6}\right.\\
&\left.-246096r^{5}-21924r^{4}+124164r^{3}-5904r^{2}-25056r+3456\right)S^{3}T^{2}\\
&+\left(-8910r^{12}+16776r^{11}+43344r^{10}-83880r^{9}-83070r^{8}+167760r^{7}+77040r^{6}\right.\\
&\left.-167760r^{5}-32490r^{4}+83880r^{3}+2880r^{2}-16776r+1206\right)S^{2}T^{3}\\
&+\left(-3240r^{12}+4212r^{11}+16848r^{10}-21060r^{9}-35640r^{8}+42120r^{7}+38880r^{6}\right.\\
&\left.-42120r^{5}-22680r^{4}+21060r^{3}+6480r^{2}-4212r-648\right)ST^{4}\,. \qquad \text{(A.9g)}
\end{aligned}
$$

For $\bar{Q}q(^1P_1^{(8)})$, we have

$$
\begin{aligned}
&D(^1P_1^{(8)}|S,T)\\
=&108S^4T^2(S+T)^4\left[(1-r^2)m_H^2+S+T\right]^2\,, \qquad \text{(A.10a)}\\
&a_0(^1P_1^{(8)}|S,T)\\
=&-8S^2(S+T)^5\left(12S^4+14S^3T+12S^2T^2+23ST^3+12T^4\right)\,, \qquad \text{(A.10b)}\\
&a_2(^1P_1^{(8)}|S,T)\\
=&S(S+T)^4\left[\left(448r^2-72r-436\right)S^5+\left(963r^2-52r+1768\right)S^4T\right.\\
&+\left(626r^2-2068r+2920\right)S^3T^2+\left(571r^2-1724r+496\right)S^2T^3\\
&\left.+\left(508r^2-628r-140\right)ST^4+\left(64r^2+64\right)T^5\right]\,, \qquad \text{(A.10c)}\\
&a_4(^1P_1^{(8)}|S,T)\\
=&(S+T)^3\left[\left(-32r^4+64r^2-32\right)T^6+\left(-864r^4+416r^3+1323r^2-966r-1517\right)S^6\right.\\
&+\left(-2731r^4+2218r^3-3313r^2+3260r+6396\right)S^5T\\
&+\left(-4555r^4+11402r^3-11223r^2+2140r+20578\right)S^4T^2\\
&+\left(-2125r^4+12642r^3-10811r^2-8216r+20400\right)S^3T^3\\
&+\left(-869r^4+5078r^3-4804r^2-7030r+8611\right)S^2T^4\\
&\left.+\left(-336r^4+476r^3-500r^2-476r+836\right)ST^5\right]\,, \qquad \text{(A.10d)}\\
&a_6(^1P_1^{(8)}|S,T)\\
=&(S+T)^2\left[\left(100r^6-300r^4+300r^2-100\right)T^6\right.\\
&+\left(896r^6-944r^5-1404r^4+4242r^3+2378r^2+3614r-5358\right)S^6\\
&+\left(3792r^6-7334r^5+1409r^4-2616r^3-2722r^2+23774r-11727\right)S^5T
\end{aligned}
$$

$$
\begin{aligned}
&+\left(11648r^6-29008r^5+6344r^4+6600r^3-19180r^2+29320r-4572\right)S^4T^2\\
&+\left(7539r^6-33372r^5+15888r^4+31388r^3-33297r^2+1984r+9870\right)S^3T^3\\
&+\left(1786r^6-13536r^5+10076r^4+21222r^3-21380r^2-7686r+9518\right)S^2T^4\\
&+\left(827r^6-1646r^5+259r^4+3292r^3-2999r^2-1646r+1913\right)ST^5\big]\ , \qquad \text{(A.10e)}
\end{aligned}
$$

$$
\begin{aligned}
&a_8({}^1P_1^{(8)}|S,T)\\
=&(S+T)\left[\left(-185r^8+740r^6-1110r^4+740r^2-185\right)T^6\right.\\
&+\left(-544r^8+1056r^7+683r^6-6546r^5+177r^4-3900r^3+6749r^2+9390r-7065\right)S^6\\
&+\left(-2940r^8+9214r^7+1151r^6-13876r^5-1885r^4\right.\\
&\left.-27538r^3+30573r^2+32200r-26899\right)S^5T\\
&+\left(-13572r^8+38994r^7+11667r^6-61632r^5-6301r^4\right.\\
&\left.-7542r^3+43409r^2+30180r-35203\right)S^4T^2\\
&+\left(-13541r^8+48794r^7+6821r^6-94948r^5+10631r^4\right.\\
&\left.+43514r^3+12439r^2+2640r-16350\right)S^3T^3\\
&+\left(-4947r^8+21118r^7+1082r^6-48990r^5+12846r^4\right.\\
&\left.+34626r^3-9150r^2-6754r+169\right)S^2T^4\\
&+\left(-1347r^8+2592r^7+2792r^6-7776r^5-294r^4\right.\\
&\left.+7776r^3-2400r^2-2592r+1249\right)ST^5\big]\ , \qquad \text{(A.10f)}
\end{aligned}
$$

$$
\begin{aligned}
&a_{10}({}^1P_1^{(8)}|S,T)\\
=&\left(198r^{10}-990r^8+1980r^6-1980r^4+990r^2-198\right)T^6\\
&+\left(192r^{10}-584r^9-266r^8+4230r^7-1322r^6-2274r^5\right.\\
&\left.+154r^4-5806r^3+3762r^2+4434r-2520\right)S^6\\
&+\left(1285r^{10}-5038r^9-2325r^8+22560r^7-1918r^6-23628r^5\right.\\
&\left.-2394r^4-272r^3+13417r^2+6378r-8065\right)S^5T\\
&+\left(7866r^{10}-26232r^9-17254r^8+94660r^7+5800r^6-119676r^5\right.\\
&\left.+1704r^4+60300r^3+8878r^2-9052r-6994\right)S^4T^2\\
&+\left(11214r^{10}-37860r^9-25534r^8+134664r^7+9012r^6-176832r^5\right.\\
&\left.+14028r^4+101112r^3-9026r^2-21084r+306\right)S^3T^3
\end{aligned}
$$

$$
\begin{aligned}
&+\left(6048r^{10}-18800r^{9}-16218r^{8}+69206r^{7}+10062r^{6}-94818r^{5}\right.\\
&\left.+6642r^{4}+57218r^{3}-8838r^{2}-12806r+2304\right)S^{2}T^{4}\\
&+\left(1521r^{10}-2718r^{9}-5733r^{8}+10872r^{7}+7722r^{6}-16308r^{5}\right.\\
&\left.-3978r^{4}+10872r^{3}+117r^{2}-2718r+351\right)ST^{5}\,, \qquad \text{(A.10g)}
\end{aligned}
$$

$$
\begin{aligned}
&a_{12}({}^{1}P_{1}^{(8)}|S,T)\\
=&\left(-81r^{12}+486r^{10}-1215r^{8}+1620r^{6}-1215r^{4}+486r^{2}-81\right)T^{5}\\
&+\left(-648r^{12}+1296r^{11}+2916r^{10}-6480r^{9}-4860r^{8}+12960r^{7}+3240r^{6}\right.\\
&\left.-12960r^{5}+6480r^{3}-972r^{2}-1296r+324\right)ST^{4}\\
&+\left(-32r^{12}+128r^{11}+100r^{10}-960r^{9}+284r^{8}+2560r^{7}-1496r^{6}\right.\\
&\left.-3200r^{5}+2264r^{4}+1920r^{3}-1484r^{2}-448r+364\right)S^{5}\\
&+\left(-225r^{12}+864r^{11}+1210r^{10}-8368r^{9}-363r^{8}+24832r^{7}-6148r^{6}\right.\\
&\left.-32928r^{5}+11897r^{4}+20512r^{3}-8598r^{2}-4912r+2227\right)S^{4}T\\
&+\left(-1692r^{12}+6048r^{11}+6336r^{10}-32832r^{9}-4860r^{8}+70848r^{7}-10080r^{6}\right.\\
&\left.-76032r^{5}+21420r^{4}+40608r^{3}-14688r^{2}-8640r+3564\right)S^{3}T^{2}\\
&+\left(-1782r^{12}+5472r^{11}+6804r^{10}-27360r^{9}-7290r^{8}+54720r^{7}-3240r^{6}\right.\\
&\left.-54720r^{5}+12150r^{4}+27360r^{3}-8748r^{2}-5472r+2106\right)S^{2}T^{3}\,. \qquad \text{(A.10h)}
\end{aligned}
$$

For $\bar{Q}q({}^{3}P_{0}^{(8)})$, we have

$$
\begin{aligned}
&D({}^{3}P_{0}^{(8)}|S,T)\\
=&108S^{4}T^{2}(S+T)^{4}\left[T+(1-r^{2})m_{H}^{2}\right]^{2}\left[(1-r^{2})mH^{2}+S+T\right]^{2}\,, \qquad \text{(A.11a)}\\
&a_{0}({}^{3}P_{0}^{(8)}|S,T)\\
=&-8S^{2}T^{2}(S+T)^{5}(4S^{4}+9ST^{3}+4T^{4})\,, \qquad \text{(A.11b)}\\
&a_{2}({}^{3}P_{0}^{(8)}|S,T)\\
=&ST(S+T)^{4}\left[\left(64r^{2}-384r+1088\right)S^{6}+\left(256r^{2}-1040r+4260\right)S^{5}T\right.\\
&+\left(257r^{2}-1212r+11608\right)S^{4}T^{2}+\left(342r^{2}-3132r+11432\right)S^{3}T^{3}\\
&\left.+\left(33r^{2}-788r-2528\right)S^{2}T^{4}+\left(372r^{2}+508r-5300\right)ST^{5}+\left(64r^{2}+64\right)T^{6}\right]\,, \qquad \text{(A.11c)}
\end{aligned}
$$

$$
\begin{aligned}
&a_4({}^3P_0^{(8)}|S,T)\\
=&(S+T)^3\left[\left(-32r^4+64r^2-32\right)T^8+\left(-32r^4+384r^3-1088r^2-384r+1120\right)S^8\right.\\
&+\left(-448r^4+3400r^3-6792r^2-4144r+7600\right)S^7T\\
&+\left(-1410r^4+8720r^3-26237r^2-14134r+30201\right)S^6T^2\\
&+\left(-2267r^4+15710r^3-52805r^2-42272r+58840\right)S^5T^3\\
&+\left(-2931r^4+31342r^3-38287r^2-52512r+37082\right)S^4T^4\\
&+\left(-237r^4+21614r^3+7417r^2-15860r-15012\right)S^3T^5\\
&+\left(-1275r^4+2658r^3+13228r^2+2518r-16347\right)S^2T^6\\
&\left.+\left(-464r^4-748r^3+20r^2+748r+444\right)ST^7\right], \qquad \text{(A.11d)}\\
&a_6({}^3P_0^{(8)}|S,T)\\
=&(S+T)^2\left[\left(164r^6-492r^4+492r^2-164\right)T^8\right.\\
&+\left(192r^6-1976r^5+3748r^4+4696r^3-6128r^2-2720r+2188\right)S^8\\
&+\left(1601r^6-12564r^5+20612r^4+35884r^3-42855r^2-23416r+20546\right)S^7T\\
&+\left(5074r^6-34072r^5+60078r^4+137630r^3-141248r^2-122566r+84512\right)S^6T^2\\
&+\left(11036r^6-81914r^5+84045r^4+337064r^3-219982r^2-281230r+140453\right)S^5T^3\\
&+\left(14100r^6-144744r^5+46512r^4+406232r^3-127288r^2-268656r+75988\right)S^4T^4\\
&+\left(5922r^6-105784r^5-3608r^4+197048r^3+16462r^2-91264r-18776\right)S^3T^5\\
&+\left(3496r^6-20488r^5-9250r^4+22194r^3+24390r^2-1706r-18636\right)S^2T^6\\
&\left.+\left(1627r^6+1398r^5-1589r^4-2796r^3-1703r^2+1398r+1665\right)ST^7\right], \qquad \text{(A.11e)}\\
&a_8({}^3P_0^{(8)}|S,T)\\
=&(S+T)\left[\left(-417r^8+1668r^6-2502r^4+1668r^2-417\right)T^8\right.\\
&+\left(-480r^8+4120r^7-4191r^6-16958r^5+13975r^4\right.\\
&\left.+21652r^3-13361r^2-8814r+4057\right)S^8\\
&+\left(-3525r^8+24758r^7-22119r^6-121988r^5+89675r^4\right.\\
&\left.+207814r^3-115629r^2-110584r+51598\right)S^7T\\
&+\left(-12659r^8+78630r^7-35065r^6-480188r^5+222937r^4\right.\\
&\left.+852390r^3-355099r^2-450832r+179886\right)S^6T^2
\end{aligned}
$$

$$
\begin{aligned}
&+\left(-31960r^8+209670r^7+8157r^6-1097328r^5+259769r^4\right.\\
&\left.+1682222r^3-494121r^2-794564r+258155\right)S^5T^3\\
&+\left(-42382r^8+330626r^7+56988r^6-1296198r^5+133770r^4\right.\\
&\left.+1627206r^3-303248r^2-661634r+154872\right)S^4T^4\\
&+\left(-25854r^8+229100r^7+43450r^6-705924r^5+16318r^4\right.\\
&\left.+724548r^3-59570r^2-247724r+25656\right)S^3T^5\\
&+\left(-10422r^8+51536r^7+15540r^6-134912r^5-8r^4\right.\\
&\left.+115216r^3-4916r^2-31840r-194\right)S^2T^6\\
&+\left(-3601r^8+816r^7+7724r^6-2448r^5-1566r^4\right.\\
&\left.+2448r^3-5636r^2-816r+3079\right)ST^7\Big]\,, \qquad \text{(A.11f)}\\
&a_{10}({}^3P_0^{(8)}|S,T)\\
=&\left(668r^{10}-3340r^8+6680r^6-6680r^4+3340r^2-668\right)T^8\\
&+\left(640r^{10}-4400r^9+288r^8+23206r^7-9346r^6-62226r^5\right.\\
&\left.+28326r^4+72434r^3-32966r^2-29014r+13058\right)S^8\\
&+\left(4810r^{10}-26146r^9-9865r^8+191036r^7-30616r^6-555784r^5\right.\\
&\left.+169562r^4+643044r^3-231866r^2-252150r+97975\right)S^7T\\
&+\left(20928r^{10}-99272r^9-86472r^8+796816r^7+13984r^6-2067584r^5\right.\\
&\left.+415728r^4+2141808r^3-632160r^2-771768r+267992\right)S^6T^2\\
&+\left(56044r^{10}-274384r^9-234910r^8+1772016r^7+145304r^6-3859024r^5\right.\\
&\left.+547700r^4+3499536r^3-871892r^2-1138144r+357754\right)S^5T^3\\
&+\left(77012r^{10}-400168r^9-290184r^8+2047918r^7+200934r^6-3779802r^5\right.\\
&\left.+415126r^4+3016522r^3-657378r^2-884470r+254490\right)S^4T^4\\
&+\left(53954r^{10}-265994r^9-183513r^8+1154628r^7+128296r^6-1867920r^5\right.\\
&\left.+176650r^4+1335932r^3-273906r^2-356646r+98519\right)S^3T^5\\
&+\left(21456r^{10}-66688r^9-67732r^8+265756r^7+52924r^6-397140r^5\right.\\
&\left.+33060r^4+263764r^3-61244r^2-65692r+21536\right)S^2T^6
\end{aligned}
$$

$$
\begin{aligned}
&+\left(5612r^{10}-4004r^9-20288r^8+16016r^7+25032r^6-24024r^5\right.\\
&\left.-9488r^4+16016r^3-3028r^2-4004r+2160\right)ST^7\,, \qquad \text{(A.11g)}\\
&a_{12}({}^3P_0^{(8)}|S,T)\\
=&\left(-662r^{12}+3972r^{10}-9930r^8+13240r^6-9930r^4+3972r^2-662\right)T^7\\
&+\left(-480r^{12}+2480r^{11}+2681r^{10}-11962r^9-6807r^8+60776r^7-7102r^6\right.\\
&\left.-135356r^5+42538r^4+123832r^3-47067r^2-39770r+16237\right)S^7\\
&+\left(-3434r^{12}+10114r^{11}+30902r^{10}-124506r^9-73334r^8+522324r^7-9564r^6\right.\\
&\left.-921076r^5+211186r^4+722634r^3-234250r^2-209490r+78494\right)S^6T\\
&+\left(-17466r^{12}+49764r^{11}+124766r^{10}-506104r^9-241980r^8+1637208r^7+364r^6\right.\\
&\left.-2372640r^5+465118r^4+1609252r^3-482442r^2-417480r+151640\right)S^5T^2\\
&+\left(-40658r^{12}+130004r^{11}+223972r^{10}-910252r^9-368178r^8+2363688r^7+17832r^6\right.\\
&\left.-2929592r^5+525722r^4+1759108r^3-508140r^2-412956r+149450\right)S^4T^3\\
&+\left(-41312r^{12}+128928r^{11}+202013r^{10}-728674r^9-318539r^8+1625416r^7+80266r^6\right.\\
&\left.-1793484r^5+269986r^4+980776r^3-268807r^2-212962r+76393\right)S^3T^4\\
&+\left(-20010r^{12}+44274r^{11}+94166r^{10}-229218r^9-159574r^8+474132r^7+96836r^6\right.\\
&\left.-489828r^5+25426r^4+252762r^3-53834r^2-52122r+16990\right)S^2T^5\\
&+\left(-5222r^{12}+4356r^{11}+26108r^{10}-21780r^9-52210r^8+43560r^7+52200r^6\right.\\
&\left.-43560r^5-26090r^4+21780r^3+5212r^2-4356r+2\right)ST^6\,. \qquad \text{(A.11h)}
\end{aligned}
$$

For $\bar{Q}q({}^3P_1^{(8)})$, we have

$$
\begin{aligned}
&D({}^3P_1^{(8)}|S,T)\\
=&54S^4T^2(S+T)^4\left[T+(1-r^2)m_H^2\right]^2\left[(1-r^2)m_H^2+S+T\right]^2\,, \qquad \text{(A.12a)}\\
&a_0({}^3P_1^{(8)}|S,T)\\
=&-8S^2T^2(S+T)^5\left(4S^4+7S^3T+14S^2T^2+5ST^3+12T^4\right)\,, \qquad \text{(A.12b)}\\
&a_2({}^3P_1^{(8)}|S,T)\\
=&ST(S+T)^4\left[\left(128r^2-128r+64\right)S^6+\left(696r^2-700r+108\right)S^5T\right.
\end{aligned}
$$

$$
\begin{aligned}
&+\left(1491r^2+530r-939\right)S^4T^2+\left(1514r^2-880r-4038\right)S^3T^3\\
&+\left(279r^2-702r-663\right)S^2T^4+\left(748r^2-776r-1308\right)ST^5+\left(64r^2+64\right)T^6\big]\ , \quad \text{(A.12c)}\\
&a_4({}^3P_1^{(8)}|S,T)\\
=&(S+T)^3\left[\left(-96r^4+128r^3-128r+96\right)S^8+\left(-32r^4+64r^2-32\right)T^8\right.\\
&+\left(-1024r^4+1616r^3+352r^2-1704r+376\right)S^7T\\
&+\left(-4046r^4+2624r^3+4302r^2-312r-3408\right)S^6T^2\\
&+\left(-7917r^4-332r^3+19620r^2-7052r-9523\right)S^5T^3\\
&+\left(-8565r^4+14072r^3+25584r^2-30472r-2359\right)S^4T^4\\
&+\left(-6711r^4+16748r^3+13212r^2-24788r+3159\right)S^3T^5\\
&+\left(-4009r^4+6032r^3+4762r^2-4336r-1565\right)S^2T^6\\
&\left.+\left(-528r^4+144r^3-392r^2-144r+920\right)ST^7\right]\ , \quad \text{(A.12d)}\\
&a_6({}^3P_1^{(8)}|S,T)\\
=&(S+T)^2\left[\left(164r^6-492r^4+492r^2-164\right)T^8\right.\\
&+\left(448r^6-788r^5-132r^4+1664r^3-400r^2-876r+84\right)S^8\\
&+\left(3555r^6-5206r^5-4293r^4+6596r^3+5321r^2-1422r-4615\right)S^7T\\
&+\left(12342r^6-5152r^5-30986r^4+17508r^3+32590r^2-21220r-9738\right)S^6T^2\\
&+\left(25554r^6-19908r^5-88588r^4+123912r^3+55290r^2-110564r+12496\right)S^5T^3\\
&+\left(37084r^6-81756r^5-113856r^4+261808r^3+31164r^2-177780r+44984\right)S^4T^4\\
&+\left(34418r^6-84056r^5-68306r^4+193320r^3-1922r^2-109264r+35810\right)S^3T^5\\
&+\left(14672r^6-26476r^5-16936r^4+48596r^3-8836r^2-22120r+11100\right)S^2T^6\\
&\left.+\left(2319r^6-1810r^5-1495r^4+3620r^3-3967r^2-1810r+3143\right)ST^7\right]\ , \quad \text{(A.12e)}\\
&a_8({}^3P_1^{(8)}|S,T)\\
=&(S+T)\left[\left(-417r^8+1668r^6-2502r^4+1668r^2-417\right)T^8\right.\\
&+\left(-864r^8+1964r^7+1242r^6-4300r^5-1726r^4+2740r^3+3214r^2-404r-1866\right)S^8\\
&+\left(-6627r^8+7880r^7+17890r^6-19632r^5-28512r^4\right.\\
&\left.+33384r^3+21478r^2-21632r-4229\right)S^7T
\end{aligned}
$$

$$
\begin{aligned}
&+\left(-23881r^8+13936r^7+96398r^6-131168r^5-121336r^4\right.\\
&\left.+269008r^3+22570r^2-151776r+26249\right)S^6T^2\\
&+\left(-57814r^8+88068r^7+241722r^6-529372r^5-222574r^4\right.\\
&\left.+818188r^3-68042r^2-376884r+106708\right)S^5T^3\\
&+\left(-93544r^8+224804r^7+309012r^6-890244r^5-183584r^4\right.\\
&\left.+1098972r^3-184684r^2-433532r+152800\right)S^4T^4\\
&+\left(-83198r^8+204408r^7+201468r^6-651232r^5-49504r^4\right.\\
&\left.+689240r^3-172604r^2-242416r+103838\right)S^3T^5\\
&+\left(-33810r^8+66712r^7+65944r^6-194568r^5+3948r^4\right.\\
&\left.+189000r^3-70488r^2-61144r+34406\right)S^2T^6\\
&+\left(-6013r^8+6492r^7+13184r^6-19476r^5-3474r^4\right.\\
&\left.+19476r^3-8552r^2-6492r+4855\right)ST^7\Big]\ , \qquad \text{(A.12f)}\\
&a_{10}({}^3P_1^{(8)}|S,T)\\
=&\left(668r^{10}-3340r^8+6680r^6-6680r^4+3340r^2-668\right)T^8\\
&+\left(896r^{10}-2536r^9-2984r^8+5596r^7+8108r^6-10436r^5\right.\\
&\left.-11172r^4+14228r^3+5476r^2-6852r-324\right)S^8\\
&+\left(7192r^{10}-6776r^9-35386r^8+45248r^7+75984r^6-154640r^5\right.\\
&\left.-57364r^4+200640r^3-7640r^2-84472r+17214\right)S^7T\\
&+\left(30152r^{10}-29556r^9-166420r^8+316200r^7+281688r^6-865184r^5\right.\\
&\left.-91632r^4+899992r^3-146880r^2-321452r+93092\right)S^6T^2\\
&+\left(83364r^{10}-164436r^9-395516r^8+1040768r^7+516696r^6-2171240r^5\right.\\
&\left.+21672r^4+1877920r^3-428188r^2-583012r+201972\right)S^5T^3\\
&+\left(135476r^{10}-335592r^9-514508r^8+1590348r^7+504724r^6-2749812r^5\right.\\
&\left.+218836r^4+2070948r^3-571192r^2-575892r+226664\right)S^4T^4\\
&+\left(115760r^{10}-281648r^9-372674r^8+1161008r^7+286656r^6-1793136r^5\right.\\
&\left.+218476r^4+1229840r^3-385024r^2-316064r+136806\right)S^3T^5
\end{aligned}
$$

$$
\begin{aligned}
&+\left(48176r^{10}-96204r^{9}-149964r^{8}+378992r^{7}+119904r^{6}-559752r^{5}\right.\\
&\left.+58312r^{4}+367344r^{3}-117360r^{2}-90380r+40932\right)S^{2}T^{6}\\
&+\left(9336r^{10}-11028r^{9}-33640r^{8}+44112r^{7}+41200r^{6}-66168r^{5}\right.\\
&\left.-15120r^{4}+44112r^{3}-5480r^{2}-11028r+3704\right)ST^{7}\,, \qquad \text{(A.12g)}\\
&a_{12}({}^{3}P_{1}^{(8)}|S,T)\\
=&\left(-662r^{12}+3972r^{10}-9930r^{8}+13240r^{6}-9930r^{4}+3972r^{2}-662\right)T^{7}\\
&+\left(-544r^{12}+1784r^{11}+2970r^{10}-4696r^{9}-10394r^{8}+18576r^{7}+14244r^{6}\right.\\
&\left.-45392r^{5}-1908r^{4}+44920r^{3}-8926r^{2}-15192r+4558\right)S^{7}\\
&+\left(-4148r^{12}+1772r^{11}+31596r^{10}-47308r^{9}-83460r^{8}+221816r^{7}+72760r^{6}\right.\\
&\left.-399320r^{5}+28740r^{4}+313564r^{3}-75012r^{2}-90524r+29524\right)S^{6}T\\
&+\left(-20066r^{12}+30880r^{11}+128764r^{10}-304896r^{9}-261462r^{8}+940320r^{7}+135720r^{6}\right.\\
&\left.-1300384r^{5}+174962r^{4}+844992r^{3}-234660r^{2}-210912r+76742\right)S^{5}T^{2}\\
&+\left(-52394r^{12}+125904r^{11}+259784r^{10}-767120r^{9}-416602r^{8}+1806304r^{7}+114480r^{6}\right.\\
&\left.-2075232r^{5}+344242r^{4}+1170512r^{3}-350072r^{2}-260368r+100562\right)S^{4}T^{3}\\
&+\left(-63032r^{12}+155480r^{11}+270682r^{10}-802152r^{9}-383546r^{8}+1653808r^{7}+88004r^{6}\right.\\
&\left.-1703312r^{5}+275924r^{4}+876408r^{3}-256894r^{2}-180232r+68862\right)S^{3}T^{4}\\
&+\left(-33468r^{12}+69404r^{11}+143436r^{10}-343132r^{9}-216708r^{8}+678488r^{7}+101832r^{6}\right.\\
&\left.-670712r^{5}+62412r^{4}+331468r^{3}-79860r^{2}-65516r+22356\right)S^{2}T^{5}\\
&+\left(-7882r^{12}+10072r^{11}+37792r^{10}-50360r^{9}-70730r^{8}+100720r^{7}+62640r^{6}\right.\\
&\left.-100720r^{5}-23230r^{4}+50360r^{3}-208r^{2}-10072r+1618\right)ST^{6}\,. \qquad \text{(A.12h)}
\end{aligned}
$$

For $\bar{Q}q({}^{3}P_{2}^{(8)})$, we have

$$
\begin{aligned}
&D({}^{3}P_{2}^{(8)}|S,T)\\
=&324S^{4}T^{2}(S+T)^{4}\left[(1-r^{2})m_{H}^{2}+S+T\right]^{2}\,, \qquad \text{(A.13a)}\\
&a_{0}({}^{3}P_{2}^{(8)}|S,T)\\
=&-8S^{2}(S+T)^{5}\left(20S^{4}+21S^{3}T+18S^{2}T^{2}+39ST^{3}+20T^{4}\right)\,, \qquad \text{(A.13b)}
\end{aligned}
$$

$$
\begin{aligned}
&a_2({}^3P_2^{(8)}|S,T)\\
=&S(S+T)^4\left[\left(960r^2-388r+332\right)S^5+\left(2125r^2+162r+7829\right)S^4T\right.\\
&+\left(1950r^2-1992r+12010\right)S^3T^2+\left(1897r^2-382r+3121\right)S^2T^3\\
&\left.+\left(1684r^2-184r+1156\right)ST^4+\left(320r^2+320\right)T^5\right]\,, \qquad \text{(A.13c)}\\
&a_4({}^3P_2^{(8)}|S,T)\\
=&(S+T)^3\left[\left(-160r^4+320r^2-160\right)T^6+\left(-2400r^4+1940r^3-576r^2-2748r+4520\right)S^6\right.\\
&+\left(-8105r^4-2996r^3-25854r^2+18260r+22463\right)S^5T\\
&+\left(-15945r^4+10512r^3-46766r^2+28472r+27535\right)S^4T^2\\
&+\left(-15315r^4+8508r^3-15626r^2+15228r+14269\right)S^3T^3\\
&+\left(-7907r^4+772r^3+2598r^2+3748r+6229\right)S^2T^4\\
&\left.+\left(-1872r^4+184r^3+1840r^2-184r+32\right)ST^5\right]\,, \qquad \text{(A.13d)}\\
&a_6({}^3P_2^{(8)}|S,T)\\
=&(S+T)^2\left[\left(500r^6-1500r^4+1500r^2-500\right)T^6\right.\\
&+\left(3200r^6-3880r^5-1016r^4+7752r^3-10328r^2+7360r+3808\right)S^6\\
&+\left(14530r^6+10364r^5+16730r^4-62104r^3-45050r^2+70236r+4334\right)S^5T\\
&+\left(47160r^6-31464r^5+9984r^4-60712r^3-52224r^2+99440r-8904\right)S^4T^2\\
&+\left(55053r^6-52530r^5-39113r^4+6484r^3-8949r^2+46046r-6991\right)S^3T^3\\
&+\left(25118r^6-15996r^5-34998r^4+6312r^3+9522r^2+9684r+358\right)S^2T^4\\
&\left.+\left(5827r^6-1150r^5-12531r^4+2300r^3+7581r^2-1150r-877\right)ST^5\right]\,, \qquad \text{(A.13e)}\\
&a_8({}^3P_2^{(8)}|S,T)\\
=&(S+T)\left[\left(-925r^8+3700r^6-5550r^4+3700r^2-925\right)T^6\right.\\
&+\left(-2400r^8+3880r^7+3184r^6-6768r^5+3224r^4\right.\\
&\left.-20568r^3+2272r^2+23456r-6280\right)S^6\\
&+\left(-13690r^8-14736r^7+26644r^6+71424r^5-28240r^4\right.\\
&\left.-139600r^3+51708r^2+82912r-36422\right)S^5T\\
&+\left(-63150r^8+51240r^7+132700r^6-47080r^5-137128r^4\right.\\
&\left.-78056r^3+138212r^2+73896r-70634\right)S^4T^2
\end{aligned}
$$

$$
\begin{aligned}
&+\left(-87559r^8+111952r^7+209720r^6-221744r^5-216798r^4\right.\\
&\left.+107632r^3+154672r^2+2160r-60035\right)S^3T^3\\
&+\left(-44601r^8+51752r^7+125912r^6-119760r^5-143106r^4\right.\\
&\left.+84264r^3+86880r^2-16256r-25085\right)S^2T^4\\
&+\left(-10395r^8+6816r^7+37084r^6-20448r^5-48882r^4\right.\\
&\left.+20448r^3+28092r^2-6816r-5899\right)ST^5\Big]\,, \qquad \text{(A.13f)}\\
&a_{10}({}^3P_2^{(8)}|S,T)\\
=&\left(990r^{10}-4950r^8+9900r^6-9900r^4+4950r^2-990\right)T^6\\
&+\left(960r^{10}-1940r^9-2676r^8+1272r^7+6456r^6+19056r^5\right.\\
&\left.-17248r^4-34168r^3+21032r^2+15780r-8524\right)S^6\\
&+\left(6593r^{10}+9554r^9-39207r^8-29576r^7+99858r^6+53868r^5\right.\\
&\left.-141206r^4-57224r^3+106701r^2+23378r-32739\right)S^5T\\
&+\left(39714r^{10}-40176r^9-168338r^8+159824r^7+310020r^6-227184r^5\right.\\
&\left.-322644r^4+135600r^3+190010r^2-28064r-48762\right)S^4T^2\\
&+\left(63606r^{10}-98436r^9-250514r^8+362832r^7+408828r^6-497880r^5\right.\\
&\left.-359460r^4+301008r^3+176462r^2-67524r-38922\right)S^3T^3\\
&+\left(38016r^{10}-56828r^9-156908r^8+212408r^7+262376r^6-296256r^5\right.\\
&\left.-225840r^4+182600r^3+102104r^2-41924r-19748\right)S^2T^4\\
&+\left(9765r^{10}-10062r^9-45423r^8+40248r^7+84042r^6-60372r^5\right.\\
&\left.-77238r^4+40248r^3+35217r^2-10062r-6363\right)ST^5\,, \qquad \text{(A.13g)}\\
&a_{12}({}^3P_2^{(8)}|S,T)\\
=&\left(-405r^{12}+2430r^{10}-6075r^8+8100r^6-6075r^4+2430r^2-405\right)T^5\\
&+\left(-160r^{12}+388r^{11}+752r^{10}+492r^9-3872r^8-5848r^7+11168r^6\right.\\
&\left.+10712r^5-15392r^4-7788r^3+9968r^2+2044r-2464\right)S^5\\
&+\left(-1125r^{12}-2736r^{11}+13106r^{10}+1504r^9-45159r^8+21344r^7+72076r^6\right.\\
&\left.-45696r^5-59459r^4+35024r^3+24546r^2-9440r-3985\right)S^4T
\end{aligned}
$$

$$
\begin{aligned}
&+\left(-8460r^{12}+14616r^{11}+47304r^{10}-82008r^{9}-106452r^{8}+181872r^{7}+121968r^{6}\right.\\
&\left.-199728r^{5}-73332r^{4}+108792r^{3}+20808r^{2}-23544r-1836\right)S^{3}T^{2}\\
&+\left(-8910r^{12}+16272r^{11}+45108r^{10}-81360r^{9}-91890r^{8}+162720r^{7}+94680r^{6}\right.\\
&\left.-162720r^{5}-50130r^{4}+81360r^{3}+11700r^{2}-16272r-558\right)S^{2}T^{3}\\
&+\left(-3240r^{12}+4212r^{11}+16848r^{10}-21060r^{9}-35640r^{8}+42120r^{7}+38880r^{6}\right.\\
&\left.-42120r^{5}-22680r^{4}+21060r^{3}+6480r^{2}-4212r-648\right)ST^{4}\,. \qquad \text{(A.13h)}
\end{aligned}
$$

The partonic cross sections for the $\bar{Q}q \to \bar{Q}q(^{2S+1}P_J^{(c)}) + g$ can be obtained from those for $qg \to \bar{Q}q(^{2S+1}P_J^{(c)}) + Q$ by applying crossing symmetry as follows. Formally, in the expressions of $\frac{d\hat{\sigma}}{d\hat{t}}[qg \to \bar{Q}q(^{2S+1}P_J^{(c)}) + Q]$, one replaces the flux factor by

$$
\frac{1}{S^2} \to \frac{1}{S^2} \quad \text{for the prefactor}\,. \qquad \text{(A.14)}
$$

Then beside this flux factor, for all the appearances of S and T, the following replacementare are implemented:

$$
\begin{aligned}
&S \to T\,,\\
&T \to U\,,\\
&U \to S\,. \qquad \text{(A.15)}
\end{aligned}
$$

After all these, one has to multiply the resulting expression by $-8/3$. The final result will be $\frac{d\hat{\sigma}}{d\hat{t}}[\bar{Q}q \to \bar{Q}q(^{2S+1}P_J^{(c)}) + g]$, with $S = \hat{s} - m_H^2$ and $T = \hat{t}$.

A.2 HADRONIC PRODUCTION OF HEAVY BARYONS

For P waves in baryon productions, there also are 8 non-perturbative parameters, corresponding to $n =^1 P_1^{(\bar{3})},\ ^3P_0^{(\bar{3})},\ ^3P_1^{(\bar{3})},\ ^3P_2^{(\bar{3})},\ ^1P_1^{(6)},\ ^3P_0^{(6)},\ ^3P_1^{(6)},\ ^3P_2^{(6)}$. They are defined by

$$\begin{aligned}
\rho[Qq(^1P_1^{(\bar{3})}) \to H] =& \frac{1}{m_Q^3}\int \frac{d\eta_1}{\eta_1}\frac{d\eta_2}{\eta_2}\frac{dw_1}{2\pi}\frac{dw_2}{2\pi}e^{-i\eta_1 w_1+i\eta_2 w_2} \\
& \times \langle 0|\bar{\mathbf{T}}\left[\bar{q}(w_2v)\mathcal{C}^\dagger\left(-\frac{i}{2}\overleftrightarrow{D}_T^\mu\right)K^a S(w_2v,0)Q_v(0)\right]a_H^\dagger \\
& \times a_H \mathbf{T}\left[\bar{Q}_v(0)\left(-\frac{i}{2}\overleftrightarrow{D}_{T\mu}\right)S(0,w_1v)K^a\mathcal{C}q(w_1v)\right]|0\rangle\,, \qquad \text{(A.16a)} \\
\rho[Qq(^3P_0^{(\bar{3})}) \to H] =& \frac{1}{m_Q^3}\int \frac{d\eta_1}{\eta_1}\frac{d\eta_2}{\eta_2}\frac{dw_1}{2\pi}\frac{dw_2}{2\pi}e^{-i\eta_1 w_1+i\eta_2 w_2} \\
& \times \langle 0|\bar{\mathbf{T}}\left[\bar{q}(w_2v)\mathcal{C}^\dagger\left(-\frac{i}{2}\overleftrightarrow{D}_T^\mu\Sigma_\mu\right)K^a S(w_2v,0)Q_v(0)\right]a_H^\dagger \\
& \times a_H \mathbf{T}\left[\bar{Q}_v(0)\left(-\frac{i}{2}\overleftrightarrow{D}_T^\nu\Sigma_\nu\right)S(0,w_1v)K^a\mathcal{C}q(w_1v)\right]|0\rangle\,, \qquad \text{(A.16b)} \\
\rho[Qq(^3P_1^{(\bar{3})}) \to H] =& \frac{1}{m_Q^3}\int \frac{d\eta_1}{\eta_1}\frac{d\eta_2}{\eta_2}\frac{dw_1}{2\pi}\frac{dw_2}{2\pi}e^{-i\eta_1 w_1+i\eta_2 w_2} \\
& \times \langle 0|\bar{\mathbf{T}}\left[\bar{q}(w_2v)\mathcal{C}^\dagger\left(-\frac{i}{2}\epsilon_{\mu\nu\alpha\beta}v^\nu\overleftrightarrow{D}_T^\alpha\Sigma^\beta\right)K^a S(w_2v,0)Q_v(0)\right]a_H^\dagger \\
& \times a_H \mathbf{T}\left[\bar{Q}_v(0)\left(-\frac{i}{2}\epsilon^\mu{}_{\rho\sigma\delta}v^\rho\overleftrightarrow{D}_T^\sigma\Sigma^\delta\right)S(0,w_1v)K^a\mathcal{C}q(w_1v)\right]|0\rangle\,, \qquad \text{(A.16c)} \\
\rho[Q\bar{q}(^3P_2^{(\bar{3})}) \to H] =& \frac{1}{m_Q^3}\int \frac{d\eta_1}{\eta_1}\frac{d\eta_2}{\eta_2}\frac{dw_1}{2\pi}\frac{dw_2}{2\pi}e^{-i\eta_1 w_1+i\eta_2 w_2} \\
& \times \langle 0|\bar{\mathbf{T}}\left[\bar{q}(w_2v)\mathcal{C}^\dagger\left(-\frac{i}{2}\overleftrightarrow{D}_T^{(\mu}\overleftrightarrow{D}_T^{\nu)}\right)K^a S(w_2v,0)Q_v(0)\right]a_H^\dagger \\
& \times a_H \mathbf{T}\left[\bar{Q}_v(0)\left(-\frac{i}{2}\overleftrightarrow{D}_{T(\mu}\overleftrightarrow{D}_{T\nu)}\right)S(0,w_1v)K^a\mathcal{C}q(w_1v)\right]|0\rangle\,, \qquad \text{(A.16d)} \\
\rho[Qq(^1P_1^{(6)}) \to H] =& \frac{1}{m_Q^3}\int \frac{d\eta_1}{\eta_1}\frac{d\eta_2}{\eta_2}\frac{dw_1}{2\pi}\frac{dw_2}{2\pi}e^{-i\eta_1 w_1+i\eta_2 w_2} \\
& \times \langle 0|\bar{\mathbf{T}}\left[\bar{q}(w_2v)\mathcal{C}^\dagger\left(-\frac{i}{2}\overleftrightarrow{D}_T^\mu\right)L^a S(w_2v,0)Q_v(0)\right]a_H^\dagger \\
& \times a_H \mathbf{T}\left[\bar{Q}_v(0)\left(-\frac{i}{2}\overleftrightarrow{D}_{T\mu}\right)S(0,w_1v)L^a\mathcal{C}q(w_1v)\right]|0\rangle\,, \qquad \text{(A.16e)}
\end{aligned}$$

$$\rho[Qq(^3P_0^{(6)}) \to H] = \frac{1}{m_Q^3}\int \frac{d\eta_1}{\eta_1}\frac{d\eta_2}{\eta_2}\frac{dw_1}{2\pi}\frac{dw_2}{2\pi}e^{-i\eta_1 w_1 + i\eta_2 w_2} \times \langle 0|\bar{\mathbf{T}}\left[\bar{q}(w_2 v)\mathcal{C}^\dagger\left(-\frac{i}{2}\overleftrightarrow{D}^\mu_T\Sigma_\mu\right)L^a S(w_2 v,0)Q_v(0)\right]a_H^\dagger \times a_H \mathbf{T}\left[\bar{Q}_v(0)\left(-\frac{i}{2}\overleftrightarrow{D}^\nu_T\Sigma_\nu\right)S(0,w_1 v)L^a\mathcal{C}q(w_1 v)\right]|0\rangle\,, \tag{A.16f}$$

$$\rho[Qq(^3P_1^{(6)}) \to H] = \frac{1}{m_Q^3}\int \frac{d\eta_1}{\eta_1}\frac{d\eta_2}{\eta_2}\frac{dw_1}{2\pi}\frac{dw_2}{2\pi}e^{-i\eta_1 w_1 + i\eta_2 w_2} \times \langle 0|\bar{\mathbf{T}}\left[\bar{q}(w_2 v)\mathcal{C}^\dagger\left(-\frac{i}{2}\epsilon_{\mu\nu\alpha\beta}v^\nu\overleftrightarrow{D}^\alpha_T\Sigma^\beta\right)L^a S(w_2 v,0)Q_v(0)\right]a_H^\dagger \times a_H \mathbf{T}\left[\bar{Q}_v(0)\left(-\frac{i}{2}\epsilon^\mu{}_{\rho\sigma\delta}v^\rho\overleftrightarrow{D}^\sigma_T\Sigma^\delta\right)S(0,w_1 v)L^a\mathcal{C}q(w_1 v)\right]|0\rangle\,, \tag{A.16g}$$

$$\rho[Qq(^3P_2^{(6)}) \to H] = \frac{1}{m_Q^3}\int \frac{d\eta_1}{\eta_1}\frac{d\eta_2}{\eta_2}\frac{dw_1}{2\pi}\frac{dw_2}{2\pi}e^{-i\eta_1 w_1 + i\eta_2 w_2} \times \langle 0|\bar{\mathbf{T}}\left[\bar{q}(w_2 v)\mathcal{C}^\dagger\left(-\frac{i}{2}\overleftrightarrow{D}^{(\mu}_T\overleftrightarrow{D}^{\nu)}_T\right)L^a S(w_2 v,0)Q_v(0)\right]a_H^\dagger \times a_H \mathbf{T}\left[\bar{Q}_v(0)\left(-\frac{i}{2}\overleftrightarrow{D}_{T(\mu}\overleftrightarrow{D}_{T\nu)}\right)S(0,w_1 v)L^a\mathcal{C}q(w_1 v)\right]|0\rangle\,. \tag{A.16h}$$

The resulting perturbative cross sections for $qg \to Qq(^{2S+1}P_J^{(c)}) + \bar{Q}$ have the form

$$\frac{d\hat{\sigma}}{d\hat{t}}[qg \to Qq(^{2S+1}P_J^{(c)}) + \bar{Q}] = -\frac{\pi^2\alpha_s^3 m_H^2}{6S^2}\frac{\mathcal{N}(^{2S+1}P_J^{(c)}|S,T)}{\mathcal{D}(^{2S+1}P_J^{(c)}|S,T)}\,, \tag{A.17}$$

where $S = \hat{s} = (p+l)^2$ and $T = \hat{t} - m_H^2 = (p_H - p)^2 - m_H^2$. Again, we will distinguish m_H from m_Q and write $m_Q = r m_H$. $\mathcal{N}(^{2S+1}P_J^{(c)}|S,T)$ is an expansion in powers of m_H:

$$\mathcal{N}(^{2S+1}P_J^{(c)}|S,T) = \sum_{n=0}^{6} c_{2n}(^{2S+1}P_J^{(c)}|S,T)m_H^{2n}\,. \tag{A.18}$$

Just as in the case of production of heavy mesons, the partonic cross sections for $Qq \to Qq(^{2S+1}P_J^{(c)}) + g$ can be obtained from those for $qg \to Qq(^{2S+1}P_J^{(c)}) + \bar{Q}$ by applying crossing symmetry, as described at the end of Section A.1.

For $Qq(^1P_1^{(\bar{3})})$, we have

$$
\begin{aligned}
&\mathcal{D}(^1P_1^{(\bar{3})}|S,T)\\
=&18S^4T^2(S+T)^4\left[(1-r^2)m_H^2+S+T\right]^2\,, &\text{(A.19a)}\\
&c_0(^1P_1^{(\bar{3})}|S,T)\\
=&-16S^2(S+T)^5(12S^4+24S^3T+32S^2T^2+33ST^3+12T^4)\,, &\text{(A.19b)}\\
&c_2(^1P_1^{(\bar{3})}|S,T)\\
=&S(S+T)^4\left[\left(896r^2-144r-872\right)S^5+\left(2001r^2-484r-1884\right)S^4T\right.\\
&+\left(2322r^2-1276r-2220\right)S^3T^2+\left(2137r^2-1668r-1648\right)S^2T^3\\
&\left.+\left(1016r^2-716r-280\right)ST^4+\left(128r^2+128\right)T^5\right]\,, &\text{(A.19c)}\\
&c_4(^1P_1^{(\bar{3})}|S,T)\\
=&(S+T)^3\left[\left(-64r^4+128r^2-64\right)T^6+\left(-1728r^4+832r^3+2781r^2-42r-1279\right)S^6\right.\\
&+\left(-4457r^4+3066r^3+6509r^2+440r-3028\right)S^5T\\
&+\left(-5025r^4+5994r^3+6479r^2-1620r-2474\right)S^4T^2\\
&+\left(-3735r^4+6474r^3+3403r^2-5052r+380\right)S^3T^3\\
&+\left(-2143r^4+3166r^3+572r^2-3290r+1777\right)S^2T^4\\
&\left.+\left(-672r^4+412r^3+80r^2-412r+592\right)ST^5\right]\,, &\text{(A.19d)}\\
&c_6(^1P_1^{(\bar{3})}|S,T)\\
=&(S+T)^2\left[\left(200r^6-600r^4+600r^2-200\right)T^6\right.\\
&+\left(1792r^6-1888r^5-3348r^4+1194r^3+2866r^2+1558r-1806\right)S^6\\
&+\left(5584r^6-7738r^5-8837r^4+2828r^3+8946r^2+6638r-6909\right)S^5T\\
&+\left(7256r^6-13836r^5-9012r^4+8000r^3+10140r^2+6700r-9104\right)S^4T^2\\
&+\left(4953r^6-12464r^5-4164r^4+13296r^3+2701r^2-832r-3490\right)S^3T^3\\
&+\left(2762r^6-5452r^5-2368r^4+8654r^3-1500r^2-3202r+1106\right)S^2T^4\\
&\left.+\left(1249r^6-862r^5-2047r^4+1724r^3+347r^2-862r+451\right)ST^5\right]\,, &\text{(A.19e)}
\end{aligned}
$$

$$
\begin{aligned}
&c_8({}^1P_1^{(\bar{3})}|S,T)\\
=&(S+T)\left[\left(-235r^8+940r^6-1410r^4+940r^2-235\right)T^6\right.\\
&+\left(-1088r^8+2112r^7+2041r^6-3642r^5-1941r^4\right.\\
&\left.-780r^3+3103r^2+2310r-2115\right)S^6\\
&+\left(-4260r^8+9658r^7+6997r^6-14832r^5-7655r^4\right.\\
&\left.-2766r^3+13791r^2+7940r-8873\right)S^5T\\
&+\left(-7164r^8+18358r^7+10829r^6-30204r^5-12007r^4\right.\\
&\left.+3606r^3+21623r^2+8240r-13281\right)S^4T^2\\
&+\left(-5887r^8+16358r^7+9187r^6-31336r^5-8983r^4\right.\\
&\left.+13598r^3+13953r^2+1380r-8270\right)S^3T^3\\
&+\left(-3009r^8+6466r^7+6674r^6-14970r^5-6198r^4\right.\\
&\left.+10542r^3+4410r^2-2038r-1877\right)S^2T^4\\
&+\left(-1209r^8+864r^7+3964r^6-2592r^5-4638r^4\right.\\
&\left.\left.+2592r^3+2220r^2-864r-337\right)ST^5\right]\,, \qquad \text{(A.19f)}\\
&c_{10}({}^1P_1^{(\bar{3})}|S,T)\\
=&\left(126r^{10}-630r^8+1260r^6-1260r^4+630r^2-126\right)T^6\\
&+\left(384r^{10}-1168r^9-802r^8+3870r^7+326r^6-3738r^5\right.\\
&\left.-502r^4+538r^3+1314r^2+498r-720\right)S^6\\
&+\left(1895r^{10}-5946r^9-4055r^8+19420r^7+2074r^6-20856r^5\right.\\
&\left.-2058r^4+7236r^3+4639r^2+146r-2495\right)S^5T\\
&+\left(4122r^{10}-12804r^9-9558r^8+42560r^7+6140r^6-49992r^5\right.\\
&\left.-3012r^4+23520r^3+5226r^2-3284r-2918\right)S^4T^2\\
&+\left(4338r^{10}-12840r^9-11458r^8+44268r^7+9624r^6-55764r^5\right.\\
&\left.-3504r^4+30084r^3+2278r^2-5748r-1278\right)S^3T^3\\
&+\left(2376r^{10}-5660r^9-7866r^8+20642r^7+9594r^6-27966r^5\right.\\
&\left.-5346r^4+16646r^3+1494r^2-3662r-252\right)S^2T^4
\end{aligned}
$$

$$
\begin{aligned}
&+\left(747r^{10}-846r^9-3231r^8+3384r^7+5454r^6-5076r^5\right.\\
&\left.-4446r^4+3384r^3+1719r^2-846r-243\right)ST^5\,, \qquad \text{(A.19g)}\\
&c_{12}({}^1P_1^{(\bar{3})}|S,T)\\
=&\left(-27r^{12}+162r^{10}-405r^8+540r^6-405r^4+162r^2-27\right)T^5\\
&+\left(-216r^{12}+432r^{11}+972r^{10}-2160r^9-1620r^8+4320r^7+1080r^6\right.\\
&\left.-4320r^5+2160r^3-324r^2-432r+108\right)ST^4\\
&+\left(-64r^{12}+256r^{11}+200r^{10}-1380r^9+28r^8+2960r^7-832r^6\right.\\
&\left.-3160r^5+1288r^4+1680r^3-808r^2-356r+188\right)S^5\\
&+\left(-315r^{12}+1188r^{11}+1070r^{10}-6476r^9-321r^8+14024r^7-3116r^6\right.\\
&\left.-15096r^5+5299r^4+8084r^3-3426r^2-1724r+809\right)S^4T\\
&+\left(-684r^{12}+2376r^{11}+2412r^{10}-12204r^9-1620r^8+25056r^7-3960r^6\right.\\
&\left.-25704r^5+7740r^4+13176r^3-5076r^2-2700r+1188\right)S^3T^2\\
&+\left(-594r^{12}+1764r^{11}+2268r^{10}-8820r^9-2430r^8+17640r^7-1080r^6\right.\\
&\left.-17640r^5+4050r^4+8820r^3-2916r^2-1764r+702\right)S^2T^3\,. \qquad \text{(A.19h)}
\end{aligned}
$$

For $Qq({}^3P_0^{(\bar{3})})$, we have

$$
\begin{aligned}
&\mathcal{D}({}^3P_0^{(\bar{3})}|S,T)\\
=&18S^4T^2(S+T)^4\left[T+(1-r^2)m_H^2\right]^2\left[(1-r^2)m_H^2+S+T\right]^2\,, \qquad \text{(A.20a)}\\
&c_0({}^3P_0^{(\bar{3})}|S,T)\\
=&-16S^2T^2(S+T)^5\left(4S^4+9ST^3+4T^4\right)\,, \qquad \text{(A.20b)}\\
&c_2({}^3P_0^{(\bar{3})}|S,T)\\
=&ST(S+T)^4\left[\left(128r^2-768r+2176\right)S^6+\left(512r^2-2080r+8520\right)S^5T\right.\\
&+\left(379r^2-2804r+12876\right)S^4T^2+\left(414r^2-3244r+7884\right)S^3T^3\\
&\left.+\left(1011r^2-2116r+184\right)S^2T^4+\left(744r^2-604r-880\right)ST^5+\left(128r^2+128\right)T^6\right]\,, \qquad \text{(A.20c)}\\
&c_4({}^3P_0^{(\bar{3})}|S,T)\\
=&(S+T)^3\left[\left(-64r^4+128r^2-64\right)T^8+\left(-64r^4+768r^3-2176r^2-768r+2240\right)S^8\right.
\end{aligned}
$$

$$
\begin{aligned}
&+\left(-896r^4+6800r^3-13584r^2-8288r+15200\right)S^7T\\
&+\left(-2550r^4+18200r^3-32619r^2-25578r+37787\right)S^6T^2\\
&+\left(-3049r^4+26550r^3-36975r^2-39884r+43880\right)S^5T^3\\
&+\left(-3297r^4+26494r^3-16449r^2-34624r+21054\right)S^4T^4\\
&+\left(-4119r^4+15878r^3+2719r^2-15520r+16\right)S^3T^5\\
&+\left(-3225r^4+4426r^3+3156r^2-3254r-889\right)S^2T^6\\
&+\left(-928r^4+124r^3+40r^2-124r+888\right)ST^7\big]\ , \qquad \text{(A.20d)}
\end{aligned}
$$

$$
\begin{aligned}
&c_6({}^3P_0^{(\bar{3})}|S,T)\\
=&(S+T)^2\left[\left(328r^6-984r^4+984r^2-328\right)T^8\right.\\
&+\left(384r^6-3952r^5+7496r^4+9392r^3-12256r^2-5440r+4376\right)S^8\\
&+\left(3067r^6-25508r^5+31304r^4+66108r^3-60005r^2-40792r+25442\right)S^7T\\
&+\left(8258r^6-66704r^5+48986r^4+183470r^3-116296r^2-119142r+59684\right)S^6T^2\\
&+\left(11812r^6-98718r^5+30195r^4+271628r^3-109354r^2-175710r+68691\right)S^5T^3\\
&+\left(12540r^6-92388r^5-2396r^4+228264r^3-46856r^2-136492r+37456\right)S^4T^4\\
&+\left(11574r^6-50948r^5-13436r^4+104076r^3-7926r^2-53128r+9788\right)S^3T^5\\
&+\left(8072r^6-13196r^5-8510r^4+22578r^3-4410r^2-9382r+4848\right)S^2T^6\\
&+\left(2849r^6-714r^5-3583r^4+1428r^3-1381r^2-714r+2115\right)ST^7\big]\ , \qquad \text{(A.20e)}
\end{aligned}
$$

$$
\begin{aligned}
&c_8({}^3P_0^{(\bar{3})}|S,T)\\
=&(S+T)\left[\left(-699r^8+2796r^6-4194r^4+2796r^2-699\right)T^8\right.\\
&+\left(-960r^8+8240r^7-7977r^6-30946r^5+23765r^4\right.\\
&\left.+37364r^3-19567r^2-14658r+4739\right)S^8\\
&+\left(-6375r^8+49926r^7-25493r^6-194136r^5+101105r^4\right.\\
&\left.+243438r^3-101303r^2-99228r+32066\right)S^7T\\
&+\left(-17353r^8+130150r^7-16235r^6-515496r^5+164539r^4\right.\\
&\left.+655070r^3-216753r^2-269724r+85802\right)S^6T^2\\
&+\left(-27200r^8+193250r^7+30899r^6-747276r^5+128343r^4\right.\\
&\left.+927074r^3-247687r^2-373048r+115645\right)S^5T^3
\end{aligned}
$$

$$
\begin{aligned}
&+\left(-28874r^8+175182r^7+56756r^6-624006r^5+56070r^4\right.\\
&\left.+724962r^3-169936r^2-276138r+85984\right)S^4T^4\\
&+\left(-22818r^8+91160r^7+43410r^6-288228r^5+21406r^4\right.\\
&\left.+302976r^3-81770r^2-105908r+39772\right)S^3T^5\\
&+\left(-13554r^8+22452r^7+26000r^6-64144r^5+2264r^4\right.\\
&\left.+60932r^3-28312r^2-19240r+13602\right)S^2T^6\\
&+\left(-4907r^8+1632r^7+12748r^6-4896r^5-8802r^4\right.\\
&\left.+4896r^3-1012r^2-1632r+1973\right)ST^7\Big]\,, \qquad \text{(A.20f)}\\
&c_{10}({}^3P_0^{(\bar{3})}|S,T)\\
=&\left(796r^{10}-3980r^8+7960r^6-7960r^4+3980r^2-796\right)T^8\\
&+\left(1280r^{10}-8800r^9+576r^8+43982r^7-15722r^6-81522r^5\right.\\
&\left.+31542r^4+66298r^3-24622r^2-19958r+6946\right)S^8\\
&+\left(8270r^{10}-53942r^9-9875r^8+272312r^7-58872r^6-509188r^5\right.\\
&\left.+159454r^4+417208r^3-144142r^2-126390r+45165\right)S^7T\\
&+\left(23496r^{10}-143444r^9-57544r^8+724032r^7-71312r^6-1341248r^5\right.\\
&\left.+338856r^4+1084176r^3-351080r^2-323516r+117584\right)S^6T^2\\
&+\left(39188r^{10}-215988r^9-122230r^8+1058292r^7-15292r^6-1899028r^5\right.\\
&\left.+400720r^4+1487132r^3-462584r^2-430408r+160198\right)S^5T^3\\
&+\left(42244r^{10}-194516r^9-137588r^8+897586r^7+38858r^6-1529454r^5\right.\\
&\left.+291122r^4+1144214r^3-359686r^2-317830r+125050\right)S^4T^4\\
&+\left(30958r^{10}-99218r^9-98951r^8+425796r^7+53932r^6-682080r^5\right.\\
&\left.+122330r^4+483644r^3-165442r^2-128142r+57173\right)S^3T^5\\
&+\left(15912r^{10}-24456r^9-53544r^8+99072r^7+51408r^6-150480r^5\right.\\
&\left.+7920r^4+101568r^3-35448r^2-25704r+13752\right)S^2T^6\\
&+\left(5284r^{10}-2068r^9-21136r^8+8272r^7+31704r^6-12408r^5\right.\\
&\left.-21136r^4+8272r^3+5284r^2-2068r\right)ST^7\,, \qquad \text{(A.20g)}
\end{aligned}
$$

$$
\begin{aligned}
&c_{12}({}^3P_0^{(\bar{3})}|S,T)\\
=&\left(-514r^{12}+3084r^{10}-7710r^8+10280r^6-7710r^4+3084r^2-514\right)T^7\\
&+\left(-960r^{12}+4960r^{11}+4147r^{10}-29594r^9-2949r^8+72952r^7-12314r^6\right.\\
&\left.-90892r^5+27566r^4+56504r^3-21369r^2-13930r+5879\right)S^7\\
&+\left(-5518r^{12}+26518r^{11}+26034r^{10}-161502r^9-27258r^8+394428r^7-47748r^6\right.\\
&\left.-479452r^5+129222r^4+289038r^3-103230r^2-69030r+28498\right)S^6T\\
&+\left(-14142r^{12}+60748r^{11}+68562r^{10}-366628r^9-84980r^8+871016r^7-70492r^6\right.\\
&\left.-1020760r^5+247866r^4+591244r^3-202294r^2-135620r+55480\right)S^5T^2\\
&+\left(-20566r^{12}+75528r^{11}+97764r^{10}-434784r^9-133426r^8+986416r^7-35736r^6\right.\\
&\left.-1105824r^5+238614r^4+613896r^3-201740r^2-135232r+55090\right)S^4T^3\\
&+\left(-17824r^{12}+50376r^{11}+83651r^{10}-272878r^9-127973r^8+587752r^7+31862r^6\right.\\
&\left.-629748r^5+103102r^4+335872r^3-101209r^2-71374r+28391\right)S^3T^4\\
&+\left(-9510r^{12}+15618r^{11}+45802r^{10}-80826r^9-82238r^8+167124r^7+61132r^6\right.\\
&\left.-172596r^5-5338r^4+89034r^3-15718r^2-18354r+5870\right)S^2T^5\\
&+\left(-3154r^{12}+1692r^{11}+16576r^{10}-8460r^9-35570r^8+16920r^7+39600r^6\right.\\
&\left.-16920r^5-23830r^4+8460r^3+7184r^2-1692r-806\right)ST^6\,. \qquad \text{(A.20h)}
\end{aligned}
$$

For $Qq({}^3P_1^{(\bar{3})})$, we have

$$
\begin{aligned}
&\mathcal{D}({}^3P_1^{(\bar{3})}|S,T)\\
=&9S^4T^2(S+T)^4\left[T+(1-r^2)m_H^2\right]^2\left[(1-r^2)m_H^2+S+T\right]^2\,, \qquad \text{(A.21a)}\\
&c_0({}^3P_1^{(\bar{3})}|S,T)\\
=&-64S^2T^2(S+T)^5\left(S^4+3S^3T+6S^2T^2+5ST^3+3T^4\right)\,, \qquad \text{(A.21b)}\\
&c_2({}^3P_1^{(\bar{3})}|S,T)\\
=&ST(S+T)^4\left[\left(256r^2-256r+128\right)S^6+\left(1552r^2-1560r+56\right)S^5T\right]\\
&+\left(3617r^2-3030r-1173\right)S^4T^2+\left(4678r^2-3280r-2426\right)S^3T^3\\
&+\left(3593r^2-1994r-1561\right)S^2T^4+\left(1576r^2-472r-536\right)ST^5+\left(128r^2+128\right)T^6\big]\,, \qquad \text{(A.21c)}
\end{aligned}
$$

$$
\begin{aligned}
&c_4({}^3P_1^{(\bar{3})}|S,T)\\
=&(S+T)^3\left[\left(-192r^4+256r^3-256r+192\right)S^8\right.\\
&+\left(-64r^4+128r^2-64\right)T^8+\left(-2128r^4+3392r^3+864r^2-3568r+672\right)S^7T\\
&+\left(-8562r^4+13428r^3+6594r^2-13604r-16\right)S^6T^2\\
&+\left(-17639r^4+25056r^3+18340r^2-26644r-1821\right)S^5T^3\\
&+\left(-21615r^4+27804r^3+23368r^2-30204r-133\right)S^4T^4\\
&+\left(-16217r^4+17216r^3+14724r^2-17956r+2693\right)S^3T^5\\
&+\left(-6663r^4+4584r^3+4494r^2-4432r+2165\right)S^2T^6\\
&\left.+\left(-1056r^4+288r^3+296r^2-288r+760\right)ST^7\right], \qquad \text{(A.21d)}\\
&c_6({}^3P_1^{(\bar{3})}|S,T)\\
=&(S+T)^2\left[\left(328r^6-984r^4+984r^2-328\right)T^8\right.\\
&+\left(896r^6-1576r^5-264r^4+3328r^3-800r^2-1752r+168\right)S^8\\
&+\left(7105r^6-14342r^5-6691r^4+30172r^3-1773r^2-15894r+1295\right)S^7T\\
&+\left(24154r^6-48844r^5-34162r^4+105176r^3+3530r^2-57320r+6794\right)S^6T^2\\
&+\left(46698r^6-89856r^5-77696r^4+198504r^3+10490r^2-109568r+21132\right)S^5T^3\\
&+\left(56408r^6-100012r^5-92992r^4+216116r^3+2408r^2-116100r+34308\right)S^4T^4\\
&+\left(42126r^6-62532r^5-61822r^4+128120r^3-9014r^2-65588r+28710\right)S^3T^5\\
&+\left(17724r^6-18172r^5-23832r^4+35732r^3-5592r^2-17560r+11700\right)S^2T^6\\
&\left.+\left(3693r^6-1730r^5-5825r^4+3460r^3+571r^2-1730r+1561\right)ST^7\right], \qquad \text{(A.21e)}\\
&c_8({}^3P_1^{(\bar{3})}|S,T)\\
=&(S+T)\left[\left(-699r^8+2796r^6-4194r^4+2796r^2-699\right)T^8\right.\\
&+\left(-1728r^8+3928r^7+2214r^6-12920r^5+1678r^4\right.\\
&\left.+14120r^3-3022r^2-5128r+858\right)S^8\\
&+\left(-12569r^8+30260r^7+22950r^6-99344r^5+716r^4\right.\\
&\left.+109948r^3-20574r^2-40864r+9477\right)S^7T\\
&+\left(-40707r^8+97352r^7+90106r^6-324636r^5-20892r^4\right.\\
&\left.+362816r^3-68410r^2-135532r+39903\right)S^6T^2
\end{aligned}
$$

$$
\begin{aligned}
&+\left(-77478r^8+178316r^7+184074r^6-589964r^5-53558r^4\right.\\
&\left.+648556r^3-137994r^2-236908r+84956\right)S^5T^3\\
&+\left(-93348r^8+197528r^7+217784r^6-628508r^5-56008r^4\right.\\
&\left.+664384r^3-168448r^2-233404r+100020\right)S^4T^4\\
&+\left(-69866r^8+124156r^7+156556r^6-377224r^5-38588r^4\right.\\
&\left.+381980r^3-113028r^2-128912r+64926\right)S^3T^5\\
&+\left(-30350r^8+38324r^7+70568r^6-113556r^5-29604r^4\right.\\
&\left.+112140r^3-31096r^2-36908r+20482\right)S^2T^6\\
&+\left(-7031r^8+4344r^7+19888r^6-13032r^5-17478r^4\right.\\
&\left.+13032r^3+3416r^2-4344r+1205\right)ST^7\Big]\ , \qquad \text{(A.21f)}\\
&c_{10}({}^3P_1^{(\bar{3})}|S,T)\\
=&\left(796r^{10}-3980r^8+7960r^6-7960r^4+3980r^2-796\right)T^8\\
&+\left(1792r^{10}-5072r^9-4888r^8+21992r^7+1636r^6-36532r^5\right.\\
&\left.+6816r^4+27376r^3-7948r^2-7764r+2592\right)S^8\\
&+\left(13024r^{10}-36152r^9-39522r^8+159096r^7+22488r^6-266840r^5\right.\\
&\left.+42332r^4+201000r^3-59160r^2-57104r+20838\right)S^7T\\
&+\left(42704r^{10}-114472r^9-137620r^8+505780r^7+94536r^6-841248r^5\right.\\
&\left.+121436r^4+623044r^3-189520r^2-173104r+68464\right)S^6T^2\\
&+\left(82448r^{10}-209692r^9-268812r^8+905656r^7+196752r^6-1463960r^5\right.\\
&\left.+202744r^4+1049720r^3-332736r^2-281724r+119604\right)S^5T^3\\
&+\left(99932r^{10}-231104r^9-321856r^8+960676r^7+247268r^6-1495284r^5\right.\\
&\left.+190732r^4+1032956r^3-335504r^2-267244r+119428\right)S^4T^4\\
&+\left(74940r^{10}-145876r^9-242818r^8+586056r^7+212112r^6-882912r^5\right.\\
&\left.+71172r^4+591160r^3-182108r^2-148428r+66702\right)S^3T^5\\
&+\left(33032r^{10}-46928r^9-114448r^8+185784r^7+127848r^6-275784r^5\right.\\
&\left.-27176r^4+181928r^3-36560r^2-45000r+17304\right)S^2T^6\\
&+\left(7872r^{10}-5856r^9-31640r^8+23424r^7+47840r^6-35136r^5\right.
\end{aligned}
$$

$$-32400r^4+23424r^3+8480r^2-5856r-152\big)\,ST^7\,, \tag{A.21g}$$

$$\begin{aligned}
&c_{12}({}^3P_1^{(\bar{3})}|S,T)\\
=&\big(-514r^{12}+3084r^{10}-7710r^8+10280r^6-7710r^4+3084r^2-514\big)\,T^7\\
&+\big(-1088r^{12}+3568r^{11}+4590r^{10}-18572r^9-5938r^8+40392r^7-1212r^6\\
&-45424r^5+9684r^4+26120r^3-8402r^2-6084r+2366\big)\,S^7\\
&+\big(-7076r^{12}+21244r^{11}+30752r^{10}-114816r^9-41340r^8+252072r^7-3640r^6\\
&-279760r^5+57580r^4+156348r^3-50184r^2-35088r+13908\big)\,S^6T\\
&+\big(-20702r^{12}+57860r^{11}+90108r^{10}-310932r^9-123114r^8+668480r^7+2560r^6\\
&-718448r^5+140454r^4+385884r^3-122460r^2-82844r+33154\big)\,S^5T^2\\
&+\big(-34298r^{12}+87848r^{11}+147208r^{10}-455660r^9-205534r^8+944048r^7+35560r^6\\
&-976664r^5+168914r^4+504584r^3-152624r^2-104156r+40774\big)\,S^4T^3\\
&+\big(-32824r^{12}+72560r^{11}+141334r^{10}-364044r^9-210482r^8+730576r^7+85068r^6\\
&-733064r^5+86708r^4+367776r^3-96418r^2-73804r+26614\big)\,S^3T^4\\
&+\big(-17336r^{12}+29268r^{11}+78592r^{10}-145044r^9-133316r^8+287496r^7+94064r^6\\
&-284904r^5-8176r^4+141156r^3-21520r^2-27972r+7692\big)\,S^2T^5\\
&+\big(-4694r^{12}+4484r^{11}+23744r^{10}-22420r^9-48310r^8+44840r^7+49680r^6\\
&-44840r^5-26210r^4+22420r^3+6064r^2-4484r-274\big)\,ST^6\,.
\end{aligned} \tag{A.21h}$$

For $Qq({}^3P_2^{(\bar{3})})$, we have

$$\begin{aligned}
&\mathcal{D}({}^3P_2^{(\bar{3})}|S,T)\\
=&54S^4T^2(S+T)^4\left[(1-r^2)m_H^2+S+T\right]^2\,,
\end{aligned} \tag{A.22a}$$

$$\begin{aligned}
&c_0({}^3P_2^{(\bar{3})}|S,T)\\
=&-32S^2(S+T)^5\left(10S^4+18S^3T+24S^2T^2+27ST^3+10T^4\right)\,,
\end{aligned} \tag{A.22b}$$

$$\begin{aligned}
&c_2({}^3P_2^{(\bar{3})}|S,T)\\
=&S(S+T)^4\left[\big(1920r^2-776r+664\big)\,S^5+\big(4775r^2-2206r+3723\big)\,S^4T\right.\\
&+\big(6570r^2-2864r+5310\big)\,S^3T^2+\big(6719r^2-1514r+3687\big)\,S^2T^3\\
&\left.+\big(3608r^2-368r+2072\big)\,ST^4+\big(640r^2+640\big)\,T^5\right]\,,
\end{aligned} \tag{A.22c}$$

$$
\begin{aligned}
&c_4({}^3P_2^{(\bar{3})}|S,T)\\
=&(S+T)^3\left[\left(-320r^4+640r^2-320\right)T^6+\left(-4800r^4+3880r^3-1152r^2-1176r+1480\right)S^6\right.\\
&+\left(-15235r^4+12768r^3-7618r^2+140r+5761\right)S^5T\\
&+\left(-23595r^4+19644r^3-8882r^2+2964r+6965\right)S^4T^2\\
&+\left(-23085r^4+13256r^3+2618r^2+2196r+4463\right)S^3T^3\\
&+\left(-13429r^4+3724r^3+7826r^2-84r+2043\right)S^2T^4\\
&\left.+\left(-3744r^4+368r^3+3680r^2-368r+64\right)ST^5\right]\,, \qquad \text{(A.22d)}\\
&c_6({}^3P_2^{(\bar{3})}|S,T)\\
=&(S+T)^2\left[\left(1000r^6-3000r^4+3000r^2-1000\right)T^6\right.\\
&+\left(6400r^6-7760r^5-2032r^4+7404r^3-3376r^2+1760r-1564\right)S^6\\
&+\left(24710r^6-29012r^5-9110r^4+19752r^3-7830r^2+12132r-9162\right)S^5T\\
&+\left(44040r^6-52008r^5-30372r^4+35836r^3+5312r^2+17640r-19688\right)S^4T^2\\
&+\left(43971r^6-43330r^5-55551r^4+37308r^3+30917r^2+6022r-19337\right)S^3T^3\\
&+\left(25306r^6-15452r^5-48326r^4+18424r^3+33214r^2-2972r-10194\right)S^2T^4\\
&\left.+\left(8009r^6-2030r^5-19797r^4+4060r^3+15567r^2-2030r-3779\right)ST^5\right]\,, \qquad \text{(A.22e)}\\
&c_8({}^3P_2^{(\bar{3})}|S,T)\\
=&(S+T)\left[\left(-1175r^8+4700r^6-7050r^4+4700r^2-1175\right)T^6\right.\\
&+\left(-4800r^8+7760r^7+6368r^6-15156r^5-572r^4\right.\\
&\left.+4224r^3+2384r^2+3172r-3380\right)S^6\\
&+\left(-21830r^8+32488r^7+35808r^6-61312r^5-20380r^4\right.\\
&\left.+19480r^3+23416r^2+9344r-17014\right)S^5T\\
&+\left(-44730r^8+66800r^7+91120r^6-134740r^5-79816r^4\right.\\
&\left.+66208r^3+66584r^2+1732r-33158\right)S^4T^2\\
&+\left(-47633r^8+65584r^7+120840r^6-145928r^5-131106r^4\right.\\
&\left.+95104r^3+90224r^2-14760r-32325\right)S^3T^3\\
&+\left(-27207r^8+28244r^7+85184r^6-70980r^5-106422r^4\right.\\
&\left.+57228r^3+66120r^2-14492r-17675\right)S^2T^4
\end{aligned}
$$

$$
\begin{aligned}
&+\left(-8505r^8+4452r^7+31508r^6-13356r^5-43494r^4\right.\\
&\left.+13356r^3+26484r^2-4452r-5993\right)ST^5\big]\,, \qquad \text{(A.22f)}\\
&c_{10}({}^3P_2^{(\bar{3})}|S,T)\\
=&\left(630r^{10}-3150r^8+6300r^6-6300r^4+3150r^2-630\right)T^6\\
&+\left(1920r^{10}-3880r^9-5352r^8+12804r^7+5352r^6-13728r^5\right.\\
&\left.-3716r^4+4564r^3+3184r^2+240r-1388\right)S^6\\
&+\left(10051r^{10}-17982r^9-32429r^8+62808r^7+41806r^6-77724r^5\right.\\
&\left.-32722r^4+38952r^3+19487r^2-6054r-6193\right)S^5T\\
&+\left(23478r^{10}-41832r^9-82146r^8+150028r^7+116220r^6-197688r^5\right.\\
&\left.-91248r^4+112620r^3+45030r^2-23128r-11334\right)S^4T^2\\
&+\left(27282r^{10}-46632r^9-103058r^8+170664r^7+157116r^6-232200r^5\right.\\
&\left.-125820r^4+138936r^3+56114r^2-30768r-11634\right)S^3T^3\\
&+\left(16092r^{10}-23096r^9-67016r^8+87416r^7+112112r^6-123672r^5\right.\\
&\left.-95160r^4+77480r^3+41588r^2-18128r-7616\right)S^2T^4\\
&+\left(4815r^{10}-4194r^9-22401r^8+16776r^7+41454r^6-25164r^5\right.\\
&\left.-38106r^4+16776r^3+17379r^2-4194r-3141\right)ST^5\,, \qquad \text{(A.22g)}\\
&c_{12}({}^3P_2^{(\bar{3})}|S,T)\\
=&\left(-135r^{12}+810r^{10}-2025r^8+2700r^6-2025r^4+810r^2-135\right)T^5\\
&+\left(-320r^{12}+776r^{11}+1504r^{10}-3876r^9-2884r^8+7744r^7+2896r^6\right.\\
&\left.-7736r^5-1624r^4+3864r^3+496r^2-772r-68\right)S^5\\
&+\left(-1575r^{12}+3168r^{11}+8122r^{10}-17512r^9-16473r^8+38368r^7+16172r^6\right.\\
&\left.-41712r^5-7273r^4+22528r^3+762r^2-4840r+265\right)S^4T\\
&+\left(-3420r^{12}+7092r^{11}+16848r^{10}-36576r^9-32544r^8+75384r^7+30096r^6\right.\\
&\left.-77616r^5-12204r^4+39924r^3+576r^2-8208r+648\right)S^3T^2\\
&+\left(-2970r^{12}+5544r^{11}+14616r^{10}-27720r^9-28530r^8+55440r^7+27360r^6\right.\\
&\left.-55440r^5-12510r^4+27720r^3+1800r^2-5544r+234\right)S^2T^3\\
&+\left(-1080r^{12}+1404r^{11}+5616r^{10}-7020r^9-11880r^8+14040r^7+12960r^6\right.
\end{aligned}
$$

$$-14040r^5 - 7560r^4 + 7020r^3 + 2160r^2 - 1404r - 216\big)\, ST^4\,. \tag{A.22h}$$

For $Qq(^1P_1^{(6)})$, we have

$$\begin{aligned}
&\mathcal{D}(^1P_1^{(6)}|S,T)\\
=&18S^4T^2(S+T)^4\left[(1-r^2)m_H^2+S+T\right]^2\,, &\text{(A.23a)}\\
&c_0(^1P_1^{(6)}|S,T)\\
=&-8S^2(S+T)^5\left(12S^4+12S^3T+8S^2T^2+21ST^3+12T^4\right)\,, &\text{(A.23b)}\\
&c_2(^1P_1^{(6)}|S,T)\\
=&S(S+T)^4\left[\left(448r^2-72r-436\right)S^5+\left(753r^2-284r-120\right)S^4T\right.\\
&+\left(654r^2-1004r+216\right)S^3T^2+\left(809r^2-1092r-320\right)S^2T^3\\
&\left.+\left(508r^2-412r-140\right)ST^4+\left(64r^2+64\right)T^5\right]\,, &\text{(A.23c)}\\
&c_4(^1P_1^{(6)}|S,T)\\
=&(S+T)^3\left[\left(-32r^4+64r^2-32\right)T^6+\left(-864r^4+416r^3+1377r^2-210r-815\right)S^6\right.\\
&+\left(-2089r^4+1950r^3+1381r^2+628r+148\right)S^5T\\
&+\left(-2601r^4+5118r^3-413r^2-780r+3206\right)S^4T^2\\
&+\left(-1839r^4+5478r^3-961r^2-4224r+4192\right)S^3T^3\\
&+\left(-1031r^4+2402r^3-692r^2-2842r+2393\right)S^2T^4\\
&\left.+\left(-336r^4+260r^3-68r^2-260r+404\right)ST^5\right]\,, &\text{(A.23d)}\\
&c_6(^1P_1^{(6)}|S,T)\\
=&(S+T)^2\left[\left(100r^6-300r^4+300r^2-100\right)T^6\right.\\
&+\left(896r^6-944r^5-1620r^4+1326r^3+1622r^2+1346r-1794\right)S^6\\
&+\left(2912r^6-4922r^5-2893r^4+1168r^3+2994r^2+7210r-5349\right)S^5T\\
&+\left(5152r^6-12096r^5-2016r^4+6040r^3+540r^2+7784r-5116\right)S^4T^2\\
&+\left(3489r^6-12340r^5+1392r^4+13116r^3-5059r^2-776r+178\right)S^3T^3\\
&+\left(1462r^6-5168r^5+988r^4+8266r^3-4716r^2-3098r+2266\right)S^2T^4\\
&\left.+\left(665r^6-674r^5-767r^4+1348r^3-461r^2-674r+563\right)ST^5\right]\,, &\text{(A.23e)}
\end{aligned}$$

$$
\begin{aligned}
&c_8({}^1P_1^{(6)}|S,T)\\
=&(S+T)\left[\left(-131r^8+524r^6-786r^4+524r^2-131\right)T^6\right.\\
&+\left(-544r^8+1056r^7+953r^6-2766r^5-741r^4-1092r^3+2591r^2+2802r-2259\right)S^6\\
&+\left(-2292r^8+5906r^7+2909r^6-9228r^5-3319r^4\right.\\
&\left.-6174r^3+11751r^2+9496r-9049\right)S^5T\\
&+\left(-5580r^8+15662r^7+6505r^6-25848r^5-6023r^4\right.\\
&\left.+1254r^3+17731r^2+8932r-12633\right)S^4T^2\\
&+\left(-5063r^8+16822r^7+5039r^6-33044r^5-1667r^4\right.\\
&\left.+15622r^3+8469r^2+600r-6778\right)S^3T^3\\
&+\left(-2193r^8+7010r^7+2926r^6-16386r^5-30r^4\right.\\
&\left.+11742r^3+54r^2-2366r-757\right)S^2T^4\\
&\left.+\left(-753r^8+864r^7+2144r^6-2592r^5-1914r^4+2592r^3+408r^2-864r+115\right)ST^5\right]\,,
\end{aligned}
\tag{A.23f}
$$

$$
\begin{aligned}
&c_{10}({}^1P_1^{(6)}|S,T)\\
=&\left(90r^{10}-450r^8+900r^6-900r^4+450r^2-90\right)T^6\\
&+\left(192r^{10}-584r^9-374r^8+2394r^7-134r^6-1950r^5\right.\\
&\left.-170r^4-946r^3+1278r^2+1086r-792\right)S^6\\
&+\left(1015r^{10}-3426r^9-2047r^8+12440r^7+326r^6-13308r^5\right.\\
&\left.-1182r^4+3000r^3+4499r^2+1294r-2611\right)S^5T\\
&+\left(3222r^{10}-10488r^9-7194r^8+36436r^7+3376r^6-44652r^5\right.\\
&\left.-624r^4+21948r^3+3786r^2-3244r-2566\right)S^4T^2\\
&+\left(3978r^{10}-12828r^9-9650r^8+45120r^7+5532r^6-58392r^5\right.\\
&\left.+1524r^4+32736r^3-934r^2-6636r-450\right)S^3T^3\\
&+\left(2160r^{10}-6064r^9-6390r^8+22258r^7+5850r^6-30390r^5\right.\\
&\left.-810r^4+18262r^3-1170r^2-4066r+360\right)S^2T^4\\
&+\left(603r^{10}-882r^9-2439r^8+3528r^7+3726r^6-5292r^5\right.\\
&\left.-2574r^4+3528r^3+711r^2-882r-27\right)ST^5\,,
\end{aligned}
\tag{A.23g}
$$

$$
\begin{aligned}
&c_{12}({}^1P_1^{(6)}|S,T)\\
=&\left(-27r^{12}+162r^{10}-405r^8+540r^6-405r^4+162r^2-27\right)T^5\\
&+\left(-216r^{12}+432r^{11}+972r^{10}-2160r^9-1620r^8+4320r^7+1080r^6\right.\\
&\left.-4320r^5+2160r^3-324r^2-432r+108\right)ST^4\\
&+\left(-32r^{12}+128r^{11}+100r^{10}-744r^9+68r^8+1696r^7-632r^6\right.\\
&\left.-1904r^5+968r^4+1056r^3-620r^2-232r+148\right)S^5\\
&+\left(-171r^{12}+648r^{11}+670r^{10}-4264r^9-201r^8+10576r^7-2476r^6\right.\\
&\left.-12624r^5+4499r^4+7336r^3-3090r^2-1672r+769\right)S^4T\\
&+\left(-612r^{12}+2160r^{11}+2232r^{10}-11448r^9-1620r^8+24192r^7-3600r^6\right.\\
&\left.-25488r^5+7380r^4+13392r^3-4968r^2-2808r+1188\right)S^3T^2\\
&+\left(-594r^{12}+1800r^{11}+2268r^{10}-9000r^9-2430r^8+18000r^7-1080r^6\right.\\
&\left.-18000r^5+4050r^4+9000r^3-2916r^2-1800r+702\right)S^2T^3\,.
\end{aligned}
\tag{A.23h}
$$

For $Qq({}^3P_0^{(6)})$, we have

$$
\mathcal{D}({}^3P_0^{(6)}|S,T)
=18S^4T^2(S+T)^2\left[T+(1-r^2)m_H^2\right]^2\left[(1-r^2)m_H^2+S+T\right]^2\,,
\tag{A.24a}
$$

$$
c_0({}^3P_0^{(6)}|S,T)
=-8S^2T^2(S+T)^5\left(4S^4+9ST^3+4T^4\right)\,,
\tag{A.24b}
$$

$$
\begin{aligned}
&c_2({}^3P_0^{(6)}|S,T)\\
=&ST(S+T)^4\left[\left(64r^2-384r+1088\right)S^6+\left(256r^2-1040r+4260\right)S^5T\right.\\
&+\left(203r^2-1444r+7512\right)S^4T^2+\left(234r^2-2084r+5640\right)S^3T^3\\
&\left.+\left(411r^2-1004r-352\right)S^2T^4+\left(372r^2-140r-1412\right)ST^5+\left(64r^2+64\right)T^6\right]\,,
\end{aligned}
\tag{A.24c}
$$

$$
\begin{aligned}
&c_4({}^3P_0^{(6)}|S,T)\\
=&(S+T)^3\left[\left(-32r^4+64r^2-32\right)T^8+\left(-32r^4+384r^3-1088r^2-384r+1120\right)S^8\right.\\
&+\left(-448r^4+3400r^3-6792r^2-4144r+7600\right)S^7T\\
&\left.+\left(-1302r^4+9184r^3-17895r^2-13458r+20515\right)S^6T^2\right.
\end{aligned}
$$

$$
\begin{aligned}
&+\left(-1673r^4+14442r^3-24231r^2-25408r+27880\right)S^5T^3\\
&+\left(-1905r^4+17546r^3-13317r^2-24992r+14718\right)S^4T^4\\
&+\left(-1695r^4+10714r^3+2891r^2-9380r-3436\right)S^3T^5\\
&+\left(-1545r^4+2342r^3+3948r^2-838r-3665\right)S^2T^6\\
&+\left(-464r^4-100r^3+20r^2+100r+444\right)ST^7\big]\ , \qquad \text{(A.24d)}\\
&c_6({}^3P_0^{(6)}|S,T)\\
=&(S+T)^2\left[\left(164r^6-492r^4+492r^2-164\right)T^8\right.\\
&+\left(192r^6-1976r^5+3748r^4+4696r^3-6128r^2-2720r+2188\right)S^8\\
&+\left(1547r^6-12796r^5+16204r^4+34020r^3-31453r^2-21320r+13606\right)S^7T\\
&+\left(4318r^6-34216r^5+28450r^4+103474r^3-68768r^2-74010r+37936\right)S^6T^2\\
&+\left(6932r^6-57510r^5+22167r^4+181024r^3-77138r^2-129690r+51447\right)S^5T^3\\
&+\left(7836r^6-66984r^5+2864r^4+175752r^3-36280r^2-110288r+27500\right)S^4T^4\\
&+\left(5814r^6-41656r^5-7576r^4+81600r^3+2322r^2-39944r-560\right)S^3T^5\\
&+\left(3928r^6-9496r^5-5254r^4+13710r^3+3114r^2-4214r-1788\right)S^2T^6\\
&+\left(1465r^6-6r^5-1751r^4+12r^3-893r^2-6r+1179\right)ST^7\big]\ , \qquad \text{(A.24e)}\\
&c_8({}^3P_0^{(6)}|S,T)\\
=&(S+T)\left[\left(-363r^8+1452r^6-2178r^4+1452r^2-363\right)T^8\right.\\
&+\left(-480r^8+4120r^7-4029r^6-15770r^5+12301r^4\right.\\
&\left.+19276r^3-10499r^2-7626r+2707\right)S^8\\
&+\left(-3255r^8+25122r^7-13261r^6-103212r^5+55177r^4\right.\\
&\left.+140658r^3-61327r^2-62568r+22666\right)S^7T\\
&+\left(-9473r^8+68786r^7-6907r^6-307596r^5+96563r^4\right.\\
&\left.+439906r^3-149361r^2-201096r+69178\right)S^6T^2\\
&+\left(-17272r^8+120634r^7+24991r^6-526296r^5+82011r^4\right.\\
&\left.+718114r^3-187139r^2-312452r+97409\right)S^5T^3\\
&+\left(-20026r^8+136638r^7+41380r^6-512802r^5+35982r^4\right.\\
&\left.+621546r^3-123344r^2-245382r+66008\right)S^4T^4
\end{aligned}
$$

$$
\begin{aligned}
&+\left(-14298r^8+82204r^7+27414r^6-256956r^5+9746r^4\right.\\
&\left.+267300r^3-44542r^2-92548r+21680\right)S^3T^5\\
&+\left(-7506r^8+19368r^7+13348r^6-52880r^5+1384r^4\right.\\
&\left.+47656r^3-12788r^2-14144r+5562\right)S^2T^6\\
&+\left(-2683r^8+816r^7+6644r^6-2448r^5-3834r^4+2448r^3-1532r^2-816r+1405\right)ST^7\Big]\,,
\end{aligned}
\tag{A.24f}
$$

$$
\begin{aligned}
&c_{10}({}^3P_0^{(6)}|S,T)\\
&=\left(452r^{10}-2260r^8+4520r^6-4520r^4+2260r^2-452\right)T^8\\
&+\left(640r^{10}-4400r^9+288r^8+22234r^7-8158r^6-45054r^5\right.\\
&\left.+18282r^4+41006r^3-16442r^2-13786r+5390\right)S^8\\
&+\left(4270r^{10}-26926r^9-7003r^8+148012r^7-27072r^6-316592r^5\right.\\
&\left.+96134r^4+296852r^3-104390r^2-101346r+38061\right)S^7T\\
&+\left(13584r^{10}-77512r^9-44552r^8+451776r^7-16048r^6-955936r^5\right.\\
&\left.+213888r^4+866592r^3-269344r^2-284920r+102472\right)S^6T^2\\
&+\left(26884r^{10}-141072r^9-101594r^8+779400r^7+35224r^6-1536536r^5\right.\\
&\left.+265628r^4+1299160r^3-364972r^2-400952r+138830\right)S^5T^3\\
&+\left(32300r^{10}-157000r^9-116032r^8+766778r^7+61330r^6-1366782r^5\right.\\
&\left.+199714r^4+1061230r^3-280790r^2-304226r+103478\right)S^4T^4\\
&+\left(23174r^{10}-92326r^9-76603r^8+399324r^7+47312r^6-644016r^5\right.\\
&\left.+85942r^4+459364r^3-123278r^2-122346r+43453\right)S^3T^5\\
&+\left(10656r^{10}-23040r^9-34884r^8+92460r^7+30828r^6-139140r^5\right.\\
&\left.+10260r^4+93060r^3-26748r^2-23340r+9888\right)S^2T^6\\
&+\left(3236r^{10}-1628r^9-12512r^8+6512r^7+17688r^6-9768r^5\right.\\
&\left.-10352r^4+6512r^3+1508r^2-1628r+432\right)ST^7\,,
\end{aligned}
\tag{A.24g}
$$

$$
\begin{aligned}
&c_{12}({}^3P_0^{(6)}|S,T)\\
&=\left(-338r^{12}+2028r^{10}-5070r^8+6760r^6-5070r^4+2028r^2-338\right)T^7\\
&+\left(-480r^{12}+2480r^{11}+2195r^{10}-14230r^9-2541r^8+41336r^7-6346r^6\right.\\
&\left.-63428r^5+19534r^4+47368r^3-17961r^2-13526r+5599\right)S^7
\end{aligned}
$$

$$
\begin{aligned}
&+\left(-2894r^{12}+12590r^{11}+16794r^{10}-89382r^{9}-26010r^{8}+261996r^{7}-21012r^{6}\right.\\
&\left.-375596r^{5}+94566r^{4}+259782r^{3}-88662r^{2}-69390r+27218\right)S^{6}T\\
&+\left(-9150r^{12}+33932r^{11}+52818r^{10}-246392r^{9}-83428r^{8}+672808r^{7}-27884r^{6}\right.\\
&\left.-879392r^{5}+193290r^{4}+556268r^{3}-178406r^{2}-137224r+52760\right)S^{5}T^{2}\\
&+\left(-16358r^{12}+55572r^{11}+84300r^{10}-352764r^{9}-128366r^{8}+860744r^{7}-9048r^{6}\right.\\
&\left.-1021368r^{5}+199710r^{4}+593700r^{3}-182164r^{2}-135884r+51926\right)S^{4}T^{3}\\
&+\left(-15392r^{12}+45456r^{11}+74143r^{10}-252446r^{9}-116257r^{8}+555224r^{7}+31438r^{6}\right.\\
&\left.-605556r^{5}+92678r^{4}+327944r^{3}-93005r^{2}-70622r+26395\right)S^{3}T^{4}\\
&+\left(-7806r^{12}+14982r^{11}+37274r^{10}-77574r^{9}-65410r^{8}+160476r^{7}+45020r^{6}\right.\\
&\left.-165804r^{5}+1750r^{4}+85566r^{3}-16454r^{2}-17646r+5626\right)S^{2}T^{5}\\
&+\left(-2306r^{12}+1548r^{11}+11852r^{10}-7740r^{9}-24670r^{8}+15480r^{7}+26280r^{6}\right.\\
&\left.-15480r^{5}-14750r^{4}+7740r^{3}+3916r^{2}-1548r-322\right)ST^{6}\,. \qquad \text{(A.24h)}
\end{aligned}
$$

For $Qq(^3P_1^{(6)})$, we have

$$
\begin{aligned}
&\mathcal{D}(^3P_1^{(6)}|S,T)\\
=&9S^4T^2(S+T)^4\left[T+(1-r^2)m_H^2\right]^2\left[(1-r^2)m_H^2+S+T\right]^2\,, \qquad \text{(A.25a)}\\
&c_0(^3P_1^{(6)}|S,T)\\
=&-16S^2T^2(S+T)^5\left(2S^4+3S^3T+6S^2T^2+ST^3+6T^4\right)\,, \qquad \text{(A.25b)}\\
&c_2(^3P_1^{(6)}|S,T)\\
=&ST(S+T)^4\left[\left(128r^2-128r+64\right)S^6+\left(680r^2-684r+124\right)S^5T\right.\\
&+\left(1225r^2-546r-537\right)S^4T^2+\left(1214r^2-728r-1498\right)S^3T^3\\
&\left.+\left(853r^2-778r-437\right)S^2T^4+\left(740r^2-344r-436\right)ST^5+\left(64r^2+64\right)T^6\right]\,, \qquad \text{(A.25c)}\\
&c_4(^3P_1^{(6)}|S,T)\\
=&(S+T)^3\left[\left(-96r^4+128r^3-128r+96\right)S^8+\left(-32r^4+64r^2-32\right)T^8\right.\\
&+\left(-1016r^4+1600r^3+336r^2-1688r+384\right)S^7T\\
&+\left(-3594r^4+4776r^3+3018r^2-4144r-848\right)S^6T^2\\
&+\left(-6319r^4+6276r^3+10100r^2-8228r-3753\right)S^5T^3
\end{aligned}
$$

$$
\begin{aligned}
&+\left(-7239r^4+10056r^3+12704r^2-14376r-1805\right)S^4T^4\\
&+\left(-6229r^4+9196r^3+7092r^2-10940r+1429\right)S^3T^5\\
&+\left(-3267r^4+3000r^3+2430r^2-2600r+673\right)S^2T^6\\
&+\left(-528r^4+144r^3+40r^2-144r+488\right)ST^7\big]\ , \qquad \text{(A.25d)}\\
&c_6({}^3P_1^{(6)}|S,T)\\
=&(S+T)^2\left[\left(164r^6-492r^4+492r^2-164\right)T^8\right.\\
&+\left(448r^6-788r^5-132r^4+1664r^3-400r^2-876r+84\right)S^8\\
&+\left(3353r^6-6298r^5-3335r^4+12188r^3+555r^2-5922r-605\right)S^7T\\
&+\left(10370r^6-16688r^5-18782r^4+37492r^3+10810r^2-22972r-1430\right)S^6T^2\\
&+\left(19110r^6-30564r^5-46156r^4+86184r^3+22774r^2-57460r+5592\right)S^5T^3\\
&+\left(24820r^6-47876r^5-56048r^4+122728r^3+13396r^2-74556r+17880\right)S^4T^4\\
&+\left(21294r^6-39264r^5-35150r^4+84712r^3-3430r^2-45448r+17286\right)S^3T^5\\
&+\left(9624r^6-12404r^5-12000r^4+23692r^3-4644r^2-11288r+7020\right)S^2T^6\\
&\left.+\left(1941r^6-1054r^5-2629r^4+2108r^3-565r^2-1054r+1253\right)ST^7\right]\ , \qquad \text{(A.25e)}\\
&c_8({}^3P_1^{(6)}|S,T)\\
=&(S+T)\left[\left(-363r^8+1452r^6-2178r^4+1452r^2-363\right)T^8\right.\\
&+\left(-864r^8+1964r^7+1134r^6-6028r^5+326r^4+6196r^3-566r^2-2132r-30\right)S^8\\
&+\left(-5953r^8+12640r^7+12558r^6-40624r^5-7016r^4\right.\\
&\left.+47696r^3-1734r^2-19712r+2145\right)S^7T\\
&+\left(-18579r^8+35608r^7+53882r^6-139248r^5-41184r^4\right.\\
&\left.+183928r^3-11570r^2-80288r+17451\right)S^6T^2\\
&+\left(-37194r^8+76780r^7+117894r^6-309220r^5-80698r^4\right.\\
&\left.+395060r^3-49086r^2-162620r+49084\right)S^5T^3\\
&+\left(-50808r^8+113932r^7+142756r^6-402532r^5-67280r^4\right.\\
&\left.+462308r^3-90836r^2-173708r+66168\right)S^4T^4\\
&+\left(-42226r^8+87344r^7+98396r^6-272336r^5-24496r^4\right.\\
&\left.+282640r^3-77292r^2-97648r+45618\right)S^3T^5
\end{aligned}
$$

$$
\begin{aligned}
&+\left(-18502r^8+28432r^7+40216r^6-83616r^5-9852r^4\right.\\
&\left.+81936r^3-26936r^2-26752r+15074\right)S^2T^6\\
&+\left(-4015r^8+3036r^7+10592r^6-9108r^5-7686r^4\right.\\
&\left.+9108r^3-344r^2-3036r+1453\right)ST^7\Big]\,, \qquad \text{(A.25f)}\\
&c_{10}({}^3P_1^{(6)}|S,T)\\
=&\left(452r^{10}-2260r^8+4520r^6-4520r^4+2260r^2-452\right)T^8\\
&+\left(896r^{10}-2536r^9-2552r^8+9916r^7+2276r^6-16700r^5\right.\\
&\left.+492r^4+13796r^3-2084r^2-4476r+972\right)S^8\\
&+\left(6248r^{10}-14776r^9-22446r^8+69168r^7+25752r^6-133504r^5\right.\\
&\left.+2260r^4+118608r^3-23232r^2-39496r+11418\right)S^7T\\
&+\left(21112r^{10}-46700r^9-85772r^8+248672r^7+100152r^6-489696r^5\right.\\
&\left.+17488r^4+420176r^3-97904r^2-132452r+44924\right)S^6T^2\\
&+\left(45892r^{10}-108044r^9-180708r^8+541136r^7+188880r^6-985432r^5\right.\\
&\left.+67832r^4+779632r^3-208932r^2-227292r+87036\right)S^5T^3\\
&+\left(63748r^{10}-152800r^9-225044r^8+679700r^7+201052r^6-1121196r^5\right.\\
&\left.+110420r^4+814492r^3-242560r^2-220196r+92384\right)S^4T^4\\
&+\left(51768r^{10}-112520r^9-168182r^8+459264r^7+140256r^6-702672r^5\right.\\
&\left.+70644r^4+477632r^3-148168r^2-121704r+53682\right)S^3T^5\\
&+\left(22648r^{10}-37852r^9-75092r^8+149472r^7+74400r^6-221304r^5\right.\\
&\left.+872r^4+145600r^3-37816r^2-35916r+14988\right)S^2T^6\\
&+\left(5016r^{10}-4548r^9-19384r^8+18192r^7+27376r^6-27288r^5\right.\\
&\left.-15984r^4+18192r^3+2296r^2-4548r+680\right)ST^7\,, \qquad \text{(A.25g)}\\
&c_{12}({}^3P_1^{(6)}|S,T)\\
=&\left(-338r^{12}+2028r^{10}-5070r^8+6760r^6-5070r^4+2028r^2-338\right)T^7\\
&+\left(-544r^{12}+1784r^{11}+2430r^{10}-8368r^9-4454r^8+19872r^7+2364r^6\right.\\
&\left.-27248r^5+3492r^4+19432r^3-5146r^2-5472r+1858\right)S^7\\
&+\left(-3460r^{12}+8372r^{11}+18100r^{10}-53388r^9-33108r^8+142152r^7+13696r^6\right.
\end{aligned}
$$

$$
\begin{aligned}
&-189848r^5+28460r^4+124932r^3-35316r^2-32220r+11628\big)\,S^6T\\
&+\big(-11614r^{12}+27760r^{11}+59916r^{10}-178992r^9-100698r^8+445936r^7+29768r^6\\
&-541456r^5+89934r^4+322272r^3-96276r^2-75520r+28970\big)\,S^5T^2\\
&+\big(-23398r^{12}+58600r^{11}+108560r^{10}-328768r^9-164414r^8+728560r^7+39320r^6\\
&-799072r^5+133894r^4+434536r^3-130504r^2-93856r+36542\big)\,S^4T^3\\
&+\big(-25376r^{12}+59440r^{11}+109670r^{10}-303288r^9-160702r^8+618752r^7+53628r^6\\
&-630928r^5+87268r^4+321552r^3-88706r^2-65528r+24218\big)\,S^3T^4\\
&+\big(-13588r^{12}+25548r^{11}+60044r^{10}-126444r^9-96868r^8+250296r^7+58792r^6\\
&-247704r^5+8212r^4+122556r^3-24020r^2-24252r+7428\big)\,S^2T^5\\
&+\big(-3454r^{12}+3808r^{11}+17056r^{10}-19040r^9-33470r^8+38080r^7+32400r^6\\
&-38080r^5-15130r^4+19040r^3+2384r^2-3808r+214\big)\,ST^6\,. \qquad \text{(A.25h)}
\end{aligned}
$$

For $Qq(^3P_2^{(6)})$, we have

$$
\begin{aligned}
&\mathcal{D}(^3P_2^{(6)}|S,T)\\
=&54S^4T^2(S+T)^4\left[(1-r^2)m_H^2+S+T\right]^2\,, \qquad \text{(A.26a)}\\
&c_0(^3P_2^{(6)}|S,T)\\
=&-16S^2(S+T)^5\left(10S^4+9S^3T+6S^2T^2+18ST^3+10T^4\right)\,, \qquad \text{(A.26b)}\\
&c_2(^3P_2^{(6)}|S,T)\\
=&S(S+T)^4\left[\left(960r^2-388r+332\right)S^5+\left(1735r^2-530r+3015\right)S^4T\right.\\
&+\left(1818r^2-1024r+4566\right)S^3T^2+\left(2347r^2-442r+2499\right)S^2T^3\\
&\left.+\left(1660r^2-184r+1180\right)ST^4+\left(320r^2+320\right)T^5\right]\,, \qquad \text{(A.26c)}\\
&c_4(^3P_2^{(6)}|S,T)\\
=&(S+T)^3\left[\left(-160r^4+320r^2-160\right)T^6+\left(-2400r^4+1940r^3-576r^2-1020r+1496\right)S^6\right.\\
&+\left(-6515r^4+3228r^3-8258r^2+4348r+7277\right)S^5T\\
&+\left(-10227r^4+7680r^3-13786r^2+8760r+9733\right)S^4T^2\\
&+\left(-10737r^4+5644r^3-3758r^2+5364r+6079\right)S^3T^3
\end{aligned}
$$

$$
\begin{aligned}
&+\left(-6593r^4+1364r^3+3010r^2+996r+2343\right)S^2T^4\\
&+\left(-1872r^4+184r^3+1840r^2-184r+32\right)ST^5\big]\ , \qquad \text{(A.26d)}\\
&c_6({}^3P_2^{(6)}|S,T)\\
=&(S+T)^2\left[\left(500r^6-1500r^4+1500r^2-500\right)T^6\right.\\
&+\left(3200r^6-3880r^5-1016r^4+4512r^3-3416r^2+2176r+136\right)S^6\\
&+\left(11590r^6-7612r^5+62r^4-6840r^3-12102r^2+19620r-2118\right)S^5T\\
&+\left(24648r^6-23376r^5-8472r^4-3808r^3-9200r^2+29544r-8176\right)S^4T^2\\
&+\left(27039r^6-25358r^5-28083r^4+11340r^3+9457r^2+14018r-8413\right)S^3T^3\\
&+\left(14786r^6-8740r^5-25690r^4+7352r^3+14990r^2+1388r-4086\right)S^2T^4\\
&\left.+\left(4369r^6-1042r^5-10425r^4+2084r^3+7743r^2-1042r-1687\right)ST^5\right]\ , \qquad \text{(A.26e)}\\
&c_8({}^3P_2^{(6)}|S,T)\\
=&(S+T)\left[\left(-655r^8+2620r^6-3930r^4+2620r^2-655\right)T^6\right.\\
&+\left(-2400r^8+3880r^7+3184r^6-7416r^5+416r^4\right.\\
&\left.-2424r^3+1408r^2+5960r-2608\right)S^6\\
&+\left(-10870r^8+8768r^7+19212r^6-7520r^5-14840r^4\right.\\
&\left.-22048r^3+20828r^2+20800r-14330\right)S^5T\\
&+\left(-29322r^8+34288r^7+62108r^6-56792r^5-62072r^4\right.\\
&\left.+5552r^3+57676r^2+16952r-28390\right)S^4T^2\\
&+\left(-35845r^8+46784r^7+90000r^6-97600r^5-98682r^4\right.\\
&\left.+54848r^3+70744r^2-4032r-26217\right)S^3T^3\\
&+\left(-19683r^8+21208r^7+59416r^6-51024r^5-72390r^4\right.\\
&\left.+38424r^3+45264r^2-8608r-12607\right)S^2T^4\\
&+\left(-5481r^8+3144r^7+20020r^6-9432r^5-27174r^4\right.\\
&\left.+9432r^3+16212r^2-3144r-3577\right)ST^5\big]\ , \qquad \text{(A.26f)}\\
&c_{10}({}^3P_2^{(6)}|S,T)\\
=&\left(450r^{10}-2250r^8+4500r^6-4500r^4+2250r^2-450\right)T^6\\
&+\left(960r^{10}-1940r^9-2676r^8+5376r^7+3432r^6-1680r^5\right.
\end{aligned}
$$

$$
\begin{aligned}
&-4936r^4 - 5008r^3 + 5480r^2 + 3252r - 2260\big)\, S^6 \\
&+ \big(5219r^{10} - 4962r^9 - 20653r^8 + 18168r^7 + 37214r^6 - 19116r^5 \\
&-42650r^4 + 3576r^3 + 30175r^2 + 2334r - 9305\big)\, S^5T \\
&+ \big(17094r^{10} - 24048r^9 - 66486r^8 + 89576r^7 + 110652r^6 - 121632r^5 \\
&-105348r^4 + 70728r^3 + 59214r^2 - 14624r - 15126\big)\, S^4T^2 \\
&+ \big(23514r^{10} - 37860r^9 - 91726r^8 + 139152r^7 + 147372r^6 - 190296r^5 \\
&-126900r^4 + 114576r^3 + 61018r^2 - 25572r - 13278\big)\, S^3T^3 \\
&+ \big(14040r^{10} - 20524r^9 - 58468r^8 + 77128r^7 + 98440r^6 - 108240r^5 \\
&-84912r^4 + 67192r^3 + 38176r^2 - 15556r - 7276\big)\, S^2T^4 \\
&+ \big(3879r^{10} - 3690r^9 - 18045r^8 + 14760r^7 + 33390r^6 - 22140r^5 \\
&-30690r^4 + 14760r^3 + 13995r^2 - 3690r - 2529\big)\, ST^5\,, \qquad \text{(A.26g)}
\end{aligned}
$$

$$
\begin{aligned}
&c_{12}({}^3P_2^{(6)}|S,T) \\
&= \big(-135r^{12} + 810r^{10} - 2025r^8 + 2700r^6 - 2025r^4 + 810r^2 - 135\big)\, T^5 \\
&+ \big(-160r^{12} + 388r^{11} + 752r^{10} - 1452r^9 - 1928r^8 + 1928r^7 + 3392r^6 \\
&-952r^5 - 3728r^4 - 12r^3 + 2192r^2 + 100r - 520\big)\, S^5 \\
&+ \big(-855r^{12} + 720r^{11} + 5870r^{10} - 6704r^9 - 15621r^8 + 19616r^7 + 20884r^6 \\
&-25824r^5 - 14801r^4 + 16016r^3 + 5214r^2 - 3824r - 691\big)\, S^4T \\
&+ \big(-3060r^{12} + 5760r^{11} + 16200r^{10} - 31032r^9 - 34308r^8 + 66528r^7 + 36432r^6 \\
&-70992r^5 - 19548r^4 + 37728r^3 + 4392r^2 - 7992r - 108\big)\, S^3T^2 \\
&+ \big(-2970r^{12} + 5472r^{11} + 14868r^{10} - 27360r^9 - 29790r^8 + 54720r^7 + 29880r^6 \\
&-54720r^5 - 15030r^4 + 27360r^3 + 3060r^2 - 5472r - 18\big)\, S^2T^3 \\
&+ \big(-1080r^{12} + 1404r^{11} + 5616r^{10} - 7020r^9 - 11880r^8 + 14040r^7 + 12960r^6 \\
&-14040r^5 - 7560r^4 + 7020r^3 + 2160r^2 - 1404r - 216\big)\, ST^4\,. \qquad \text{(A.26h)}
\end{aligned}
$$

A.3 PHOTOPRODUCTION OF HEAVY MESONS

For P waves in photoproduction of mesons, we have the same set of ρ's (Eqs. A.1) as in the case of hadronic production. The corresponding partonic cross sections have the form

$$\frac{d\hat{\sigma}}{d\hat{t}}[q\gamma \to \bar{Q}q(^{2S+1}P_J^{(c)}) + Q] = -\frac{16\pi^2 e_Q^2 \alpha \alpha_s^2 m_H^2}{9S^2} \frac{N_\gamma(^{2S+1}P_J^{(c)}|S,T)}{D_\gamma(^{2S+1}P_J^{(c)}|S,T)}\,, \tag{A.27}$$

where again $N_\gamma(^{2S+1}P_J^{(c)}|S,T)$ is an expansion in powers of m_H:

$$N_\gamma(^{2S+1}P_J^{(c)}|S,T) = \sum_{n=0}^{6} b_{2n}(^{2S+1}P_J^{(c)}|S,T) m_H^{2n}\,. \tag{A.28}$$

Define $\kappa \equiv e_q/e_Q$, where $e_q e$ and $e_Q e$ are the electric charges of the incoming light quark and the outgoing heavy quark respectively.

For $\bar{Q}q(^1P_1^{(1)})$, we have

$$\begin{aligned}
&D_\gamma(^1P_1^{(1)}|S,T) \\
=&S^4T^2(S+T)^4\left[(1-r^2)m_H^2+S+T\right]^2\,, \qquad \text{(A.29a)}\\
&b_0(^1P_1^{(1)}|S,T) \\
=&-2S^2(S+T)^5\left[3S^4+4(\kappa+1)S^3T+2\left(\kappa^2+4\kappa+1\right)S^2T^2+4\kappa(\kappa+1)ST^3+3\kappa^2T^4\right]\,, \qquad \text{(A.29b)}\\
&b_2(^1P_1^{(1)}|S,T) \\
=&S(S+T)^4\left[\left(28r^2-16\right)S^5+S^4T\left(-28\kappa+24\kappa r^2+30r^2+8\kappa r-28\right)\right.\\
&+S^3T^2\left(-24\kappa^2-52\kappa+8\kappa^2r^2+40\kappa r^2+8r^2+8\kappa r-16\right)\\
&+S^2T^3\left(-44\kappa^2-24\kappa+18\kappa^2r^2+16\kappa r^2+8\kappa^2 r+8\kappa r\right)\\
&\left.+ST^4\left(-20\kappa^2+16\kappa^2r^2+8\kappa^2 r\right)+T^5\left(4\kappa^2+4\kappa^2r^2\right)\right]\,, \qquad \text{(A.29c)}\\
&b_4(^1P_1^{(1)}|S,T) \\
=&(S+T)^3\left[T^6\left(-2\kappa^2-2\kappa^2r^4+4\kappa^2r^2\right)+\left(-54r^4+8r^3+54r^2-12r-20\right)S^6\right.\\
&+S^5T\left(-8\kappa-24\kappa r^4-46r^4-28\kappa r^3+8r^3+56\kappa r^2+66r^2+20\kappa r-12r-40\right)\\
&+S^4T^2\left(-24\kappa^2-8\kappa-4\kappa^2r^4-32\kappa r^4-4r^4-44\kappa r^3+4r^3+30\kappa^2r^2+76\kappa r^2\right.\\
&\left.\left.+20r^2+4\kappa^2 r+56\kappa r+4r-24\right)\right.
\end{aligned}$$

$$
\begin{aligned}
&+S^3T^3\left(-52\kappa^2+4\kappa-14\kappa^2r^4-8\kappa r^4-12\kappa^2r^3-36\kappa r^3+66\kappa^2r^2\right.\\
&\left.+16\kappa r^2+20\kappa^2r+56\kappa r\right)\\
&+S^2T^4\left(-30\kappa^2+4\kappa-20\kappa^2r^4-16\kappa^2r^3-12\kappa r^3+48\kappa^2r^2-4\kappa r^2+20\kappa^2r+12\kappa r\right)\\
&+ST^5\left(-4\kappa^2-12\kappa^2r^4-4\kappa^2r^3+16\kappa^2r^2+4\kappa^2r\right)\big]\ , \qquad \text{(A.29d)}\\
&b_6({}^1P_1^{(1)}|S,T)\\
=&(S+T)^2\left[T^6\left(-4\kappa^2+4\kappa^2r^6-12\kappa^2r^4+12\kappa^2r^2\right)\right.\\
&+\left(56r^6-32r^5-72r^4+48r^3+44r^2-16r-12\right)S^6\\
&+S^5T\left(24\kappa+8\kappa r^6+40r^6+36\kappa r^5-32r^5-36\kappa r^4-52r^4\right.\\
&\left.-56\kappa r^3+32r^3+4\kappa r^2+52r^2+20\kappa r-24\right)\\
&+S^4T^2\left(-4\kappa^2+56\kappa+8\kappa r^6+76\kappa r^5-8r^5-8\kappa^2r^4-32\kappa r^4-152\kappa r^3\right.\\
&\left.-16r^3+12\kappa^2r^2-32\kappa r^2+16r^2+76\kappa r+24r-16\right)\\
&+S^3T^3\left(-16\kappa^2+40\kappa+6\kappa^2r^6+4\kappa^2r^5+68\kappa r^5-36\kappa^2r^4+12\kappa r^4\right.\\
&\left.-8\kappa^2r^3-152\kappa r^3+46\kappa^2r^2-52\kappa r^2+4\kappa^2r+84\kappa r\right)\\
&+S^2T^4\left(-24\kappa^2+8\kappa+16\kappa^2r^6+8\kappa^2r^5+28\kappa r^5-60\kappa^2r^4+8\kappa r^4\right.\\
&\left.-16\kappa^2r^3-56\kappa r^3+68\kappa^2r^2-16\kappa r^2+8\kappa^2r+28\kappa r\right)\\
&+ST^5\left(-16\kappa^2+14\kappa^2r^6+4\kappa^2r^5-44\kappa^2r^4-8\kappa^2r^3+46\kappa^2r^2+4\kappa^2r\right)\big]\ , \qquad \text{(A.29e)}\\
&b_8({}^1P_1^{(1)}|S,T)\\
=&(S+T)\left[ST^5\left(-8\kappa^2-6\kappa^2r^8+26\kappa^2r^6-42\kappa^2r^4+30\kappa^2r^2\right)\right.\\
&+T^6\left(-2\kappa^2-2\kappa^2r^8+8\kappa^2r^6-12\kappa^2r^4+8\kappa^2r^2\right)\\
&+S^4T^2\left(-2\kappa^2+28\kappa-52\kappa r^7+4r^7+2\kappa^2r^6+16\kappa r^6-6r^6+144\kappa r^5\right.\\
&\left.+36r^5-6\kappa^2r^4-4\kappa r^4+6r^4-132\kappa r^3-84r^3+6\kappa^2r^2-40\kappa r^2+6r^2+40\kappa r+44r-6\right)\\
&+\left(-34r^8+48r^7+50r^6-84r^5-30r^4+24r^3+14r^2+12r\right)S^6\\
&+S^5T\left(12\kappa-24r^8-20\kappa r^7+48r^7+12\kappa r^6+20r^6+52\kappa r^5-44r^5-12\kappa r^4-4r^4\right.\\
&\left.-44\kappa r^3-56r^3-12\kappa r^2+12r^2+12\kappa r+52r-4\right)\\
&+S^3T^3\left(-8\kappa^2+20\kappa-2\kappa^2r^8-52\kappa r^7+14\kappa^2r^6+152\kappa r^5-30\kappa^2r^4\right.\\
&\left.+20\kappa r^4-148\kappa r^3+26\kappa^2r^2-40\kappa r^2+48\kappa r\right)
\end{aligned}
$$

$$
\begin{aligned}
&+S^2T^4\left(-12\kappa^2+4\kappa-6\kappa^2r^8-20\kappa r^7+30\kappa^2r^6-4\kappa r^6+60\kappa r^5-54\kappa^2r^4\right.\\
&\left.+12\kappa r^4-60\kappa r^3+42\kappa^2r^2-12\kappa r^2+20\kappa r\right)\Big]\,, \qquad \text{(A.29f)}\\
&b_{10}({}^1P_1^{(1)}|S,T)\\
=&S^2T^4\left(4\kappa r^9-16\kappa r^7+24\kappa r^5-16\kappa r^3+4\kappa r\right)\\
&+\left(12r^{10}-32r^9-20r^8+72r^7+4r^6-24r^5+4r^4-40r^3+24r\right)S^6\\
&+S^4T^2\left(12\kappa r^9-8\kappa r^8+4r^8-48\kappa r^7-32r^7+24\kappa r^6-8r^6+72\kappa r^5\right.\\
&\left.+96r^5-24\kappa r^4-48\kappa r^3-96r^3+8\kappa r^2+8r^2+12\kappa r+32r-4\right)\\
&+S^3T^3\left(12\kappa r^9-4\kappa r^8-48\kappa r^7+12\kappa r^6+72\kappa r^5-12\kappa r^4-48\kappa r^3+4\kappa r^2+12\kappa r\right)\\
&+S^5T\left(10r^{10}+4\kappa r^9-32r^9-4\kappa r^8-8r^8-16\kappa r^7+40r^7+12\kappa r^6\right.\\
&\left.-16r^6+24\kappa r^5+72r^5-12\kappa r^4+12r^4-16\kappa r^3-136r^3+4\kappa r^2+6r^2+4\kappa r+56r-4\right)\,, \qquad \text{(A.29g)}\\
&b_{12}({}^1P_1^{(1)}|S,T)\\
=&\left(-2r^{10}+8r^9+6r^8-32r^7-4r^6+48r^5-4r^4-32r^3+6r^2+8r-2\right)S^4T\\
&+\left(-2r^{12}+8r^{11}+4r^{10}-24r^9+2r^8+16r^7-8r^6+16r^5+2r^4-24r^3+4r^2+8r-2\right)S^5\,. \qquad \text{(A.29h)}
\end{aligned}
$$

For $\bar{Q}q({}^3P_0^{(1)})$, we have

$$
\begin{aligned}
&D_\gamma({}^3P_0^{(1)}|S,T)\\
=&S^4T^2(S+T)^4\left[T+(1-r^2)m_H^2\right]^2\left[(1-r^2)m_H^2+S+T\right]^2\,, \qquad \text{(A.30a)}\\
&b_0({}^3P_0^{(1)}|S,T)\\
=&-2S^2T^2(S+T)^5\left(S^4+\kappa^2T^4\right)\,, \qquad \text{(A.30b)}\\
&b_2({}^3P_0^{(1)}|S,T)\\
=&ST(S+T)^4\left[\left(4r^2-24r+68\right)S^6+\left(16r^2-56r+156\right)S^5T\right.\\
&+S^4T^2\left(-4\kappa+2r^2+8\kappa r-32r+104\right)+S^2T^4\left(-60\kappa^2-8\kappa+6\kappa^2r^2+16\kappa^2r\right)\\
&+ST^5\left(-32\kappa^2+12\kappa^2r^2+16\kappa^2r\right)+T^6\left(4\kappa^2+4\kappa^2r^2\right)\\
&\left.+S^3T^3\left(-24\kappa^2-20\kappa+16\kappa r-16r+16\right)\right]\,, \qquad \text{(A.30c)}
\end{aligned}
$$

$$
\begin{aligned}
&b_4({}^3P_0^{(1)}|S,T)\\
=&(S+T)^3\left[T^8\left(-2\kappa^2-2\kappa^2r^4+4\kappa^2r^2\right)+\left(-2r^4+24r^3-68r^2-24r+70\right)S^8\right.\\
&+\left(-28r^4+208r^3-312r^2-160r+268\right)S^7T\\
&+S^6T^2\left(64\kappa-60r^4-16\kappa r^3+408r^3-40\kappa r^2-382r^2+40\kappa r-236r+302\right)\\
&+S^5T^3\left(-48\kappa^2+144\kappa-14r^4-68\kappa r^3+232r^3+48\kappa^2r^2-112\kappa r^2\right.\\
&\left.-106r^2+100\kappa r-132r+76\right)\\
&+S^4T^4\left(-170\kappa^2+112\kappa-6\kappa^2r^4-32\kappa^2r^3-68\kappa r^3+44r^3+182\kappa^2r^2\right.\\
&\left.-92\kappa r^2+32r^2+44\kappa^2r+64\kappa r-60r-24\right)\\
&+S^3T^5\left(-188\kappa^2+44\kappa-30\kappa^2r^4-84\kappa^2r^3-4\kappa r^3+234\kappa^2r^2-32\kappa r^2+100\kappa^2r\right)\\
&+S^2T^6\left(-52\kappa^2+4\kappa-42\kappa^2r^4-56\kappa^2r^3-4\kappa r^3+104\kappa^2r^2-4\kappa r^2+60\kappa^2r+4\kappa r\right)\\
&\left.+ST^7\left(12\kappa^2-20\kappa^2r^4-4\kappa^2r^3+8\kappa^2r^2+4\kappa^2r\right)\right]\,, \qquad \text{(A.30d)}\\
&b_6({}^3P_0^{(1)}|S,T)\\
=&(S+T)^2\left[T^8\left(-8\kappa^2+8\kappa^2r^6-24\kappa^2r^4+24\kappa^2r^2\right)\right.\\
&+\left(12r^6-128r^5+232r^4+208r^3-284r^2-80r+40\right)S^8\\
&+S^7T\left(68\kappa+86r^6+8\kappa r^5-728r^5+44\kappa r^4+756r^4-40\kappa r^3\right.\\
&\left.+1016r^3-112\kappa r^2-794r^2+32\kappa r-240r\right)\\
&+S^6T^2\left(-24\kappa^2+284\kappa+136r^6+72\kappa r^5-1216r^5-24\kappa^2r^4+316\kappa r^4\right.\\
&\left.+728r^4-256\kappa r^3+1416r^3+48\kappa^2r^2-600\kappa r^2-500r^2+184\kappa r-200r-252\right)\\
&+S^5T^3\left(-120\kappa^2+412\kappa+2\kappa^2r^6+42r^6+16\kappa^2r^5+164\kappa r^5\right.\\
&-632r^5-136\kappa^2r^4+672\kappa r^4+124r^4-56\kappa^2r^3-496\kappa r^3+680r^3+254\kappa^2r^2\\
&\left.-1060\kappa r^2+214r^2+40\kappa^2r+316\kappa r-96r-332\right)\\
&+S^4T^4\left(-216\kappa^2+268\kappa+24\kappa^2r^6+88\kappa^2r^5+108\kappa r^5-40r^5-296\kappa^2r^4\right.\\
&+548\kappa r^4-72r^4-256\kappa^2r^3-320\kappa r^3+104r^3+488\kappa^2r^2-792\kappa r^2\\
&\left.+192r^2+168\kappa^2r+196\kappa r-64r-120\right)\\
&+S^3T^5\left(-152\kappa^2+72\kappa+72\kappa^2r^6+140\kappa^2r^5+12\kappa r^5-324\kappa^2r^4+148\kappa r^4\right.\\
&\left.-368\kappa^2r^3-56\kappa r^3+404\kappa^2r^2-220\kappa r^2+228\kappa^2r+44\kappa r\right)\\
&+S^2T^6\left(-24\kappa^2+88\kappa^2r^6+80\kappa^2r^5+12\kappa r^5-208\kappa^2r^4-192\kappa^2r^3\right.
\end{aligned}
$$

$$
\begin{aligned}
&-24\kappa r^3+144\kappa^2r^2+112\kappa^2r+12\kappa r\big)\\
&+ST^7\left(46\kappa^2r^6+12\kappa^2r^5-92\kappa^2r^4-24\kappa^2r^3+46\kappa^2r^2+12\kappa^2r\right)\big]\ , \qquad \text{(A.30e)}\\
&b_8({}^3P_0^{(1)}|S,T)\\
=&(S+T)\ \big[\big(-30r^8+280r^7-258r^6-620r^5+478r^4+352r^3-110r^2-12r-80\big)\,S^8\\
&+T\left(-150r^8-20\kappa r^7+1312r^7-136\kappa r^6-806r^6+116\kappa r^5-2572r^5\right.\\
&\left.+320\kappa r^4+1458r^4-172\kappa r^3+1160r^3-232\kappa r^2-170r^2+76\kappa r+100r+48\kappa-332\right)S^7\\
&+T^2\left(-200r^8-100\kappa r^7+1924r^7+14\kappa^2r^6-660\kappa r^6-816r^6+12\kappa^2r^5+536\kappa r^5-3364r^5\right.\\
&-36\kappa^2r^4+1384\kappa r^4+1344r^4-24\kappa^2r^3-740\kappa r^3+1196r^3+30\kappa^2r^2-836\kappa r^2\\
&\left.+160r^2+12\kappa^2r+304\kappa r+244r-8\kappa^2+112\kappa-488\right)S^6\\
&+T^3\left(-6\kappa^2r^8-70r^8-20\kappa^2r^7-140\kappa r^7+904r^7+62\kappa^2r^6-1100\kappa r^6-246r^6+148\kappa^2r^5\right.\\
&+792\kappa r^5-1456r^5-146\kappa^2r^4+2128\kappa r^4+258r^4-236\kappa^2r^3-1084\kappa r^3+440r^3+130\kappa^2r^2\\
&\left.-1076\kappa r^2+358r^2+108\kappa^2r+432\kappa r+112r-40\kappa^2+48\kappa-300\right)S^5\\
&+T^4\left(-40\kappa^2r^8-72\kappa^2r^7-44\kappa r^7+16r^7+164\kappa^2r^6-728\kappa r^6+6r^6+408\kappa^2r^5+396\kappa r^5\right.\\
&-48r^5-276\kappa^2r^4+1320\kappa r^4-78r^4-600\kappa^2r^3-612\kappa r^3+48r^3+220\kappa^2r^2-528\kappa r^2\\
&\left.+138r^2+264\kappa^2r+260\kappa r-16r-68\kappa^2-64\kappa-66\right)S^4\\
&+T^5\left(-96\kappa^2r^8-96\kappa^2r^7+8\kappa r^7+308\kappa^2r^6-136\kappa r^6+456\kappa^2r^5+48\kappa r^5-384\kappa^2r^4\right.\\
&\left.+208\kappa r^4-624\kappa^2r^3-120\kappa r^3+228\kappa^2r^2-8\kappa r^2+264\kappa^2r+64\kappa r-56\kappa^2-64\kappa\right)S^3\\
&+T^6\left(-108\kappa^2r^8-56\kappa^2r^7-8\kappa r^7+350\kappa^2r^6+16\kappa r^6+220\kappa^2r^5+24\kappa r^5-416\kappa^2r^4\right.\\
&\left.-48\kappa r^4-272\kappa^2r^3-24\kappa r^3+214\kappa^2r^2+48\kappa r^2+108\kappa^2r+8\kappa r-40\kappa^2-16\kappa\right)S^2\\
&+T^7\left(-58\kappa^2r^8-12\kappa^2r^7+206\kappa^2r^6+36\kappa^2r^5-270\kappa^2r^4\right.\\
&\left.-36\kappa^2r^3+154\kappa^2r^2+12\kappa^2r-32\kappa^2\right)S\\
&+T^8\left(-12\kappa^2r^8+48\kappa^2r^6-72\kappa^2r^4+48\kappa^2r^2-12\kappa^2\right)\big]\ , \qquad \text{(A.30f)}\\
&b_{10}({}^3P_0^{(1)}|S,T)\\
=&\left(40r^{10}-320r^9+72r^8+880r^7-340r^6-720r^5+300r^4+80r^3-68r^2+80r-4\right)S^8\\
&+T\left(160r^{10}+12\kappa r^9-1312r^9+108\kappa r^8+176r^8-88\kappa r^7+3336r^7-260\kappa r^6\right.\\
&-1100r^6+176\kappa r^5-2472r^5+156\kappa r^4+1076r^4-136\kappa r^3+184r^3\\
&\left.+36\kappa r^2-356r^2+36\kappa r+264r-40\kappa+44\right)S^7
\end{aligned}
$$

$$
\begin{aligned}
&+T^2\left(192r^{10}+28\kappa r^9-1728r^9+8\kappa^2r^8+424\kappa r^8+108r^8-24\kappa^2r^7-280\kappa r^7+4160r^7\right.\\
&-20\kappa^2r^6-968\kappa r^6-1144r^6+72\kappa^2r^5+592\kappa r^5-2880r^5+12\kappa^2r^4+480\kappa r^4+1344r^4\\
&-72\kappa^2r^3-456\kappa r^3+192r^3+4\kappa^2r^2+248\kappa r^2-648r^2+24\kappa^2r\\
&\left.+116\kappa r+256r-4\kappa^2-184\kappa+148\right)S^6\\
&+T^3\left(6\kappa^2r^{10}+70r^{10}+4\kappa^2r^9-20\kappa r^9-744r^9+4\kappa^2r^8+572\kappa r^8-4r^8-112\kappa^2r^7\right.\\
&-168\kappa r^7+1744r^7-28\kappa^2r^6-1228\kappa r^6-404r^6+312\kappa^2r^5+512\kappa r^5-1200r^5+420\kappa r^4\\
&+680r^4-304\kappa^2r^3-440\kappa r^3+144r^3+38\kappa^2r^2+556\kappa r^2-482r^2+100\kappa^2r\\
&\left.+116\kappa r+56r-20\kappa^2-320\kappa+140\right)S^5\\
&+T^4\left(32\kappa^2r^{10}+16\kappa^2r^9-84\kappa r^9-8r^9-104\kappa^2r^8+296\kappa r^8-208\kappa^2r^7+184\kappa r^7+40r^7\right.\\
&+168\kappa^2r^6-560\kappa r^6-40r^6+528\kappa^2r^5-96\kappa r^5-72r^5-200\kappa^2r^4-24\kappa r^4+120r^4\\
&-496\kappa^2r^3-24\kappa r^3+56r^3+152\kappa^2r^2+544\kappa r^2-120r^2\\
&\left.+160\kappa^2r+20\kappa r-16r-48\kappa^2-256\kappa+40\right)S^4\\
&+T^5\left(68\kappa^2r^{10}+24\kappa^2r^9-56\kappa r^9-296\kappa^2r^8+32\kappa r^8-192\kappa^2r^7+192\kappa r^7+552\kappa^2r^6\right.\\
&-8\kappa r^6+432\kappa^2r^5-240\kappa r^5-560\kappa^2r^4-168\kappa r^4-384\kappa^2r^3+128\kappa r^3+308\kappa^2r^2\\
&\left.+232\kappa r^2+120\kappa^2r-24\kappa r-72\kappa^2-88\kappa\right)S^3\\
&+T^6\left(72\kappa^2r^{10}+16\kappa^2r^9-8\kappa r^9-344\kappa^2r^8-8\kappa r^8-88\kappa^2r^7+32\kappa r^7+668\kappa^2r^6+32\kappa r^6\right.\\
&+168\kappa^2r^5-48\kappa r^5-660\kappa^2r^4-48\kappa r^4-136\kappa^2r^3+32\kappa r^3+332\kappa^2r^2\\
&\left.+32\kappa r^2+40\kappa^2r-8\kappa r-68\kappa^2-8\kappa\right)S^2\\
&+T^7\left(38\kappa^2r^{10}+4\kappa^2r^9-188\kappa^2r^8-16\kappa^2r^7+372\kappa^2r^6+24\kappa^2r^5-368\kappa^2r^4\right.\\
&\left.-16\kappa^2r^3+182\kappa^2r^2+4\kappa^2r-36\kappa^2\right)S\\
&+T^8\left(8\kappa^2r^{10}-40\kappa^2r^8+80\kappa^2r^6-80\kappa^2r^4+40\kappa^2r^2-8\kappa^2\right), \qquad \text{(A.30g)}
\end{aligned}
$$

$$
\begin{aligned}
&b_{12}({}^3P_0^{(1)}|S,T)\\
&=\left(-30r^{12}+200r^{11}+50r^{10}-652r^9+60r^8+752r^7-220r^6\right.\\
&\left.-344r^5+250r^4+40r^3-150r^2+4r+40\right)S^7\\
&+T\left(-74r^{12}+4\kappa r^{11}+528r^{11}-20\kappa r^{10}+166r^{10}-12\kappa r^9-1680r^9+44\kappa r^8+20r^8\right.\\
&+24\kappa r^7+1920r^7-420r^6-40\kappa r^5-960r^5-64\kappa r^4+590r^4+36\kappa r^3+240r^3\\
&\left.+52\kappa r^2-386r^2-12\kappa r-48r-12\kappa+104\right)S^6
\end{aligned}
$$

$$
\begin{aligned}
&+T^2\left(-42r^{12}+32\kappa r^{11}+340r^{11}+2\kappa^2r^{10}-44\kappa r^{10}+146r^{10}-148\kappa r^9-1104r^9-10\kappa^2r^8\right.\\
&+104\kappa r^8-136r^8+304\kappa r^7+1352r^7+20\kappa^2r^6-24\kappa r^6-124r^6-344\kappa r^5-832r^5\\
&-20\kappa^2r^4-112\kappa r^4+358r^4+208\kappa r^3+324r^3+10\kappa^2r^2+100\kappa r^2\\
&\left.-278r^2-52\kappa r-80r-2\kappa^2-24\kappa+76\right)S^5\\
&+T^3\left(-2\kappa^2r^{12}+64\kappa r^{11}+4r^{11}+20\kappa^2r^{10}-40\kappa r^{10}+12r^{10}-320\kappa r^9-44r^9-70\kappa^2r^8\right.\\
&+136\kappa r^8-36r^8+656\kappa r^7+136r^7+120\kappa^2r^6-168\kappa r^6+24r^6-688\kappa r^5-184r^5\\
&-110\kappa^2r^4+88\kappa r^4+24r^4+368\kappa r^3+116r^3+52\kappa^2r^2-16\kappa r^2\\
&\left.-36r^2-80\kappa r-28r-10\kappa^2+12\right)S^4\\
&+T^4\left(-8\kappa^2r^{12}+48\kappa r^{11}+60\kappa^2r^{10}-28\kappa r^{10}-244\kappa r^9-180\kappa^2r^8+136\kappa r^8+496\kappa r^7\right.\\
&+280\kappa^2r^6-264\kappa r^6-504\kappa r^5-240\kappa^2r^4+256\kappa r^4+256\kappa r^3+108\kappa^2r^2\\
&\left.-124\kappa r^2-52\kappa r-20\kappa^2+24\kappa\right)S^3\\
&+T^5\left(-12\kappa^2r^{12}+12\kappa r^{11}+80\kappa^2r^{10}-12\kappa r^{10}-60\kappa r^9-220\kappa^2r^8+60\kappa r^8+120\kappa r^7\right.\\
&+320\kappa^2r^6-120\kappa r^6-120\kappa r^5-260\kappa^2r^4+120\kappa r^4+60\kappa r^3+112\kappa^2r^2\\
&\left.-60\kappa r^2-12\kappa r-20\kappa^2+12\kappa\right)S^2\\
&+T^6\left(-8\kappa^2r^{12}+50\kappa^2r^{10}-130\kappa^2r^8+180\kappa^2r^6-140\kappa^2r^4+58\kappa^2r^2-10\kappa^2\right)S\\
&+T^7\left(-2\kappa^2r^{12}+12\kappa^2r^{10}-30\kappa^2r^8+40\kappa^2r^6-30\kappa^2r^4+12\kappa^2r^2-2\kappa^2\right). \qquad \text{(A.30h)}
\end{aligned}
$$

For $\bar{Q}q(^3P_1^{(1)})$, we have

$$
\begin{aligned}
&D_\gamma(^3P_1^{(1)}|S,T)\\
=&S^4T^2(S+T)^4\left[T+(1-r^2)m_H^2\right]^2\left[(1-r^2)m_H^2+S+T\right]^2, \qquad \text{(A.31a)}\\
&b_0(^3P_1^{(1)}|S,T)\\
=&-4S^2T^2(S+T)^5\left(S^2+2ST+3T^2\right)(S+\kappa T)^2, \qquad \text{(A.31b)}\\
&b_2(^3P_1^{(1)}|S,T)\\
=&ST(S+T)^4\left[\left(16r^2-16r+8\right)S^6+S^5T\left(-16\kappa+16\kappa r^2+80r^2-16\kappa r-112r+16\right)\right.\\
&+S^4T^2\left(-8\kappa^2-24\kappa+8\kappa^2r^2+104\kappa r^2+116r^2-112\kappa r-112r+8\right)\\
&+S^3T^3\left(-40\kappa^2-56\kappa+40\kappa^2r^2+192\kappa r^2+72r^2-24\kappa^2r-152\kappa r-24r-24\right)
\end{aligned}
$$

$$
\begin{aligned}
&+S^2T^4\left(-20\kappa^2-64\kappa+88\kappa^2r^2+128\kappa r^2-40\kappa^2r-32\kappa r\right)\\
&+ST^5\left(-16\kappa^2-8\kappa+72\kappa^2r^2+8\kappa r^2-16\kappa^2r\right)+T^6\left(8\kappa^2+8\kappa^2r^2\right)\big]\ , \qquad \text{(A.31c)}\\
&b_4({}^3P_1^{(1)}|S,T)\\
=&(S+T)^3\left[\left(-12r^4+16r^3-16r+12\right)S^8+ST^7\left(16\kappa^2-48\kappa^2r^4+32\kappa^2r^2\right)\right.\\
&+T^8\left(-4\kappa^2-4\kappa^2r^4+8\kappa^2r^2\right)\\
&+S^7T\left(-8\kappa-8\kappa r^4-120r^4+16\kappa r^3+240r^3+16\kappa r^2-8r^2-16\kappa r-224r+64\right)\\
&+S^6T^2\left(-4\kappa^2+32\kappa-4\kappa^2r^4-128\kappa r^4-340r^4+224\kappa r^3+752r^3+8\kappa^2r^2\right.\\
&\left.+96\kappa r^2-32r^2-272\kappa r-496r+140\right)\\
&+S^5T^3\left(-48\kappa^2+224\kappa-48\kappa^2r^4-464\kappa r^4-364r^4+48\kappa^2r^3+736\kappa r^3+592r^3\right.\\
&\left.+96\kappa^2r^2+232\kappa r^2-4r^2-48\kappa^2r-768\kappa r-304r+104\right)\\
&+S^4T^4\left(-4\kappa^2+256\kappa-184\kappa^2r^4-624\kappa r^4-140r^4+184\kappa^2r^3+776\kappa r^3+88r^3\right.\\
&\left.+204\kappa^2r^2+352\kappa r^2+68r^2-208\kappa^2r-760\kappa r-24r-8\right)\\
&+S^3T^5\left(52\kappa^2+56\kappa-304\kappa^2r^4-320\kappa r^4+216\kappa^2r^3+208\kappa r^3\right.\\
&\left.+252\kappa^2r^2+288\kappa r^2-208\kappa^2r-240\kappa r\right)\\
&+S^2T^6\left(32\kappa^2-24\kappa-208\kappa^2r^4-40\kappa r^4+80\kappa^2r^3+8\kappa r^3\right.\\
&\left.\left.+160\kappa^2r^2+64\kappa r^2-48\kappa^2r-8\kappa r\right)\right]\ , \qquad \text{(A.31d)}\\
&b_6({}^3P_1^{(1)}|S,T)\\
=&(S+T)^2\left[T^8\left(-16\kappa^2+16\kappa^2r^6-48\kappa^2r^4+48\kappa^2r^2\right)\right.\\
&+\left(56r^6-112r^5+24r^4+208r^3-104r^2-96r+24\right)S^8\\
&+S^7T\left(40\kappa+40\kappa r^6+356r^6-96\kappa r^5-944r^5-40\kappa r^4+112r^4+240\kappa r^3+1408r^3\right.\\
&\left.-40\kappa r^2-556r^2-144\kappa r-432r+120\right)\\
&+S^6T^2\left(-16\kappa^2+440\kappa+16\kappa^2r^6+352\kappa r^6+736r^6-24\kappa^2r^5-776\kappa r^5-2040r^5\right.\\
&-48\kappa^2r^4-216\kappa r^4+272r^4+48\kappa^2r^3+1616\kappa r^3+2464r^3+48\kappa^2r^2-576\kappa r^2\\
&\left.-1120r^2-24\kappa^2r-840\kappa r-488r+224\right)\\
&+S^5T^3\left(28\kappa^2+1072\kappa+128\kappa^2r^6+936\kappa r^6+580r^6-200\kappa^2r^5-1872\kappa r^5-1312r^5\right.\\
&-260\kappa^2r^4-528\kappa r^4+240r^4+448\kappa^2r^3+3600\kappa r^3+1280r^3+104\kappa^2r^2\\
&\left.-1504\kappa r^2-844r^2-248\kappa^2r-1696\kappa r-64r+120\right)
\end{aligned}
$$

$$
\begin{aligned}
&+S^4T^4\left(144\kappa^2+968\kappa+384\kappa^2r^6+1032\kappa r^6+128r^6-480\kappa^2r^5-1696\kappa r^5-128r^5\right.\\
&-664\kappa^2r^4-784\kappa r^4+32r^4+984\kappa^2r^3+3216\kappa r^3+32r^3+136\kappa^2r^2-1240\kappa r^2\\
&\left.-144r^2-504\kappa^2r-1488\kappa r+96r-16\right)\\
&+S^3T^5\left(152\kappa^2+272\kappa+536\kappa^2r^6+488\kappa r^6-464\kappa^2r^5-512\kappa r^5-904\kappa^2r^4-648\kappa r^4\right.\\
&\left.+832\kappa^2r^3+1040\kappa r^3+216\kappa^2r^2-112\kappa r^2-368\kappa^2r-528\kappa r\right)\\
&+S^2T^6\left(48\kappa^2-24\kappa+368\kappa^2r^6+80\kappa r^6-168\kappa^2r^5-32\kappa r^5-664\kappa^2r^4-184\kappa r^4\right.\\
&\left.+264\kappa^2r^3+64\kappa r^3+248\kappa^2r^2+128\kappa r^2-96\kappa^2r-32\kappa r\right)\\
&+ST^7\left(-20\kappa^2+120\kappa^2r^6-8\kappa^2r^5-260\kappa^2r^4+16\kappa^2r^3+160\kappa^2r^2-8\kappa^2r\right)\Big]\,, \qquad \text{(A.31e)}
\end{aligned}
$$

$$
\begin{aligned}
&b_8({}^3P_1^{(1)}|S,T)\\
=&(S+T)\left[\left(-108r^8+304r^7-704r^5+304r^4+464r^3-208r^2-64r+12\right)S^8\right.\\
&+T\left(-80\kappa r^8-556r^8+208\kappa r^7+1776r^7+40\kappa r^6-20r^6-608\kappa r^5-3520r^5+320\kappa r^4\right.\\
&\left.+1516r^4+592\kappa r^3+1808r^3-440\kappa r^2-1004r^2-192\kappa r-64r+160\kappa+64\right)S^7\\
&+T^2\left(-24\kappa^2r^8-496\kappa r^8-952r^8+56\kappa^2r^7+1224\kappa r^7+3000r^7+68\kappa^2r^6+288\kappa r^6\right.\\
&-148r^6-192\kappa^2r^5-3368\kappa r^5-5240r^5-44\kappa^2r^4+1712\kappa r^4+2668r^4+216\kappa^2r^3\\
&+3000\kappa r^3+2024r^3-20\kappa^2r^2-2256\kappa r^2-1628r^2-80\kappa^2r\\
&\left.-856\kappa r+216r+20\kappa^2+752\kappa+60\right)S^6\\
&+T^3\left(-160\kappa^2r^8-1072\kappa r^8-588r^8+296\kappa^2r^7+2432\kappa r^7+1616r^7+428\kappa^2r^6+816\kappa r^6\right.\\
&-236r^6-912\kappa^2r^5-6528\kappa r^5-2432r^5-276\kappa^2r^4+2952\kappa r^4+1828r^4+936\kappa^2r^3\\
&+5600\kappa r^3+432r^3-92\kappa^2r^2-3944\kappa r^2-948r^2-320\kappa^2r\\
&\left.-1504\kappa r+384r+100\kappa^2+1248\kappa-56\right)S^5\\
&+T^4\left(-416\kappa^2r^8-1048\kappa r^8-68r^8+576\kappa^2r^7+2008\kappa r^7+96r^7+1120\kappa^2r^6+1232\kappa r^6\right.\\
&-108r^6-1656\kappa^2r^5-5384\kappa r^5-16r^5-816\kappa^2r^4+1632\kappa r^4+356r^4+1584\kappa^2r^3\\
&+4648\kappa r^3-256r^3-64\kappa^2r^2-2696\kappa r^2-116r^2-504\kappa^2r\\
&\left.-1272\kappa r+176r+176\kappa^2+880\kappa-64\right)S^4\\
&+T^5\left(-552\kappa^2r^8-472\kappa r^8+512\kappa^2r^7+640\kappa r^7+1568\kappa^2r^6+904\kappa r^6-1416\kappa^2r^5\right.\\
&-1760\kappa r^5-1376\kappa^2r^4-168\kappa r^4+1296\kappa^2r^3+1600\kappa r^3+256\kappa^2r^2-488\kappa r^2\\
&\left.-392\kappa^2r-480\kappa r+104\kappa^2+224\kappa\right)S^3
\end{aligned}
$$

$$
\begin{aligned}
&+T^6\left(-400\kappa^2r^8-80\kappa r^8+200\kappa^2r^7+48\kappa r^7+1244\kappa^2r^6+240\kappa r^6-552\kappa^2r^5-144\kappa r^5\right.\\
&\left.-1332\kappa^2r^4-240\kappa r^4+504\kappa^2r^3+144\kappa r^3+532\kappa^2r^2+80\kappa r^2-152\kappa^2r-48\kappa r-44\kappa^2\right)S^2\\
&+T^7\left(-152\kappa^2r^8+24\kappa^2r^7+532\kappa^2r^6-72\kappa^2r^5-684\kappa^2r^4\right.\\
&\left.+72\kappa^2r^3+380\kappa^2r^2-24\kappa^2r-76\kappa^2\right)S\\
&+T^8\left(-24\kappa^2r^8+96\kappa^2r^6-144\kappa^2r^4+96\kappa^2r^2-24\kappa^2\right)\Big]\ , \qquad \text{(A.31f)}\\
&b_{10}({}^3P_1^{(1)}|S,T)\\
=&\left(112r^{10}-416r^9-112r^8+1136r^7-224r^6-976r^5+336r^4+208r^3-112r^2+48r\right)S^8\\
&+T\left(80\kappa r^{10}+504r^{10}-208\kappa r^9-1872r^9-88\kappa r^8-472r^8+704\kappa r^7+4736r^7-312\kappa r^6\right.\\
&\left.-1008r^6-832\kappa r^5-3648r^5+640\kappa r^4+1392r^4+384\kappa r^3+576r^3\right.\\
&\left.-392\kappa r^2-392r^2-48\kappa r+208r+72\kappa-24\right)S^7\\
&+T^2\left(16\kappa^2r^{10}+400\kappa r^{10}+752r^{10}-40\kappa^2r^9-1000\kappa r^9-2632r^9-56\kappa^2r^8-512\kappa r^8\right.\\
&\left.-664r^8+152\kappa^2r^7+3376\kappa r^7+6288r^7+56\kappa^2r^6-1200\kappa r^6-1472r^6-216\kappa^2r^5\right.\\
&\left.-3968\kappa r^5-4352r^5+8\kappa^2r^4+2552\kappa r^4+1808r^4+136\kappa^2r^3+1808\kappa r^3+368r^3\right.\\
&\left.-40\kappa^2r^2-1456\kappa r^2-304r^2-32\kappa^2r-216\kappa r+328r+16\kappa^2+216\kappa-120\right)S^6\\
&+T^3\left(96\kappa^2r^{10}+752\kappa r^{10}+388r^{10}-184\kappa^2r^9-1744\kappa r^9-1216r^9-356\kappa^2r^8-1184\kappa r^8\right.\\
&\left.-312r^8+704\kappa^2r^7+5856\kappa r^7+2720r^7+432\kappa^2r^6-1368\kappa r^6-744r^6-1008\kappa^2r^5\right.\\
&\left.-6880\kappa r^5-1536r^5-120\kappa^2r^4+3520\kappa r^4+704r^4+640\kappa^2r^3+3168\kappa r^3-224r^3\right.\\
&\left.-112\kappa^2r^2-1960\kappa r^2+132r^2-152\kappa^2r-400\kappa r+256r+60\kappa^2+240\kappa-168\right)S^5\\
&+T^4\left(240\kappa^2r^{10}+664\kappa r^{10}+24r^{10}-336\kappa^2r^9-1352\kappa r^9-40r^9-944\kappa^2r^8-1320\kappa r^8\right.\\
&\left.-8r^8+1296\kappa^2r^7+4528\kappa r^7+32r^7+1328\kappa^2r^6-240\kappa r^6-48r^6-1872\kappa^2r^5-5376\kappa r^5\right.\\
&\left.+144r^5-720\kappa^2r^4+1928\kappa r^4-48r^4+1200\kappa^2r^3+2576\kappa r^3-224r^3+32\kappa^2r^2-1176\kappa r^2\right.\\
&\left.+152r^2-288\kappa^2r-376\kappa r+88r+64\kappa^2+144\kappa-72\right)S^4\\
&+T^5\left(320\kappa^2r^{10}+272\kappa r^{10}-304\kappa^2r^9-432\kappa r^9-1336\kappa^2r^8-696\kappa r^8+1184\kappa^2r^7\right.\\
&\left.+1472\kappa r^7+2112\kappa^2r^6+384\kappa r^6-1728\kappa^2r^5-1824\kappa r^5-1520\kappa^2r^4+304\kappa r^4+1120\kappa^2r^3\right.\\
&\left.+960\kappa r^3+448\kappa^2r^2-336\kappa r^2-272\kappa^2r-176\kappa r-24\kappa^2+72\kappa\right)S^3\\
&+T^6\left(240\kappa^2r^{10}+40\kappa r^{10}-136\kappa^2r^9-32\kappa r^9-1064\kappa^2r^8-136\kappa r^8+536\kappa^2r^7+128\kappa r^7\right.\\
&\left.+1848\kappa^2r^6+144\kappa r^6-792\kappa^2r^5-192\kappa r^5-1560\kappa^2r^4-16\kappa r^4+520\kappa^2r^3+128\kappa r^3\right.
\end{aligned}
$$

$$
\begin{aligned}
&+632\kappa^2r^2-56\kappa r^2-128\kappa^2r-32\kappa r-96\kappa^2+24\kappa\big)\,S^2\\
&+T^7\left(96\kappa^2r^{10}-24\kappa^2r^9-452\kappa^2r^8+96\kappa^2r^7\right.\\
&\left.+848\kappa^2r^6-144\kappa^2r^5-792\kappa^2r^4+96\kappa^2r^3+368\kappa^2r^2-24\kappa^2r-68\kappa^2\right)S\\
&+T^8\left(16\kappa^2r^{10}-80\kappa^2r^8+160\kappa^2r^6-160\kappa^2r^4+80\kappa^2r^2-16\kappa^2\right)\,, \qquad \text{(A.31g)}\\
&b_{12}({}^3P_1^{(1)}|S,T)\\
=&\big(-68r^{12}+304r^{11}+144r^{10}-992r^9-28r^8+1152r^7-96r^6\\
&-544r^5+36r^4+80r^3+16r^2-4\big)\,S^7\\
&+T\left(-40\kappa r^{12}-204r^{12}+96\kappa r^{11}+832r^{11}+104\kappa r^{10}+448r^{10}-400\kappa r^9-2656r^9\right.\\
&\left.-24\kappa r^8-180r^8+608\kappa r^7+3008r^7-120\kappa r^6-64r^6-384\kappa r^5-1408r^5+64\kappa r^4\right.\\
&\left.-148r^4+64\kappa r^3+256r^3+48\kappa r^2+192r^2+16\kappa r-32r-32\kappa-44\right)S^6\\
&+T^2\left(-4\kappa^2r^{12}-136\kappa r^{12}-152r^{12}+8\kappa^2r^{11}+312\kappa r^{11}+552r^{11}+20\kappa^2r^{10}+376\kappa r^{10}\right.\\
&\left.+368r^{10}-40\kappa^2r^9-1272\kappa r^9-1736r^9-40\kappa^2r^8-168\kappa r^8-320r^8+80\kappa^2r^7+1904\kappa r^7\right.\\
&\left.+1904r^7+40\kappa^2r^6-320\kappa r^6+352r^6-80\kappa^2r^5-1200\kappa r^5-816r^5-20\kappa^2r^4+248\kappa r^4\right.\\
&\left.-536r^4+40\kappa^2r^3+216\kappa r^3+104r^3+4\kappa^2r^2+72\kappa r^2\right.\\
&\left.+368r^2-8\kappa^2r+40\kappa r-8r-72\kappa-80\right)S^5\\
&+T^3\left(-20\kappa^2r^{12}-160\kappa r^{12}-4r^{12}+32\kappa^2r^{11}+344\kappa r^{11}+8r^{11}+104\kappa^2r^{10}+456\kappa r^{10}\right.\\
&\left.+44r^{10}-160\kappa^2r^9-1384\kappa r^9-8r^9-220\kappa^2r^8-224\kappa r^8-176r^8+320\kappa^2r^7+2064\kappa r^7\right.\\
&\left.-48r^7+240\kappa^2r^6-440\kappa r^6+344r^6-320\kappa^2r^5-1328\kappa r^5+112r^5-140\kappa^2r^4+504\kappa r^4\right.\\
&\left.-356r^4+160\kappa^2r^3+280\kappa r^3-88r^3+40\kappa^2r^2-112\kappa r^2\right.\\
&\left.+188r^2-32\kappa^2r+24\kappa r+24r-4\kappa^2-24\kappa-40\right)S^4\\
&+T^4\left(-40\kappa^2r^{12}-72\kappa r^{12}+48\kappa^2r^{11}+136\kappa r^{11}+216\kappa^2r^{10}+200\kappa r^{10}-240\kappa^2r^9-552\kappa r^9\right.\\
&\left.-480\kappa^2r^8-40\kappa r^8+480\kappa^2r^7+848\kappa r^7+560\kappa^2r^6-400\kappa r^6-480\kappa^2r^5-592\kappa r^5\right.\\
&\left.-360\kappa^2r^4+520\kappa r^4+240\kappa^2r^3+168\kappa r^3+120\kappa^2r^2\right.\\
&\left.-248\kappa r^2-48\kappa^2r-8\kappa r-16\kappa^2+40\kappa\right)S^3\\
&+T^5\left(-40\kappa^2r^{12}-8\kappa r^{12}+32\kappa^2r^{11}+8\kappa r^{11}+224\kappa^2r^{10}+16\kappa r^{10}-160\kappa^2r^9-40\kappa r^9\right.\\
&\left.-520\kappa^2r^8+40\kappa r^8+320\kappa^2r^7+80\kappa r^7+640\kappa^2r^6-160\kappa r^6-320\kappa^2r^5-80\kappa r^5-440\kappa^2r^4\right.\\
&\left.+200\kappa r^4+160\kappa^2r^3+40\kappa r^3+160\kappa^2r^2-112\kappa r^2-32\kappa^2r-8\kappa r-24\kappa^2+24\kappa\right)S^2
\end{aligned}
$$

$$
\begin{aligned}
&+T^6\left(-20\kappa^2r^{12}+8\kappa^2r^{11}+116\kappa^2r^{10}-40\kappa^2r^9-280\kappa^2r^8+80\kappa^2r^7+360\kappa^2r^6-80\kappa^2r^5\right.\\
&\left.-260\kappa^2r^4+40\kappa^2r^3+100\kappa^2r^2-8\kappa^2r-16\kappa^2\right)S\\
&+T^7\left(-4\kappa^2r^{12}+24\kappa^2r^{10}-60\kappa^2r^8+80\kappa^2r^6-60\kappa^2r^4+24\kappa^2r^2-4\kappa^2\right). \qquad \text{(A.31h)}
\end{aligned}
$$

For $\bar{Q}q(^3P_2^{(1)})$, we have

$$
\begin{aligned}
&D_\gamma(^3P_2^{(1)}|S,T)\\
=&3S^4T^2(S+T)^4\left[(1-r^2)m_H^2+S+T\right]^2, \qquad \text{(A.32a)}\\
&b_0(^3P_2^{(1)}|S,T)\\
=&-2S^2(S+T)^5\left[5S^4+6(\kappa+1)S^3T+3\left(\kappa^2+4\kappa+1\right)S^2T^2+6\kappa(\kappa+1)ST^3+5\kappa^2T^4\right], \qquad \text{(A.32b)}\\
&b_2(^3P_2^{(1)}|S,T)\\
=&S(S+T)^4\left[\left(60r^2-40r-4\right)S^5+S^4T\left(4\kappa+60\kappa r^2+70r^2-32\kappa r-40r-8\right)\right.\\
&+S^3T^2\left(-4\kappa+24\kappa^2r^2+120\kappa r^2+24r^2-12\kappa^2r-52\kappa r-20r-16\right)\\
&+S^2T^3\left(14\kappa^2-40\kappa+64\kappa^2r^2+72\kappa r^2-28\kappa^2r-24\kappa r\right)\\
&\left.+ST^4\left(28\kappa^2-12\kappa+64\kappa^2r^2+12\kappa r^2-16\kappa^2r\right)+T^5\left(20\kappa^2+20\kappa^2r^2\right)\right], \qquad \text{(A.32c)}\\
&b_4(^3P_2^{(1)}|S,T)\\
=&(S+T)^3\left[T^6\left(-10\kappa^2-10\kappa^2r^4+20\kappa^2r^2\right)+\left(-150r^4+200r^3+36r^2-120r-10\right)S^6\right.\\
&+S^5T\left(-48\kappa-120\kappa r^4-170r^4+128\kappa r^3+200r^3+4\kappa r^2+26r^2-64\kappa r-120r-28\right)\\
&+S^4T^2\left(-22\kappa^2-144\kappa-36\kappa^2r^4-240\kappa r^4-36r^4+36\kappa^2r^3+228\kappa r^3+60r^3+22\kappa^2r^2\right.\\
&\left.+88\kappa r^2-10r^2-24\kappa^2r-188\kappa r-20r-34\right)\\
&+S^3T^3\left(-38\kappa^2-144\kappa-120\kappa^2r^4-156\kappa r^4+92\kappa^2r^3+136\kappa r^3\right.\\
&\left.+94\kappa^2r^2+168\kappa r^2-72\kappa^2r-144\kappa r\right)\\
&+S^2T^4\left(-22\kappa^2-28\kappa-146\kappa^2r^4-36\kappa r^4+72\kappa^2r^3+28\kappa r^3\right.\\
&\left.+140\kappa^2r^2+64\kappa r^2-64\kappa^2r-28\kappa r\right)\\
&\left.+ST^5\left(-16\kappa^2-72\kappa^2r^4+16\kappa^2r^3+88\kappa^2r^2-16\kappa^2r\right)\right], \qquad \text{(A.32d)}\\
&b_6(^3P_2^{(1)}|S,T)\\
=&(S+T)^2\left[T^6\left(-20\kappa^2+20\kappa^2r^6-60\kappa^2r^4+60\kappa^2r^2\right)\right.
\end{aligned}
$$

$$
\begin{aligned}
&+\left(200r^6-400r^5-104r^4+480r^3-56r^2-80r-32\right)S^6\\
&+S^5T\left(-68\kappa+120\kappa r^6+220r^6-192\kappa r^5-400r^5\right.\\
&\left.-36\kappa r^4-40r^4+232\kappa r^3+400r^3-4\kappa r^2-124r^2-72\kappa r-56\right)\\
&+S^4T^2\left(-8\kappa^2-148\kappa+24\kappa^2r^6+240\kappa r^6+24r^6-36\kappa^2r^5-372\kappa r^5-60r^5-44\kappa^2r^4\right.\\
&-168\kappa r^4+116r^4+60\kappa^2r^3+600\kappa r^3-40r^3+28\kappa^2r^2+88\kappa r^2\\
&\left.-104r^2-24\kappa^2r-260\kappa r+100r-36\right)\\
&+S^3T^3\left(-46\kappa^2-72\kappa+96\kappa^2r^6+156\kappa r^6-100\kappa^2r^5-248\kappa r^5-214\kappa^2r^4\right.\\
&\left.-196\kappa r^4+176\kappa^2r^3+488\kappa r^3+164\kappa^2r^2+112\kappa r^2-76\kappa^2r-240\kappa r\right)\\
&+S^2T^4\left(-88\kappa^2+8\kappa+140\kappa^2r^6+36\kappa r^6-92\kappa^2r^5-64\kappa r^5-356\kappa^2r^4-64\kappa r^4\right.\\
&\left.+172\kappa^2r^3+128\kappa r^3+304\kappa^2r^2+20\kappa r^2-80\kappa^2r-64\kappa r\right)\\
&+ST^5\left(-70\kappa^2+88\kappa^2r^6-28\kappa^2r^5-246\kappa^2r^4+56\kappa^2r^3+228\kappa^2r^2-28\kappa^2r\right)\Big]\ ,\\
&b_8({}^3P_2^{(1)}|S,T)\\
=&(S+T)\left[T^6\left(-10\kappa^2-10\kappa^2r^8+40\kappa^2r^6-60\kappa^2r^4+40\kappa^2r^2\right)\right.\\
&+\left(-150r^8+400r^7+136r^6-720r^5+152r^4+240r^3-128r^2+80r-10\right)S^6\\
&+S^5T\left(24\kappa-60\kappa r^8-160r^8+128\kappa r^7+400r^7+44\kappa r^6+44r^6-272\kappa r^5-520r^5\right.\\
&\left.+104\kappa r^4+372r^4+192\kappa r^3-160r^3-112\kappa r^2-236r^2-48\kappa r+280r-20\right)\\
&+S^4T^2\left(-4\kappa^2+100\kappa-6\kappa^2r^8-120\kappa r^8-6r^8+12\kappa^2r^7+268\kappa r^7+20r^7+22\kappa^2r^6\right.\\
&+88\kappa r^6-148r^6-36\kappa^2r^5-652\kappa r^5+180r^5-30\kappa^2r^4+272\kappa r^4+300r^4+36\kappa^2r^3\\
&\left.+532\kappa r^3-420r^3+18\kappa^2r^2-340\kappa r^2-132r^2-12\kappa^2r-148\kappa r+220r-14\right)\\
&+S^3T^3\left(-22\kappa^2+128\kappa-28\kappa^2r^8-72\kappa r^8+36\kappa^2r^7+184\kappa r^7+106\kappa^2r^6+28\kappa r^6\right.\\
&-108\kappa^2r^5-512\kappa r^5-150\kappa^2r^4+288\kappa r^4+108\kappa^2r^3\\
&\left.+472\kappa r^3+94\kappa^2r^2-372\kappa r^2-36\kappa^2r-144\kappa r\right)\\
&+S^2T^4\left(-42\kappa^2+52\kappa-48\kappa^2r^8-12\kappa r^8+36\kappa^2r^7+44\kappa r^7+186\kappa^2r^6-16\kappa r^6-108\kappa^2r^5\right.\\
&\left.-132\kappa r^5-270\kappa^2r^4+120\kappa r^4+108\kappa^2r^3+132\kappa r^3+174\kappa^2r^2-144\kappa r^2-36\kappa^2r-44\kappa r\right)\\
&+ST^5\left(-34\kappa^2-36\kappa^2r^8+12\kappa^2r^7+142\kappa^2r^6-36\kappa^2r^5\right.\\
&\left.-210\kappa^2r^4+36\kappa^2r^3+138\kappa^2r^2-12\kappa^2r\right)\Big]\ ,
\end{aligned}
\tag{A.32e}
$$

$$
\begin{aligned}
&b_{10}({}^3P_2^{(1)}|S,T)\\
=&S^2T^4\left(28\kappa-8\kappa r^9+28\kappa r^8+32\kappa r^7-112\kappa r^6-48\kappa r^5+168\kappa r^4+32\kappa r^3-112\kappa r^2-8\kappa r\right)\\
&+\left(60r^{10}-200r^9-84r^8+480r^7-96r^6-240r^5+200r^4-160r^3-76r^2+120r-4\right)S^6\\
&+S^5T\left(28\kappa+12\kappa r^{10}+62r^{10}-32\kappa r^9-200r^9-16\kappa r^8-32r^8+104\kappa r^7+320r^7-52\kappa r^6\right.\\
&-260r^6-120\kappa r^5+240r^5+132\kappa r^4+352r^4+56\kappa r^3-640r^3\\
&\left.-104\kappa r^2-106r^2-8\kappa r+280r-16\right)\\
&+S^4T^2\left(84\kappa+24\kappa r^{10}-72\kappa r^9-4\kappa r^8+68r^8+240\kappa r^7-160r^7-216\kappa r^6-192r^6\right.\\
&-288\kappa r^5+480r^5+432\kappa r^4+168r^4+144\kappa r^3-480r^3\\
&\left.-320\kappa r^2-32r^2-24\kappa r+160r-12\right)\\
&+S^3T^3\left(84\kappa+12\kappa r^{10}-48\kappa r^9+40\kappa r^8+168\kappa r^7-276\kappa r^6\right.\\
&\left.-216\kappa r^5+468\kappa r^4+120\kappa r^3-328\kappa r^2-24\kappa r\right)\,, \qquad \text{(A.32f)}\\
&b_{12}({}^3P_2^{(1)}|S,T)\\
=&\left(-10r^{10}+40r^9+30r^8-160r^7-20r^6+240r^5-20r^4-160r^3+30r^2+40r-10\right)S^4T\\
&+\left(-10r^{12}+40r^{11}+20r^{10}-120r^9+10r^8+80r^7-40r^6\right.\\
&\left.+80r^5+10r^4-120r^3+20r^2+40r-10\right)S^5\,. \qquad \text{(A.32g)}
\end{aligned}
$$

The color-octet cross sections are given by

$$
\frac{d\hat{\sigma}}{dt}\left[q\gamma\to\bar{Q}q({}^{2S+1}P_J^{(8)})+Q\right]=\frac{1}{8}\frac{d\hat{\sigma}}{dt}\left[q\gamma\to\bar{Q}q({}^{2S+1}P_J^{(1)})+Q\right]\,. \qquad \text{(A.33)}
$$

APPENDIX B

ANALYTIC EXPRESSIONS FOR THRESHOLD RESUMMATION

In this appendix, we list the functions needed for the threshold resummation of Chap 5, taken from Ref. [58].

The running kernel U is defined as

$$U(M,\mu_h,\mu_s,\mu_f) = \left(\frac{M^2}{\mu_h^2}\right)^{-2a_\Gamma(\mu_h,\mu_s)} \exp\left[4S(\mu_h,\mu_s) - 2a_{\gamma^V}(\mu_h,\mu_s) + 4a_{\gamma^\phi}(\mu_s,\mu_f)\right] , \quad \text{(B.1)}$$

where a_γ is the anomalous exponent of γ defined by

$$a_\gamma(\nu,\mu) = -\int_{\alpha_s(\nu)}^{\alpha_s(\mu)} d\alpha \frac{\gamma(\alpha)}{\beta(\alpha)} , \quad \text{(B.2)}$$

and S is the Sudakov exponent

$$S(\nu,\mu) = -\int_{\alpha_s(\nu)}^{\alpha_s(\mu)} d\alpha \frac{\Gamma_{\rm cusp}(\alpha)}{\beta(\alpha)} \int_{\alpha_s(\nu)}^{\alpha} \frac{d\alpha'}{\beta(\alpha')} . \quad \text{(B.3)}$$

The renormalization group equations, Eqs. (B.2) and (B.3), can be solved perturbatively. The anomalous dimensions are expanded as

$$\gamma(\alpha_s) = \gamma_0 \frac{\alpha_s}{4\pi} + \gamma_1 \left(\frac{\alpha_s}{4\pi}\right)^2 + \gamma_2 \left(\frac{\alpha_s}{4\pi}\right)^3 + \cdots . \quad \text{(B.4)}$$

The solutions to Eqs. (B.2) and (B.3) are then

$$\begin{aligned} a_\gamma(\nu,\mu) \;=\; & \frac{\gamma_0}{2\beta_0}\left\{\ln\frac{\alpha_s(\mu)}{\alpha_s\nu} + \left(\frac{\gamma_1}{\gamma_0} - \frac{\beta_1}{\beta_0}\right)\frac{\alpha_s(\mu)-\alpha_s(\nu)}{4\pi}\right. \\ & \left. + \left[\frac{\gamma_2}{\gamma_0} - \frac{\beta_2}{\beta_0} - \frac{\beta_1}{\beta_0}\left(\frac{\gamma_1}{\gamma_0} - \frac{\beta_1}{\beta_0}\right)\right]\frac{\alpha_s^2(\mu)-\alpha_s^2(\nu)}{32\pi^2} + \cdots\right\} , \end{aligned} \quad \text{(B.5)}$$

and

$$
\begin{aligned}
S(\nu,\mu) \;=\; & \frac{\Gamma_0}{4\beta_0^2}\left\{\frac{4\pi}{\alpha_s(\nu)}\left(1-\frac{1}{r}-\ln r\right)+\left(\frac{\Gamma_1}{\Gamma_0}-\frac{\beta_1}{\beta_0}\right)(1-r+\ln r)+\frac{\beta_1}{2\beta_0}\ln^2 r\right. \\
& +\frac{\alpha_s(\nu)}{4\pi}\left[\left(\frac{\beta_1\Gamma_1}{\beta_0\Gamma_0}-\frac{\beta_2}{\beta_0}\right)(1-r+r\ln r)+\left(\frac{\beta_1^2}{\beta_0^2}-\frac{\beta_2}{\beta_0}\right)(1-r)\ln r\right. \\
& \qquad \left.-\left(\frac{\beta_1^2}{\beta_0^2}-\frac{\beta_2}{\beta_0}-\frac{\beta_1\Gamma_1}{\beta_0\Gamma_0}+\frac{\Gamma_2}{\Gamma_0}\right)\frac{(1-r)^2}{2}\right] \\
& +\left(\frac{\alpha_s(\nu)}{4\pi}\right)^2\left[\left(\frac{\beta_1\beta_2}{\beta_0^2}-\frac{\beta_1^3}{2\beta_0^3}-\frac{\beta_3}{2\beta_0}+\frac{\beta_1}{\beta_0}\left(\frac{\Gamma_2}{\Gamma_0}-\frac{\beta_2}{\beta_0}+\frac{\beta_1^2}{\beta_0^2}-\frac{\beta_1\Gamma_1}{\beta_0\Gamma_0}\right)\frac{r^2}{2}\right)\ln r\right. \\
& \qquad +\left(\frac{\Gamma_3}{\Gamma_0}-\frac{\beta_3}{\beta_0}+\frac{2\beta_1\beta_2}{\beta_0^2}+\frac{\beta_1^2}{\beta_0^2}\left(\frac{\Gamma_1}{\Gamma_0}-\frac{\beta_1}{\beta_0}\right)-\frac{\beta_2\Gamma_1}{\beta_0\Gamma_0}-\frac{\beta_1\Gamma_2}{\beta_0\Gamma_0}\right)\frac{(1-r)^3}{3} \\
& \qquad +\left(\frac{3\beta_3}{4\beta_0}-\frac{\Gamma_3}{2\Gamma_0}+\frac{\beta_1^3}{\beta_0^3}-\frac{3\beta_1^2\Gamma_1}{4\beta_0^2\Gamma_0}+\frac{\beta_2\Gamma_1}{\beta_0\Gamma_0}+\frac{\beta_1\Gamma_2}{4\beta_0\Gamma_0}-\frac{7\beta_1\beta_2}{4\beta_0^2}\right)(1-r)^2 \\
& \qquad \left.\left.+\left(\frac{\beta_1\beta_2}{\beta_0^2}-\frac{\beta_3}{\beta_0}-\frac{\beta_1^2\Gamma_1}{\beta_0^2\Gamma_0}+\frac{\beta_1\Gamma_2}{\beta_0\Gamma_0}\right)\frac{1-r}{2}\right]+\cdots\right\}, \qquad \text{(B.6)}
\end{aligned}
$$

where $r \equiv \alpha_s(\mu)/\alpha_s(\nu)$.

The cusp anomalous dimension is known to three-loops [74, 75]. The coefficients are

$$
\begin{aligned}
\Gamma_0 &= 4C_F, \\
\Gamma_1 &= 4C_F\left[\left(\frac{67}{9}-\frac{\pi^2}{3}\right)C_A-\frac{20}{9}T_F n_f\right], \\
\Gamma_2 &= 4C_F\left[C_A^2\left(\frac{245}{6}-\frac{134\pi^2}{27}+\frac{11\pi^4}{45}+\frac{22}{3}\zeta_3\right)+C_A T_F n_f\left(-\frac{418}{27}+\frac{40\pi^2}{27}-\frac{56}{3}\zeta_3\right)\right. \\
&\qquad \left.+C_F T_F n_f\left(-\frac{55}{3}+16\zeta_3\right)-\frac{16}{27}T_F^2 n_f^2\right]. \qquad \text{(B.7)}
\end{aligned}
$$

The four-loop coefficient Γ_3 has not yet been calculated, so we use the Padé approximate $\Gamma_3 = \Gamma_2^2/\Gamma_1$. The anomalous dimension γ^V can be obtained from the partial three-loop

on-shell quark form factor [76]. The coefficients are

$$
\begin{aligned}
\gamma_0^V &= -6C_F\,, \\
\gamma_1^V &= C_F^2(-3+4\pi^2-48\zeta_3)+C_FC_A\left(-\frac{961}{27}-\frac{11\pi^2}{3}+52\zeta_3\right)+C_FT_Fn_f\left(\frac{260}{27}+\frac{4\pi^2}{3}\right), \\
\gamma_2^V &= C_F^3\left(-29-6\pi^2-\frac{16\pi^4}{5}-136\zeta_3+\frac{32\pi^2}{3}\zeta_3+480\zeta_5\right) \\
&\quad +C_F^2C_A\left(-\frac{151}{2}+\frac{410\pi^2}{9}+\frac{494\pi^4}{135}-\frac{1688}{3}\zeta_3-\frac{16\pi^2}{3}\zeta_3-240\zeta_5\right) \\
&\quad +C_FC_A^2\left(-\frac{139345}{1458}-\frac{7163\pi^2}{243}-\frac{83\pi^4}{45}+\frac{7052}{9}\zeta_3-\frac{88\pi^2}{9}\zeta_3-272\zeta_5\right) \\
&\quad +C_F^2T_Fn_f\left(\frac{5906}{27}-\frac{52\pi^2}{9}-\frac{56\pi^4}{27}+\frac{1024}{9}\zeta_3\right) \\
&\quad +C_FC_AT_Fn_f\left(-\frac{34636}{729}+\frac{5188\pi^2}{243}+\frac{44\pi^4}{45}-\frac{3856}{27}\zeta_3\right) \\
&\quad +C_FT_F^2n_f^2\left(\frac{19336}{729}-\frac{80\pi^2}{27}-\frac{64}{27}\zeta_3\right). \qquad \text{(B.8)}
\end{aligned}
$$

The final anomalous dimension, γ^ϕ, is known from the NNLO calculation of the Altarelli-Parisi splitting function [75]. The coefficients are

$$
\begin{aligned}
\gamma_0^\phi &= 3C_F\,, \\
\gamma_1^\phi &= C_F^2\left(\frac{3}{2}-2\pi^2+24\zeta_3\right)+C_FC_A\left(\frac{17}{6}+\frac{22\pi^2}{9}-12\zeta_3\right)-C_FT_Fn_f\left(\frac{2}{3}+\frac{8\pi^2}{9}\right), \\
\gamma_2^\phi &= C_F^3\left(\frac{29}{2}+3\pi^2+\frac{8\pi^4}{5}+68\zeta_3-\frac{16\pi^2}{3}\zeta_3-240\zeta_5\right) \\
&\quad +C_F^2C_A\left(\frac{151}{4}-\frac{205\pi^2}{9}-\frac{247\pi^4}{135}+\frac{844}{3}\zeta_3+\frac{8\pi^2}{3}\zeta_3+120\zeta_5\right) \\
&\quad +C_FC_A^2\left(-\frac{1657}{36}+\frac{2248\pi^2}{81}-\frac{\pi^4}{18}-\frac{1552}{9}\zeta_3+40\zeta_5\right) \\
&\quad +C_F^2T_Fn_f\left(-46+\frac{20\pi^2}{9}+\frac{116\pi^4}{135}-\frac{272}{3}\zeta_3\right) \\
&\quad +C_FC_AT_Fn_f\left(40-\frac{1336\pi^2}{81}+\frac{2\pi^4}{45}+\frac{400}{9}\zeta_3\right) \\
&\quad +C_FT_F^2n_f^2\left(-\frac{68}{9}+\frac{160\pi^2}{81}-\frac{64}{9}\zeta_3\right). \qquad \text{(B.9)}
\end{aligned}
$$

The other functions needed are the Wilson coefficient C_V and the soft function $\tilde{s}_{\rm DY}$. The Wilson coefficient C_V has the expansion,

$$C_V(-M^2-i\epsilon,\mu) = 1+\frac{C_F\alpha_s}{4\pi}\left(-L^2+3L-8+\frac{\pi^2}{6}\right)+C_F\left(\frac{\alpha_s}{4\pi}\right)^2\left(C_F H_F+C_A H_A+T_F n_f H_f\right), \tag{B.10}$$

where $L=\ln(M^2/\mu^2)-i\pi$, and

$$\begin{aligned}
H_F &= \frac{L^4}{2}-3L^3+\left(\frac{25}{2}-\frac{\pi^2}{6}\right)L^2+\left(-\frac{45}{2}-\frac{3\pi^2}{2}+24\zeta_3\right)L+\frac{255}{8}+\frac{7\pi^2}{2}-\frac{83\pi^4}{360}-30\zeta_3\,,\\
H_A &= \frac{11}{9}L^3+\left(-\frac{233}{18}+\frac{\pi^2}{3}\right)L^2+\left(\frac{2545}{54}+\frac{11\pi^2}{9}-26\zeta_3\right)L\\
&\quad -\frac{51157}{648}-\frac{337\pi^2}{108}+\frac{11\pi^4}{45}+\frac{313}{9}\zeta_3\,,\\
H_f &= -\frac{4}{9}L^3+\frac{38}{9}L^2+\left(-\frac{418}{27}-\frac{4\pi^2}{9}\right)L+\frac{4085}{162}+\frac{23\pi^2}{27}+\frac{4}{9}\zeta_3\,.
\end{aligned} \tag{B.11}$$

This agrees with the corresponding expression in [77].

The soft function to two-loops is

$$\tilde{s}_{\rm DY}(\ell,\mu) = 1+\frac{C_F\alpha_s}{4\pi}\left(2\ell^2+\frac{\pi^2}{3}\right)+C_F\left(\frac{\alpha_s}{4\pi}\right)^2\left(C_F W_F+C_A W_A+T_F n_f W_f\right), \tag{B.12}$$

where

$$\begin{aligned}
W_F &= 2\ell^4+\frac{2\pi^2}{3}\ell^2+\frac{\pi^4}{18}\,,\\
W_A &= -\frac{22}{9}\ell^3+\left(\frac{134}{9}-\frac{2\pi^2}{3}\right)\ell^2+\left(-\frac{808}{27}+28\zeta_3\right)\ell+\frac{2428}{81}+\frac{67\pi^2}{54}-\frac{\pi^4}{3}-\frac{22}{9}\zeta_3\,,\\
W_f &= \frac{8}{9}\ell^3-\frac{40}{9}\ell^2+\frac{224}{27}\ell-\frac{656}{81}-\frac{10\pi^2}{27}+\frac{8}{9}\zeta_3\,.
\end{aligned} \tag{B.13}$$

This again agrees with the moment-space expression in [77].

The QCD β-function

$$\beta(\alpha_s)\equiv\mu^2\frac{d\alpha_s}{d\mu^2} \tag{B.14}$$

is expanded as

$$\beta(\alpha_s) = -\alpha_s\left[\beta_0\left(\frac{\alpha_s}{4\pi}\right)+\beta_1\left(\frac{\alpha_s}{4\pi}\right)^2+\beta_2\left(\frac{\alpha_s}{4\pi}\right)^3+\cdots\right], \tag{B.15}$$

where

$$
\begin{aligned}
\beta_0 &= \frac{11}{3}C_A - \frac{4}{3}T_F n_f \,, \\
\beta_1 &= \frac{34}{3}C_A^2 - \frac{20}{3}C_A T_F n_f - 4C_F T_F n_f \,, \\
\beta_2 &= \frac{2857}{54}C_A^3 + \left(2C_F^2 - \frac{205}{9}C_F C_A - \frac{1415}{27}C_A^2\right) T_F n_f + \left(\frac{44}{9}C_F + \frac{158}{27}C_A\right) T_F^2 n_f^2 \,, \\
\beta_3 &= \frac{149753}{6} + 3564\zeta_3 - \left(\frac{1078361}{162} + \frac{6508}{27}\zeta_3\right) n_f + \left(\frac{50065}{162} + \frac{6472}{81}\zeta_3\right) n_f^2 + \frac{1093}{729}n_f^3 \,.
\end{aligned}
\tag{B.16}
$$

BIBLIOGRAPHY

[1] P. A. R. Ade *et al.* [Planck Collaboration], [arXiv:1502.01589 [astro-ph.CO]].

[2] G. Aad *et al.* [ATLAS Collaboration], Phys. Lett. B **716**, 1 (2012) [arXiv:1207.7214 [hep-ex]].

[3] S. Chatrchyan *et al.* [CMS Collaboration], Phys. Lett. B **716**, 30 (2012) [arXiv:1207.7235 [hep-ex]].

[4] The ATLAS and CMS Collaborations, ATLAS-CONF-2015-044.

[5] Christenson, J. H. and Cronin, J. W. and Fitch, V. L. and Turlay, R. Phys. Rev. Lett. **13**, 138 (1964).

[6] A. D. Sakharov, Pisma Zh. Eksp. Teor. Fiz. **5**, 32 (1967).

[7] M. B. Gavela, P. Hernandez, J. Orloff and O. Pene, Mod. Phys. Lett. A **9**, 795 (1994) [hep-ph/9312215].

[8] M. B. Gavela, P. Hernandez, J. Orloff, O. Pene and C. Quimbay, Nucl. Phys. B **430**, 382 (1994) [hep-ph/9406289].

[9] K. Abe *et al.* [Belle Collaboration], Phys. Rev. Lett. **87**, 091802 (2001) [hep-ex/0107061].

[10] B. Aubert *et al.* [BaBar Collaboration], Phys. Rev. Lett. **87**, 091801 (2001) [hep-ex/0107013].

[11] R. Aaij *et al.* [LHCb Collaboration], Phys. Lett. B **718**, 902 (2013) [arXiv:1210.4112 [hep-ex]].

[12] K. A. Olive *et al.* [Particle Data Group Collaboration], Chin. Phys. C **38**, 090001 (2014).

[13] R. K. Ellis, W. J. Stirling and B. R. Webber, *QCD and Collider Physics*, Cambridge university Press (1996).

[14] R. Brock *et al.* [CTEQ Collaboration], Rev. Mod. Phys. **67**, 157 (1995).

[15] S. Heinemeyer *et al.* [LHC Higgs Cross Section Working Group Collaboration], arXiv:1307.1347 [hep-ph].

[16] C. Anastasiou, C. Duhr, F. Dulat, F. Herzog and B. Mistlberger, Phys. Rev. Lett. **114**, 212001 (2015) [arXiv:1503.06056 [hep-ph]].

[17] A. Manohar and M. Wise, *Heavy Quark Physics*, Cambridge Unversity Press (2000).

[18] R. J. Eden, P. V. Landshoff, D. I. Olive and J. C. Polkinghorne, *The Analytic S-Matrix*, Cambridge University Press (1966).

[19] J. Collins, *Foundations of Perturbative QCD*, Cambridge University Press (2011).

[20] C. W. Bauer, S. Fleming and M. E. Luke, Phys. Rev. D **63**, 014006 (2000) [hep-ph/0005275].

[21] C. W. Bauer, D. Pirjol and I. W. Stewart, Phys. Rev. D **65**, 054022 (2002) [hep-ph/0109045].

[22] C. W. Bauer, D. Pirjol and I. W. Stewart, Phys. Rev. D **66**, 054005 (2002) [hep-ph/0205289].

[23] A. V. Manohar, T. Mehen, D. Pirjol and I. W. Stewart, Phys. Lett. B **539**, 59 (2002) [hep-ph/0204229].

[24] J. N. Butler *et al.* (Quark Flavor Physics Working Group Collaboration, "Working Group Report: Quark Flavor Physics"), [arXiv:1311.1076].

[25] M. Artuso, B. Meadows, and A. A. Petrov, Annu. Rev. Nucl. Part. Sci. **58**, 249 (2008) [arXiv:0802.2934].

[26] E. M. Aitala *et al.* (E791 Collaboration), Phys. Lett. B **371**, 157 (1996) ; *ibid.* **411**, 230 (1997); G. A. Alves *et al.* (E769 Collaboration), Phys. Rev. Lett. **72**, 812 (1994); *ibid.* **77**, 2392 (1996); M. Adamovich *et al.* (BEATRICE Collaboration), Nucl. Phys. B **495**, 3 (1997); M. Adamovich *et al.* (WA82 Collaboration), Phys. Lett. B **305**, 402 (1993); F. G. Garcia *et al.* (SELEX Collaboration), Phys. Lett. B **528**, 49 (2002); E. M. Aitala *et al.* (E791 Collaboration), Phys. Lett. B **495**, 42 (2000); M. I. Adamovich *et al.* (WA89 Collaboration), Eur. Phys. J. C **8**, 593 (1999).

[27] J. C. Collins, D. E. Soper and G. F. Sterman, Nucl. Phys. B **263**, 37 (1986).

[28] E. Norrbin and T. Sjostrand, Eur. Phys. J. C **17**, 137 (2000) [hep-ph/0005110].

[29] E. R. Cazaroto, V. P. Goncalves, F. S. Navarra and M. Nielsen, Phys. Lett. B **724**, 108 (2013) [arXiv:1302.0035].

[30] E. Braaten, Y. Jia and T. Mehen, Phys. Rev. D **66**, 034003 (2002) [hep-ph/0108201].

[31] E. Braaten, Y. Jia and T. Mehen, Phys. Rev. D **66**, 014003 (2002) [hep-ph/0111296].

[32] E. Braaten, Y. Jia and T. Mehen, Phys. Rev. Lett. **89**, 122002 (2002) [hep-ph/0205149].

[33] E. Braaten, M. Kusunoki, Y. Jia and T. Mehen, Phys. Rev. D **70**, 054021 (2004) [hep-ph/0304280].

[34] W. K. Lai, A. K. Leibovich and A. A. Petrov, Phys. Rev. D **90**, no. 5, 054022 (2014) [arXiv:1408.2843 [hep-ph]].

[35] W. K. Lai and A. K. Leibovich, Phys. Rev. D **91**, no. 5, 054022 (2015) doi:10.1103/PhysRevD.91.054022 [arXiv:1410.2091 [hep-ph]].

[36] C. Peterson, D. Schlatter, I. Schmitt and P. M. Zerwas, Phys. Rev. D **27**, 105 (1983).

[37] S. Chekanov *et al.* (ZEUS Collaboration), JHEP **0904**, 082 (2009) [arXiv:0901.1210].

[38] H. Abramowicz *et al.* (ZEUS Collaboration), JHEP **1309**, 058 (2013) [arXiv:1306.4862].

[39] T. Affolder *et al.* [CDF Collaboration], Phys. Rev. Lett. **84**, 1663 (2000) [hep-ex/9909011].

[40] S. Chatrchyan *et al.* [CMS Collaboration], Phys. Lett. B **714**, 136 (2012) [arXiv:1205.0594 [hep-ex]].

[41] R. C. Hwa, Phys. Rev. D **51**, 85 (1995).

[42] R. Vogt and S. J. Brodsky, Nucl. Phys. B **438**, 261 (1995) [hep-ph/9405236].

[43] J. L. Rosner, Phys. Rev. D **86**, 014011 (2012) [arXiv:1205.1529 [hep-ph]].

[44] S. L. Glashow, D. V. Nanopoulos and A. Yildiz, Phys. Rev. D **18**, 1724 (1978).

[45] A. Stange, W. J. Marciano and S. Willenbrock, Phys. Rev. D **50**, 4491 (1994) [hep-ph/9404247].

[46] [Tevatron New Physics Higgs Working Group and CDF and D0 Collaborations], arXiv:1207.0449 [hep-ex].

[47] J. M. Butterworth, A. R. Davison, M. Rubin and G. P. Salam, Phys. Rev. Lett. **100**, 242001 (2008) [arXiv:0802.2470 [hep-ph]].

[48] S. Dittmaier *et al.* [LHC Higgs Cross Section Working Group Collaboration], arXiv:1101.0593 [hep-ph].

[49] S. Dittmaier *et al.*, arXiv:1201.3084 [hep-ph].

[50] O. Brein, A. Djouadi and R. Harlander, Phys. Lett. B **579**, 149 (2004) [hep-ph/0307206].

[51] O. Brein, R. Harlander, M. Wiesemann and T. Zirke, Eur. Phys. J. C **72**, 1868 (2012) [arXiv:1111.0761 [hep-ph]].

[52] T. Han and S. Willenbrock, Phys. Lett. B **273**, 167 (1991).

[53] H. Baer, B. Bailey and J. F. Owens, Phys. Rev. D **47**, 2730 (1993).

[54] J. Ohnemus and W. J. Stirling, Phys. Rev. D **47**, 2722 (1993).

[55] J. Campbell, R. Ellis, and C. Williams, *M*CFM-Monte Carlo for FeMtobarn processes, http://mcfm.fnal.gov/ (2012).

[56] G. F. Sterman, Nucl. Phys. B **281**, 310 (1987).

[57] G. F. Sterman and W. Vogelsang, JHEP **0102**, 016 (2001) [hep-ph/0011289].

[58] T. Becher, M. Neubert and G. Xu, JHEP **0807**, 030 (2008) [arXiv:0710.0680 [hep-ph]].

[59] S. Dawson, T. Han, W. K. Lai, A. K. Leibovich and I. Lewis, Phys. Rev. D **86**, 074007 (2012) [arXiv:1207.4207 [hep-ph]].

[60] S. Catani and L. Trentadue, Nucl. Phys. B **327**, 323 (1989).

[61] L. Magnea, Nucl. Phys. B **349**, 703 (1991).

[62] G. Korchemsky and G. Marchesini, Phys. Lett. B **313**, 433 (1993).

[63] P. Bolzoni, Phys. Lett. B **643**, 325 (2006) [hep-ph/0609073].

[64] A. Mukherjee and W. Vogelsang, Phys. Rev. D **73**, 074005 (2006) [hep-ph/0601162].

[65] V. Ravindran and J. Smith, Phys. Rev. D **76**, 114004 (2007) [arXiv:0708.1689 [hep-ph]].

[66] V. Ravindran, J. Smith and W. L. van Neerven, Nucl. Phys. B **767**, 100 (2007) [hep-ph/0608308].

[67] T. Becher, M. Neubert and B. D. Pecjak, JHEP **0701**, 076 (2007) [hep-ph/0607228].

[68] J. C. Collins, D. E. Soper and G. Sterman, Nucl. Phys. B **261**, 104 (1985).

[69] A. D. Martin, W. J. Stirling, R. S. Thorne and G. Watt, Eur. Phys. J. C **63**, 189 (2009) [arXiv:0901.0002 [hep-ph]].

[70] M. L. Ciccolini, S. Dittmaier and M. Kramer, Phys. Rev. D **68**, 073003 (2003) [hep-ph/0306234].

[71] N. D. Christensen, T. Han and T. Li, Phys. Rev. D **86**, 074003 (2012) [arXiv:1206.5816 [hep-ph]].

[72] R. Mertig, M. Bhm, and A. Denner, "Feyn Calc - Computer-algebraic calculation of Feynman amplitudes", Comput. Phys. Commun., **64**, 345-359, 1991.

[73] V. I. Borodulin, R. N. Rogalev and S. R. Slabospitsky, [hep-ph/9507456].

[74] I. A. Korchemskaya and G. P. Korchemsky, Phys. Lett. B **287**, 169 (1992).

[75] S. Moch, J. A. M. Vermaseren and A. Vogt, Nucl. Phys. B **688**, 101 (2004) [hep-ph/0403192].

[76] S. Moch, J. A. M. Vermaseren and A. Vogt, JHEP **0508**, 049 (2005) [hep-ph/0507039].

[77] A. Idilbi, X. d. Ji and F. Yuan, Nucl. Phys. B **753**, 42 (2006) [hep-ph/0605068].